ALFRED-WEGENER-INSTITUT
HELMHOLTZ-ZENTRUM FÜR POLAR- UND MEERESFORSCHUNG

Hochschule Bremerhaven

Bioactive substances in marine phytoplankton: salinity effects on growth and toxin production of the dinophyte *Alexandrium ostenfeldii*

Master's Thesis

A thesis submitted to the
University of Applied Science Bremerhaven
for the degree of

Master of Science

written by

Jörn Helge Martens

Conducted at the
Alfred Wegener Institute
Helmholtz Centre for Polar and Marine Research

2014

First Examiner: Prof. Dr. Boris Koch
University of Applied Science Bremerhaven
Alfred Wegener Institute Helmholtz Centre for Polar and Marine Research

Second Examiner: Prof. Dr. Allan Cembella
University of Bremen
Alfred Wegener Institute Helmholtz Centre for Polar and Marine Research

Table of contents

Declaration of Authorship

I hereby declare that I have developed and written the enclosed Master's Thesis completely by myself, and have not used sources or means without declaration in the text. Any thoughts from others or literal quotations are clearly marked. The thesis was not used in the same or in a similar version to achieve an academic grading before.

Bremerhaven, 21 November 2014 _____

Jörn Helge Martens

Acknowledgement

Though only my name appears on the cover letter of this thesis, many people have contributed to its completion. Special thanks go to

Dr. Urban Tillmann
for his excellent supervision

Prof. Dr. Boris Koch and **Prof. Dr. Allan Cembella**
for the possibility to work at AWI, their interest in my work
and their willingness to be my examiners

Dr. Bernd Krock
for his introduction into marine toxins, his guidance and assistance with LC-MS analysis and his scientific advice and troubleshooting

Dr. Dedmer van de Waal
for the possibility to work at NIOO, a great stay in Wageningen and his help and guidance in data interpretation

Annegret Müller and **Wolfgang Drebing**
for their technical assistance, their help and advice with all kinds of problems

Nico Helmsing
for his help with elemental analysis during my stay at NIOO

Denise Bachmann
for constructive proofreading the manuscript

Jörg Lehmann
for support with the DOC analysis.

For great years of study I am deeply grateful to
Denise Bachmann, Katharina Straumer, Gerrit Rohner, **Jörg Lehmann**
and **Theresa Sigges.**

And finally I would like to thank
my parents and my sister
who were always supporting and encouraging me with their best wishes.

Abstract

Alexandrium ostenfeldii is one of the most intensely studied toxic dinophyta in the world's oceans and coastal waters. Its toxins are highly potent neurotoxins and causatives of food intoxications by contaminated sea food. In the last few years harmful algal blooms (HAB) of *A. ostenfeldii* have become a recurrent phenomenon in coastal waters. In 2012 such a dense bloom occurred in the Ouwerkerkse Kreek. This creek system in The Netherlands is discharging water in the Oosterschelde estuary, a large stock of mussels, oysters and fishery. Only little information is available about this *A. ostenfeldii* population, both in terms of its toxin profile and concerning its physiological characteristics in a highly variable ecosystem.

We used multiple isolates of a bloom population for a thorough characterization of the phycotoxin profile and its variability in the population. A total of 68 *A. ostenfeldii* isolates were analyzed and revealed the presence of both, paralytic shellfish toxins (PSP) and cyclic imine toxins. Whereas the relative composition of PSP-toxins, consisting of saxitoxin, gonyautoxin and C-toxins, was almost identical among isolates, cyclic imine toxins were quite diverse. We detected a total of 23 different compounds with both spirolides (mainly 13-desmethyl spirolide C) and gymnodimines (both gymnodimine A and 12-methyl gymnodimine A) present and with a high variability in cyclic imine toxin profile among all isolates. Toxin cell quota was found to range 8-fold for total PSP-toxins and 11-fold for total cyclic imine toxins.

Furthermore, for one selected isolate, the impact of variable salinities from 3 to 34 on growth and toxin content was determined. With similar growth rates from 0.13 to 0.2 d^{-1} over a salinity range from 6 to 34, a broad salinity tolerance of the Dutch *A. ostenfeldii* population was demonstrated. Furthermore, toxin composition and the expression of single PSP- and cyclic imine toxins were depended on salinity. Highest toxin cell quota was observed for exceptionally low and high salinities. In addition, isolates were found to produce lytic compounds with EC_{50} values (i.e. the concentration of *A. ostenfeldii* causing 50 % cell lysis of the target species *Rhodomonas salina*) of about 659 cells ml^{-1}. A comparison of lytic activity in various fractions (whole cultures, culture supernatant, cell extract) revealed that whole cultures and also cell-free supernatants were about 5-fold more lytic than cell extracts. The lytic potency was susceptible for variable salinities: at very low salinities lytic effects of extracellular compounds were larger. At very high salinities, a larger amount of lytic substances was measured inside the cells.

During the toxin screening a potentially new spirolide (m/z 696) was detected. LC-MS data allowed a hypothetical characterization of the compound as 23-hydroxy-13,19-didesmethyl spirolide D. For further NMR-analyzes, *A. ostenfeldii* was mass cultured and a total of 140 µg of the new compound was collected.

Kurzdarstellung

Alexandrium ostenfeldii ist einer der am häufigsten untersuchten, toxischen Dinophyten der Ozeane und Küstengewässer. Die vom Organismus gebildeten Toxine zählen zu den stärksten, bislang bekannten Nervengiften. Insbesondere durch die Aufnahme von kontaminierten Schalentieren und Fischen können Lebensmittelvergiftungen verursacht werden. In den letzten Jahren ist ein vermehrtes Auftreten von Algenblüten, sogenannten „harmful algal blooms" (HAB), der Art *A. ostenfeldii* zu beobachten. Im Jahr 2012 wurde eine solche Blüte im niederländischen Ouwerkerkse Kreek in der Oosterschelde, einem zum Anbau von Schalentieren genutzten Mündungsdelta, festgestellt. Bis heute sind nur wenige Informationen zu dieser *A. ostenfeldii* Population hinsichtlich Toxizität und physiologischer Eigenschaften in diesem höchst variablen Ökosystem bekannt.

Für eine genaue Charakterisierung des Toxinprofils und einer möglichen Variabilität innerhalb der Population, wurden 68 Isolate hinsichtlich enthaltener „paralytic shellfish toxins" (PST) und einer weiteren Toxinklasse, der zyklischen Imine, untersucht. Während die relative Zusammensetzung der PSP-Toxine hauptsächlich aus STX, GTX2/3 und C1/C2 weitgehend gleich für alle Isolate war, waren die zyklischen Imine in ihrer Zusammensetzung äußerst divers. Insgesamt konnten 23 Komponenten, bestehend aus Spiroliden (insbesondere 13-desmethyl Spirolide C) und Gymnodiminen (sowohl Gymnodimine A, als auch 12-methyl Gymnodimine A), in hoher Variabilität nachgewiesen werden. Der Toxingehalt pro Zelle variierte dabei um das 8-fache für PSP-Toxine und um das 11-fache für zyklische Imine.

Des Weiteren wurde für ein ausgewähltes Isolat der Einfluss von unterschiedlichen Salzgehalten (S = 3 bis 34) auf Wachstum und Toxingehalt ermittelt. Bei ähnlichen Wachstumsraten im Bereich von 0,13 bis 0,2 pro Tag, wurde ein breiter Toleranzbereich von S = 6 bis 34 für die niederländischen Isolate ermittelt. Auch konnte gezeigt werden, dass der Toxingehalt und die Zusammensetzung der Toxine vom Salzgehalt abhängig waren. Die höchsten Toxinkonzentrationen pro Zelle waren bei besonders niedrigen oder hohen Salzgehalten messbar. Zusätzlich wurde die Produktion lytischer Substanzen mit EC_{50} Werten (die *A. ostenfeldii* Konzentration, bei der 50 % der Zellen in einem *Rhodomonas salina* Assay lysiert werden) von 659 Zellen mL^{-1} ermittelt. Es zeigte sich, dass die Vollkultur, sowie der zellfreie Überstand einer Kultur, etwa 5-fach lytischer waren, als ein Zellextrakt. Die Lysefähigkeit war dabei deutlich vom Salzgehalt abhängig: Bei besonders niedrigen Salzgehalten waren extrazelluläre Fraktionen besonders lytisch. Bei hohen Salzgehalten hingegen, waren die Zellextrakte verstärkt lytisch.

Während des Toxin-Screenings wurde ein neues Spirolide (m/z 696) detektiert. LC-MS-Untersuchungen ermöglichten eine hypothetische Charakterisierung des Toxins als 23-hydroxy-13,19-didesmethyl Spirolide D. Für weitere NMR-Analysen wurde eine Massenkultivierung mit *A. ostenfeldii* durchgeführt und eine Gesamtmenge von 140 µg der neuen Komponente gesammelt.

List of abbreviations

Δm	mass difference
°C	degree Celsius
µmol	micromole
ANOVA	analysis of variance
ASP	amnesic shellfish poisoning
AZA	azaspiracid
AZP	azaspiracid poisoning
CAD	collision-induced dissociation
CE	collision energy
CFP	ciguatera fish poisoning
CI	chemical ionization
CID	collision-induced dissociation
Cps	counts per second
Da	Dalton
dcSTX	decarbamoylsaxitoxin
DNA	deoxyribonucleic acid
DOC	dissolved organic carbon
DOM	dissolved organic matter
DON	dissolved organic nitrogen
DSP	diarrheic shellfish poisoning
EI	electron ionization
EPI	enhanced product ion scan
ESI	electrospray ionization
et al.	et alli
exp	exponential
FAB	fast atom bombardment
FT	fourier transform
g	gram
GTX	gonyautoxins
GYM	gymnodimine
h	hour
HAB	harmful algal bloom
HCl	hydrochloric acid
HPLC	high-performance liquid chromatography
HSD	honest significant difference
kV	kilo Volt
L	liter

LC	liquid chromatography
LC-FD	liquid chromatography with fluorescence detection
LC-MS	liquid chromatography–mass spectrometry
LOD	limit of detection
LOQ	limit of quantitation
m	meter
M	mol
m/z	mass-to-charge ratio
MALDI	matrix-assisted laser desorption/ionization
MeOH	methanol
min	minute
mL	milliliter
mm	millimeter
mM	millimolar
mmol	milimole
MRM	multiple reaction monitoring
MS	mass spectrometer
ms	millisecond
MU	mouse units
MW	molecular weight
n/a	not available
ND	not detectable
ng	nanogram
nm	nanometer
NMR	nuclear magnetic resonance
NP-HPLC	normal-phase chromatography
NSP	neurotoxic shellfish poisoning
pg	picogram
POC	particulate organic carbon
PON	particulate organic nitrogen
POP	particulate organic phosphorus
PSI	Pound-force per square inch
PSP	paralytic shellfish poisoning
PSS	practical salinity scale
PST	paralytic shellfish toxin
PSU	practical salinity unit
QqQ	triple quadruple
RP-HPLC	reversed-phase chromatography
rpm	rounds per minute

S	Practical salinity
s	second
S/N	signal-to-noise ratio
SPATT	solid phase adsorption toxin tracking
SPX-1	13-desmethyl spirolide C
SRM	selective reaction monitoring
SSP	spiroimine shellfish poisoning
stat	stationary
STX	saxitoxin
T	temperature
THF	tetrahydrofuran
TIC	total ion chromatogram
TOF	time of flight
UV	ultraviolet
UV/VIS	ultraviolet/visible
V	volt
v	volume
v/v	volume/volume
µg	microgram
µL	microliter
µM	micromolar

1 Introduction

The planktonic algae of the world's oceans form the basis for marine food webs and are thus of major importance for marine ecosystems. Today there are about 5,000 known species of planktonic microscopic algae (Hallegraeff 1993; Sournia et al. 1991; Gerssen et al. 2010). Some of these at times occur in high cell numbers and sometimes even discolor the surface of the sea. These obvious events are often termed as red-tides because many were composed of dinoflagellates containing red pigments (Glibert et al. 2005). During an algal bloom the density of cells can achieve a number of one million cells per liter or even more (Hallegraeff 1993). It is reported that 300 of all estimated phytoplankton species produce blooms and 60 - 80 of them are actually assumed to be toxic (Gerssen et al. 2010; Smayda 1997) and are therefore of major interest. In the case of a bloom of a toxic species, the phenomenon is commonly known as "harmful algal bloom" (HAB). The occurrence of HABs is a worldwide phenomenon. Commonly such blooms can be observed in coastal waters. In the last years blooms of harmful algae occurred with an increasing frequency (Glibert et al. 2005; Hallegraeff 1993). An increasing nutrient load through agriculture and the boom of the aquaculture industries supported anthropogenic eutrophication of coastal waters through polluted water and sewage disposal. Also natural influence by climate change and global warming are discussed as reasons for spreading of HAB-species (Glibert et al. 2005). Inter-annual oscillations like the El-Niño-Southern-Oscillation, the North-Atlantic-Oscillation or the Pacific-Decadal-Oscillation take part in spreading blooms along coastal waters (Glibert et al. 2005). The increasing carriage of freight with container ship caused also an anthropogenic spreading of organisms in ballast water of the ships (Hallegraeff 1998). Also the worldwide transportation and breeding of marine organisms contribute to a global spreading.

About 75 % of HAB species are dinoflagellates but cyanobacteria and other classes of algae can also cause HABs (Guéret and Brimble 2010; Glibert et al. 2005). HAB-species can produce a quit extensive range of different toxins including ciguatoxin, which cause ciguatera fish poisoning, domoic acid, which causes amnesic shellfish poisoning (ASP), azaspiracid, which causes azaspiracid shellfish poisoning (AZP), brevetoxins, which cause neurotoxic shellfish poisoning (NSP), saxitoxin, which causes paralytic shellfish poisoning (PSP), spirolides, which cause spiroimine shellfish poisoning (SSP), okadaic acid, which causes diarrheic shellfish poisoning (DSP) (Glibert et al. 2005; Guéret and Brimble 2010). One of the first documented cases of human poisoning after eating seafood contaminated with algal toxins occurred in 1793 in British Columbia (Hallegraeff 1993). The transfer of toxins to higher tropic levels is usually carried out by vectors like zooplankton, crustacean,

mollusks or fish. For humans especially fish, shellfish and bivalves are important transport vectors (Ciminiello and Fattorusso 2006; Röder et al. 2011). Also other marine animals like whales, tunas or seabirds can be affected by toxic algae through the food chain (Geraci et al. 1989). The toxins accumulate in tissue of the digestive tract of these organisms, sometimes without affecting the organism itself (Gerssen et al. 2010). After consumption of contaminated seafood by humans, the toxins are causing food poisonings with typical symptoms like headache, dizziness, nausea and vomiting or diarrhea. In case of high intoxications of some of the toxins, neurological deficits like respiratory paralysis could lead to death. There are no known antidotes for food intoxication caused by HAB-toxins (Glibert et al. 2005). Another significant way in which HABs can be harmful is via high biomass accumulation which may damage the environment. Particularly hypoxia or anoxia in addition to degradation of submerged vegetation are major problems (Glibert et al. 2005). In some areas HAB events can affect local public and economic interest. Losses in fishery, aquaculture industries and other economics which depend on the water quality are difficult to quantify. Costs range from direct expenses for public health, for losses in commercial fishing and in declines in tourism.

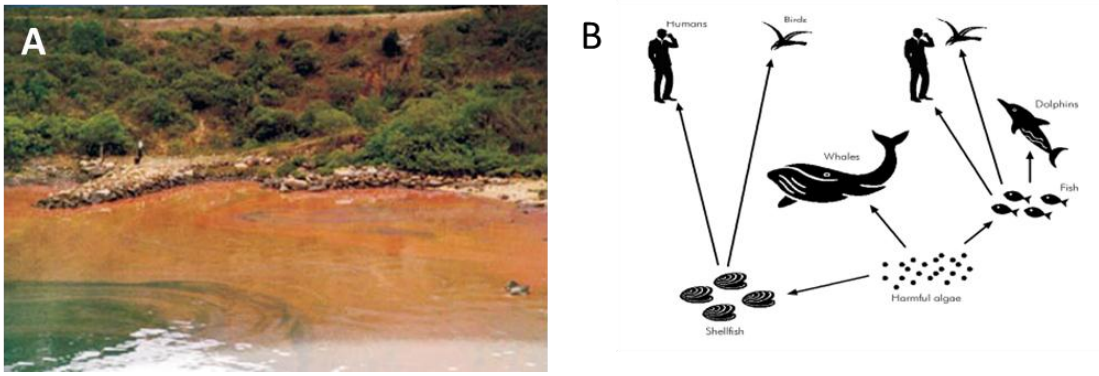

Figure 1: A) A bloom in Hong Kong, China caused by dinoflagellates (Glibert et al. 2005). **B)** Harmful algae blooms and the route of HAB-toxins in the food chain of marine organisms (Gerssen et al. 2010).

1.1 The marine dinoflagellate *Alexandrium* (Halim)

One of the most intensively studied planktonic dinoflagellate is the genus *Alexandrium* (Halim) Balech. Species of this genus are widely distributed around the world and common in temperate waters. Most *Alexandrium* species occur in background concentrations and are often outnumbered by co-occurring phytoplankton. High concentrations and almost monospecific blooms of *Alexandrium* seem to be the exception but do occur. Many species of the genus *Alexandrium* produce several highly potent neurotoxins, such as PSP-toxins and spirolides (Balech 1995), therefore blooms of *Alexandrium* species are in public interest.

The genus was formally established by the description of *A. minutum* which caused a red-tide in the harbor of Alexandria, Egypt (Bolch et al. 1991; Anderson et al. 2012). The *Alexandrium* genus includes about 31 species nowadays (Balech 1995), many of them were originally described with a different genus name, e.g. *Gonyaulax*, *Goniodoma* or *Pyrodinium* (Anderson et al. 2012). According to Balech (1995) the most important characters for species separation of *Alexandrium* are the ability to form chains, the morphological shape of the pore plate, the anterior and posterior sulcal plates, the first apical plate, the sixth precingular plate, the presence/absence of a ventral pore and the connection between the pore plate and the first apical plate. The genus *Alexandrium* is subdivided by Balech (1995) into the subgenera *Alexandrium sensu strictu*, where the apical pore complex is connected to the first apical plate and the homogenous subgenera *Gessnerium*, where the connection is interrupted. Moreover, some *Alexandrium* morphospecies which share similar morphological characteristics are grouped in species-complexes.

The morphologically based species concept of some *Alexandrium* species, however, is not supported by phylogenetic analysis based on ribosomal DNA sequences (Gu et al. 2013; MacKenzie et al. 2004). Lilly et al. (2007) and Kremp et al. (2014) performed phylogenetic analysis which resulted in different classifications as it was reported for morphologic descriptions before. For this reasons morphological and genetic examinations formally required a redefinition of several morphospecies into species complexes. Especially the *A. tamarense*, *A. fudyense* and *A. catenella* complex (Lilly et al. 2007) and also the *A. ostenfeldii* and *A. peruvianum* complex (Kremp et al. 2014) have to be revised because previous morphological classifications are untenable since phylogenetic elucidations were published.

1.1.1 The Alexandrium ostenfeldii *species complex*

The *A. ostenfeldii* species group is an important complex defined by Balech (1995). Based on similar morphological characters, Balech considered three species to be closely related and classified them as a complex: *A. ostenfeldii* Paulsen (Balech and Tangen 1985), *A. peruvianum* (Balech and Tangen 1985; Balech and de Mendiola 1977) and *Gonyaulax dimorpha* (Biecheler 1957). The first species was described from the Faroe Islands by Paulsen (1904) under the species name *Goniodoma ostenfeldii*. This species often co-occurs with *Alexandrium tamarense* (Hansen et al. 1992) and was often classified as *A. tamarense* var. *globosa* (Braarud 1945; Paulsen 1949; Balech and Tangen 1985; Balech 1995). After a redescription by Balech and Tangen (1985) the species was named under its current name *A. ostenfeldii*.

All three species of the *Alexandrium ostenfeldii* complex are globally distributed (Kremp et al. 2014). Published records include the Northern Adriatic Sea (Ciminiello et al. 2006), the Northern Baltic Sea (Kremp et al. 2009), the Danish coast (MacKinnon et al. 2006b; Moestrup and Hansen 1988), the Irish coast (Touzet et al. 2011) and the Scottish coast (John et al. 2003). *A. ostenfeldii* is also reported from Washington State on the Pacific coast of North America (Hansen et al. 1992), from Rhode Island, USA (Borkman et al. 2012) as well as from New Zealand and Northern Africa (MacKenzie et al. 1996).

According to Moestrup and Hansen (1988) *A. ostenfeldii* occurred throughout the year. Gu (2011) mentioned an optimal growth temperature between 12 - 24 °C for *A. ostenfeldii* cultures from Bohai Sea, China.

A. ostenfeldii cells are morphological characterized by a medium cell size, a globular shape and a thin walled theca. Moestrup and Hansen (1988) reported an averaged cell length of 45.5 µm and width of 49.0 µm. Balech and Tangen (1985) considered a cell size in the range 40 - 50 µm. In general the overall cell size seems to be very variable within a population (Figure 2).

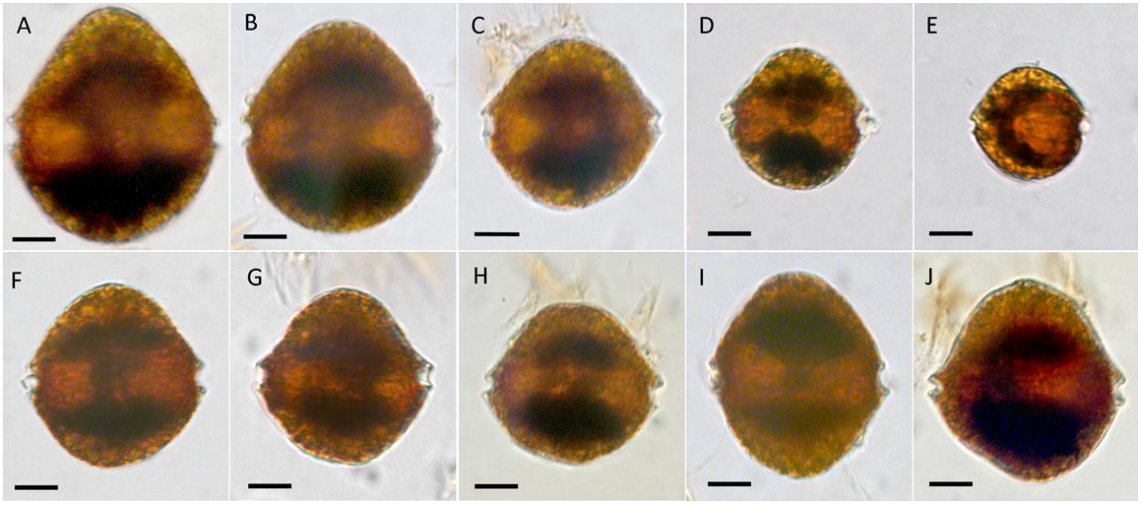

Figure 2: *Alexandrium ostenfeldii*. Light micrographs of single cells in ventral view to illustrate the variable cell size and shape. Scale bars = 20 µm. Adapted from Tillmann (2014, unpublished data).

The general cell shape of *A. ostenfeldii* is characterized by a broad and convex-conical formed epitheca and a hemispherical hypotheca without any spines or other antapical extensions (Gu 2011). Epi- and hypotheca are separated by a left-descending cingulum which is slightly excavated. The sulcus on the hypotheca is quite shallow but with elevated margins. A large amount of pores of various sizes are distributed over the whole surface, but are difficult to detect with light microscopy. The plate pattern of the thin theca can be observed after calcofluor staining. It is similar to other species of the *Alexandrium* genus and is described by Balech and Tangen (1985): An apical pore (AP) on a pore plate (Po) is

enclosed by series of four apical plates (4'), followed by six precingular plates (6''), six cingular plates (6C), 10 sulcal plates (10S), five postcingular plates (5''') and two antapical plates (2''''). The general plate pattern can be summarized with the Kofoidean plate formula: Po, 4', 6'', 6C, 10S, 5''', 2'''' (Balech and Tangen 1985; Balech 1995). MacKenzie et al. (1996) reported a plate pattern for *Alexandrium* with only 9 instead of 10 sulcal plates.

The first apical plate of *A. ostenfeldii* is very characteristic. It is asymmetric and comes with a prominent and large ventral pore on the cells left side as the most characteristic feature of the species (Kremp et al. 2014; Balech 1995; Moestrup and Hansen 1988). Another characteristic feature of *A. ostenfeldii* is the shape of the sixth precingular plate which is higher than wide (Figure 3) in contrast to some species in the genus *Alexandrium* (Moestrup and Hansen 1988).

Like other *Alexandrium* species, *A. ostenfeldii* possesses chloroplasts and a nucleus, which is horseshoe-shaped and oriented in the equatorial plane; the chloroplasts are radially oriented around the nucleus (Balech and Tangen 1985).

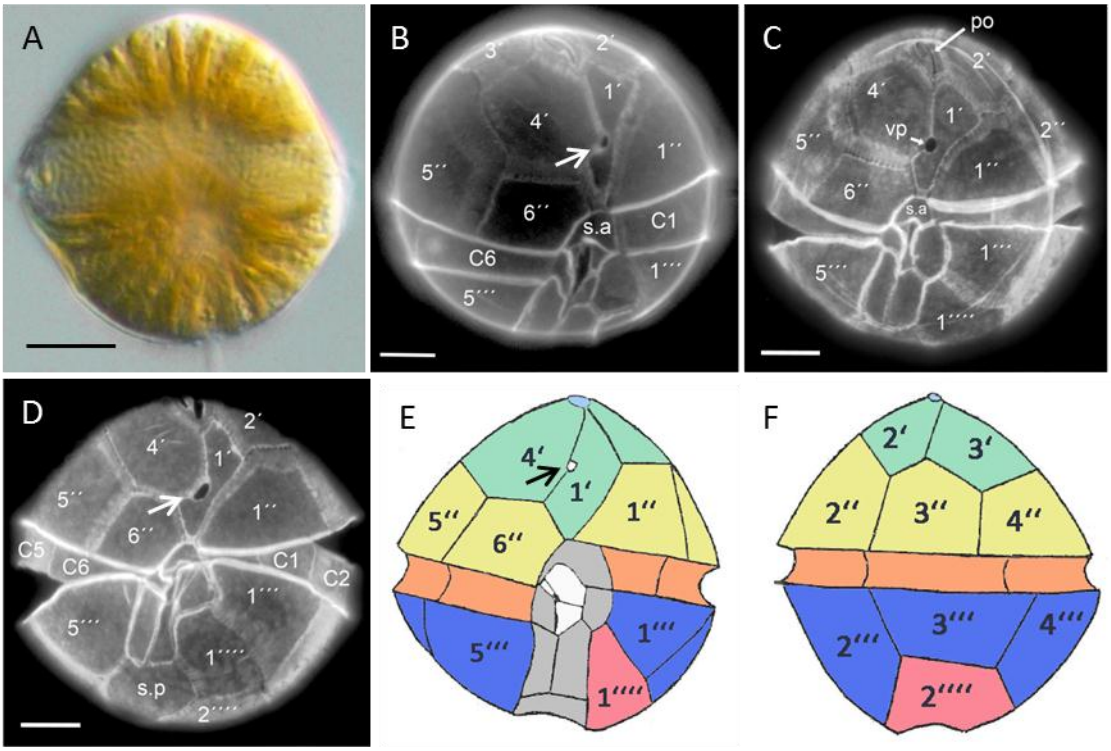

Figure 3: *A. ostenfeldii*. **A)** Light micrograph of a single cell in ventral view. **B)** Ventral view showing the typical cell shape. The positions of the cingulum, the large ventral pore (arrow) and some details of the tabulations are visible. **C-D)** As B. Note the typically formed shape of the first apical plate (1'). **E)** Tabulation of *A. ostenfeldii* in ventral views and **F)** in dorsal view. Scale bars = 10 µm. A-D) Adapted from Tillmann (2014, unpublished data). E-F) Adapted from Balech (1995).

Two different species, *A. ostenfeldii* and *A. peruvianum,* have been formally described with merely subtle differences in cell size and cell shape, especially in features of the first apical plate, sulcal anterior plate and the sixth precingular plate (Balech and de Mendiola 1977; Tomas et al. 2012). In addition, *A. ostenfeldii* cells generally are assumed to be larger and longer than wide, whereas *A. peruvianum* is generally described as being slightly wider than long (Kremp et al. 2014). *G. dimorpha* was originally described by Biecheler (1957) using material from a Mediterranean lagoon in the south of France. This species comes with distinctive differences to *A. ostenfeldii* and *A. peruvianum:* the first apical plate is anteriorly extended and some of the sulcal plates appear slightly different.

A clear morphological separation of *A. ostenfeldii* and *A. peruvianum*, however, has been challenged. A recent detailed and global study compiled and compared morphological and sequence data of *A. ostenfeldii* and *A. peruvianum* isolates. Phylogenetic analysis of rDNA sequences from cultures characterized as *A. ostenfeldii* or *A. peruvianum* formed a monophyletic clade consisting of six distinct groups. However, each examined group contained strains morphologically identified as either *A. ostenfeldii* or *A. peruvianum.* Thus Kremp et al (2014) concluded that the *A. ostenfeldii* complex should be regarded as a single genetically structured species, until more material and alternative criteria for species delimitation are available. Moreover, they proposed that *A. peruvianum* is a heterotypic synonym of *A. ostenfeldii* and that this taxon name should be discontinued (Kremp et al. 2014).

1.2 Life cycle of *Alexandrium* species

It is reported that some of the yet studied *Alexandrium* species have alternative asexual and sexual reproduction phases (Bolch et al. 1991; Anderson 1980; Gracia et al. 2013). Also for *A. ostenfeldii* a combined asexual and sexual life cycle is mentioned by several authors (MacKenzie et al. 1996). *Alexandrium* cells are meroplanktonic, so they spend only a part of their life as plankton (Wyatt and Jenkinson 1997). Other life phases they spend in the sediment. Repeated cell divisions of motile, vegetative cells form an asexual reproduction and could lead to high cell densities. For *A. ostenfeldii* division rates of 0.2 - 0.3 (divisions per day) are mentioned (Jensen and Moestrup 1997). This phase of exponential population growth is usually being terminated by external factors which then might also trigger and lead to a sexual reproduction. Anderson (1998) reported that sexuality has been induced in some culture by a limitation of nutrients, especially a limitation of nitrogen and phosphorus. Sexual stages were also observed by other authors in nutrient limited cultures (Jensen and Moestrup 1997). A potential role of short-term and sudden changes of environmental conditions like light, temperature or salinity on sexual cyst formation is

poorly known (Anderson 1998; Anderson et al. 1984) but often lead to the formation of temporary ecdysal cysts of normal vegetative cells. These temporary cyst may not be important for overwintering but to resist sudden or unusual environmental changes (Jensen and Moestrup 1997). Sexual reproduction starts with the formation of gametes, which could be in equal or in non-equal size. After fusion of two gametes, the planozygotes settle down to the sediment after a few days and start dormancy by forming a resting cyst. The period of dormancy seem to be species-specific and range from 12 hours to 6 month (Anderson 1980) or even years (Wyatt and Jenkinson 1997). When the resting interval is complete, the cysts are ready to hatch once the external conditions are favorable. Otherwise the cysts can stay in resting phase until e.g. the temperature increases due to seasonal warming. Cyst are able to germinate in a broad temperature range from 5 °C to 21 °C (Anderson 1980; Anderson and Morel 1979). This broad range may explain why some species like *Alexandrium* can bloom twice a year, one bloom in the spring and one in the fall (Anderson 1980). However, cysts are also found in water depths in which water temperature does not change much during the year and thus the germination process may be regulated by an endogenous annual clock mechanism. Such a mechanism was verified for one *A. tamarense* isolate but also postulated for other *Alexandrium* species (Anderson 1980). The molecular pathway of a clock mechanism regulating the germination is basically unknown. In general germination leads to a naked, ecdysal cell which – like the planocygotes before encystement – is characterized by two longitudinal flagella (Jensen and Moestrup 1997).

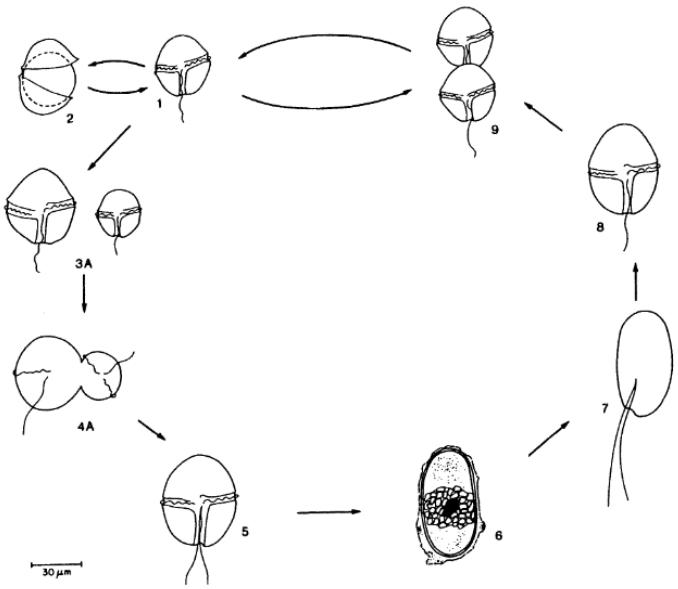

Figure 4: Life cycle diagram of *Alexandrium*. **1)** Vegetative, motile cell, **2)** temporary cyst, **3)** gametes, **4)** fusing gametes, **5)** swimming zygote, **6)** resting cyst, **7-8)** motile, germinated cell, **9)** pair of vegetative cells following division. Adapted from Anderson (1998).

1.3 Allelochemical interactions and lytic effects of *Alexandrium*

It is well known that some members of the genus *Alexandrium* produce highly potent phycotoxins like paralytic shellfish poisoning toxins, spirolides or gymnodimines. In addition there is increasing evidence that probably all species of *Alexandrium* produce lytic substances and other allelochemicals (Tillmann et al. 2008). Lytic activity was found to be unrelated to the known phycotoxins; non-toxic (in terms of phycotoxins) isolates of *Alexandrium* have been shown to cause cell lysis of other protists. This clearly indicate that neither the PSP-toxins (Tillmann and John 2002) nor the spirolides, the most common cyclic imine toxins (Tillmann et al. 2007) are the causative agent but allelochemicals with a yet unknown chemical composition (Alpermann et al. 2010; Tillmann et al. 2008; Ma et al. 2011).

Species-specific interactions through resource competitions or predator-prey interactions are important factors in biotic associations (Tillmann et al. 2008). Allelopathy describes all kinds of chemical interactions between species including both harmful and beneficial effect. Plankton species may interact with other organisms in an indirect way when they, e.g., exploit limiting resources, or in a direct way through the release of chemical compounds (Gross et al. 2012). These direct chemical interactions are an important part of the ecology of phytoplanktonic organisms (Gross et al. 2012; Tillmann and Hansen 2009). Weissbach (2011) pointed out several ways an organism in marine environments can benefit from allelochemical compounds: bioactive substances may function as chemical defense with effects varying from deterring, immobilization or lysis of grazers In addition, these compounds are also able to incapacitate or to kill competitors (Tillmann et al. 2008; Cembella 2003). In addition to reducing grazing loss and to eliminate competitors, allelochemicals may enable mixotrophy by either as a mean to subdue potential prey (Tillmann 2003) or by enlarging the pool of dissolved matter. By lysis of other protistan species, dissolved and particulate organic matter are available in the environment (Weissbach 2011).

In the aquatic realm, allelochemicals are inevitably diluted after being released by the organism. Consequently, the concentrations have to be high enough to counteract the dilution or the compounds have to be effective at very low concentrations. Only a few allelochemicals from phytoplankton have been structurally elucidated. Described compounds shown a large chemical variety. It is reported that physicochemical stress factors like nutrient limitation, temperature, changes of pH-value and acidification, light limitation and salinity can enhance the production of allelochemicals (Fistarol 2004; Tillmann 2003; Hansen 2002; Pedersen and Hansen 2003).

1.4 Toxic *Alexandrium* bloom in Ouwerkerkse Kreek, The Netherlands

The isolates of *A. ostenfeldii* used for the experiments presented in this thesis derived from a HAB-event in the Ouwerkerkse Kreek, located in the south-western part of The Netherlands. The creek is a shallow brackish water creek used as a drainage channel for local agriculture and the village Ouwerkerk (Figure 5). The water course is split into a southern and a northern part and flows along a campground. A pumping station regulates the water level in the creek to prevent flooding of the surroundings by discharging water into the Oosterschelde estuary, a tidal estuary with commercially used oyster beds. In addition to economic activities the estuary is quite important for populations of seabirds. As a semi-enclosed shallow brackish water system the creek is prone to substantial fluctuations in salinity on both temporal and spatial scales, mainly due to varying levels of drainage, flushing, or rainfall. For example, a depth profile of the creek in August showed a strong salinity-depth gradient ranging from $S < 10$ at the surface to values $S > 20$ in 2 m depth (Burson et al. 2014).

A dense bloom of *A. ostenfeldii* in this brackish creek was first observed in 2012 and described by Burson et al. (2014). The bloom in 2012 was first noticed after the death of a dog, probably caused by intoxication through contaminated material. Burson et al. (2014) reported about postmortem examinations which revealed a saxitoxin concentration of 2 - 4 mg kg^{-1}. Water analyses of the creek revealed considerably concentrations of saxitoxin and its analogs. *A. ostenfeldii* was found to be the most dominant phytoplankton organism in water samples from the creek (Burson et al. 2014). To prevent a further damage of the environment the bloom was terminated by adding hydrogen peroxide to the entire creek system (Burson et al. 2014).

However, in July 2013 a next and notably dense bloom of more than 3,000 cells mL^{-1} of *A. ostenfeldii* was recorded (van de Waal et al., in prep.). The author reported about highly variable salinities between 5 and 20 over the year. The creek showed highly fluctuating pH-values ranging between 7.3 and 9.0. Salinity and pH-value were maximal in August and September (pH 9.0, salinity 20) which was also the maximum of cell density of *A. ostenfeldii* in the water (Figure 5 D). The temperature was seasonable and maximal during the bloom in August and September (25 °C). In October cell density, salinity and pH-value decreased abruptly which maybe is caused by a temperature drop.

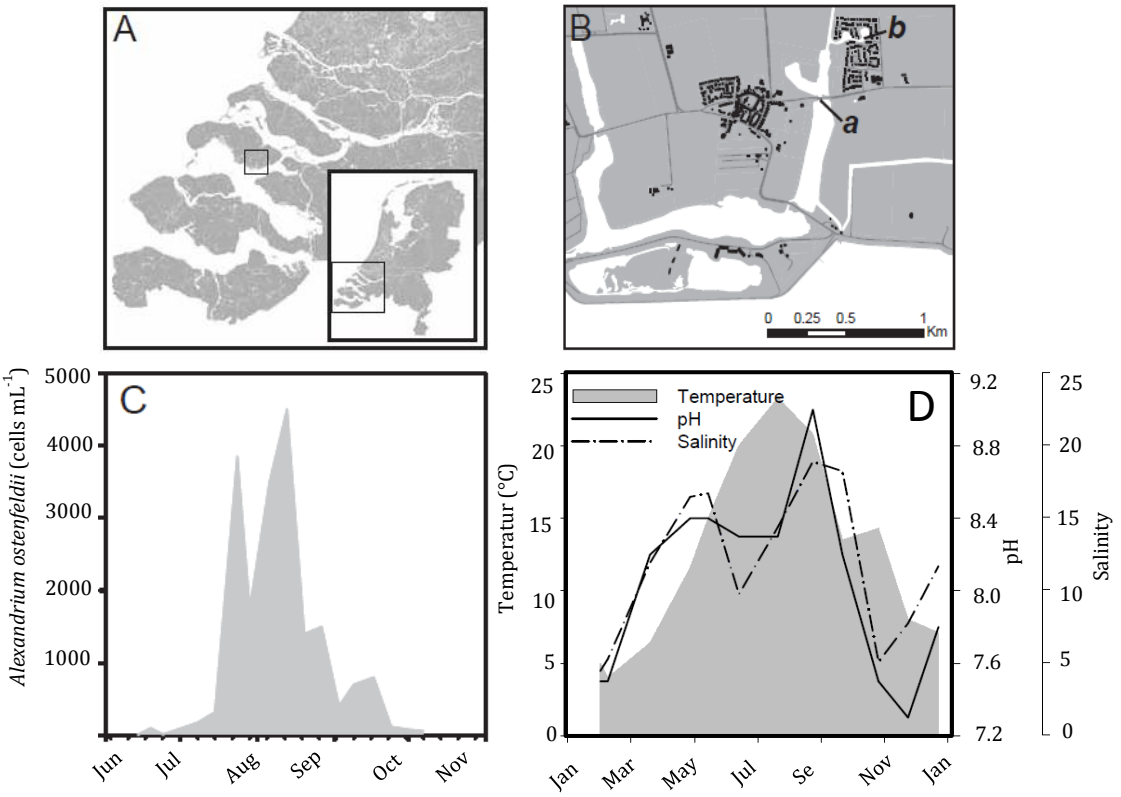

Figure 5: A, B) Overview of the sampling location in the Ouwerkerkse Kreek in the southwest of The Netherlands and the Rhine-Muesse-Scheldt delta. **C)** *A. ostenfeldii* population densities during the 2012 bloom. **D)** Field sampling data of the 2013 bloom. A-C) Adapted from Burson et al. (2014). D) Unpublished data, D. van de Waal.

2 Aims of this thesis

Because of the recent occurrences of the *A. ostenfeldii* blooms in the Ouwerkerkse Kreek, only little is known about the local *A. ostenfeldii* population. The overall aim of this thesis thus is to characterize the Dutch bloom population of *A. ostenfeldii* in terms of toxins and bioactive compounds and – more specifically – to elucidate effects of different salinities on growth and bioactive compound production of *A. ostenfeldii*.

It is well known that the toxin composition within a clonal isolate of *Alexandrium* is rather stable under a range of environmental conditions (Boyer et al. 1987; Cembella et al. 1987; Ogata et al. 1987) indicating that the relative toxin composition might be used as a chemotaxonomic trait to differentiate populations from diverse geographical regions (Cembella et al. 1998). However, only single strains or just a few isolates per population have usually been studied, but there is increasing evidence that geno- and phenotypic variability, including variability in toxin profile, may be extraordinary large within populations of *Alexandrium* (Alpermann et al. 2010; Tillmann et al. 2014). We therefore used a large number of 68 isolate for a thorough characterization in terms of toxin profile and cell quota.

Because of the local hydrographic situation in the brackish water of the Ouwerkerkse Kreek, local blooms are exposed to different salinities, which may vary spatially and temporally in both short term (rainfall) and long term (season, increased/reduced flushing), but the ecophysiological consequences for the local *A. ostenfeldii* population are completely unknown. Consequently, a particulate aim of this thesis is to analyze salinity effects on growth and toxin production of *A. ostenfeldii.* Growth rate measured over a broad range of salinities should allow to determined lower and upper growth limitations at extreme salinities. As a main focus, changes in PSP- and cyclic imine toxin content (intra- and extracellular) and toxin composition, as well as the production of lytic compounds as a response to different salinities will be measured in order to understand and predict the physiological response of the local *A. ostenfeldii* bloom to natural salinity fluctuations but also to anthropogenic changes in salinity due to regional water management decisions (i.e increased pumping and/or flushing).

3 Theoretical background

3.1 Marine phycotoxins

Marine phycotoxins are naturally occurring chemical substances of the metabolism of marine algae. They are non-proteinaceous compounds of high molecular weight and are very diverse concerning their chemical characteristics. A useful characteristic for classification is the subdivision in hydrophilic and lipophilic toxins. Also they can be classified by different functional groups or chemical classes like amino acids or polyketides. The mechanism of action and the toxicity of different algal toxins are highly variable. The symptoms they cause after human consumption are used to classify different eponymous poisonings (Campàs et al. 2007). Two of the major known poisonings caused by *A. ostenfeldii* are paralytic shellfish poisoning (PSP) and spiroimine shellfish poisoning (SSP).

3.1.1 Paralytic shellfish poisoning (PSP)

Paralytic shellfish poisoning is a severe world-wide problem for public health and fishery industries. In areas where dinoflagellates occur, planktonic feeders like bivalve shellfish may accumulate PSP-toxins. The safety consumption level of PSP-toxins in shellfish is monitored by public authorities who are able to ban the local shellfish market to avoid intoxications if toxicity exceeds threshold limits. Because of these possible sanctions, serious intoxications of humans due to PSP-toxins are rare in developed countries.

Paralytic shellfish poisoning toxins (PSTs) are consisting of a group of chemical compounds which are derived from saxitoxin (STX). Various derivatives of STX (Figure 6) have been isolated from different toxic algae, including *A. ostenfeldii, Gymnodinium catenatum* and *Pyrodinium bahamense* (Reyero et al. 1999). Currently more than 30 different compounds of PSP-toxins are reported (Sato and Kodama 2008). Derivatives of saxitoxin are chemical variable in the presence or absence of an N1-hydroxyl group, the presence or absence of an epimeric sulfate group at C11 position, a carbamoyl group at the side-chain R4, which additionally contains an N-sulfonate at N21. The carbamoyl group also can be absent (Botana 2014). The chemical stability varies depending on the structure of the toxin. In general, the toxins are water soluble and very stable over time. They are also stable under acidic or heat conditions but degenerate quickly at alkaline pH (Sato and Kodama 2008; Kentala et al. 1985). The toxicity varies among different PSTs, basically depending on its charge. PSTs are able to interact with sodium channels of cell membranes and can cause dysfunctions of these channels. A higher positive charge of the PST causes a stronger bond to the channel and results in increased toxic effects. The toxicity is also different between

epimers (e.g. GTX2 and GTX3) and between those epimers which belong to the R1-H or to the R1-OH group.

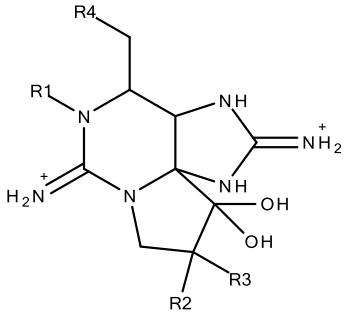

	R1	R2	R3	R4
Saxitoxin (STX)	H	H	H	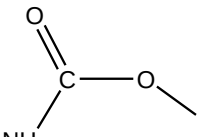
Neosaxitoxin (neoSTX)	OH	H	H	
Gonyautoxin 1 (GTX1)	OH	OSO_3^-	H	
Gonyautoxin 2 (GTX2)	H	OSO_3^-	H	
Gonyautoxin 3 (GTX3)	H	H	OSO_3^-	
Gonyautoxin 4 (GTX4)	OH	H	OSO_3^-	
Gonyautoxin 5 (GTX5) B1	H	H	H	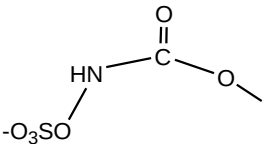
Gonyautoxin 6 (GTX6) B2	OH	H	H	
C1	H	OSO_3^-	H	
C2	H	H	OSO_3^-	
C3	OH	OSO_3^-	H	
C4	OH	H	OSO_3^-	
Decarbamoyl saxitoxin (dcSTX)	H	H	H	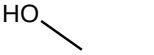
Decarbamoyl neosaxitoxin (dcneoSTX)	OH	H	H	
Decarbamoyl gonyautoxin 1 (dcGTX1)	OH	OSO_3^-	H	
Decarbamoyl gonyautoxin 2 (dcGTX2)	H	OSO_3^-	H	
Decarbamoyl gonyautoxin 3 (dcGTX3)	H	H	OSO_3^-	
Decarbamoyl gonyautoxin 4 (dcGTX4)	OH	H	OSO_3^-	
GC1	H	H	OSO_3^-	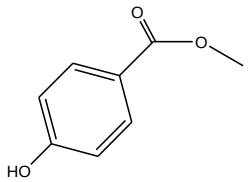
GC2	H	OSO_3^-	H	
GC3	H	H	H	
GC4	OH	H	OSO_3^-	
GC5	OH	OSO_3^-	H	
GC6	OH	H	H	

Carbamoyl

N-sulphocarbamoyl

Decarbamoyl

p-hydroxybenzoyl

Figure 6: Structures of saxitoxin and its derivatives. In addition, GC toxins are also reported as di-hydroxybenzoyl and sulphobenbenzoyl derivatives (Molgó et al. 2014; Vale 2008).

3.1.2 Spiroimine shellfish poisoning (SSP)

The spiroimine shellfish poisoning (SSP) is caused by a heterogeneous group of cyclic imine toxins sharing an imine moiety as bioactive pharmacophore (Cembella and Krock 2008). Basically the group contains gymnodimines, spirolides, pinnatoxins, prorocentrolides, pteriatoxins and spiro-prorocentrolides. Gymnodimines and spirolides are produced by *Alexandrium ostenfeldii* and are therefore discussed in this thesis (Cembella et al. 2000; van Wagoner et al. 2011). Spirolides are the largest group within SSP-toxins, which consist of 14 commonly studied derivatives with related chemical structures (Molgó et al. 2014). The main components (spirolide A-I) are complemented by different methyl, desmethyl or didesmethyl derivatives (Figure 7). The derivative 13-desmethyl spirolide C is commonly known as SPX-1 and the only available technical standard. Due to the lack of other spirolide standards, concentrations of spirolides other than SPX-1 in samples are expressed as SPX-1 equivalents.

Spirolides and gymnodimines are both fast acting toxins. The toxicity is strongly depended on the cyclic imine group as pharmacophore. For the first time, spirolides were discovered in *A. ostenfeldii* samples from Canada in 1998, three years after the discovery of spirolides in digestive glands of shellfish (Hu et al. 1995). The dinoflagellate was confirmed as the source organism of the spirolides A, B, C and D as well as two C and D isomers and some derivatives (13-Desmethyl spirolide C and D) (Cembella et al. 1998; Hu et al. 2001). Non-toxic derivatives of spirolides (e.g. spirolides E and F) suggest an important role of the imine group: Both, spirolide E and F, are shellfish metabolites of spirolide A and B and are formed by keto amine hydrolysis (Hu et al. 1996). Cembella and Krock (2008) reported about an dramatic decrease in biological activity after separating the imine ring from the molecule. Spirolide E and F have not been found in dinoflagellates (Christian et al. 2008). The toxic spirolide G and its derivative 20-methyl spirolide G are also found in cultures of *A. ostenfeldii* (Aasen et al. 2005). Recent researches reported *A. ostenfeldii* as the producer of two new spirolide H and I isolated from Canadian samples (Roach et al. 2009).

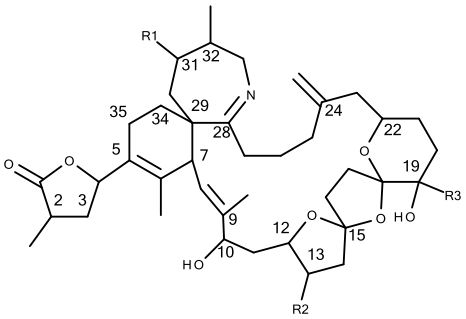

Spirolide	R1	R2	R3	$\Delta^{2,3}$	MW
A	H	CH_3	CH_3	+	691.5
B	H	CH_3	CH_3	-	693.5
C	CH_3	CH_3	CH_3	+	705.5
D	CH_3	CH_3	CH_3	-	707.5
13-desMe-C	CH_3	H	CH_3	+	691.5
13,19-didesMe-C	CH_3	H	H	+	677.5

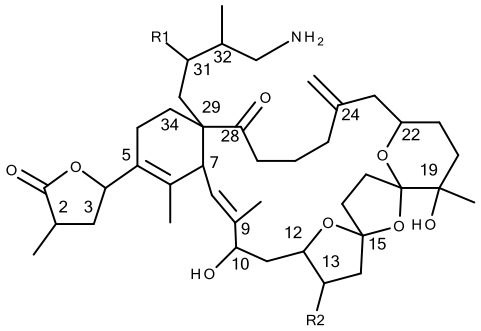

Spirolide	R1	R2	$\Delta^{2,3}$	MW
E	H	CH_3	+	709.5
F	H	CH_3	-	711.5

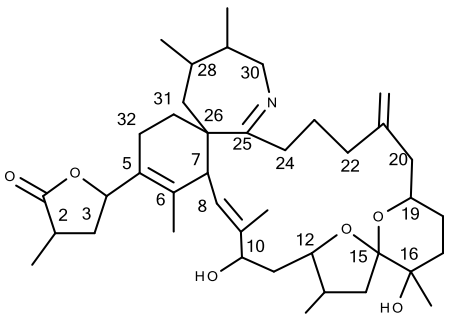

Spirolide	$\Delta^{2,3}$	MW
H	+	649.5
I	-	651.5

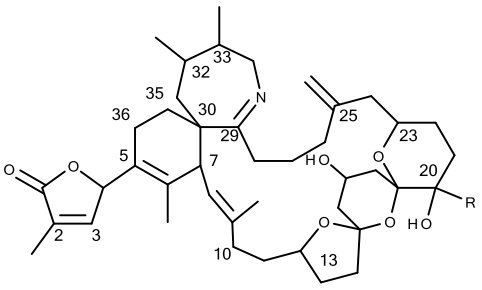

Spirolide	R	MW
G	H	691.5
20-Me-G	CH_3	705.5

Figure 7: Structures of spirolides (modified as per Christian et al. 2008; van Wagoner et al. 2011; Roach et al. 2009).

In addition, gymnodimines are reported as highly potent SSP toxins. In 1995 the dinoflagellate *Gymnodinium* cf. *mikimotoi* was found to produce gymnodimine A and to have caused an oyster contamination in New Zealand (Seki et al. 1995). Later the oxidized derivative gymnodimine B and its isomeric analog gymnodimine C were recognized as toxins produced by the dinoflagellate *Karenia selliformis* (Miles et al. 2000, 2003). Gymnodimines and its production was thus attributed to this group of species until in samples from *A. ostenfeldii* from North Carolina and Rhode Island in the United States a 12-methyl gymnodimine A analogue was isolated (Borkman et al. 2012; Tatters et al. 2012; van Wagoner et al. 2011).

Gymnodimines are reported to have a molecular weight of approximate 500 Da (Figure 8) and are one of the smallest molecules within the cyclic imine toxins (Cembella and Krock 2008).

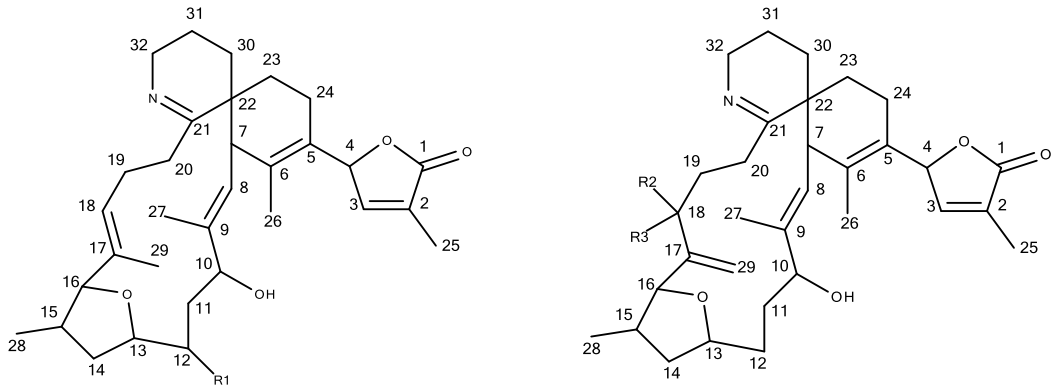

Gymnodimine	R1	MW
A	H	507.7
12-Me-A	CH_3	521.3

Gymnodimine	R2	R3	MW
B	H	OH	523.7
C	OH	H	523.7

Figure 8: Structures of gymnodimines (modified as per Molgó et al. 2014).

To date there are no reports of human intoxication which are caused only by cyclic imine toxins. Most intoxications are caused by a variety of different toxins in shellfish. The symptoms of intoxication in mice with purified toxins are the same as for all cyclic imine toxins and include neurological symptoms like hyperactivity, pilo-erection, hyperextension of the back, paralysis and respiratory arrest (Molgó et al. 2014). The toxicity of 13-desmethyl spirolide C, spirolide C and 20-methyl spirolide G is exceptionally high in comparison to other toxins (Munday 2008). There are some reports that spirolides affect Ca^{++}-channels and that gymnodimines activates Na^{+}-channels (Hu et al. 1996). Also acetylcholine receptors in the central and peripheral nervous system seem to be affected by cyclic imine toxins. A high affinity of toxins to these receptors causes a blockage of the signal conduction (Gill et al. 2003; Kharrat et al. 2008) which lead to neurological disorder.

3.2 High-performance liquid chromatography

High-performance liquid chromatography (HPLC) is a very efficient technique used in analytical chemistry for separating, identifying and quantifying different components in a mixture. The measurement principle based on a highly pressurized liquid solvent ("mobile phase") containing the sample mixture which flows through a column filled with a solid adsorbent material ("stationary phase"). Each of the components contained in the sample mixture interacts in a different way with the stationary phase. Thereby different retention times of the components cause a separation of the sample. The active compound of the column ("sorbent") consists of a porose material (e.g. silica gel, polymers) and is a decisive factor for the separation process. The interaction between the mobile phase and the stationary phase is basically done by chemical interactions (e.g. hydrophobic, ionic, dipol-dipol). The first developed HPLC application was the normal-phase chromatography (NP-HPLC). A polar material with a highly specific surface is used as stationary phase (e.g. silica). The mobile phase consists of a non-polar solvent, for example pentane, hexane or tetrahydrofuran. Because of the highly polar (or hydrophilic) stationary phase, it has a strong affinity to hydrophilic compounds in the mobile phase. In consequence, highly polar compounds will be later eluted than non-polar (or hydrophobic) compounds.

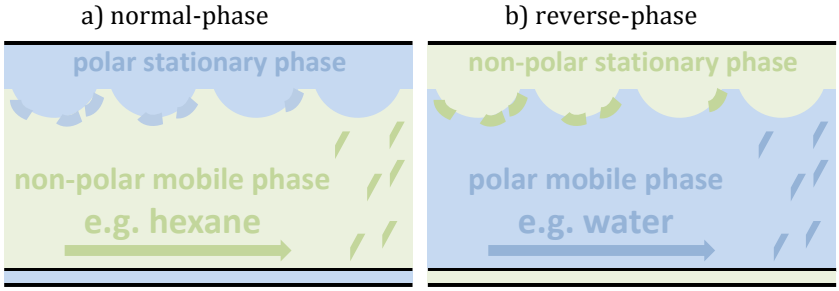

Figure 9: Schematic diagram of different columns for HPLC. **A)** Normal-phase column. **B)** Reverse-phase column.

In contrast, the reversed-phase chromatography (RP-HPLC) uses a stationary phase consisting of an inert, non-polar substance. Water or a mixture of water and acetonitrile or methanol is often used as mobile phase. In isocratic separations the polarity of the mobile phase is constant over the time. With a gradient elution, the polarity changes during separation runtime. A common stationary phase for reverse phase chromatography is an octadecyl carbon chain (C18)-bonded silica gel. The surface of the silica gel is chemically modified with long-chained fatty acids which decrease the polarity of the surface. In consequence the retention time is longer for molecules which are less polar because non-polar compounds can interact with the stationary phase. The interaction between analytes and stationary phase depends on interactions of hydrophobic substituents like alkyl chains. Retention times increase with a higher hydrophobic and non-polar characteristics of a

compound. The elution profile of a reverse phase chromatography with polar compounds first and non-polar compounds later is the opposite of a normal phase chromatography (Meyer 2006).

In general there are two common types of detectors used to analyze the separated sample. Concentration-dependent detectors analyses the concentration of an analyte in a specific volume of the flowing mobile phase, rather than quantity-dependent detector which measure the total quantity of an analyte.

The most common concentration-dependent detectors are UV/VIS-detectors (e.g. diode-array-detectors), fluorescence detectors, refractometric detectors and electro-analytical detectors. The UV/VIS detector is the most common detector because it is very universal and can be used for most of the analyte which absorb light in visible or ultraviolet spectra (≥200 nm). For UV/VIS detection it is necessary that the analyte includes aromatic compounds or conjugated double bonds. During absorption, conjugated electrons of the molecule are excited to a higher molecular orbital. The light absorption is measured by a detector. In addition to UV/VIS-detectors a refractometric detector can be used to measure different refractive indexes in the sample. The higher the refractive index of the analyte is in comparison to the pure mobile phase, the higher is the signal. A more sensitive detector principle is the fluorescence detector which directly measures fluorescent compounds or compounds which can be modified into fluorescent derivatives. In contrast to the UV/VIS detector, the fluorescence detector measures an emission of fluorescent light. The eluent itself does not contain any fluorescent compounds and only compounds of the sample contribute to the fluorescent signal which results in a distinctly lower background noise and a lower signal-to-noise ratio and therefore in a higher sensitivity. Especially conjugated cyclic compounds like aromatics emit fluorescent light and are detectable.

The detection of marine toxins like PSP-toxins can be carried out by a HPLC with fluorescence detection if a derivatisation system is used. In a chemical reaction, the analytes are selectively modified and afterwards emits fluorescent light under excitation. The derivatisation can be done previous to the separation on the column (“pre-column”) or after separation (“post-column”). The advantages of a pre-column derivatisation are basically a higher variability in experimental settings and an easier sample handling by doing the derivatisation simultaneously with a pre-cleaning step or the sample treatment. Excessive derivatisation reagent can be removed before separation. A pre-column derivatisation can have problematical impact on the separation if the derivatives of different compounds get chemically similar to each other due to the derivatisation process. In addition, the derivatisation reaction can result in different unrequested byproducts.

A post-column derivatisation is done by a reagent added to the sample after separation. A high concentration of the reagent is needed to avoid diluting effects in the sample. The separation is carried out before the derivatisation and therefore also analytes which result in similar derivatisation products can be individually detected. Previous to the derivatisation the separated compounds can be detect by another detector (e.g. an UV-detector). It is important that the derivatisation reagent itself is not detectable by the fluorescent detector to avoid noise and false signals. Furthermore the derivatisation reaction in the mobile phase must be reproducible for a comprehensible experiment.

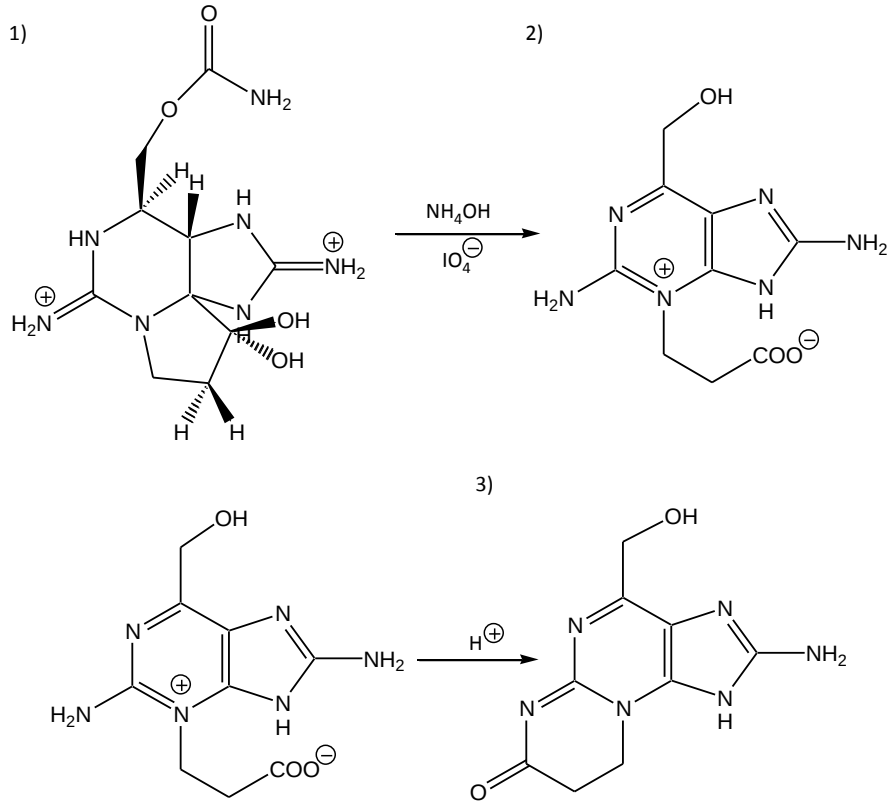

Figure 10: The chemistry of the post-column reactor used for the detection of PSP-toxins. **1)** Saxitoxin, **2)** open carboxylic oxidation product of the purine derivatives, **3)** fluorescent purine derivatives of saxitoxin.

The derivatisation of PSP-toxins based on the chemistry of Wong et al. (1971) and can be done in two steps (Figure 10): First the molecule is oxygenized by periodic acid which leads to fluorescent purine derivatives. The reaction is carried out in an alkaline solution by adding ammonia. In this alkaline solution the stability of the molecule is much lower and the binding between C12 and C4 in the molecule can be broken. Subsequently the resulting oxidation product of saxitoxin is reoriented into a planar aromatic system proposed as an open carboxylic acid form of the purine derivative (Quilliam et al. 1993; Boyer and Goddard 1999). In a second step an increased fluorescent signal of the intermediate is yielded by acidification with nitric acid. The acidic solution promotes the formation of pyrimidino-

purine lactams. The florescent signal of the derivative can be measured using an excitation wavelength of 333 nm and an emission peak at 395 nm. (Boyer and Goddard 1999; Asp et al. 2004)

3.3 Mass spectrometry

Mass spectrometry is a standard tool for analyzing chemical substances in terms of mass, structure and chemical composition. The basic principle is based on the detection of ions which are separated because of a different mass-charge ratio (m/z). It is necessary to apply a high vacuum to avoid inadvertent collisions of the ion with molecules contained in the air. In general, a mass spectrometer consists of four main components: an intake system, an ion source, a mass analyzer and a detector (Figure 11).

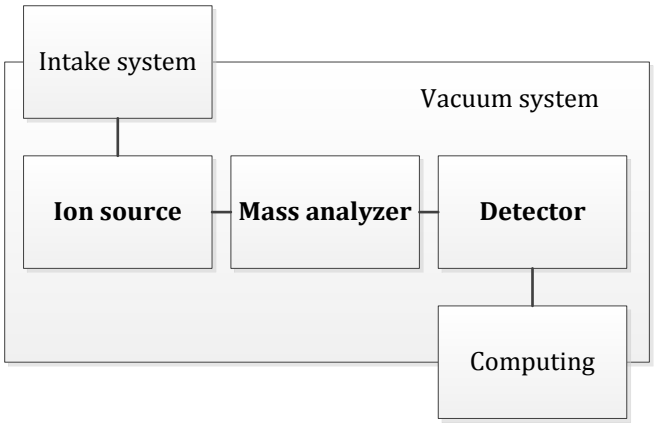

Figure 11: Schematic illustration of a mass spectrometer.

Depending on the phase of the unknown substance, different intake systems can be used to apply the sample to the mass spectrometer: Samples in liquid phase can be applied by a liquid chromatographic (LC) system to the ion source. Especially reverse phase LC/MS systems are often used because of the easier ionization of polar solvents. Volatile samples in gas-phase could be applied by a gas chromatograph or by a direct intake system. For non-volatile samples, a desorption intake system provides an intake of sample in condensed form.

For ionization, different ionization techniques can be classified as hard ionization and soft ionization methods: The hard ionization, especially the Electron Impact ionization (EI) leads to a high amount of fragmentation. The gaseous sample is radiated by an electron beam and the applied energy leads to ionization and fragmentation of the molecule. Soft ionization methods applied low residual energy on the analyte and lead to a lower amount of fragmentation. Typical applications of the letter method are the Chemical Ionization (CI), the Fast Atom Bombardment (FAB), the Matrix Assisted Laser Desorption Ionization (MALDI) and the Electrospray Ionization (ESI).

Three different types of mass analyzer can be distinguished because of their functional concept: First, ions can be separated in electric or magnetic fields (e.g. sector field instruments). Second, ions with different masses can be filtered in alternating electrical fields (e.g. quadrupole, ion trap or cyclotron resonance analyzer). And third, ions can be separated due to different flight times in a field-free vacuum in Time-of-Flight (TOF) analyzers.

3.3.1 Electrospray ionization and triple quadrupole mass spectrometer

Especially for analyzing and quantifying of complex substance mixtures, it could be necessary to separate the compounds of the sample first: It is a common method to analyze e.g. marine toxins with a coupled liquid chromatograph (LC) and a mass spectrometer. The toxin sample can be separated with an LC due to differences in polarity of its compounds before it is injected to the mass spectrometer (Turrell et al. 2008; Krauss et al. 2010). The presented results in this thesis were analyzed with a triple quadrupole (QqQ) mass spectrometer using ESI ionization coupled with a liquid chromatograph:

The electrospray ionization is commonly used as an ion source in mass spectrometry, especially for polar compounds (Hesse et al. 2012). It is based on the nebulization of the HPLC eluate by a capillary tube (Figure 12). The spraying takes place at atmospheric pressure which enables to couple the mass spectrometer with a high performance liquid chromatograph. An advantage of the electrospray ionization is that only weak fragmentation occurs to the sample because of the smooth treatment (Ekman 2009).

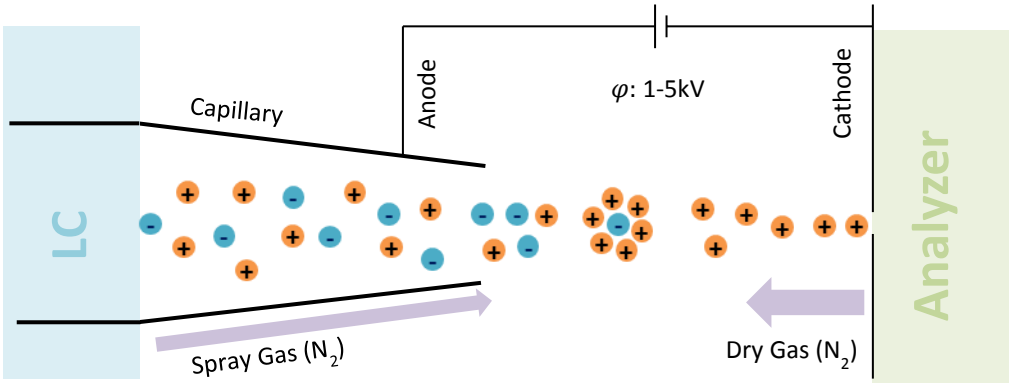

Figure 12: Schematic illustration of an electrospray ionization. Modified as per Hesse et al. (2012).

After separating the sample with a HPLC, the analyte is continuously injected into the ion source of the mass spectrometer and dispersed. The nebulization is done by a capillary tube carrying a potential difference of 1-5 kV between the capillary and the spray shied, which provides the entrance to the vacuum of the analyzer of the mass spectrometer (Hesse et al. 2012). In some large-flow electrospray applications the nebulization is supported by an inert gas (e.g. nitrogen) as a spray gas. The droplets which leave the capillary are highly positive charged depending on the impressed voltage. To decrease the droplet size the solvent is evaporated by an inverted dry gas flow of e.g. heated nitrogen (Banerjee and Mazumdar 2012). After reaching its Rayleigh limit the droplet becomes unstable (Li et al. 2005). At this point the electrostatic repulsion exceeds the surface tension of the drop. At a threshold level a Coulomb-Explosion occurs and single gas-phase ions are pulled out and carried over into the analyzer of the mass spectrometer. The observed ions are quasimolecular and are created by the addition of a hydrogen or sodium cation in positive mode, noted as $[M + nX]^{n+}$ or by the removal of hydrogen in negative mode, noted as $[M - nH]^{n-}$ (Hesse et al. 2012).

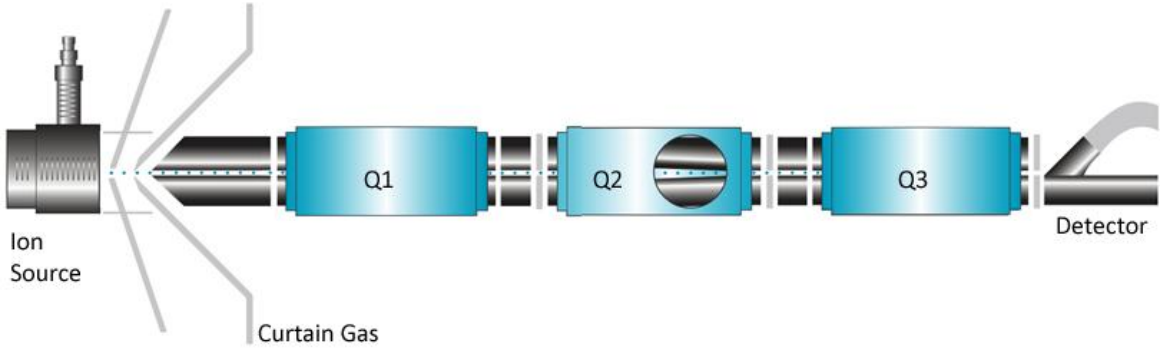

Figure 13: Schematic illustration of a triple quadrupole mass spectrometer. Modified as per AB Sciex (2010).

Quadrupole mass spectrometers are the most commonly used analyzers because of their easy and economic handling and their compact construction. They could be used with the most common ion sources and can be easily coupled with chromatographic systems. Advantageous to this is the high scanning speed (5000 m/z s^{-1}) of quadrupole mass spectrometers (Hesse et al. 2012). In contrast to other analyzers, the mass range (up to 4000 m/z) and a lower resolution are characteristic (Hesse et al. 2012). Quadrupole mass spectrometers are often used for analyzing mixtures and environmental samples with different components and are therefore especially convenient for analyzing marine toxins (Hunt et al. 1980; Fux et al. 2007). A quadrupole analyzer is built out of four hyperbolic metal rods arranged in pairs. An electric field with direct-current voltage is set up between two proximate rods. The electric field is overlaid by a radio-frequent, alternating-current voltage. This setup applied an electric field which enables ions with a specific mass-charge

ratio to pass the field unchallenged and to reach the detector. Ions with a different m/z ratio are distracted under the same conditions. A triple quadrupole mass spectrometer couples three quadrupoles (Q1, Q2 and Q3) in series. Q1 and Q3 are used for filtering the ions by means of the m/z ratio and to select a precursor ion in this way. The second quadrupole Q2 is used for fragmentation of the precursor ion. The fragmentation is carried out by a collision (CID) of the ion with an inert collision gas (e.g. nitrogen, argon). The fragmentation leads to characteristic fragments which are filtered in Q3 and registered by the detector. This approach is also known as tandem mass spectrometry (or MS/MS, MS^2) and is schematically presented in Figure 14 A. To get information about the structure of the analyte, a high amount of different fragments is preferred. It is necessary to apply a vacuum to avoid inadvertent collisions of the ion with molecules contained in the gas phase. In linear ion trap hybrid instruments, Q3 can be used in normal mode or as a linear ion trap (Hopfgartner et al. 2004). In the latter case, an electric field traps the ions due to their m/z ratio after applying a voltage at an electrode at the end of the quadrupole. By changing the electric potential, ions with a specific m/z ratio can leave in axial orientation and can be detected. This method increases the sensibility and the limit of detection (LOD) and is useful for samples with low concentrations of the analyte.

3.3.2 Scan experiments and ion detection methods

There are four different main types of scan experiments used in QqQ-mass spectrometry (Figure 14): product-ion scan, precursor-ion scan, neutral loss scan and selected reaction monitoring. In a product-ion scan, a precursor-ion with a specific mass is selected in the first analyzer. The selected ion is fragmentized and all resulting fragment masses are detected in the second analyzer. The precursor-ion scan modus is used to detect only signals from precursor ions which form fragments with a defined mass. For that the first analyzer is scanning the complete mass range but the second analyzer selects only one specific mass. In a neutral loss scan both analyzers a scanning the same mass range but the second analyzer with specific shift (Δm). In this way, only signals which differ about Δm are detected and possible losses of neutral particles can be monitored. The most specific scan modus is the single- or multiple-reaction monitoring. Both analyzers are set up to a specific mass and thus only signals of a selected precursor-ion (which lead to fragments with a specific mass) are detected. This experiment is often performed to detect transitions used for quantifications.

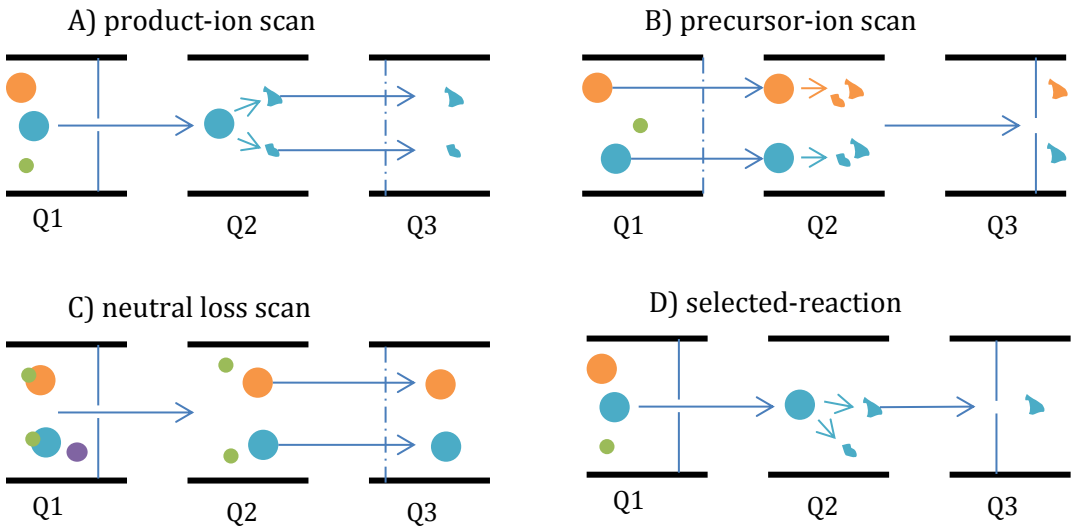

Figure 14: Schematic diagram of different scanning methods in mass spectrometry. **A)** product-ion scan **B)** precursor-ion scan **C)** neutral loss scan and **D)** selected-reaction monitoring.

The detection of ions can be done in basically two different ways: In most cases ions are registered by destructive detector systems. After leaving the analyzer the ions collide with a collection device, e.g. a Faraday Cup. This detector is able to measure ionic currents but only provides weak signals by directly impacting particles. Therefore the signal is increased by secondary particles (e.g. electrons or photons) which are created by the clash of the ion on the detector. These secondary particles are amplified by a secondary electron multiplier or a photo multiplier and provide a suitable signal for data processing. (Hesse et al. 2012)

Otherwise ions can be detected by Fourier-Transform (FT) detector systems. Contrary to destructive detectors ions are not destroyed in Fourier-Transform detectors. The measurement principle of Fourier-Transform detectors bases on the conversion of signals from a time-based domain into a frequency-based domain and subsequently to calculate m/z-values. The amplitude of the signal is directly proportional to the occurrence of the observed ions. Thereby this detection system is advantageous for quantifications. Because of the non-destructive measurements, Fourier-Transform detector systems can be coupled with multiple tandem mass spectrometers and increase the resolution of the resulting signals by using the same ion population in multiple measurements. (Hesse et al. 2012)

4 Material and methods

4.1 General part

4.1.1 Practical Salinity Scale

In this thesis the Practical Salinity Scale 1978 (PSS-78) is used, which has been recommended by the Joint Panel on Oceanographic Tables and Standards (UNESCO / ICES / SCOR / IAPSO Joint Panel on Oceanographic tables and Standards, Sidney, BC, Canada, 1-5 September 1980) as the scale in which salinity data should be reported. Practical salinity (symbol: S) is expressed by dimensionless numbers.

4.1.2 Culture media

All clonal *A. ostenfeldii* isolates were maintained in half-strength K-medium using the following recipe (Keller et al. 1987). A requested salinity was achieved by diluting seawater (salinity 36, AWI, Bremerhaven, Germany) with deionized and purified Milli-Q water (Millipore GmbH, Eschborn, Germany).

Following ingredients were added to 1 L as it is described by Keller et al. (1987):

- 500 µL $NaNO_3$ (stock solution 75.0 g/L)
- 500 µL NH_4Cl (stock solution 2.68 g/L)
- 500 µL $NaH_2PO_4 \cdot H_2O$ (stock solution 5.00 g/L)
- 50 µL H_2SeO_3 (stock solution 12.50 mg/L)
- 500 µL Trace metal solution (see below)
- 250 µL Vitamin solution (see below)
- 500 µL Tris-base (stock solution 121.10 g/L)

The trace metal solution (Keller et al. 1987) contained the following ingredients dissolved by heating in 1.0 liter Milli-Q water:

- 41.6 g $Na_2EDTA \cdot 2H_2O$
- 3.15 g $FeCl_3 \cdot 6H_2O$
- 1.0 mL $Na_2MoO_4 \cdot 2H_2O$ (stock solution 6.3 g/L)
- 1.0 mL $ZnSO_4 \cdot 7H_20$ (stock solution 22.0 g/L)
- 1.0 mL $CoCl_2 \cdot 6H_2O$ (stock solution 10.0 g/L)
- 1.0 mL $MnCl_2 \cdot 4H_2O$ (stock solution 180.0 g/L)
- 0.5 mL $CuSO_4 \cdot 5H_2O$ (stock solution 9.8 g/L)

The vitamin solution (Guillard and Ryther 1962; Guillard 1975) contained the following ingredients and was dissolved for a final volume up to 0.25 liter with Milli-Q water.

- 2.5 mL Vitamin B12 (stock solution 0.1 g/L)
- 2.5 mL Biotin (stock solution 0.1 g/L)
- 50 mg Thiamine HCL

After addition of all solutions, the pH-value of the culture medium was adjusted to 8.0 with a pH-meter (EcoScan Series, Eutech instruments, Singapore) by adding 1N hydrochloric acid. Finally all media were filter-sterilized (pore-size 0.2 µm, Sartorius AG, Goettingen, Germany) and stored at 10 °C.

4.1.3 Analytical methods for toxin analysis

Extraction of intracellular PSP-toxins and analysis with LC-FD

The PSP-toxin extraction and analysis followed the protocol described by Krock et al. (2007). For analyzing the intracellular PSP-toxins with liquid chromatography with fluorescence detection (LC-FD) cell pellets were transferred into a 2 mL microcentrifuge tube (neoLab, Heidelberg, Germany) containing 0.5 g of lysing matrix D (Thermo Savant, Illkirch, France) and 500 µL of 0.03 M acetic acid (Merck, Darmstadt, Germany). All samples were homogenized by reciprocal shaking at maximum speed (6.5 m s^{-1}) for 45 s in a FP 120 FastPrep instrument (Bio101, Thermo Savant, Illkirch, France). After homogenization the tubes were centrifuged (13200 rpm, 15 min, 4 °C, Centrifuge 5415R, Eppendorf, Hamburg, Germany). The supernatant was completely transferred to a spin-filter (pore-size 0.45 mm, Millipore Ultrafree, Eschborn, Germany) and centrifuged for 30 s at 5000 rpm. Finally the filtrate was transferred to a vial (Agilent Technologies, Waldbronn, Germany) and analyzed by LC-FD and stored at -20 °C.

The LC-FD analysis was done with a LC1100 series liquid chromatograph (Agilent Technologies, Waldbronn, Germany) linked up with a postcolumn derivatization system (Pickering Laboratories, Mountain View, USA). The LC-system was equipped with a degasser (Pickering Laboratories, No. G1379A), a quaternary pump (G1311A), an autosampler (G1229A), an autosampler thermostat (G1330B), a column thermostat (G1316A) and a fluorescence detector (G1321A). A chromatographic separation of the analysts was carried out under the following conditions: The mobile phase A consisted of 6 mM 1-octanesulphonic acid and 6 mM 1-heptanesulphonic acid in 40 mM ammonium phosphate, adjusted to pH 7.0 with dilute phosphoric acid and 0.75 % tetrahydrofuran (THF). The second mobile Phase B consisted of 13 mM 1-octanesulphonic acid in 50 mM phosphoric acid adjusted to pH 6.9 with ammonium hydroxide and 15 % of acetonitrile and

1.5 % of THF. The flow rate was adjusted to 1 mL min^{-1} for the following gradient condition: 0 min, 100 % mobile phase A, switched to 100 % mobile phase B until 16 min. Up to 36 min the gradient switched back to 100 % mobile phase A and stayed constant until 45 min (total run time). The samples were cooled down to 4 °C using the autosampler thermostat. The injection volume of the samples was 10 µL. The analytes were separated on a 250 mm x 4.6 mm Luna C18 reversed-phase column (Phenomenex, Aschaffenburg, Germany) equipped with a Phenomenex SecuriGuard pre-column. For postcolumn derivatization the eluate was oxidized in a reaction coil at a flow rate of 0.4 mL min^{-1} with 10 mM of periodic acid in 550 mM ammonium hydroxide and 0.75N nitric acid. Toxins were detected by a dual monochromatic fluorescence detector (λ_{ex} 333 nm; λ_{em} 395 nm). All toxins were identified using a standard solution (provided by Bernd Krock, AWI, Bremerhaven, Germany Limits of detection (LOD) and limits of quantification (LOQ) values for the toxin measurement are presented in Appendix II (p. 98). Data acquisition and processing was performed with the ChemStation software (edition for LC&LC-MS, version C01.04 (35), Agilent Technologies, Waldbronn, Germany).

Extraction of cyclic imine toxins and analysis with LC-MS

The extraction method of intracellular cyclic imine toxins followed the protocol for PSP-toxin extraction but was modified for lipophilic toxin measurements. Cell pellets were transferred to a 2 mL microcentrifuge tube (neoLab, Heidelberg, Germany) containing 0.5 g lysing matrix D (Thermo Savant, Illkirch, France). Subsequently the pellets were suspended in 500 µL methanol (LiChrosolv, for liquid chromatograph, Merck, Darmstadt, Germany) and homogenized by reciprocal shaking at maximum speed (6.5 m s^{-1}) for 45 s in a FP 120 FastPrep instrument (Bio101, Thermo Savant, Illkirch, France). After homogenization the samples were centrifuged (13200 rpm, 15 min, 4 °C, Centrifuge 5415R, Eppendorf, Hamburg, Germany) and the supernatant was transferred to a spin-filter (pore-size 0.45 mm, Millipore Ultrafree, Eschborn, Germany) and centrifuged for 30 s at 5000 rpm. For later measurement the filtered supernatant was stored in a vial (Agilent Technologies, Waldbronn, Germany) at -20 °C.

The cyclic imine toxin measurement (described by Krock et al. 2008; Kremp et al. 2014) was performed on an ABI-Sciex 4000 Q Trap triple-quadrupole mass spectrometer (Applied Biosystems, Darmstadt, Germany) with a Turbo V ion source coupled to an Agilent 1100 LC liquid chromatograph (Waldbronn, Germany). The LC was equipped with a solvent reservoir, in-line degasser (Pickering Laboratories, No. G1379A), binary pump (G1311A), refrigerated autosampler (G1329A/G1330B) and a temperature-controlled column oven (G1316A). The separation was carried out with an analytical C8 reverse phase column

(50 mm × 2 mm) packed with 3 µm Hypersil BDS 120 Å (Phenomenex, Aschaffenburg, Germany) and tempered at 20 °C. The flow-rate was 0.2 mL min^{-1} and performed by a gradient, where eluent A consisted of water and eluent B was methanol/water (95:5 v/v), both containing 2.0 mmol L^{-1} ammonium formate and 50 mmol L^{-1} formic acid. Initial conditions were reached after 10 min column equilibration with 5% of eluent B. After equilibration a linear gradient to 100% B in 10 min and isocratic elution until 10 min was followed by a return to initial conditions within 1 min followed by 9 min column equilibration. The total run time was 30 min. The mass spectrometric parameters were as follows: Curtain gas: 20 psi, CAD gas: medium, ion-spray voltage: 5500 V, temperature: 650 °C, nebulizer gas: 40 psi, auxiliary gas: 70 psi, interface heater: on, declustering potential: 121 V, entrance potential: 10 V, exit potential: 22 V. The collision energy was 57 V for each transition. Different multiple reaction monitoring (MRM) transitions were measured in positive ion-mode and are shown in Appendix I (p. 97). Dwell times of 40 ms were used for each transition. For quantizing the toxin concentrations, standard solutions with accurate concentration were measured. Due to the lack of other spirolide standards, concentrations of spirolides other than 13-desmethyl spirolide C (SPX-1) are expressed as SPX-1 peak area equivalents. For quantifications the following concentrations of SPX-1 were used: 10 pg/µL, 50 pg/µL, 100 pg/µL and 1000 pg/µL. For quantifying gymnodimines the following concentrations of a standard solution of gymnodimine A were used: 10 pg/µL, 50 pg/µL, 500 pg/µL and 1000 pg/µL (provided by Bernd Krock, AWI, Bremerhaven, Germany). LOD and LOQ values for the toxin measurement are presented in Appendix II (p. 98). Data acquisition and processing was performed with the Analyst Software (version 1.5, Applied Biosystems, Darmstadt, Germany).

4.1.4 Statistical analysis

t-test

A t-test was performed to determine significant differences between two data sets. The test-statistic follows a Student's t-distribution. The following function was used for performing a t-test by using the R software (R Foundation for Statistical Computing, Vienna, Austria).

```
t.test(x, y = NULL, alternative = c("two.sided", "less", "greater"),
 mu = 0, paired = FALSE, var.equal = FALSE, conf.level = 0.95, ...)
```

Analysis of Variances and Tukey's HSD

An Analysis of Variances (ANOVA) was used to analyze group means with more than three groups for statistical significance. In conjunction with an ANOVA a multiple comparison procedure was performed. Therefore results of an ANOVA were analyzed with a Tukey's HSD (honest significant difference) test. The Tukey's test compares means of different treatments with each other to find sub-groups which are significantly different from others.

The following function was used to perform an ANOVA and a Tukey's HSD by using the R software.

```
aov(formula, data = NULL, projections = FALSE, qr = TRUE,
 contrasts = NULL, ...)

TukeyHSD(x, which, ordered = FALSE, conf.level = 0.95, ...)
```

Pearson correlation coefficient

Pearson product-moment correlation coefficients were calculated to measure the linear dependence between two data sets. The resulting value ranges between -1 and +1, where 1 means total positive correlated, -1 means total negative correlated and 0 means no correlation. The statistical significance of the result was proven by using a t-test. The following function was used to calculate a correlation coefficient with the R software.

```
cor.test(x, y,
 alternative = c("two.sided", "less", "greater"),
 method = c("pearson", "kendall", "spearman"),
 exact = NULL, conf.level = 0.95, continuity = FALSE, ...)
```

4.2 Experimental part

4.2.1 Experiment 1: Toxin screening of 68 isolates from Ouwerkerkse Kreek

Origin of cultures

A total of 68 isolates of *A. ostenfeldii* were isolated after a blooming event in 2013 in Ouwerkerkse Kreek (51°62' N, 3°99' E) in The Netherlands (van de Waal et al., in prep.). Isolates had been established by single cell isolation using microcapillary into individual wells of a 96-well plate pre-filled with diluted North Sea water with a salinity of about 10 and were provided Urban Tillmann (AWI, Bremerhaven, Germany).

Cultivation of isolates

All isolates were grown at AWI (Bremerhaven, Germany) in walk-in growth chambers under controlled conditions with artificial cool-white fluorescent light at a photon flux density of 80 – 100 µmol $m^{-2}s^{-1}$ on a 16:8 h light–dark photocycle. The ambient air

temperature was 15 °C. Cultures were maintained in half-strength K-medium (Keller et al. 1987) with a salinity of 10 (Chapter 4.1.2).

Toxin screening

For toxin analysis, all isolates were grown in 65 mL plastic culture flasks at the standard culture conditions described above. For each harvest, cell density was determined by settling Lugol fixed samples (2 % final concentration) and counting > 600 cells in a 2 mL counting chamber with an inverted microscope (Zeiss Axiovert 40C, Göttingen, Germany) at 200 × magnification. Cultures at a cell density ranging from 1,000 – 3,500 cells mL^{-1} were harvested by centrifugation (Eppendorf 5810R, Hamburg, Germany) at 3,220 g for 10 min, 40 mL for analyzing PSP-toxins and 15 mL for analysis of cyclic imine toxins. Cell pellets were transferred to 1 mL microtubes, again centrifuged (Eppendorf 5415, 16,000 g, 5 min), and stored frozen (–20 °C) until use. Toxin analyzes were carried out as it is described in Chapter 4.1.3.

4.2.2 Experiment 2: Salinity tolerance of a pre-selected isolate

Origin of culture

The *A. ostenfeldii* isolate OKNL21 was used for this experiment. It was originally isolated after a blooming event in 2013 in the Ouwerkerkse Kreek (51°62' N, 3°99' E) in The Netherlands (van de Waal et al., in prep.) as part of a collection of 68 isolates. OKNL21 was chosen because of its representative results in the toxin screening in the previous experiment (Chapter 4.2.1).

Culture media

Eight salinity treatments with salinities of 3, 4.5, 6, 10, 16, 22, 28 and 34 were prepared as it is described in Chapter 4.1.2. The following dilutions of seawater (salinity 36, AWI, Bremerhaven, Germany) and Milli-Q water (Millipore GmbH, Eschborn, Germany) were prepared in 1 L bottles:

- S = 3: 80 mL seawater and 920 mL Milli-Q water
- S = 4.5: 125 mL seawater and 875 mL Milli-Q water
- S = 6: 160 mL seawater and 840 mL Milli-Q water
- S = 10: 280 mL seawater and 720 mL Milli-Q water
- S = 16: 440 mL seawater and 560 mL Milli-Q water
- S = 22: 610 mL seawater and 390 mL Milli-Q water
- S = 28: 780 mL seawater and 220 mL Milli-Q water
- S = 34: 940 mL seawater and 60 mL Milli-Q water

Conductivities were checked with a SB80PC salinometer (VWR sympHony Meters, Beverly, USA) and converted into salinities by using a formula described by Eaton et al. (1998).

Culture conditions

All salinity experiments were performed under controlled conditions with artificial cool-white fluorescent light at a photon flux density of 80 - 100 µmol $m^{-2}s^{-1}$ on a 16:8 h light–dark photocycle. The ambient air temperature was 15 °C.

Pre-acclimation of inoculum cultures

Prior to the salinity experiment, cells of the isolate OKNL21 were pre-acclimated to the different salinities as follows. To prevent high cell stress due to a too drastically change of salinity, cells of a stock culture (salinity 10) were first transferred to salinities 6, 10 and 16. An initial cell density of 500 cells mL^{-1} was attempted and cells were pre-acclimatized for two weeks. After acclimation the cell density was counted every 2 - 3 days. As soon as the cell count of the S = 16 culture increased exponentially and reached a density of approximately 2,500 cells mL^{-1}, a sufficient volume was transferred to fresh media with a salinity of 22 to archive an initial cell density of 500 cells mL^{-1}. This procedure was also repeated for transferring cells from the S = 22 medium to S = 28 medium and for transferring cells from S = 28 medium to S = 34 medium. Cells from the S = 6 medium were transferred to S = 4.5 and from there to S = 3 medium as soon as the culture reached exponential growth. The step-wise acclimation is schematically presented in Figure 15.

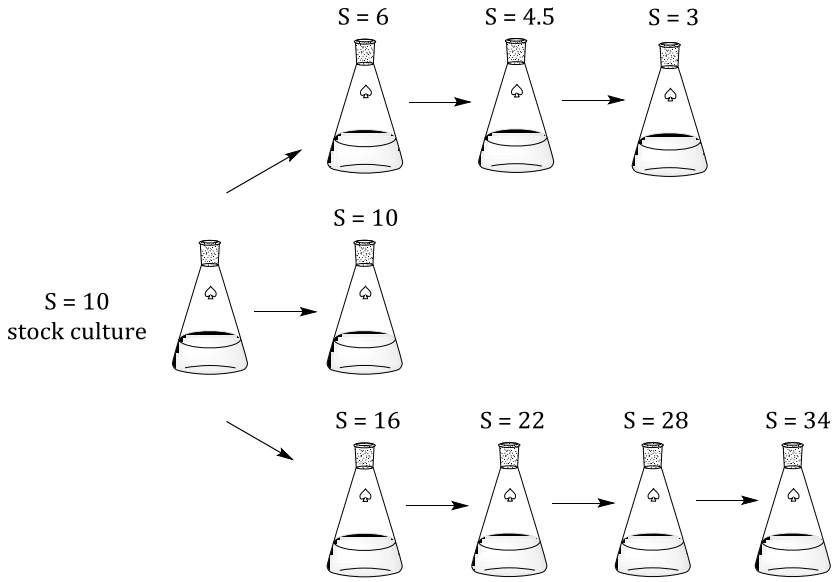

Figure 15: Schematic diagram of the pre-acclimation of the cultures for the salinity tolerance experiment.

Cultivating of experimental cultures

After *A. ostenfeldii* cells were acclimatized to the different salinities, exponential growing cells (based on consecutive cell counts of the inoculum culture) were transferred to fresh media for growth experiments. An initial cell density of 300 cells mL^{-1} in the experimental cultures was obtained. All cultures were set up in triplicates in 1 L Erlenmeyer flasks containing 600 mL of K-medium (Figure 16 A). Growth was followed by cell counts every second day by selecting an adequate volume containing about 400 cells. The samples were fixed with 2 % Lugol's iodine solution and counted in a 2 mL counting chamber. Samples for toxin measurements, lytic capacity, elemental composition and cell size determination (Table 1) were taken in exponential growth phase at a density of about 2,000 cells mL^{-1} and in stationary growth phase, when three consecutive cell counts shows that the population did not increased (>10,000 cells mL^{-1}; Figure 16 B). Samples for toxin measurement, lytic capacity and elemental analysis were frozen at -20 °C for later measurements. Samples for cell size and cell count determination were stored in the refrigerator.

Table 1: Sample volumes for measurements performed in exponential and in stationary growth phase.

	Sample volume	
	Exponential growth phase	Stationary growth phase
PSP-toxins	50 mL, in duplicates	30 mL, in duplicates
Cyclic imine toxins	15 mL, in duplicates	15 mL, in duplicates
Lytic capacity	50 mL, in duplicates	30 mL, in duplicates
Elemental composition	50 mL, in duplicates	30 mL, in duplicates
Cell size	4 mL	4 mL
Cell count	100 µL	30 µL

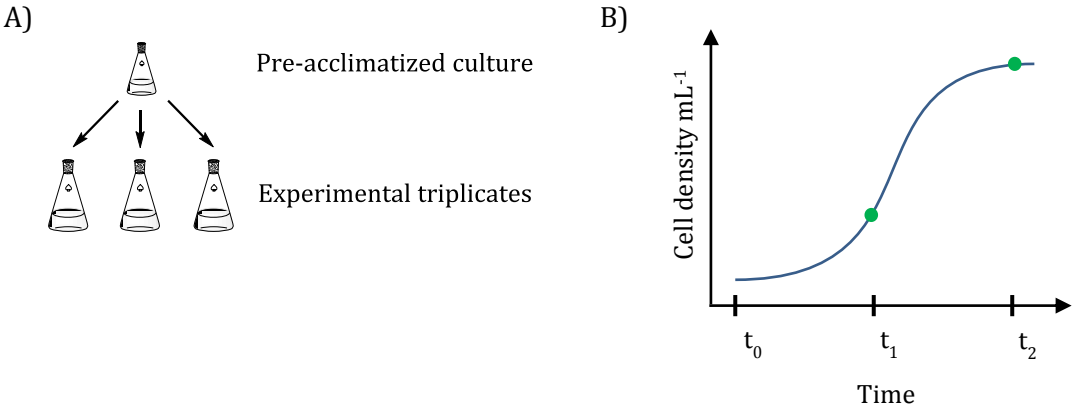

Figure 16: Schematic diagram. **A)** After pre-acclimation each salinity treatment was set up from one inoculum culture into three replicated experimental cultures. **B)** Schematic growth curve of an exponentially growing culture. The first sampling was done at t_1 (~2500 cells mL^{-1}) while exponential growth and the second sampling at t_2 as soon as the culture achieved stationary phase.

PSP-toxin analysis with LC-FD

Cultures were harvested by centrifugation (Eppendorf 5810R, Hamburg, Germany) at 3,220 g for 10 min, 50 mL for analyzing cultures in exponential growth phase and 30 mL for analysis of cultures in stationary growth phase. Cell pellets were transferred to 1 mL microtubes, again centrifuged (Eppendorf 5415, 16,000 g, 5 min), and stored frozen (-20 °C) until use. Toxin analyzes were carried out as it is described in Chapter 4.1.3.

Intracellular cyclic imine toxin analysis with LC-MS

Cultures were harvested by centrifugation (Eppendorf 5810R, Hamburg, Germany) at 3,220 g for 10 min. Volumes of 15 mL were used for analyzing cultures in exponential growth phase and in stationary growth phase. Cell pellets were transferred to 1 mL microtubes, centrifuged (Eppendorf 5415, 16,000 g, 5 min) and stored frozen (-20 °C) until use. Toxin analyzes were carried out as it is described in Chapter 4.1.3.

Cultures supernatants were also stored frozen (-30 °C) for the subsequent analysis of extracellular cyclic imine toxins.

Extracellular cyclic imine toxin analysis with LC-MS

The following clean-up procedure was developed and applied to culture supernatant, which was collected from each sample: A C_{18} cartridge (Supelclean LC-18 tubes 6 mL, Supelco, Bellefonte, USA) was conditioned in a Visiprep Solid-Phase-Extraction vacuum chamber (Supelco, Bellefonte, USA) with 2 mL of methanol and 5 mL of distilled water. The eluate was discarded. Then the whole sampled was step-wise loaded onto the cartridge. After flow through, the cartridge was washed with 5 mL of distilled water. The eluate was discarded again. The elution of the cyclic imine toxins was done with 5 mL methanol and followed the manufacturers' instructions. After elution, the 5 mL extract was evaporated with a rotary evaporator to an accurate volume of 1 mL. The extract was transferred to a glass vial (Agilent Technologies, Waldbronn, Germany) and stored at -30 °C for later measurement with LC-MS (Chapter 4.1.3).

The efficiency of the described extraction procedure for extracellular cyclic imine toxins was determined in a pretest: 100 mL of pure culture medium were mixed with 50 µL cell extract which contained a known amount of cyclic imine toxins. This mixture was treated with the described SPE extraction procedure. The pretest was repeated for three times and the recovery rate of cyclic imine toxins was calculated.

Dissolved and particulate elemental composition

For analyzing the carbon, nitrogen, and phosphorus content of the cells, duplicate samples of 30 - 50 mL culture each were filtered over a glass-fibre filter (GF/C; pre-combusted at 500 °C for 8 h; Whatman, Maidstone, UK). The filter was frozen at -30 °C and stored for later elemental analysis in a petri dish (Greiner bio-one, Orlando, USA).

For analyzing dissolved organic carbon (DOC) and nitrogen (DON), 30 - 50 mL of culture supernatant obtained after centrifugation was stored in a high-density polyethylene bottle (capacity: 60 mL; VWR International, Radnor, USA) and frozen at -30°C.

Blank samples of each salinity for analyzing dissolved and particulate elements were set up in duplicates by filtering pure culture medium over glass-fibre filters (GF/C; pre-combusted at 500 °C for 8 h; Whatman, Maidstone, UK) and collecting the filtrate. Because of high DOC and DON values in the blank samples no blanks were taken into account for DOC and DON calculations. For analyzing the particulate carbon, nitrogen, and phosphorus composition each blank value were subtracted from sample values.

Dissolved organic carbon (DOC) and nitrogen (DON)

DOC and DON were determined by catalytic oxidation at a high temperature and subsequent detection by infrared spectroscopy and chemiluminescence (TOC-VCPN/TNM-1, Shimadzu, Kyōto, Japan). Final concentrations are calculated out of triplicate measurements. Each batch of five samples was followed by one reference standard (DOC-DSR, Hansell Research Lab, University of Miami, USA), one Mili-Q water blank and a mixed potassium hydrogen phthalate (KHP) and potassium nitrate (KNO_3) standard with an alternating concentration ratio of 80:40, 120:60, 160:80, 240:120, 320:160 and 480:240 (in µg).

Particulate carbon, nitrogen and phosphorus

For analyzing the carbon and nitrogen content the filters were dried at 60 °C for 24 h. Subsequently, six small pieces (d = 3 mm; A = 7.07 mm^2) were pierced out of the filter and folded into thin capsules (Elemental Microanalysis, Okehampton, UK). The area on the filter covered by particles was A = 346.36 mm^2 (d = 21 mm). The carbon and nitrogen content was determined by a FLASH 2000 organic elemental analyzer (Brechbueler Incorporated, Interscience B.V., Breda, The Netherlands).

Subsequently, the remaining part of the filter was used for measuring the phosphorus content. First the samples were incinerated for 30 min at 500 °C, followed by a 2 % persulphate digestion step for 30 min at 121 °C in the autoclave. The digested samples

were analyzed using a QuAAtro segmented flow analyzer (Seal Analytical Incorporated, Beun de Ronde, Abcoude, The Netherlands).

Lytic compounds

Cell harvesting and sample preparation

For a quantitative comparison of different culture fractions one detailed bioassay was performed using whole cell culture, supernatant and cell extracts. For cell harvesting 40 mL of the *A. ostenfeldii* experimental culture grown at a salinity of 16 were centrifuged (4,750 rpm, 15 min, Allegra X-15R Centrifuge, Beckman Coulter, Brea, USA). An ultrasonic extraction of the cell pellet was performed by a Sonoplus HD70 sonotrode (Bandelin Electronics, Berlin, Germany). The optimal settings for sample extraction were taken from Eschbach et al. (2001) and defined as: 50 % pulse cycle and 70 % amplitude for 60 sec. Samples were kept on ice while ultrasonic treatment. Bioassays from whole cell culture, cell extracts and cell-free supernatant were set up as described below with one modification: we here used a culture of the target species *Rhodomonas salina* (Kalmar culture collection, strain KAC30) that was pre-adapted from S = 34 to the reduced salinity of S = 16 for at least four weeks.

Quantitative estimation of lytic activity for the salinity growth experiments were performed after the experiments by using frozen samples. At each sampling, *A. ostenfeldii* cells were harvested in a 50 mL Falcon tube by centrifugation. The supernatant was stored at -30 °C for estimating extracellular lytic activity. The pellet was subsequently transferred to a 2 mL microcentrifuge tube (neoLab, Heidelberg, Germany), centrifuged again (Eppendorf 5415, 16,000 g, 5 min) and frozen at -30 °C for later extraction.

Bioassay system set-up

The photosynthetic cryptophyte *Rhodomonas salina* was used as the target species in a microalgal bioassay system (Ma et al. 2009; Tillmann et al. 2009) to quantify lytic activity of either *A. ostenfeldii* whole cultures, cell extracts or cell-free culture supernatants. In these assays, intact *R. salina* cells were counted after 24 h incubation. The *R. salina* cultures were maintained in culture media (S = 34) under the same culture conditions as described before for the *A. ostenfeldii* cultures.

To avoid any salinity stress of the bioassay target organism *R. salina* treated with the different salinities of the supernatant, we decided to artificially adjust all supernatant samples to a salinity of 34 prior to the bioassay and to use the same *R. salina* culture acclimated to this salinity condition for all bioassay. Salinity was adjusted by adding an adequate amount of sodium chloride (pro analysi, Merck, Darmstadt, Germany).

The bioassays were set up in a total volume of 4 mL in 6 mL glass vials. Each sample contains 0.1 mL of a *R. salina* culture which was adjusted to an initial concentration of approximately 1 × 10^4 cells mL^{-1}. Samples were incubated at 15 °C for 24 h in darkness. Subsequently, 500 µL subsamples were fixed with 2 % Lugol's iodine solution in a 2 mL counting chamber. Counts of intact *R. salina* cells in a sub-area of the chamber corresponding to ca. 600 cells in the control were carried out with an inverted microscope (Zeiss Axiovert 40C, Göttingen, Germany) at maximum (400 ×) magnification. All *R. salina* counts were compared to a triplicate mean of a control (incubated with culture medium) to calculate the percent intact *R. salina*.

The bioassays were performed as series of several dilutions of culture supernatants, *A. ostenfeldii* whole cultures or cell extracts with an increasing concentration to allow dose-response calculation. Plotting percent intact *R. salina* against the logarithmic-scaled *A. ostenfeldii* concentration allowed calculating EC_{50} values, i.e. the *A. ostenfeldii* cell concentration yielding a 50 % mortality of *R. salina*.

Calculations were carried out by Statistica (StatSoft, Tulsa, USA) using a non-linear fit:

$$N_{final} = \frac{N_{control}}{1 + \left(\left(\frac{x}{EC_{50}}\right)^{h}\right)}$$

where N_{final} is the final target cell concentration, $N_{control}$ is the final target cell concentration in control samples, x is the log-transformed *A. ostenfeldii* concentration and EC_{50} and h are fit parameters. Results are presented as EC_{50} (cells ml^{-1}) within the 95 % confidence interval.

When performing a bioassay system with *A. ostenfeldii* cell extracts, a respective *A. ostenfeldii* cell concentration of the dilution in the bioassay sample was calculated as:

$$n = \frac{c_{A.ostenfeldii} * v_{sample}}{v_{extraction}} * \frac{v_{extract}}{v_{bioassay}}$$

where n is the corresponding *A. ostenfeldii* cell count in the assay, $c_{A.ostenfeldii}$ the cell concentration in the original *A. ostenfeldii* culture, v_{sample} the volume of the original *A. ostenfeldii* culture, $v_{extraction}$ the extraction volume, $v_{extract}$ the concentration of the extract in the assay and $v_{bioassay}$ the total volume of the bioassay.

Specific cell growth rate

For growth rate estimates the cell density was measured every second day by microscopic counting. Cell counts were performed with an inverted microscope (Zeiss Axiovert 40C, Göttingen, Germany) at 200 × magnification in 2 mL counting chambers containing 30 - 1000 µL of the sample fixed with Lugol's iodine solution (2 % final concentration). The specific growth rate (µ, unit: day^{-1}) for each replicate was calculated by exponential regression of the cell density of 8 - 10 data points in exponential growth. Growth curves for each clonal isolate were plotted from mean cell density of the three replicates.

Cell size estimates

500 µL samples for cell size measurement were fixed with 2 % Lugol's iodine solution in a 2 mL counting chamber. Measurement was carried out with an inverted microscope (Axiovert 200 M, Zeiss, Göttingen, Germany) at 200 × magnification. The mean cell size (width and lengths in µm) was calculated from a total of 30 cell measurements of cell width and cell length using the AxioVision software (version 4.9.1.0, Zeiss, Göttingen, Germany).

4.2.3 Experiment 3: Mass production of A. ostenfeldii *and crude extract preparation for future work on a new and yet undescribed spirolide*

Origin of culture

Based on results of the toxin screening the *A. ostenfeldii* isolate OKNL48 was used for this task as this isolate contained the highest amount of the new spirolide (Chapter 5.3). As part of a collection of 68 isolates the strain was originally isolated after a blooming event in 2013 in the Ouwerkerkse Kreek (51°62' N, 3°99' E) in The Netherlands.

Mass cultivation of algae

For structural elucidation and toxicity testing a relatively large amount of purified compound is needed. Based on previous work on cyclic imine toxins it was concluded that a minimum amount of 100 µg as raw extract should be collected. To achieve this goal, consecutive batch cultures of about 20 L each were grown and extracted over a period of several months until the desired amount of compound was reached.

Culture conditions of the isolate

The isolate was cultivated under controlled conditions with artificial cool-white fluorescent light at a photon flux density of 80 - 100 µmol $m^{-2}s^{-1}$ on a 16:8 h light–dark photocycle. The ambient air temperature was 15 °C.

The isolate was grown maintained in 2 L Erlenmeyer flasks or 5 L Schott flasks containing half-strength K-medium (Keller et al. 1987) with a salinity of 16. The preparation of the culture medium is described in Chapter 4.1.2.

Extraction of spirolides using Solid Phase Adsorption Toxin Tracking (SPATT)

In this experiment the extraction of intracellular spirolides was carried out by Solid Phase Adsorption Toxin Tracking (SPATT). For extraction, 1.5 g/L of HP-20 resins (Diaion, Supelco, Bellefonte, USA) were pre-conditioned with methanol overnight. Afterward the resins were filtered and dried at the air. Subsequently the pre-treated resins were transferred with Milli-Q water (Millipore GmbH, Eschborn, Germany) into the algal culture and gently mixed. An air-pump was used for a soft turbulent flow in the Erlenmeyer flask. Adding 70 mL/L acetone (HPLC grade, AppliChem, Darmstadt, Germany) to the culture led to cell lysis and to a release of intracellular toxins. The toxin adsorption to the resins was done overnight. Afterwards the toxin-loaded resins were filtered using a 20 µm nylon mesh and washed with Milli-Q water. Subsequently the dried resins were transferred in 10 mL of methanol and incubated overnight. For toxin elution a chromatographic separation column (L: 24 cm, d: 1 cm, with frit) was prepared with 1 g of quartz sand (pro analysi, Merck, Darmstadt, Germany). The resin-methanol suspension was loaded onto the column by adding additional 5 mL of methanol. Air bubbles were removed carefully by knocking. The resins in the column were covered by another 1 g of quartz sand. The methanol fraction was briskly desisted from the column until it rinsed into the top layer of the quartz sand. Another volume of 15 mL of methanol was loaded onto the column and slowly eluted (approx. 10 drops/min.). The complete methanol fraction was collected in a Falcon tube. For measuring the cyclic imine toxin concentration, 1 mL of the extract was transferred to a glass vial (Agilent Technologies, Waldbronn, Germany). This subsample was analyzed and quantified with LC-MS following the description in chapter 4.1.3.

Finally, the extract was evaporated with a rotatory evaporator (200 mbar, 50 °C, approx. 1 h, Rotavapor Laborota 4002, Heidolph Instruments, Schwabach, Germany) and adjusted to a final volume of 1-3 mL.

All crude extracts were collected in glass vials and frozen at -20 °C for later treatment.

The efficiency of the described cyclic imine toxin extraction procedure for large-scaled mass cultures was determined in a pretest. Using one sample culture (1.6 L, 3,784 cells mL^{-1}) the extraction procedure was successional repeated for three times. All three methanol extracts were collected separately and analyzed with LC-MS.

Purification and concentration of crude extracts

The collected crude extracts which contain the yet undescribed spirolide were merged and evaporated to dryness with a rotatory evaporator (75 mbar, 50 °C, approx. 1 h, Rotavapor Laborota 4002, Heidolph Instruments, Schwabach, Germany). The remainder was resolved in 30 mL Milli-Q water and transferred to a Falcon tube.

To remove salt and solid residues from the sample a purification step with an analytical Solid-Phase-Extraction column was performed: A C_{18} cartridge (Supelclean LC-18 tubes 6 mL, Supelco, Bellefonte, USA) was conditioned in a Visiprep Solid-Phase-Extraction vacuum chamber (Supelco, Bellefonte, USA) with 2 mL of methanol and 5 mL of distilled water. The eluate was discarded. Then the complete sampled was loaded onto the cartridge. After flow through, the cartridge was washed with 5 mL of distilled water. The eluate was discarded again. The elution of the cyclic imine toxins was done with 30 mL methanol.

A subsample of the eluate was taken to quantify the final toxin concentration in the sample. The subsample was diluted (1:100 v/v) and analyzed with LC-MS (Chapter 4.1.3).

After elution, the extract was evaporated with a rotary evaporator to an accurate volume of 1.8 mL. The extract was transferred to a glass vial (Agilent Technologies, Waldbronn, Germany) and dried under a nitrogen gas flow.

Further treatment

Further sample treatment, i.e. further sample clean-up and subsequent purification of the yet undescribed spirolide is not part of this thesis and will be done by Carmela Dell'Aversano (University of Naples Federico II, Napoli, Italy) who will proceed with structural elucidation.

5 Results

5.1 Experiment 1: Toxin screening of 68 isolates from Ouwerkerkse Kreek

The first objective was to determine the PSP- and cyclic imine toxin profile and the total toxin amount per cell of all 68 isolates obtained from a bloom population of *A. ostenfeldii*. Toxins were analyzed in samples harvested from cultures in exponential growth phase.

5.1.1 Cyclic imine toxins

The total cell quota of cyclic imine toxins ranged between 2.3 to 24.1 pg cell^{-1} (Figure 17). In all isolates, multiple peaks corresponding to various cyclic imine toxins were measured. In total 23 compounds were detected in the samples and six of them occurred in high relative abundances (>5 %, Table 2). All cyclic imine toxins occurred with a very high variability among the isolates (Figure 18).

Over all, gymnodimine A was the most dominant cyclic imine toxin. The mean toxin content of gymnodimine A was 4.1 pg cell^{-1}, which was almost 47 % of the total cyclic imine toxin content per cell. Only in four isolates the gymnodimine A content was less than 10 % of the total cyclic imine toxin content per cell. In one isolate (OKNL24) no gymnodimine A was detected (confirmed in a second independent analysis). The derivative 12-methyl gymnodimine A occurred much lesser in amount (0.56 ± 0.63 pg cell^{-1}, which was 6.5 % of the total cyclic imine toxin content) but in average as the third-most abundant cyclic imine toxin. 14 isolates contained no or less than 1 % of 12-methyl gymnodimine A per cell (Figure 18).

The 13-desmethyl spirolide C derivative, which was also used as analytical standard, occurred as the most abundant spirolide and was the second-most abundant cyclic imine toxin within all isolates (2.75 pg ± 1.22 cell^{-1} or 31.7 % of all cyclic imine toxins per cell). 13-desmetyl spirolide D was found to be the fourth leading cyclic imine toxin (0.63 ± 0.3 pg cell^{-1}). Two unknown cyclic imine toxins (transitions 674-164 m/z and 696-164 m/z, respectively) also occurred in high abundances within the isolates (Table 2). Whereas the former one occurred in all isolates with a high mean content per cell (0.41 ± 0.18 pg cell^{-1}), the latter one only occurred in three isolates (OKNL35, 48, 61) with a notable high toxin concentration. Because of this results, the isolate OKNL48 was selected for the toxin accumulation experiment of the yet undescribed spirolide (transition: 696-164 m/z) in experiment 3.

Two compounds with the mass transitions m/z 766-164 and 784-164, which are characteristic for pinnatoxin E and F (Table 2) occurred in 42 isolates. The mean intracellular amount the first compounds was about 9.6 ± 18.4 fg cell^{-1}, which is 1 % of the total cyclic imine content. For the second compound, the mean value was determined as 0.3 ± 0.7 fg cell^{-1} (> 0.1 % of total cyclic imine toxins per cell).

Table 2: Minimum, maximum and mean cyclic imine toxin cell quotas of all 68 isolates. Concentrations are in fg cell^{-1}. Transitions of cyclic imine toxins are mentioned in m/z. (ND = not detectable)

Transition	Toxin	Maximum	Mean (%)	SD (%)	Minimum
508-490	**GYM-A**	**18046.5**	**4100.2 (47.2)**	**3939.4 (96.1)**	**ND**
522-504	**12-me GYM -A**	**2339.9**	**560.8 (6.5)**	**629.4 (112.2)**	**ND**
640-164	undescribed	14.0	1.9 (0.02)	2.3 (155.2)	ND
644-164	undescribed	6.4	0.3 (0.00)	0.8 (278.6)	ND
650-164	H	38.3	3.0 (0.03)	7.2 (238.8)	ND
658-164	undescribed	54.2	12.9 (0.15)	9.1 (70.6)	1.4
674-164	**undescribed**	**1051.5**	**408.3 (4.7)**	**179.1 (43.8)**	**111.2**
678-164	13,19-didesme C	398.9	16.0 (0.18)	61.2 (382.0)	ND
678-150	undescribed	16.1	4.6 (0.05)	3.9 (83.8)	ND
692-164	**13-desme C**	**7359.3**	**2752.2 (31.7)**	**1224.3 (44.5)**	**765.1**
692-150	A, undescribed	33.8	10.0 (0.12)	6.7 (67.3)	ND
694-164	**13-desme D**	**1900.7**	**627.8 (7.22)**	**300.7 (47.9)**	**160.6**
694-150	B	10.4	1.9 (0.02)	1.7 (88.2)	ND
696-164	**undescribed**	**1093.0**	**54.7 (0.63)**	**199.9 (365.6)**	**1.6**
698-164	undescribed	157.6	30.3 (0.35)	37.7 (124.5)	ND
706-164	C, 20-me G	2.9	0.1 (0.00)	0.4 (661.2)	ND
708-164	D	14.7	3.9 (0.04)	3.9 (100.0)	ND
710-164	undescribed	57.6	21.1 (0.24)	13.9 (65.7)	0.6
710-150	undescribed	2.9	0.3 (0.00)	0.5 (148.2)	ND
720-164	undescribed	178.8	50.2 (0.58)	45.4 (90.5)	ND
722-164	undescribed	60.1	19.6 (0.23)	17.8 (90.6)	ND
766-164	pinnatoxin F	88.4	9.6 (0.11)	18.4 (191.1)	ND
784-164	pinnatoxin E	5.8	0.3 (0.00)	0.7 (214.4)	ND

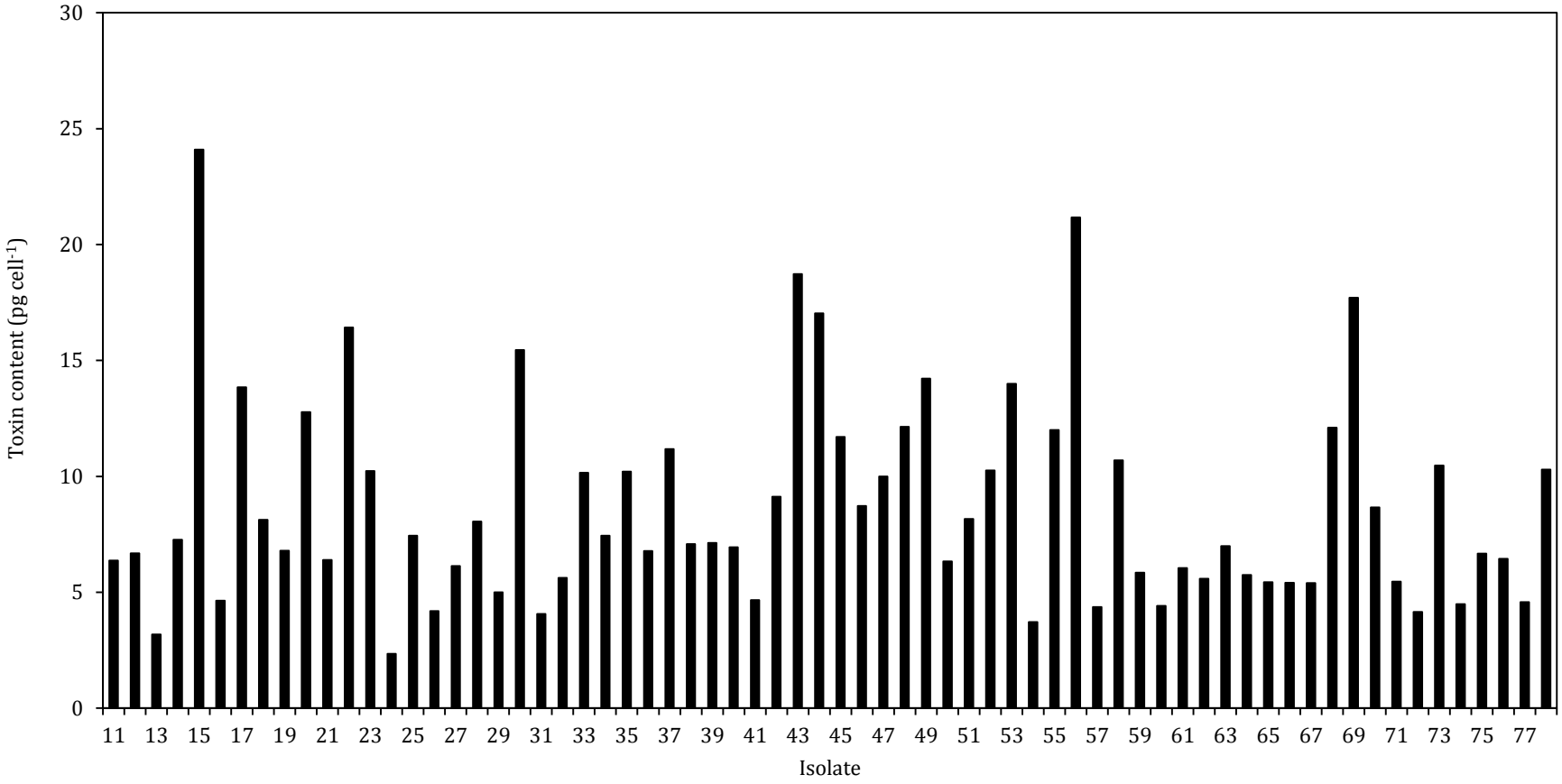

Figure 17: Total content of cyclic imine toxins in all isolates (OKNL11-78).

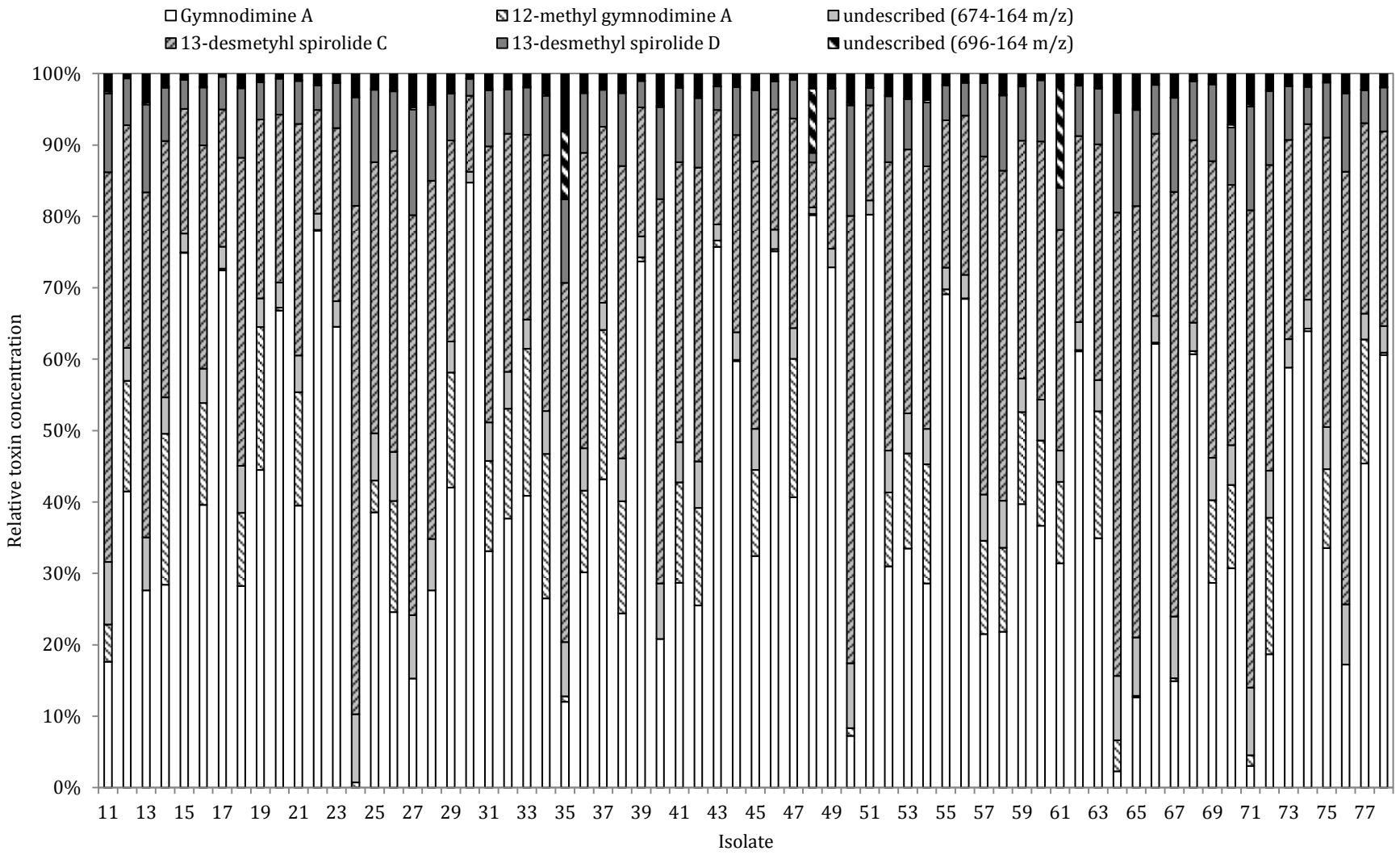

Figure 18: Cyclic imine toxins profile of all 68 isolates. Toxin concentrations are in relation to the total amount of cyclic imine toxins per cell. "Minor components" include all cyclic imine toxins except the six most abundant compounds.

The six most abundant cyclic imine toxins were also checked for significant correlations between the occurrences of single compounds. The correlation coefficients of these analyses are presented in Table 3.

A significant correlation between gymnodimine A and 12-methyl gymnodimine A was calculated for all isolates which contain a minimum concentration of 0.2 pg cell^{-1} of 12-methyl gymnodimine A (r = 0.83, n = 35, p-value = 8.71e10).

Table 3: Correlation coefficients of the six most frequent cyclic imine toxins. For two unknown spirolides only the corresponding mass transition are mentioned in m/z.

	12-me GYM-A	674-164	13-desme C	13-desme D	696-164
GYM-A	0.83*	0.11	0.10	0.11	0.03
12-me GYM-A	-	0.22	0.20	0.17	-0.10
674-164	-	-	0.99*	0.96*	-0.01
13-desme C	-	-	-	0.96*	-0.02
13-desme D	-	-	-	-	-0.03

* = significant correlation

The results of the student's t-tests indicated that there was no observable significant correlation between the tested gymnodimines and spirolides. Likewise there was no correlation between any of the six tested cyclic imine toxin with the unknown spirolide with the mass transition 696-164 m/z.

Furthermore, there were highly significant correlations between 13-desmethyl spirolide C, 13-desmethyl spirolide D and another unknown spirolide (transition: 674-164 m/z).

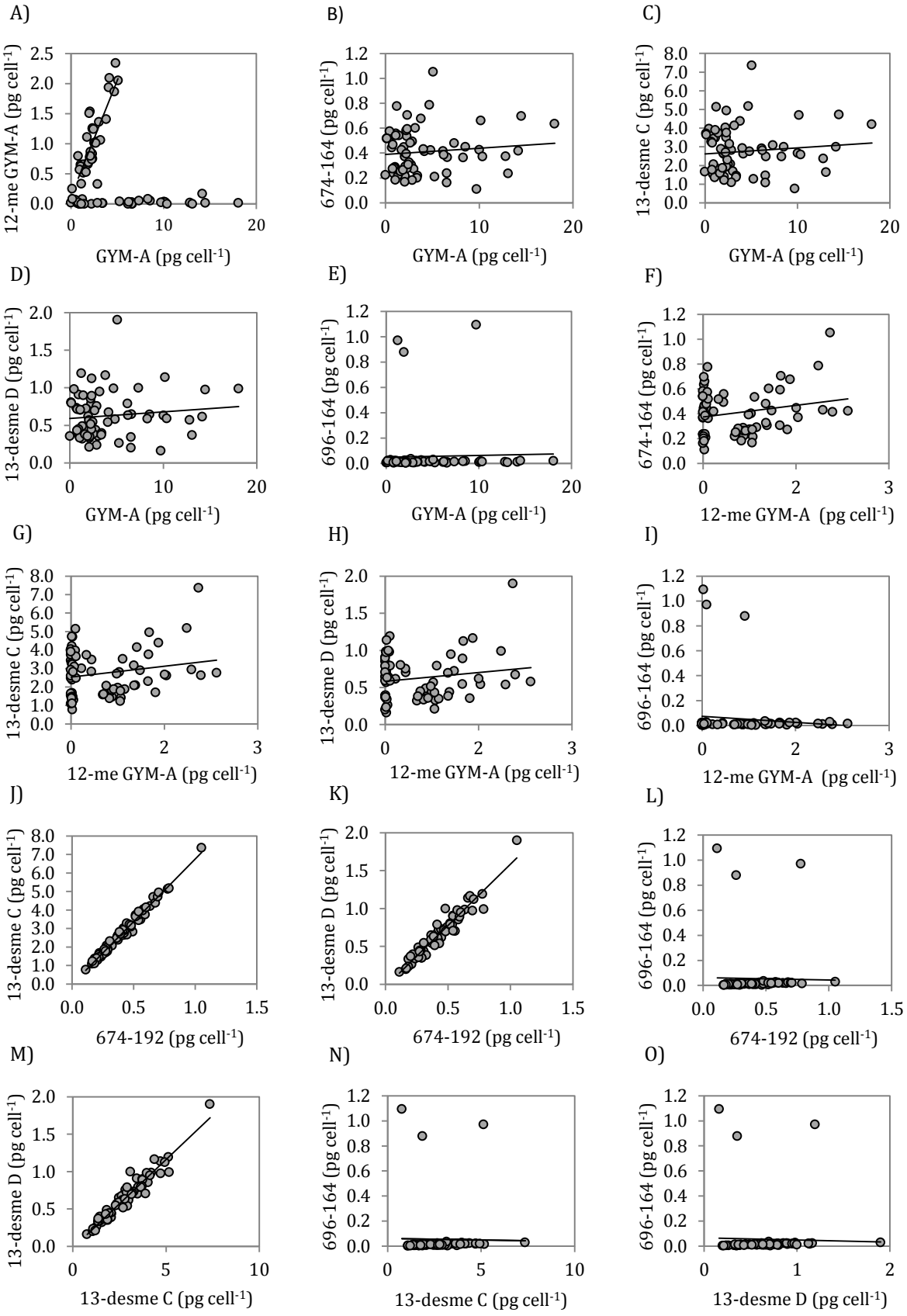

Figure 19: Correlations of the occurrence of the six most abundant cyclic imine toxins. Transitions of unknown compounds are in m/z. (n = 68) Each dot represents one of the 68 isolates.

5.1.2 PSP-toxins

LC-FD analyses were performed to check the presence of PSP-toxins in The Netherlands bloom population of *A. ostenfeldii*. The chromatograms (not shown) indicated that all isolates had similar PSP-profiles. The PSP-toxin analysis was carried out using an analytic standard solution containing different PSP-toxins (C1/C2, GTX 1-5, dcGTX2-3, STX, dcSTX and NeoSTX). From all known PSP-toxins, only C1/C2, dcGTX2-3, GTX2/3, GTX5 and STX were found in the samples. The total PSP-toxin content ranged from 11.34 pg cell^{-1} to 88.20 pg cell^{-1} (Figure 20). The total PSP content of all isolates on average was 45.73 ± 17.79 pg cell^{-1}. The PSP-toxin profile was very consistent over all isolates. The relative mean abundances of PSP-toxins per cell were 82.3 % for C1/C2, 0.1 % for dcGTX2/3, 1.0 % for GTX5, 12.6 % for GTX2/3 and 3.6 % for STX (Table 4; Figure 21).

Only for one isolate (OKNL68) the relative contribution of the different PSP compounds was distinctly different. OKNL68 contained 44.6 % of C1/C2, which was much lower than the average of all isolates. Consequently, GTX2/3 in this isolate occurred in a high abundance of 42.1 %. STX (10.2 %) and GTX5 (3.1 %) were slightly increased. These results have been verified by a second independent measurement of isolate OKNL68.

Table 4: Cell quotas for PSP-toxins expressed as maximum, minimum and mean values calculated from all 68 isolates. All toxin concentrations are in pg cell^{-1}. (ND = not detectable)

	Maximum	Mean (%)	SD (%)	Minimum
C1/C2	74.4	37.9 (82.3)	15.08 (39.8)	7.2
dcGTX 2/3	0.1	0.0 (0.1)	0.01 (0.04)	ND
GTX5	0.9	0.4 (1.0)	0.20 (0.5)	ND
GTX2/3	12.8	5.8 (12.6)	2.68 (7.1)	1.5
STX	6.8	1.7 (3.6)	1.05 (2.8)	0.4

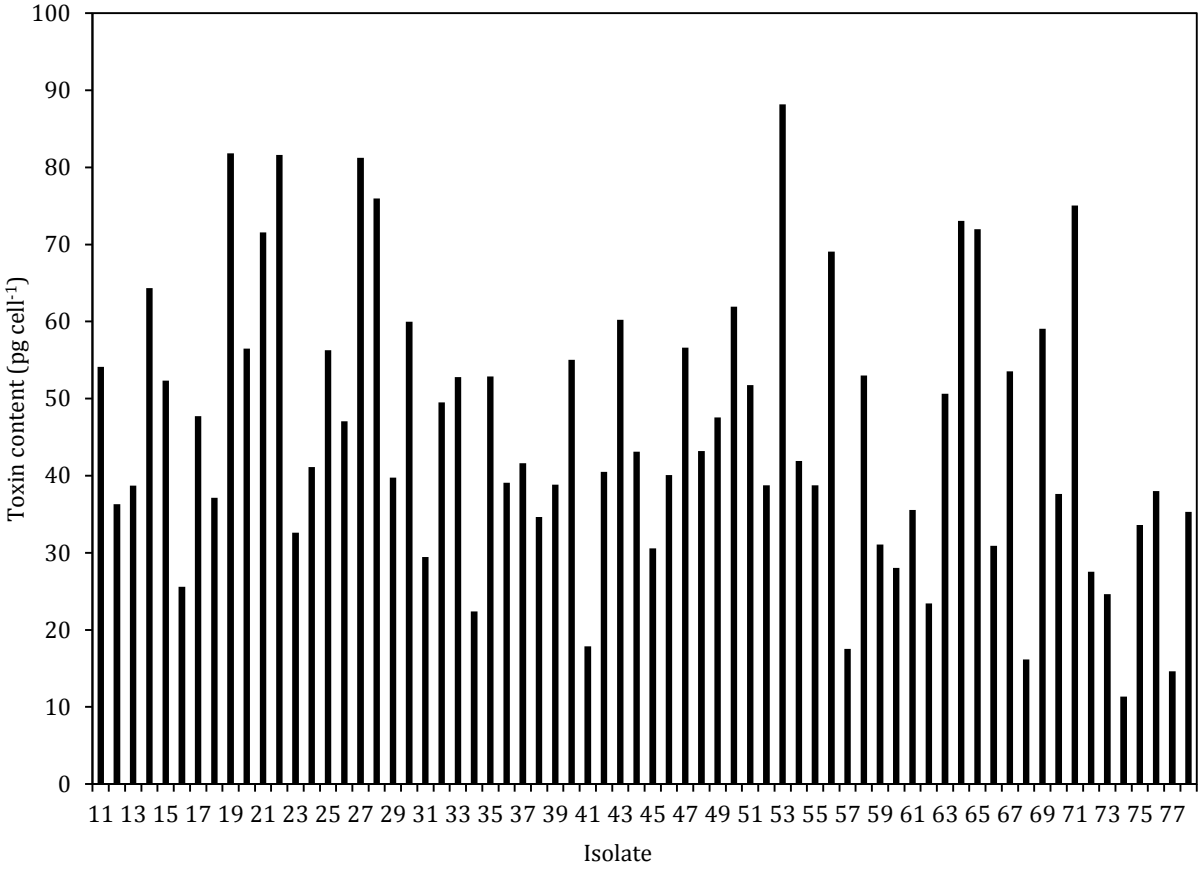

Figure 20: Total content of PSP-toxins in all isolates (OKNL11-78).

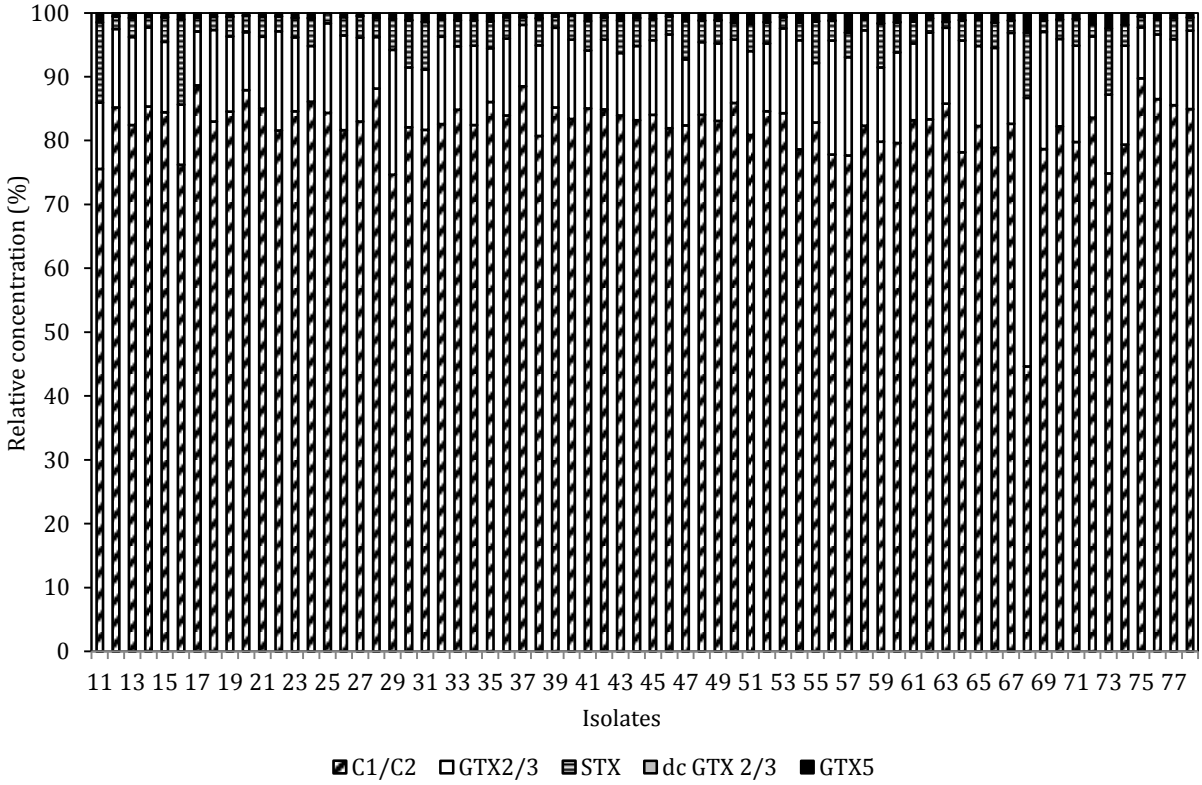

Figure 21: Relative distribution and outlier (OKNL68) of PSP-toxins in all isolates.

Correlation coefficients of measured PSP-toxins were tested with a student's t-test. The t-tests indicated that there are significant correlations between all PSP-toxins found in the samples. A very high correlation was determined between the C1/C2 toxin and GTX2/3 and between C1/C2 and dcGTX2/3. Furthermore, the occurrence of dcGTX2/3 and GTX2/3 was also highly correlated. Saxitoxin (STX) showed the highest correlation to GTX5. All results are presented in Table 5.

Table 5: Correlation coefficients of the measured PSP-toxins in all isolates.

	dcGTX2/3	GTX5	GTX2/3	STX
C1/C2	0.68*	0.42*	0.79*	0.37*
dcGTX2/3	-	0.31*	0.48*	0.23*
GTX5	-	-	0.45*	0.51*
GTX2/3	-	-	-	0.26*

* = significant correlation ($P < 0.05$)

For the data set of all isolates, cell quota of PSP-toxins and cyclic imine toxins were significantly correlated ($r = 0.31$, $n = 68$, p-value = 0.016) with PSP-toxins being about six times more abundant than the cyclic imine toxin content (compare Figure 17, 20).

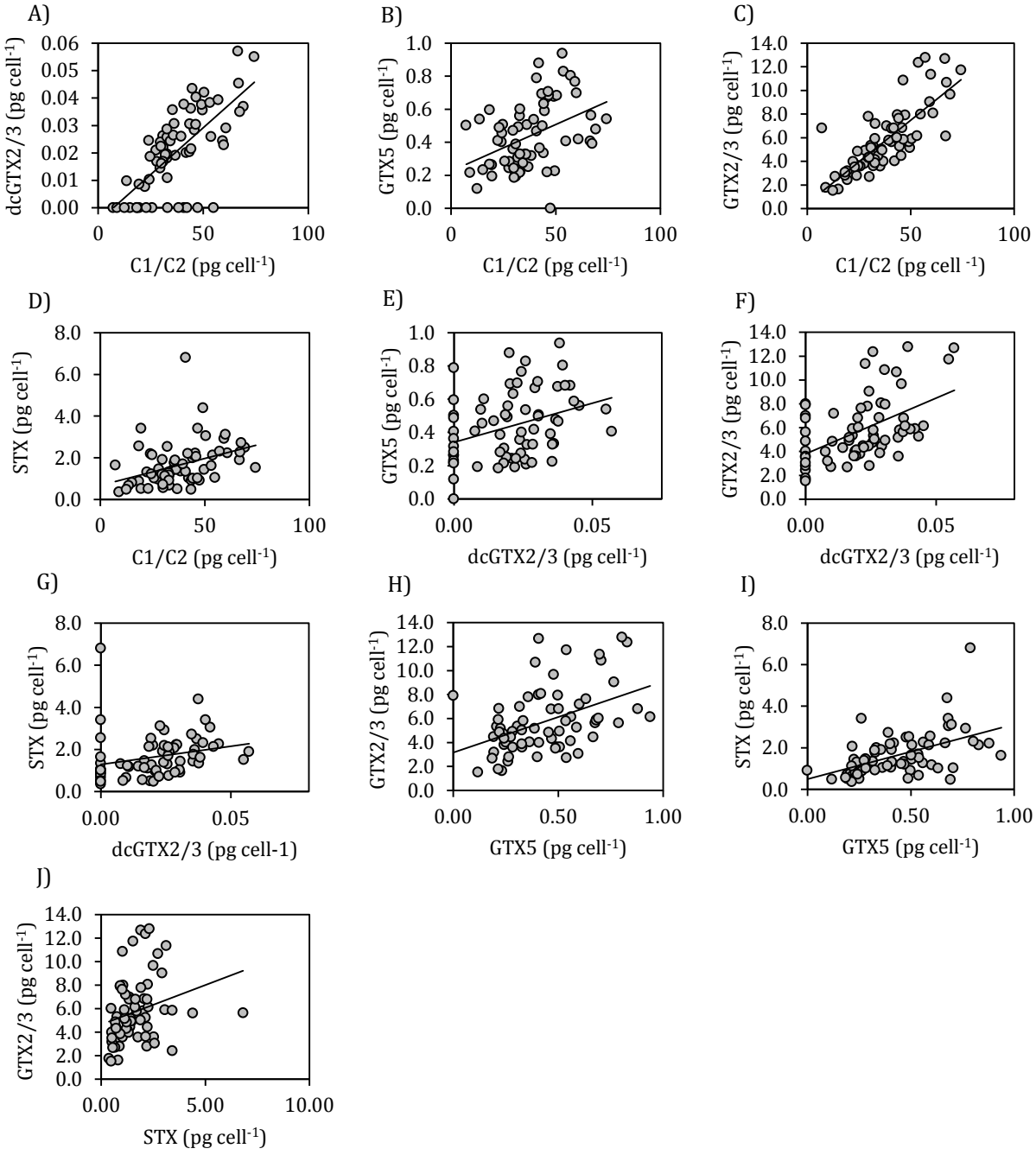

Figure 22: Correlations between PSP-toxins in the isolates. Each dot represents one of the 68 isolates.

5.2 Experiment 2: Salinity tolerance of a pre-selected isolate

Because of the results of the toxin screening for PSP- and cyclic imine toxins the isolate OKNL21 was found to be representative for the population in terms of toxin composition and cell quota and thus was selected for the salinity treatment experiment. The response to different salinity treatments were measured with respect to the growth rate, the lytic capacity, the intracellular PSP-toxin content, the intra- and extracellular cyclic imine toxin content, the particulate carbon, nitrogen and phosphorus content, the dissolved content of carbon and nitrogen, and the cell size.

5.2.1 Growth rate

Growth curves of cultures at S = 4.5 to 34 are plotted in Figure 23. At S = 3, no experimental cultures could be started because the inoculum culture did not survive in S = 3 medium. No significant growth was observable in the experimental culture at S = 4.5, even though growth was observed in the inoculum culture. For salinities 6, 16 and 34 a lag phase of 1-3 day was observed after starting the experimental culture with pre-acclimated cells.

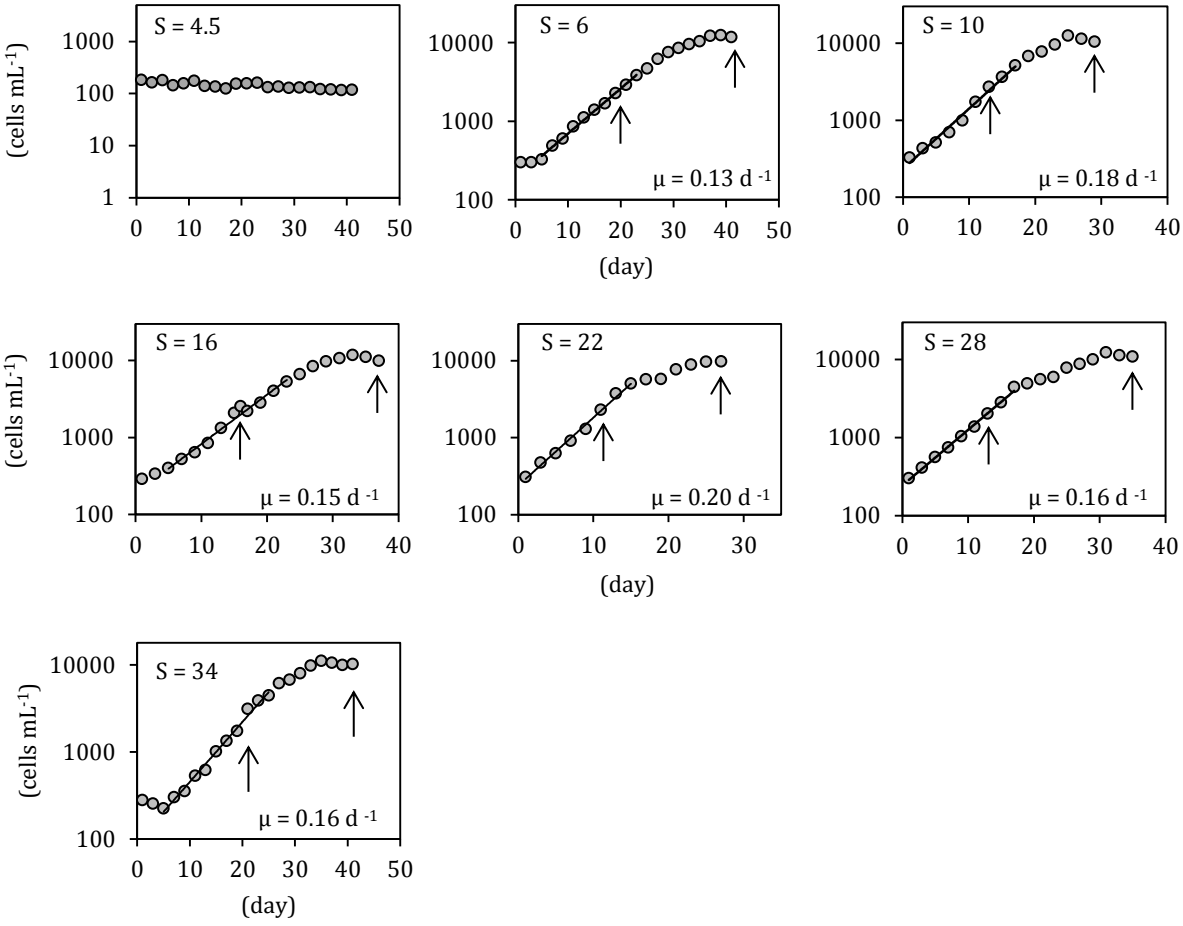

Figure 23: Growth curves of culture at S = 4.5 to 34. The data points represent mean cell counts of three replicates (n = 3, ± 1 SD, error bars are not visible as they are smaller than the dots). Values from time points connected by a trend line were used to calculate exponential growth rate. Arrows indicate sampling points.

The specific growth rate (μ) ranged between 0.13 and 0.20 d^{-1} and was significantly different among salinities (ANOVA, F = 1678, P < 0.0001). Tukey's HSD test indicated the presence of one homogenous subgroup of cultures at salinities 16, 28 and 34 (ANOVA, Tukey's HSD test, P < 0.05) (Figure 24). Maximum cell concentration at stationary phase was similar for salinities 6 to 34, ranging between 9 × 10^3 cells mL^{-1} to 12 × 10^3 cells mL^{-1}.

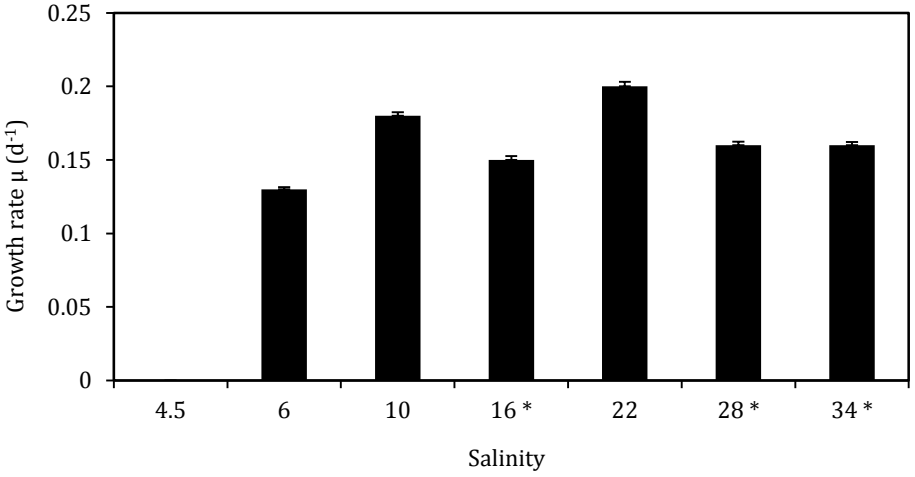

Figure 24: Mean growth rates (n=3, ± 1 SD) of *A. ostenfeldii* cultures at S = 4.5 to 34. Asterisks indicate classification of cultures forming a homogenous group (ANOVA, Tukey's HSD test, P < 0.05).

5.2.2 Quantification of the lytic capacity

Comparison of culture fractions

For one of the experimental cultures (OKNL21, grown at a salinity of 16 and sampled at exponential phase) a detailed comparison of three fractions (whole culture, supernatant, and cell extract) was performed using high resolution dose response curves (Figure 25). The EC_{50} value for the whole cell culture was 659 ± 57 cells mL^{-1}, for the culture supernatant it was 983 ± 85 cells mL^{-1} and for the cell extract fraction it is 4737 ± 113 cells mL^{-1}. EC_{50} values of the cell extract fraction were significantly different to the whole cell culture fraction and the supernatant fraction (ANOVA, Tukey's HSD, F= 2192, P < 0.0001). In comparison, the whole cell culture fraction and supernatant fraction are not significantly different within the 95 % confidence interval (P > 0.05).

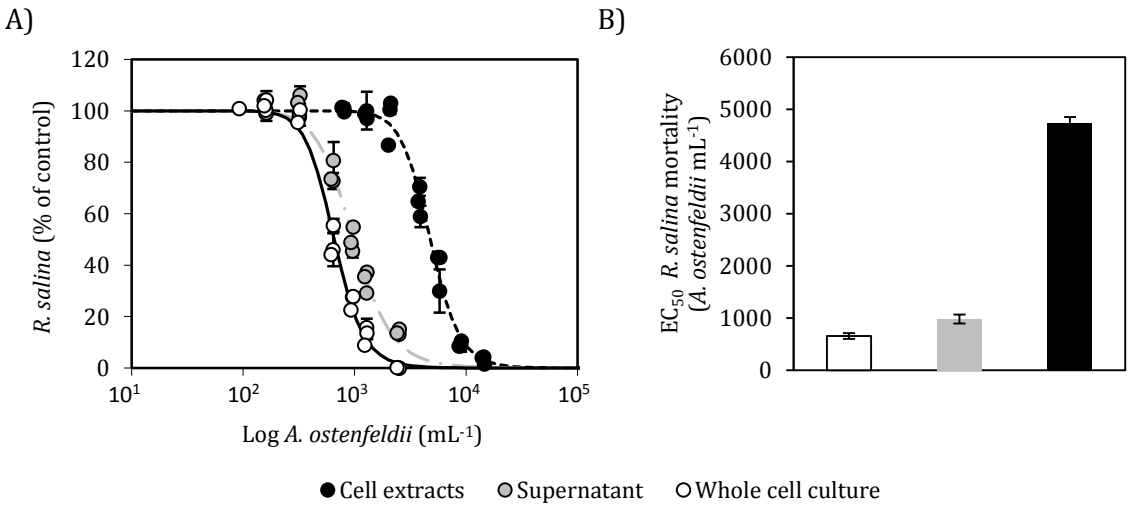

Figure 25: A) Dose-response curve describing lytic capacity of cell extracts, supernatant and whole cell culture of an *A. ostenfeldii* culture maintained at S = 16 in exponential growth phase as quantified with the *R. salina* bioassay. The graph shows the concentration of *R. salina* after 24 h incubation (as % of control) as a log-transformed function of triplicate cultures. White, grey, and black dots represent triplicate cultures with each data point representing the mean and range of two technical replicates. **B)** EC_{50} values for all three fractions. The EC_{50} value is defined as the *A. ostenfeldii* cell concentration causing lysis of 50 % of target *R. salina* cells.

Comparison of salinity treatments

All samples collected from different salinity treatments caused cell lysis of the target species *R. salina*. After 24 h incubation of the bioassays, there was a sharp decline in target species cell count with increasing *A. ostenfeldii* concentration (Figure 26, 27). For the S = 16 supernatant fraction in exponential phase, a decline of the target species cell count was observed at the highest dose only in two replicates and thus no EC_{50}-value could be calculated (Figure 26, S = 16; Exp.).

The calculated EC_{50}-values (Figure 28) of the supernatant fraction were significantly higher than EC_{50} values of the cell extract fractions (ANOVA, Tukey's HSD, $F = 11.84$, $P < 0.05$ for exponential growth phase, $P < 0.01$ for stationary growth phase).

Over all, extracellular lytic capacities in stationary phase were higher than in exponential phase; however, because of the high standard deviations, the differences were not statistically significant, (ANOVA, Tukey's HSD, $F = 11.84$, $P > 0.5$). For cell extracts, there was no difference in lytic activity between exponential and stationary phase (Figure 28).

Comparing the different salinities, EC_{50}-values of the supernatant fractions in stationary phase was almost 2-fold lower (i.e. lytic capacity was higher) in the S = 6 treatment than in the 16, 22 and 34 salinities treatments (t-test, $P < 0.001$ for stationary growth phase). Vice versa, in both growth phases the EC_{50}-values of the cell extract fractions of the S = 34 treatment was significantly lower than in the 22, 16 and 6 salinity treatments (t-test, $P < 0.001$ for both growth phases).

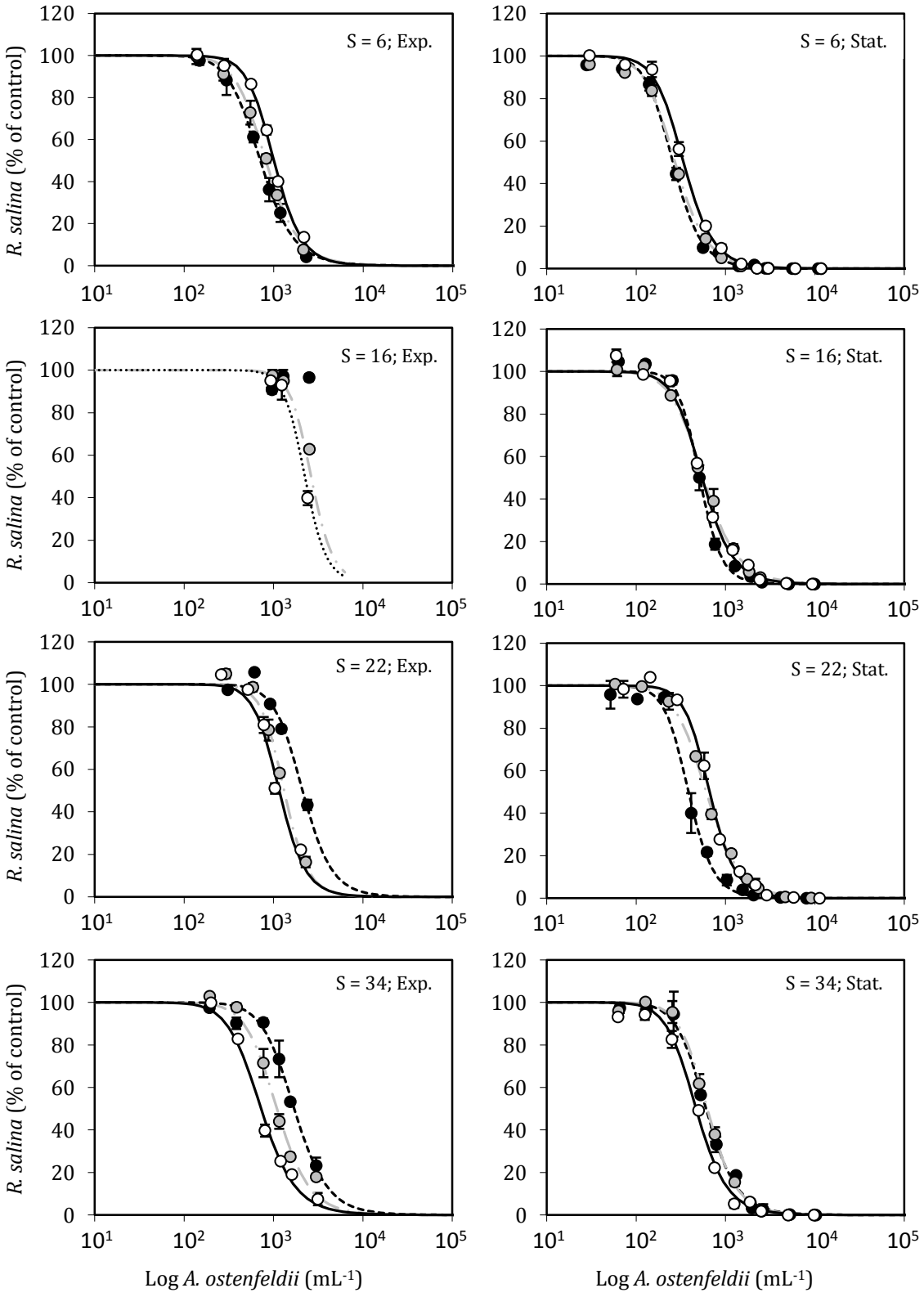

Figure 26: Dose-response curve describing lytic capacity of supernatants of different salinity treatments of *A. ostenfeldii* cultures as quantified with the *R. salina* bioassay. Each graph shows the concentration of *R. salina* after 24 h incubation (as % of control) as a log-transformed function of triplicate cultures. Each data point represents a mean (n = 2, ± 1 SD). (Exp. = Exponential, Stat. = Stationary)

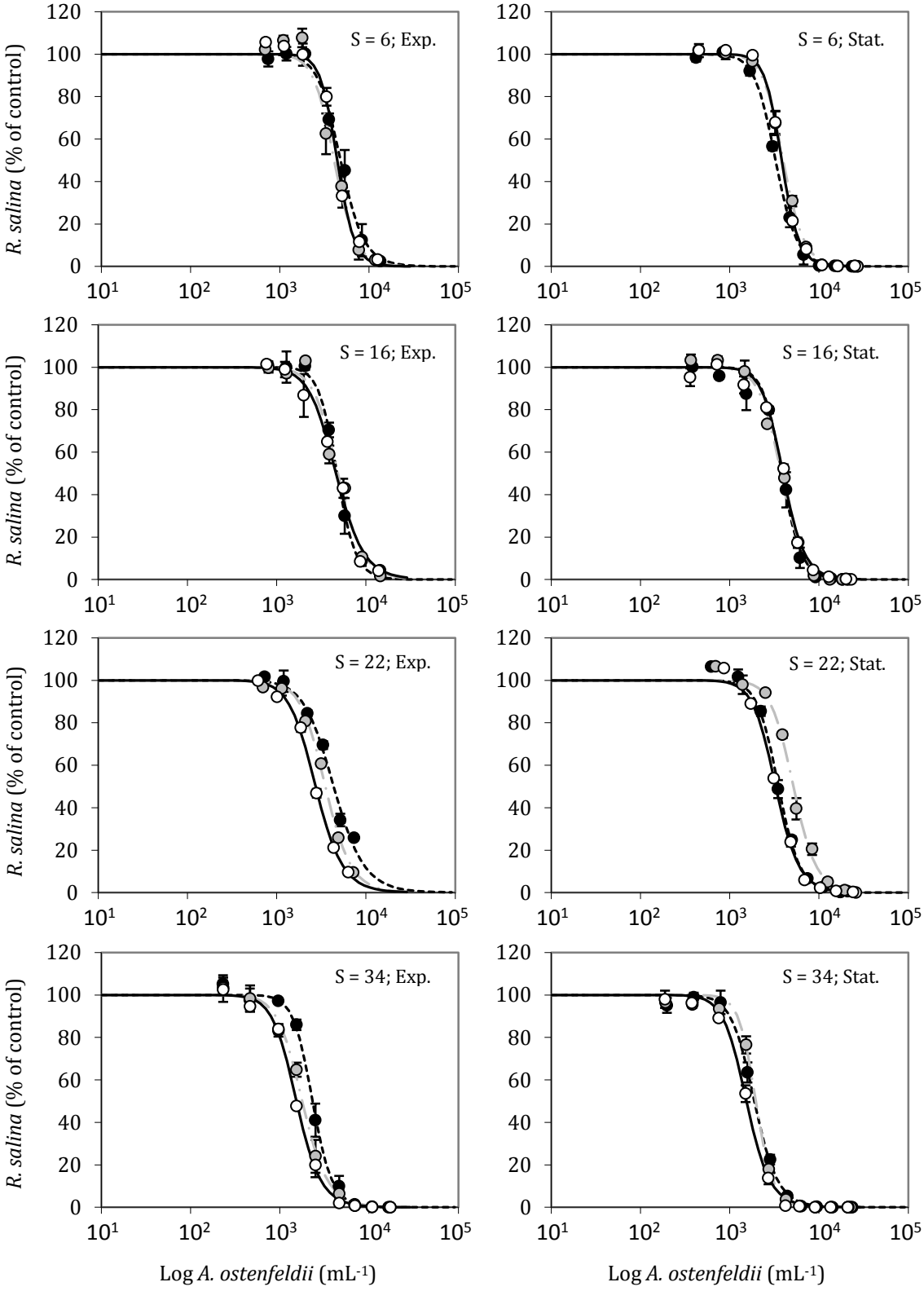

Figure 27: Dose-response curve describing lytic capacity of cell extracts of different salinity treatments of *A. ostenfeldii* cultures as quantified with the *R. salina* bioassay. Each graph shows the concentration of *R. salina* after 24 h incubation (as % of control) as a log-transformed function of triplicate cultures. Each data point represents a mean (n = 2, ± 1 SD). (Exp. = Exponential, Stat. = Stationary)

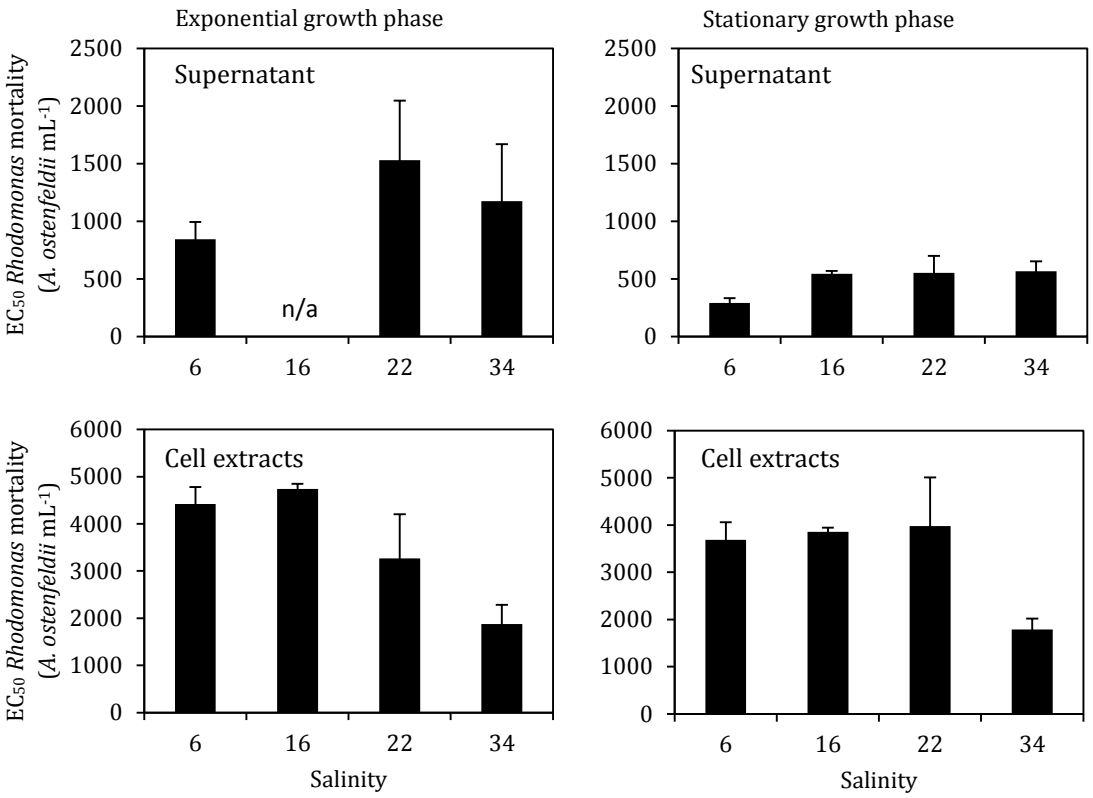

Figure 28: EC_{50}-values for the supernatant and the cell extract fractions of different salinity treatments for exponential growth phase and for stationary growth phase. No value is available for the S = 16 treatment of the supernatant fraction in exponential growth phase. Each data point represents a mean (n = 3, ± 1 SD). (n/a = not available)

5.2.3 PSP-toxins

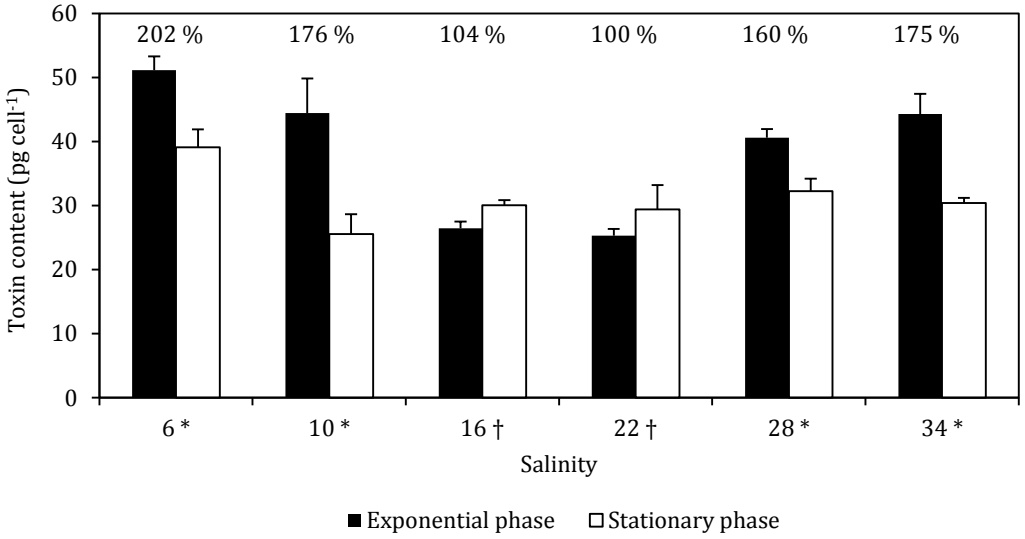

Figure 29: Total PST content of triplicate cultures (n = 3, ± 1 SD). Symbols indicate classification of cultures during exponential growth phase forming homogenous groups (ANOVA, Tukey's HSD test, P < 0.05). Changes in total PSP-content during exponential phase are also expressed as relative abundances in relation to the amount of the S = 22 treatment.

The qualitative PSP-toxin composition was similar for all salinity treatments sampled during exponential and stationary growth phase (Table 6). All cultures contained the toxins C1/C2, dcGTX3, GTX5, STX and GTX2/3 with C1/C2, STX and GTX2/3 present with highest relative abundances. Decarbamoyl toxins (dcGTX3) only occurred at very low abundances (< 0.1 %).

The total PSP-toxin cell quota ranged between 25.3 and 51.2 pg cell^{-1} in the exponential growth phase and between 25.4 and 39.1 pg cell^{-1} in the stationary growth phase (Figure 29). It is notable that the total toxin content in exponential growth phase was minimal at the salinities 16 and 22 and was higher for lower and higher ranges of salinity. This trend was not observed for stationary growth phase: in stationary phase, only PSTs in cultures maintained at S = 6 were significantly higher (t-test, $P < 0.05$) compared to all other treatments.

Table 6: PST profiles of triplicate cultures. Values are in percentages of the total PST content (n = 3, ± SD).

	Salinity	C1/C2	dc GTX 3	GTX 5	STX	GTX 2/3
Exponential Growth	6	77.8 ± 0.2	0.1 ± 0.0	1.2 ± 0.1	11.8 ± 0.1	9.2 ± 0.3
	10	79.1 ± 0.4	0.1 ± 0.0	2.7 ± 0.1	13.4 ± 0.3	4.7 ± 0.0
	16	80.6 ± 0.3	0.0 ± 0.0	0.5 ± 0.0	7.0 ± 0.2	11.9 ± 0.1
	22	82.6 ± 0.3	0.1 ± 0.0	1.8 ± 0.1	9.6 ± 0.2	6.1 ± 0.0
	28	85.5 ± 0.1	0.0 ± 0.0	0.7 ± 0.1	5.5 ± 0.1	8.3 ± 0.0
	34	85.3 ± 0.1	0.1 ± 0.0	2.1 ± 0.0	8.4 ± 0.1	4.2 ± 0.1
Stationary Growth	6	86.7 ± 0.1	0.1 ± 0.0	1.0 ± 0.2	5.3 ± 0.2	7.0 ± 0.4
	10	86.2 ± 0.2	0.1 ± 0.0	2.4 ± 0.1	7.5 ± 0.2	3.8 ± 0.1
	16	87.6 ± 0.2	0.1 ± 0.0	1.0 ± 0.1	5.0 ± 0.2	6.5 ± 0.1
	22	86.3 ± 0.2	0.1 ± 0.0	2.8 ± 0.1	6.8 ± 0.1	4.0 ± 0.1
	28	87.6 ± 0.2	0.1 ± 0.0	1.5 ± 0.1	4.7 ± 0.1	6.1 ± 0.2
	34	86.1 ± 0.1	0.1 ± 0.0	3.3 ± 0.1	6.2 ± 0.1	4.3 ± 0.1

Table 7: Correlation coefficients of the relative abundances of C1/C2, STX and GTX2/3 calculated from mean PST content of triplicate cultures.

A) Exponential Phase

	STX	GTX2/3
C1/C2	-0.93*	-0.77
STX	-	0.51

B) Stationary Phase

	STX	GTX2/3
C1/C2	-0.97*	-0.58
STX	-	0.44

* = significant correlation ($P < 0.05$)

A significant but negative correlation (Table 7; Pearson correlation, $p < 0.05$,) was present between the relative occurrence of the C1/C2 toxins and saxitoxin, both for exponential and stationary phases (Figure 30). At low salinities the relative amount of C1/C2 was lower than at high salinities. In contrast, the relative amount of saxitoxin was maximal for low

salinities and minimal for high salinities. Saxitoxin and GTX2/3 were not significantly correlated.

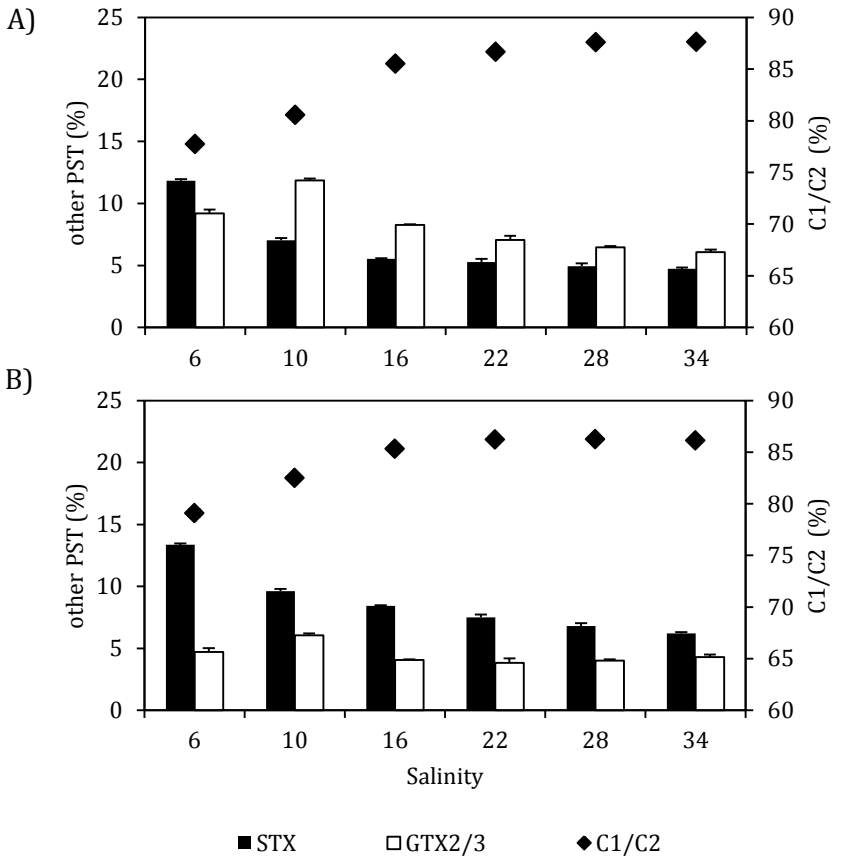

Figure 30: Mean content of STX, GTX2/3 and C1/C2 **A)** in exponential phase and **B)** in stationary phase of triplicate cultures (n = 3, ± 1 SD) in relation to the total PST content.

5.2.4 Intracellular cyclic imine toxin determination

Cyclic imine toxins were present in the cells at all salinity treatments; however, significant differences in the total toxin cell quota were observed (Figure 31). The highest concentration per cell was obtained in exponential and in stationary phase in cultures with S = 6 (12 - 14 pg cell^{-1}). The lowest amount of cyclic imine toxins was observed at a salinity of 22 (4 - 6 pg cell^{-1}). Generally in stationary phase toxin content was very similar to exponential phase. Especially in stationary phase the toxin content was very similar for cultures with salinity of 10 to 34 (5 - 6 pg cell^{-1}). For S = 4.5 only data for not growing cells are available (Figure 31 A). The most abundant toxins in exponential and stationary growth phase were gymnodimine A, 12-methyl gymnodimine A, 13-desmethyl spirolide C, 13-desmethyl spirolide D and two yet undescribed spirolides. Relative proportions of the sixth most abundant cyclic imine toxins are shown in Figure 31. Although the toxin composition was similar for all salinities. For both growth phases, an increasing concentration of 13-desmethyl spirolide C per cell was observed for increasing salinities. On the other hand, a

decreasing cell quota of gymnodimine A was evident for increasing salinities (Figure 32). A significant negative correlation between 13-desmethyl spirolide C and gymnodimine A were estimated for both growth phases (Pearson correlation, $p < 0.05$, $r = -0.91$ for exponential growth, $r = -0.96$ for stationary growth).

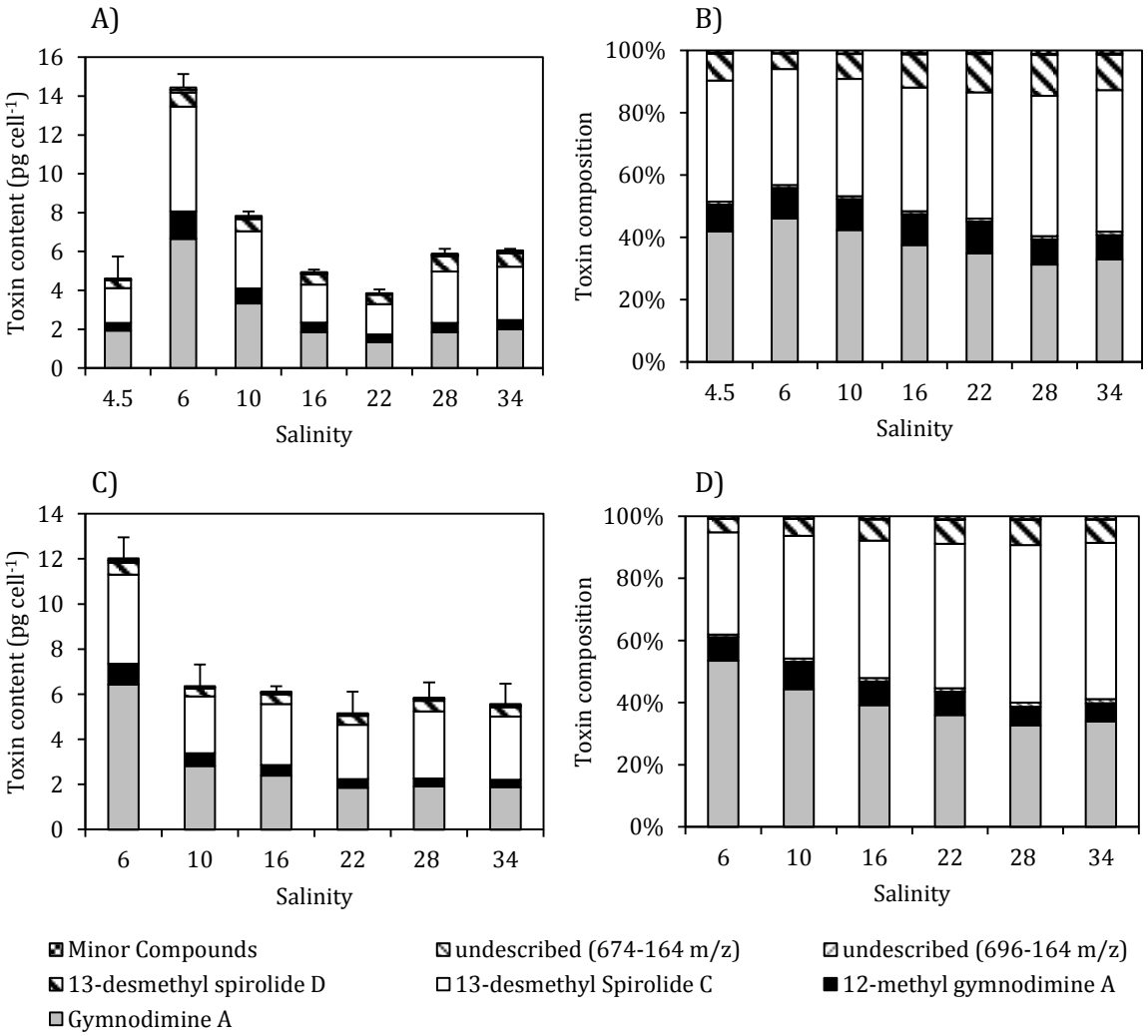

Figure 31: Intracellular cyclic imine toxins. **(A,C)** Toxin content (n = 3, ± 1 SD of total toxin content) and **(B, D)** toxin profiles of spirolides and gymnodimine in **A-B)** exponential growth phase and in **C-D)** stationary growth phase.

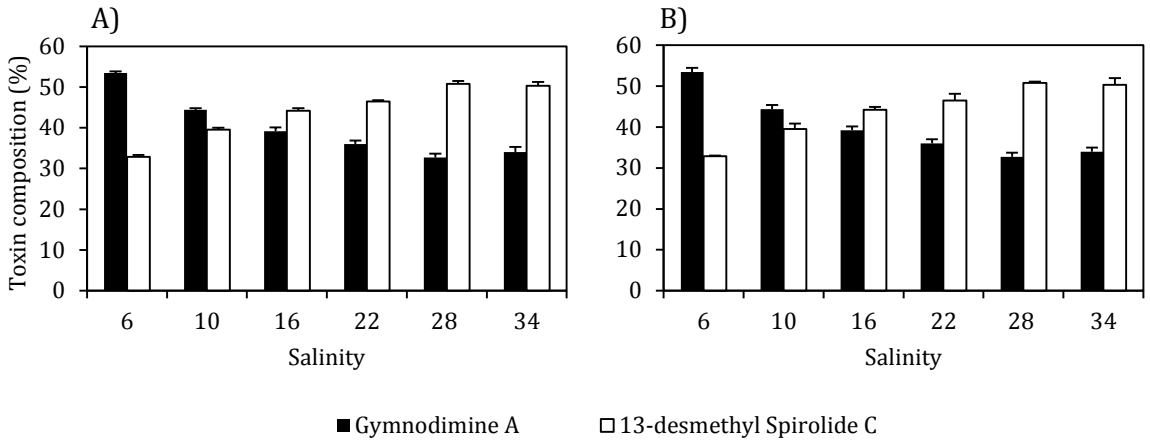

Figure 32: Relative toxin content (n = 3, ± 1 SD) of 13-desmethyl spirolide C and gymnodimine A in **A)** exponential growth phase and **B)** stationary growth phase.

5.2.5 Extracellular cyclic imine toxin determination

The efficiency of the SPE toxin extraction procedure was tested by estimating the recovery rate of cyclic imine toxins from a solution where a known amount of toxins was added. In three independent experiments, 50 mL of pure culture medium was mixed with 150 µL of cyclic imine toxin extracts with known concentrations. The mean recovery rate of all three solution using SPE purification was determined as 98.7 % (Table 8).

Table 8: Recovery rates of cyclic imine toxins using the SPE extraction method.

Replicate No.	Added toxin amount (ng)	Recovered amount in SPE eluat (ng)	Recovery rate (%)
1	147	157	106
2	136	124	91
3	149	147	99

Extracellular cyclic imine toxins were present in all salinity treatments. The extracellular toxin content was expressed as per cell equivalents and was variable among all treatments. It ranged between 175.5 ± 27.3 fg cell^{-1} (S = 28 treatment) and 644.5 ± 138.7 fg cell^{-1} (S = 10 treatment) for samples of the exponential growth phase. For stationary growth phase the extracellular amount of cyclic imine toxins was lower compared to exponential phase and ranged between 69.4 ± 0.7 (S = 10 treatment) and 177.8 ± 17.6 fg cell^{-1} (S = 6 treatment). In the exponential growth phase extracellular cyclic imine toxins were exceptionally high in the S = 6 and 10 treatments and it was exceptionally low in the stationary phase at a salinity of 10 (Figure 33 A, C).

The qualitative composition of extracellular cyclic imine toxins was similar for all salinity treatments and was almost the same for both growth phase samplings (Figure 33 B, D). The

highest percentage was found for gymnodimine A (20 - 30 %) and 13-desmethyl spirolide C (40 - 50 %). 12-methyl gymnodimine A was not detected in the S = 22 treatment and occurred only in low amounts in the exponential growth phase of the S = 28 treatment. Whereas spirolide D was present in all extracellular samples (1.5 to 4 % of the total toxin content), 13-desmethyl spirolide D could not be detected in extracellular medium.

The relative amount of the extracellular cyclic imine toxins in relation to the total cyclic imine toxin content varied between 1 to 8 % and was higher in exponential phase than in stationary phase (Table 9, 10). Furthermore there was no significant correlation between the occurrence of intra- and extracellular cyclic imine toxins (Figure 34), neither for exponential growth phase (t-test, $p > 0.05$), nor for stationary growth phase (t-test, $p > 0.05$).

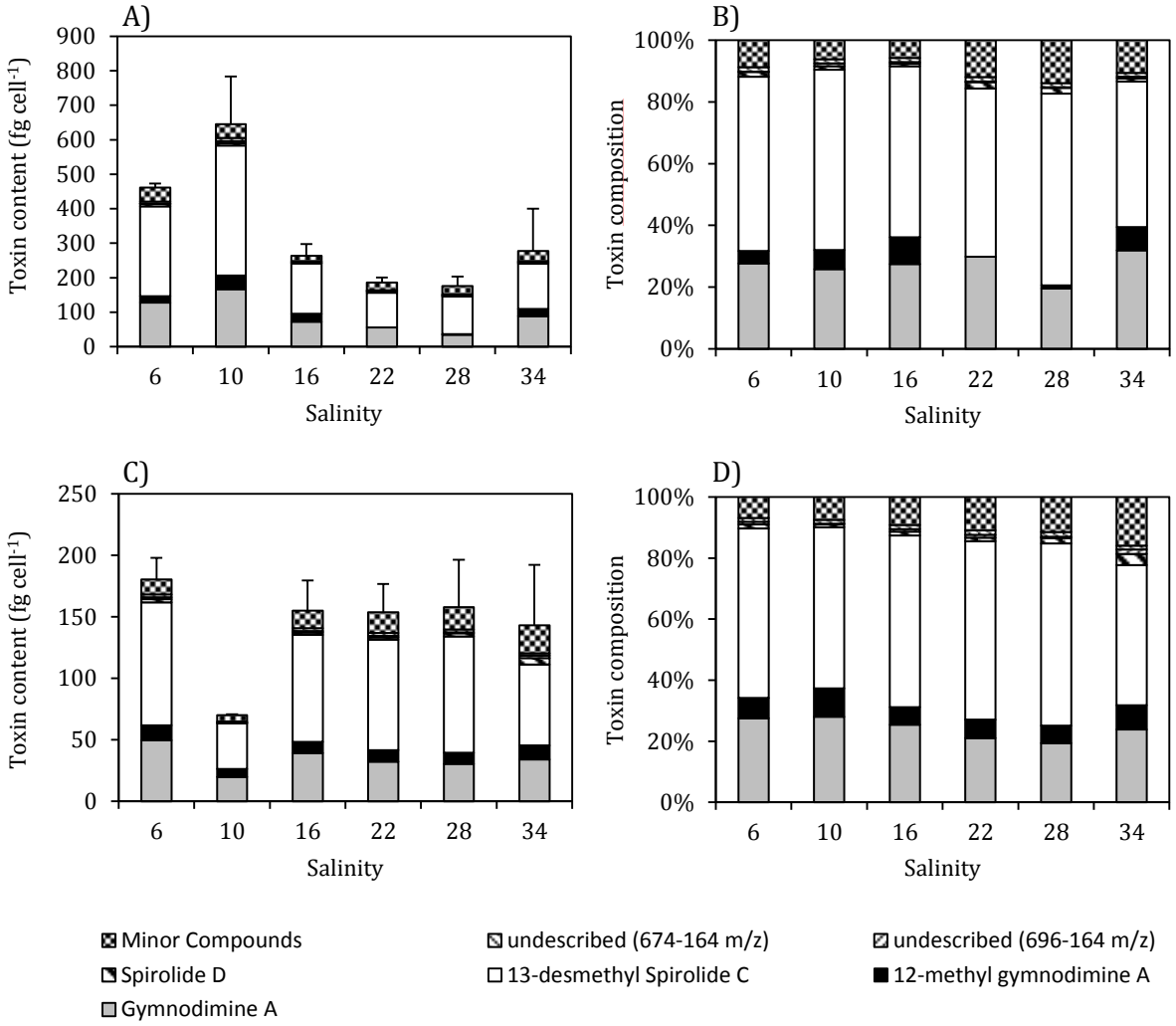

Figure 33: Extracellular cyclic imine toxins. Toxin content (n = 3, ± 1 SD of total toxin content) and toxin profiles of spirolides and gymnodimine in **A-B)** exponential growth phase and in **C-D)** stationary growth phase.

Table 9: Total amount of extracellular and intracellular cyclic imine toxins in exponential growth and stationary growth phase. (pg cell^{-1}, n = 3, ± 1 SD)

		S = 4.5	S = 6	S = 10	S = 16	S = 22	S = 28	S = 34
Extracellular toxin content	Exponential growth	n/a	0.46 ± 0.0	0.64 ± 0.1	0.26 ± 0.0	0.19 ± 0.0	0.18 ± 0.0	0.28 ± 0.1
	Stationary growth	n/a	0.18 ± 0.0	0.07 ± 0.0	0.15 ± 0.0	0.15 ± 0.0	0.16 ± 0.0	0.14 ± 0.0
Intracellular toxin content	Exponential growth	4.60 ± 1.1	14.40 ± 0.7	7.84 ± 0.2	4.93 ± 0.1	3.85 ± 0.2	5.89 ± 0.2	6.05 ± 0.1
	Stationary growth	n/a	12.04 ± 0.9	6.37 ± 0.9	6.13 ± 0.2	5.17 ± 0.9	5.86 ± 0.7	5.57 ± 0.9

Table 10: Percentages of extracellular cyclic imine related to the total amount of intracellular cyclic imine toxins.

	S = 6	S = 10	S = 16	S = 22	S = 28	S = 34
Exponential growth	3.1	7.6	5.1	4.6	2.9	4.4
Stationary growth	1.5	1.1	2.4	2.9	2.6	2.4

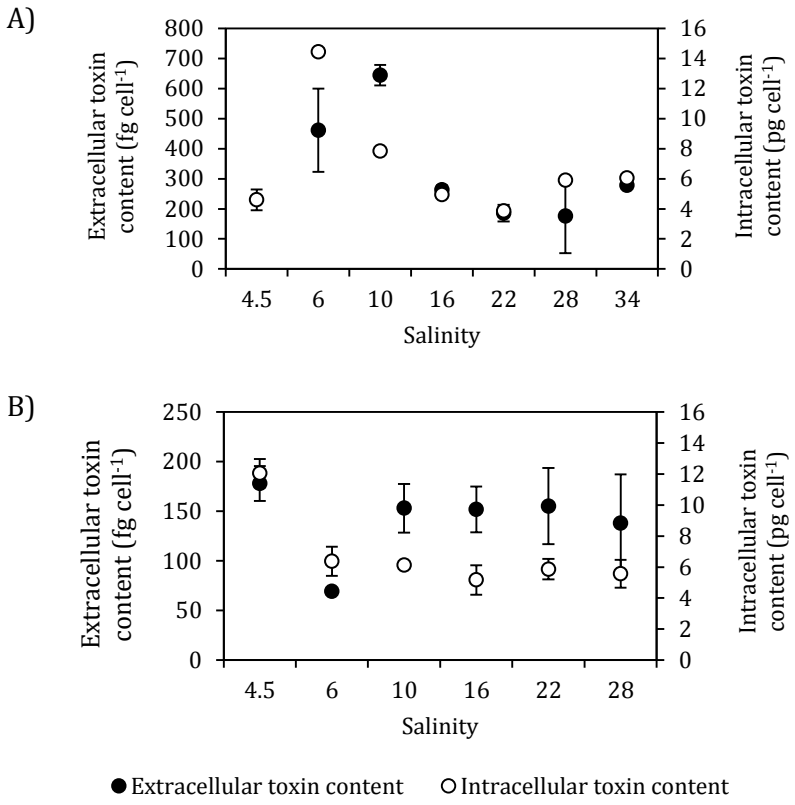

Figure 34: Intra- and extracellular cyclic imine toxin content per cell in **A)** exponential growth phase and **B)** in stationary growth phase. (n = 3, ± 1 SD)

5.2.6 Particulate carbon, nitrogen and phosphorus

The particulate carbon cell quota for exponential and stationary growth phase ranged from 2.0 to 4.5 ng cell^{-1}. Among all treatments the carbon quota was minimal at a salinity of 16 for the exponential growth phase. For the stationary growth phase the carbon quota was minimal a salinity of 10. For both growth phases the cellular carbon content increased gradually for lower and higher salinities and was maximal at salinities 6 and 34

(Figure 35 A). The nitrogen cell quota ranged between 0.4 and 0.6 ng cell^{-1}. For exponential phase samples there was a tendency of a slight increase from the middle salinities to both lower and higher salinities. Except for the salinity treatments 16 and 22, which nearly yielded the same amount of nitrogen per cell in both growth phases (Figure 35 B), the nitrogen concentrations was significant higher in exponential growth phase (t-test, $p < 0.05$). The phosphorus cell quotas ranged from 0.08 to 0.11 ng cell^{-1} for exponential growth and from 0.05 to 0.07 ng cell^{-1} for stationary growth. In exponential phase the intracellular phosphorus concentration was minimal at a salinity of 16 and 22 and increased at higher and lower salinities. In contrast, in stationary phase the phosphorus concentration was maximal at salinity 16 and decreased for lower and higher salinities (Figure 35 C).

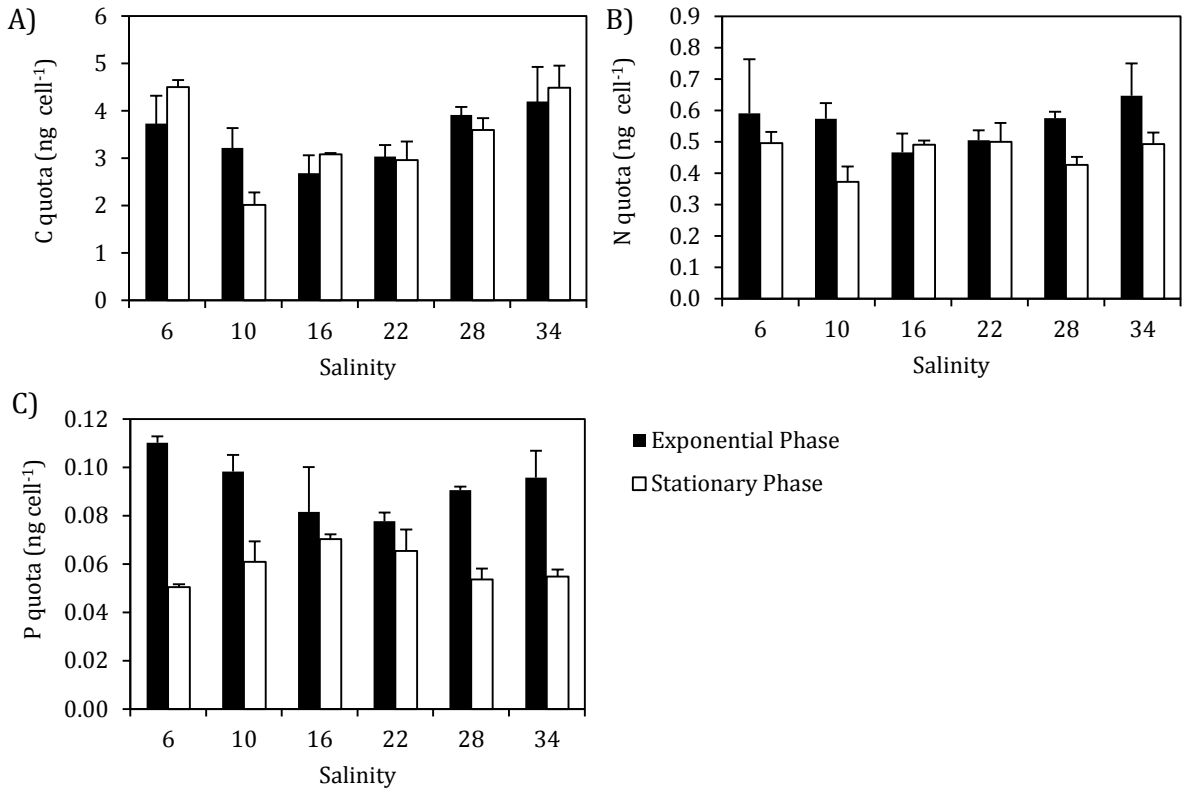

Figure 35: Cell quotas of particulate **A)** carbon (C), **B)** nitrogen (N) and **C)** phosphorus (P). Each data point represents a mean of triplicate cultures. (n = 3, ± 1 SD)

Elemental ratios of cells in exponential phase were quite similar for all salinities ranging from 6.5 to 7.8 for C/N ratios, 84.7 to 111.5 for C/P ratios, and 11.8 to 15.0 for N/P ratios, respectively. In stationary phase C/N, C/P, and N/P ratios were significantly higher for a number of treatments. C/N ratios of about 10 were observed for both low and high salinities, i.e. for the 6, 28 and 34 salinity treatment (Figure 36 A). For C/P ratios at stationary phase, significantly higher values up to 230 were observed again for the 6, 28

and 34 salinity treatments (Figure 36 B). Similarly, the N/P ratio of cultures in stationary phase was most different to exponential phase for the lowest salinity (Figure 36 C).

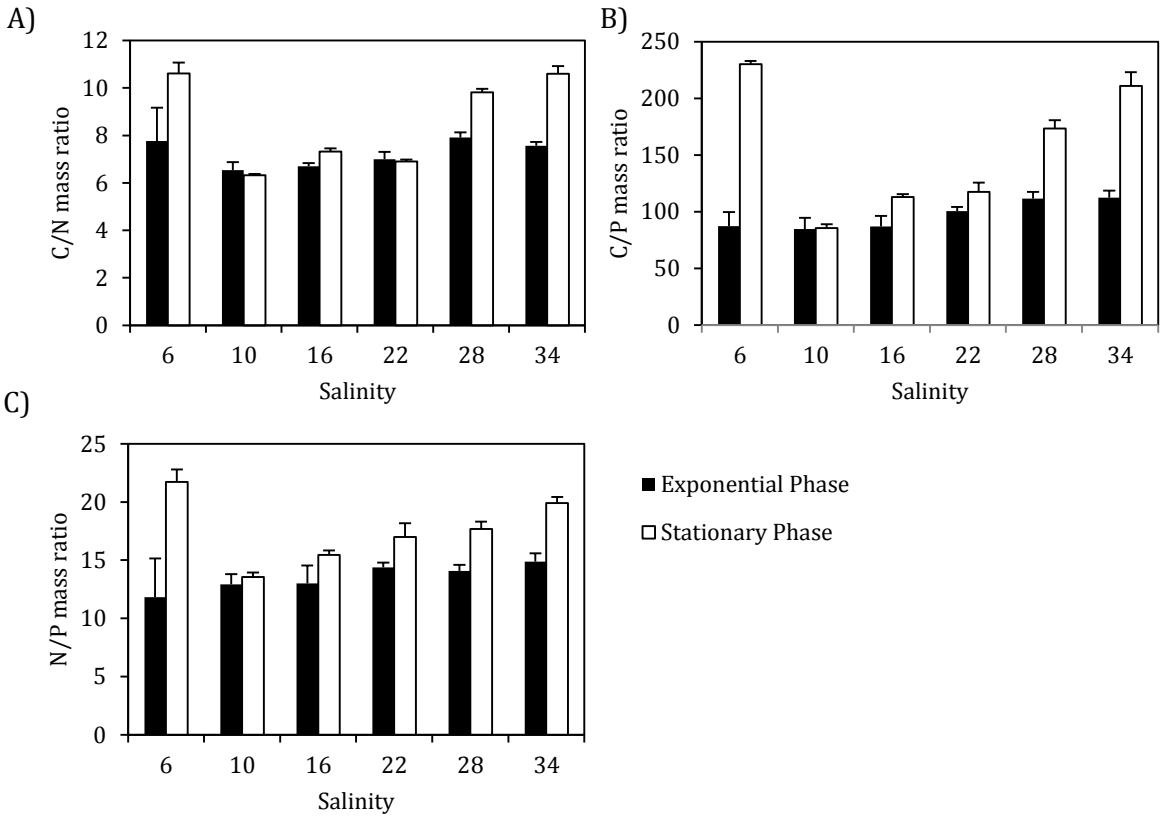

Figure 36: C/N, C/P and N/P mass ratios for triplicate cultures in exponential and stationary growth phase. (n = 3, ± 1 SD)

5.2.7 Dissolved organic carbon (DOC) and total dissolved organic nitrogen (DON)

The DOC measurement resulted in similar amounts of dissolved carbon among all treatments in exponential growth phase and in more variable amounts of DOC in cultures in stationary growth phase. Generally, DOC concentrations were higher for cultures in exponential growth phase and varied from 3.5 to 4.5 mM. For cultures in stationary growth phase the DOC concentration varied from 2.5 to 4.2 mM (Figure 37 A).

In exponential growth phase DON values ranged between 1.1 to 1.5 mM (Figure 37 B). DON values for cultures in stationary growth phase were lower and more variable than values from exponential growth phase, except for the S = 22 treatment, in which DON remained the same quota compared to cultures in exponential growth phase. The DON content in stationary phase was minimal at S = 6 (0.18 mM) and maximal at S = 22 (1.2 mM).

The ratio of DOC to DON was about 4.0 for all salinities. In stationary growth this ratio was enhanced for the salinities 6 and 16 (Figure 37 C).

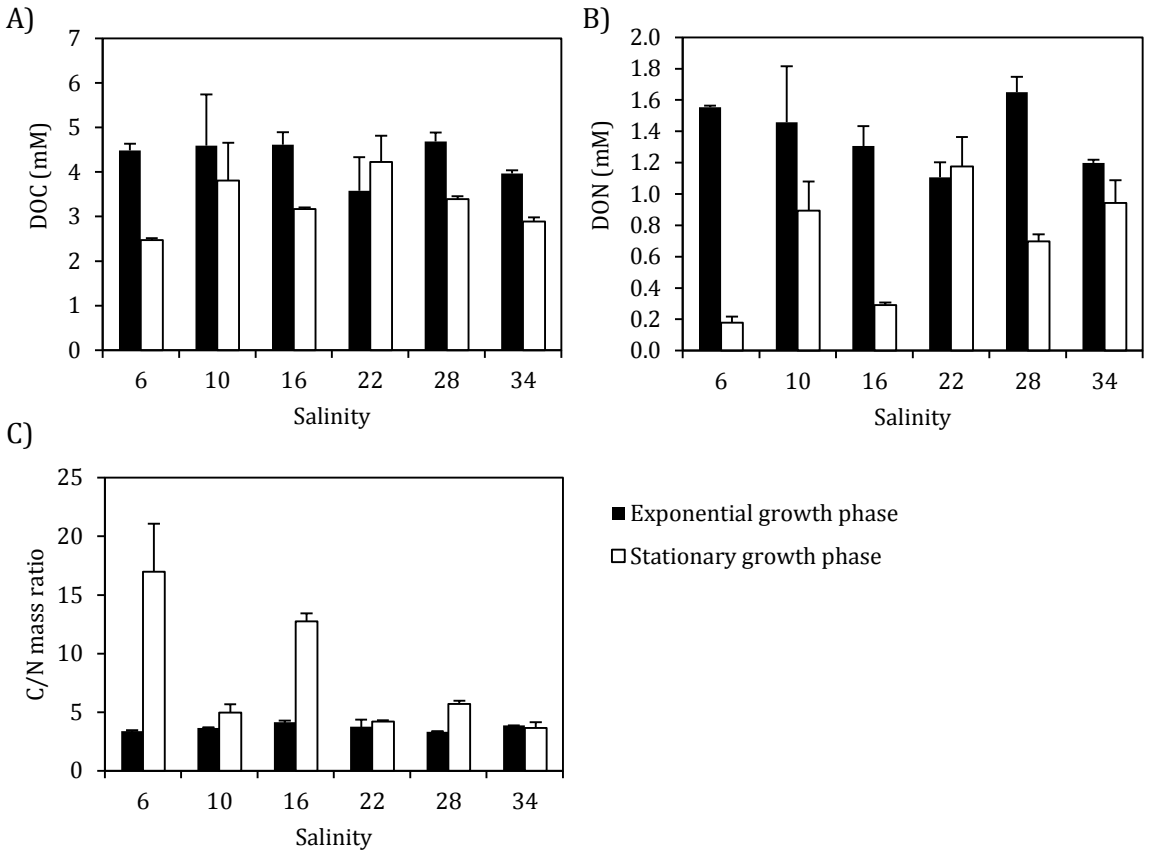

Figure 37: A) Dissolved organic carbon (DOC), **B)** dissolved organic nitrogen (DON) and **C)** C/N mass ratio of dissolved organic carbon to nitrogen of cultures in exponential and stationary growth phase. (n = 3, ± 1 SD)

5.2.8 Cell size determination

Generally, cell sizes ranged from 28.8 µm to 35.2 µm for cell width and ranged from 31.2 µm to 40.6 µm for cell length within and among all treatments. There was a distinct pattern of cell size in relations to salinity. Cells were smaller at the middle salinities and increased in size to both lower and higher salinities. At the three lowest salinities tested, cells during exponential phase were almost of the same size as cells in exponential growth. In contrast, cells in stationary phase at the three highest salinities were significantly smaller compared to cells during exponential growth (Figure 38). Among all salinity treatments cell size (both, cell width and cell length) were significant different (ANOVA, $F = 12.15$, $p < 0.0001$, for both growth phases). A homogenous subgroup of the salinities 22 and 28 was defined by performing a Tukey's HSD test (ANOVA, Tukey's HSD test, $P < 0.05$, for both growth phases).

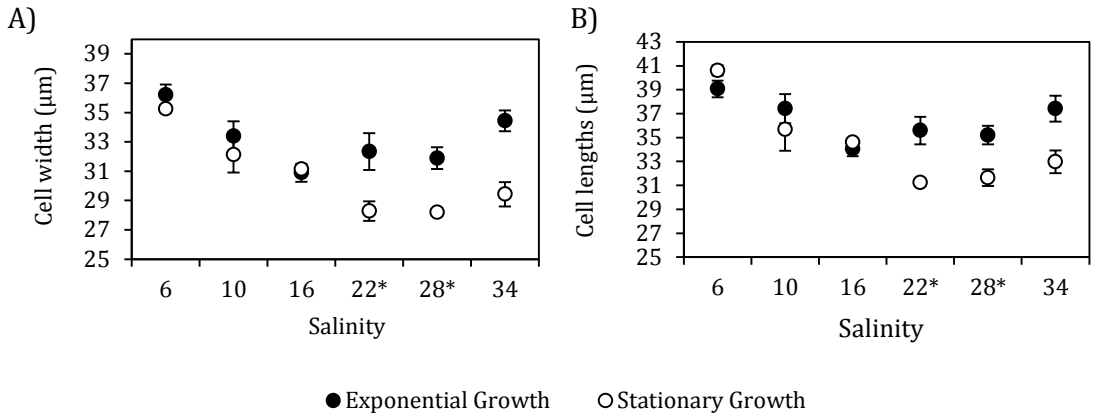

Figure 38: A) Determination of cell width and **B)** cell lengths of *A. ostenfeldii* cells for different salinity treatments. Each data point represents a mean of triplicate cultures with 30 measurements each (n = 3, ± 1 SD). (*) A homogenous subgroup of the 22 and 28 salinity treatments was defined by performing a Tukey's HSD test (ANOVA, Tukey's HSD test, $p < 0.05$).

5.3 Experiment 3: LC-MS characterization and collection of a novel spirolide

LC-MS analysis and toxin screening of 68 isolates from Ouwerkerkse Kreek in The Netherlands proved that 13-desmethyl spirolide C was the main spirolide produced by the *A. ostenfeldii* population. The presence of a 13-desmethyl spirolide C ($[M+H]^+$ ion at m/z 692.5) was determined by the observation of three characteristic fragment clusters acquired with an ESI triple quadrupole MS instrument (Figure 39). Three water loss of the precursor ion caused fragmentation ions at m/z 674, 656 and 638. Furthermore fragmentation and associated water losses caused ions at m/z 462, 444, 426 and 408 and an residual fragment at m/z 164 (Hu et al. 2001; Ciminiello et al. 2007).

During the toxin screening it was noticed that three samples contained an unknown substance at m/z 696. A product ion scan of the $[M+H]^+$ ion at m/z 696.5 was performed using an ESI triple quadrupole MS instrument. The LC-MS spectrum of the ion contained three cluster which are characteristic for spirolides plus one additional characteristic fragment cluster (Figure 40): (1) ions at m/z 696, 678, 660, 642 and 624 were caused because of four losses of water molecules. (2) Another fragmentation ion and associated water losses caused peaks at m/z 446, 428, 410 and 392. (3) Two fragmentation ions and three water losses were observable at m/z 310, 392, 274 and at m/z 248 and 230. (4) As it is described for 13-desmethyl spirolide C, a residual fragment was determined at m/z 164.

For a detailed elucidation of the chemical structure of the novel spirolide, 1D and 2D NMR analysis will be necessary, which, however, require a relatively large amount of purified compound. According to our Italian colleagues who are experienced with NMR structural elucidation of spirolides, an amount of at least 100 µg of the yet undescribed toxin is required. Cell quota of the 696-compound as estimated in the toxin screening was highest

for strain OKNL48 and accounted for 1.1 pg per cell, indicating that large-scale culturing is needed to produce an sufficient amount of material for structure elucidation.

The efficiency of toxin extraction of large-volume cultures using HP-20 resins was tested in a pre-experiment. It was confirmed that almost all (>98 %) of both SPX-1 and the yet unknown toxin can be extracted from the cultures with just one round of the extraction procedure (Table 11).

Table 11: Extraction efficiency using acetone lysis of cells and toxin binding to HP-20 resins. Almost all toxins were extracted after the first run of the extraction procedure. Toxin amounts are in ng per sample.

Run	SPX-1 (%)	Unknown spirolide (696-164 m/z) (%)
1	1968.8 (99.1)	14224.6 (98.4)
2	12.8 (0.6)	179.1 (1.2)
3	5.3 (0.3)	58.3 (0.4)

Batch cultures of the *A. ostenfeldii* isolate OKNL48 were cultivated and toxin extractions were done as it is described in Chapter 4.2.3. In total, 100 L of batch culture were grown, harvested and extracted. All extract finally were combined and analyzed by LC-MS/MS and the toxin concentration was determined. The final amount of compound m/z 696 in the dried sample was 143.8 µg and this sample now is provided for NMR analyses. Due to time constrains, the NMR analysis itself will not be part of this thesis, but will be done in co-operation by Carmela Dell'Aversano (University of Naples Federico II, Napoli, Italy).

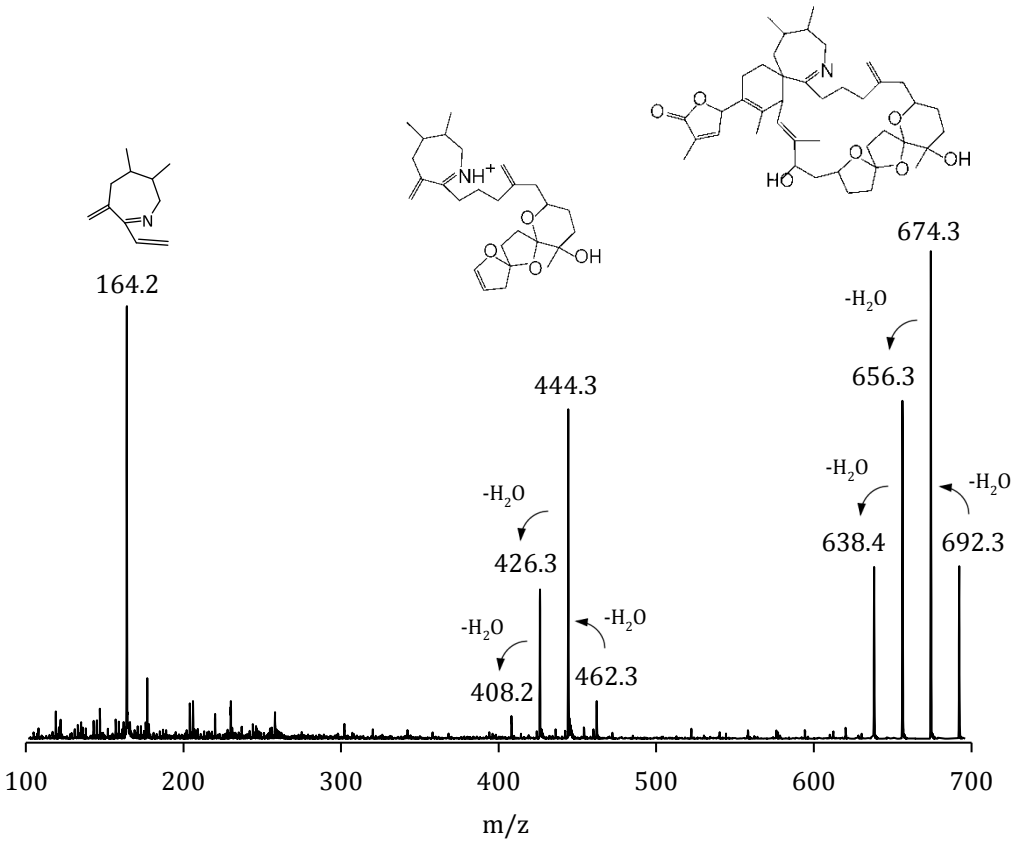

Figure 39: MS² product ion spectra of the $[M+H]^+$ ion at m/z 692.5 of a standard solution of 13-desmetyhl spirolide C. (Structural information as per Ciminiello et al. (2006))

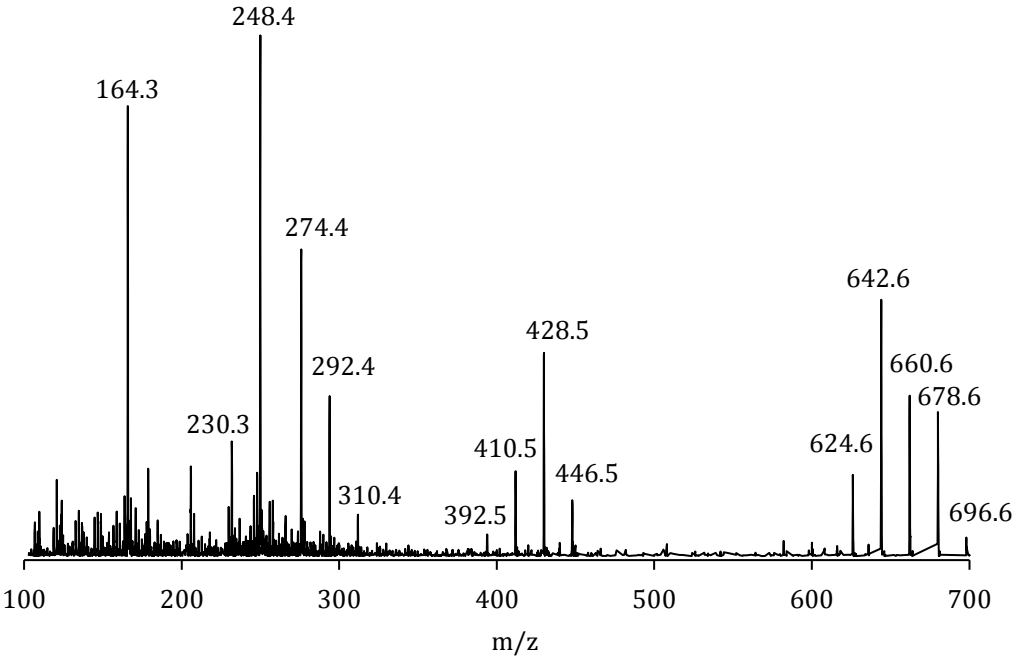

Figure 40: MS² product ion spectra of the $[M+H]^+$ ion at m/z 696.5 of a potentially unknown spirolide.

6 Discussion

6.1 Population diversity of *A. ostenfeldii*

With the first bloom description of *Alexandrium ostenfeldii* in the Ouwerkerkse Kreek in 2012 (Burson et al. 2014), dense proliferations of this toxic dinoflagellate now seem to be a serious and recurrent threat for brackish inland waters in The Netherlands. Although *A. ostenfeldii* for a long time has been considered mainly occurring at low cell concentrations mixed with other bloom forming dinoflagellates (Balech and Tangen, 1985; Moestrup and Hansen, 1988), there now are numerous recent reports of dense blooms of this species (or its synonym *A. peruvianum*) from various coastal brackish areas around the world (e.g. from South America (Sánchez et al. 2004), the Northern Baltic Sea (Kremp et al. 2009), the estuaries of the US East coast (Tomas et al. 2012), the Adriatic sea (Ciminiello et al. 2007) and, most recently, the Netherlands (Burson et al. 2014). Isolates of these blooms differed significantly in their toxin profile: whereas a Mediterranean bloom isolate was found to produce only spirolides (Ciminiello et al. 2007), Baltic blooms have been described to contain both spirolides and PSP-toxins (Kremp et al. 2009), and blooms from the US coast have been described to contain a cocktail of PSTs, spirolides, and 12-methyl gymnodimine (Tomas et al. 2012; Borkman et al. 2012). However, almost nothing was known on the toxins of the Dutch population. High PST concentrations in plankton and shellfish samples during the 2012 bloom (Burson et al. 2014) suggested that the local *A. ostenfeldii* population was the PST source organisms, but that had not yet been confirmed by culture studies as no bloom isolate had been established. For every work using microalgal isolates it is becoming more and more clear that intraspecific variability in microalgae populations is an important matter. The importance of intraspecific geno- and phenotypic variability has been recognized in traits ranging from morphology, life history, DNA, growth rates, chemical composition, toxicity and physiology (Burkholder and Glibert 2009). Intraspecific variability in toxin profile and toxicity has been reported for many harmful algae (Bachvaroff et al. 2009), including *Alexandrium tamarense* and *A. ostenfeldii* (Alpermann et al. 2010; Tillmann et al. 2014). We here thus used a multi-isolate approach to (1) provide a thorough characterisation of bioactive compounds produced by the local Dutch *A. ostenfeldii* population and (2) to explicitly determine the variability in both qualitative and quantitative aspects of toxins in a bloom population of a toxigenic dinoflagellate.

In brief, the results clearly showed that the Dutch *A. ostenfeldii* population produced a whole suite of toxic compounds including not only PSP-toxins, spirolides, and gymnodimines but also yet undescribed lytic compounds.

Lytic capacity

Allelochemical substances with the capacity to cause cell lysis of protistan targets like *Rhodomonas salina* seem to be common for the genus *Alexandrium* (Tillmann and John 2002) and have already been documented for *A. ostenfeldii* (Hakanen et al. 2014; Tillmann et al. 2014; Tillmann et al. 2007; Hansen et al. 1992). In comparative studies it was shown that the lytic activity of *Alexandrium* is unrelated to the production of PST (Tillmann and John 2002) and spirolides (Tillmann et al. 2007). The EC_{50}-value, i.e the concentration of *A. ostenfeldii* which caused 50 % cell lysis of the target *R. salina*, of 659 cells mL^{-1} is in the range of EC_{50} value estimated for other *A. ostenfeldii* isolates (Tillmann et al. 2009; Hakanen et al. 2014), which have been shown to range from 0.3 to 1.9 $x10^3$ cells ml^{-1}. EC_{50} values for haemolysis of *A. ostenfeldii* from the US coast given by (Tomas et al. 2012) and (Tatters et al. 2012), seem to be orders of magnitude higher (i.e. lytic capacity is lower) but refer to different target cells and procedures than used in standard assays. Moreover, by using their erythrocyte lysis assay, (Tomas et al. 2012) found only little lysis in cell free supernatant of their *A. ostenfeldii* from coastal North Carolina, whereas particularly cell pellets had the highest lytic activity. The authors thus concluded that the lytic agents were most likely intracellular or membrane bound (Tomas et al. 2012). However, our comparison of whole culture, cell-free supernatant, and cell extract show that the majority of lytic activity of *A. ostenfeldii* is mainly excreted and acting extracellular, underlining a rather unspecific role in grazer impairment and competition (Cembella 2003; Legrand et al. 2003). Nevertheless, lytic compounds produced by *A. ostenfeldii* may also be involved in cell communication or in interspecific cell-to-cell interactions, e.g. in prey capture and resource acquisition via mixotrophy. *A. ostenfeldii* has been shown to be mixotrophic (Gribble et al. 2005) and it has been speculated that allelochemicals are used for predation. In our co-incubation bioassay we did not observe the presence of large food vacuoles in *A. ostenfeldii* as an indication for ingestion of *R. salina*, but it is possible that *A. ostenfeldii* probably benefits from a lysis induced enhancement of dissolved organic matter.

During the bloom period in the Ouwerkerkse Kreek, cell concentrations of *A. ostenfeldii* were well above 1,000 cell mL^{-1} (Figure 5) and thus far above the concentration causing significant cell lysis of *R. salina* in our bioassay. Although the role of lytic compounds for bloom initiation at much lower cell concentrations is more difficult to evaluate, deleterious effect of lytic extracellular compounds on both competitors and grazers most likely played an important role for the high population density and persistence of the bloom.

Toxin concentration

Coming back to the known phycotoxins, it is noteworthy that we identified quite a range of different PSP-toxins and cyclic imine toxins in the Dutch *A. ostenfeldii* isolates. In quantitative terms, we found a high diversity in total toxin content per cell among all isolates. For total PSP-toxins, cell quota among isolates varied 8-fold, and for total cyclic imine toxins were observed an 11-fold variation. Toxin cell quotas are well known to be modulated by environmental factors (Maclean et al. 2003; Tatters et al. 2012). However, all isolates harvested for toxin screening were grown under identical environmental conditions (growth medium, nutrients, light, and temperature) and were sampled during active growth at a comparable cell density of about 1,000 – 3,500 cells mL^{-1}, which, according to the growth curves obtained in the salinity experiment, correspond to a mid-exponential phase. We therefore conclude that even within a bloom population there is considerable intraspecific variability in the quantity of toxins produced.

Such a high intraspecific variability of course complicates a straightforward comparison of toxin content of the Dutch *A. ostenfeldii* to other global records of the species. Nevertheless, the mean PSP-toxin cell quota of the Dutch population of 45.7 ± 17.8 pg per cell were distinctly higher than cell quotas reported for brackish water blooms of *A. ostenfeldii* in the Baltic, where cell quotas of about 18 pg per cell (Suikkanen et al. 2013) or 2-5 pg per cell (Kremp et al. 2009) have been determined. For *A. ostenfeldii* (reported as *A. perivianum*) from brackish estuaries of the US east coast, PSP-toxin profile but no quantitative measurements of cell quota are reported (Tomas et al. 2012; Borkman et al. 2012) and thus a comparison is not possible. The highest PSP-toxin cell quota of *A. ostenfeldii* reported in the literature comes from an New Zealand isolate with about 170 pg PSP-toxins per cell (MacKenzie et al. 2004) which is about two-fold higher than the most toxic one of the Dutch isolates (88 pg per cell).

Likewise, a mean cell quota of about 8.7 ± 4.5 pg $cell^{-1}$ for cyclic imine toxins might at least roughly be used in a comparison of the Netherlands bloom to other *A. ostenfeldii*. The results of a literature search suggested that cyclic imine toxin cell quota is variable depending on the geographic origin of the isolate, but it has to be kept in mind that many reports are based on just one or a few isolates. Ciminiello et al. (2006) reported about a bloom in the northern Adriatic Sea. A local isolate was found to produce only cyclic imine toxins with a cellular concentration of 3.7 pg $cell^{-1}$ of 13-desmethyl spirolide C. The author mentioned the occurrence of several other cyclic imine toxins which were neither quantified nor identified in their study. The most abundant spirolide of *A. ostenfeldii* from a bloom in Nova Scotia was determined as 13-desmetyhl spirolide C and occurred in a

distinct higher cell quota, compared to the Dutch isolates, of 54 pg cell^{-1} (Cembella et al. 2000). One strain of *A. ostenfeldii* from Canada has been described with notably high cell quotas ranging from about 30 to 240 pg cell^{-1}, depending on the environmental conditions (Maclean et al. 2003). Total spirolide cell quotas of Greenland *A. ostenfeldii* populations varied considerably among different isolated ranging from as low as 0.02 pg cell^{-1} up to 66 pg cell^{-1} (Tillmann et al. 2014). Likewise, a high variability in total spirolide quota was reported both field samples from the Gulf of Maine, U.S. ranging from almost no detectable spirolides up to a maximum of 169 pg cell^{-1} (Gribble et al. 2005). 13-desmethyl spirolide C was quite abundant in *A. ostenfeldii (as A. peruvianum)* isolates from New River Estuary, USA (Tomas et al. 2012) with cell quota for one strain ranging from 6 to 54 pg cell^{-1}, depending on culture growth phase and nutrient limitation (Tatters et al. 2012). In the same study, high per cell concentrations of 12-methylgymnodimine of 12 - 96 pg cell^{-1} were reported as well, indicating that total cyclic imine toxin quota of this American group I *A. ostenfeldii* with up to 150 pg per cell was almost an order of magnitude higher compared to representatives of the Dutch bloom.

Toxin composition

In contrast to the quantitative range in PSP-toxin cell quota, we detected almost no intraspecific variability in terms of PSP-toxin profile, i.e the relative composition of all saxitoxin analogs. The relative contribution of C1/C2, GTX2/3, GTX5, and STX was almost identical for all but one isolate (which had a lower contribution for C1/C2 and a higher contribution for STX). Among other PST producing isolates of *A. ostenfeldii* this profile is identical to isolates from the US coast but different to all Baltic strains which lack C1/2 and GTX5 (Kremp et al. 2014). One available isolate from China differed by its unique presence of neo-saxitoxin and an isolate from Peru was unique in its absence of both C1/C2 and GTX5 (Kremp et al. 2014).

Whereas the PSP-toxin profile in the Dutch bloom population was rather stable, the relative composition of cyclic imine toxin within all isolates was much more variable. In addition to four PSP-toxin analogues we identified a total of 23 different cyclic imine compounds to be present indicating a particularly high diversity of this toxin group. Older studies on *A. ostenfeldii* usually reported the presence of just a few (if any) minor spirolide compounds, but some recent reports indicate that a high diversity of different cyclic imine toxins might be the rule and not the exception (Ciminiello et al. 2006; Gribble et al. 2005; Tillmann et al. 2014) and thus its detections and documentation strongly depends on the applied methods.

Among the 23 compounds detected (Table 2), 17 have been classified as minor compounds but at least 6 cyclic imine toxins have been classified as major components with relative abundance of > 5 %. Among those, both gymnodimines (gymnodimine A, and 12-methyl gymnodimine A) were found to be absent in some of the isolates, and for the other 4 major cyclic imine toxins the range in relative concentration was 6 to 8-fold or exceptionally as high as 450-fold for the novel compound (m/z 696) among isolates. Within the minor compounds, the majority has not yet been described in detail. For some of the transitions a product ion scan is needed to be performed to verify the identity of the compound. As an example, two mass transitions corresponding to pinnatoxins have been detected at very low amounts. With the new species *Vulcanodinium rugosum,* a dinoflagellate source of pinnatoxins was recently identified (Rhodes et al. 2011). The presence of these compounds, even in low concentration, as never been reported before in *A. ostenfeldii* and thus need more confirmation and further analysis. Structural similarities of spirolide, gymnodimines and pinnatoxins have been noted earlier in the literature (MacKinnon et al. 2006a; Hu et al. 1995) and it is thus conceivable that all three compounds might be interrelated in one biochemical pathway and thus are simultaneously present in the cells. However, with a lack of significant correlations between the major gymnodimines and spirolides (Figure 19), our data set provided no conclusive evidence for such a close link.

All isolates of *A. ostenfeldii* obtained so far were found to produce a number of different cyclic imine toxins, which for the Dutch isolates included both spirolides and gymnodimines. In terms of spirolides, a recent comparison of multiple strains from various locations clearly showed that the gross qualitative composition of spirolides was in clear accordance with the phylogenetic structure, which identified 5 clusters or groups in the *A. ostenfeldii* species complex (Kremp et al. 2014). Isolates of Group 1 (and also group 2) almost exclusively produced 13-desmethyl spirolide C, whereas isolates from the other phylogenetic clusters had a more diverse composition of other major spirolides. This is in agreement with our result of a major contribution of 13-desmethyl spirolide C among total spirolides and with a phylogenetic analysis of some selected isolates of the Dutch bloom, which clearly showed that they belong to group I together with other brackish waters isolates from the Baltic and from the west coast of the U.S. (van de Waal et al., in prep.). In addition to a number of different spirolides, the Dutch isolates produced at least two different gymnodimines. Reports about the occurrence of both spirolides and gymnodimines in *A. ostenfeldii* seem to be rather exceptional, but a first record of a gymnodimine in *A. ostenfeldii* was the report of occurrence of 12-methyl gymnodimine A in isolates from the U.S. (van Wagoner et al. 2011). In any case, the presence of gymnodimine A, which has been identified from the toxic *Gymnodinium* sp. (Seki et al. 1995), has not been

reported before for *A. ostenfeldii*. Moreover, with a cell quota of up to 18 pg cell^{-1} gymnodimine A was even found to be the most abundant cyclic imine toxin among the Dutch bloom population of *A. ostenfeldii*.

A phylogenetic analysis of the Dutch *A. ostenfeldii* population revealed a close relationship with clones covering a wide geographical distribution, ranging from the coastal areas in the Baltic Sea to embayments in the North-East coast of the US, and the East coast of Japan (van de Waal et al., in prep.). The recent and sudden emergence of *A. ostenfeldii* blooms in the Ouwerkerkse Kreek may indicate a recent anthropogenic-driven dispersal. Within Group I of the *A. ostenfeldii* species complex, toxin profile of the Netherland isolates are most similar to two isolated from North America, which are the only representatives which produce an identical PSP-toxin profile, which contain the same major spirolides, and which also produce gymnodimines (van Wagoner et al. 2011; Tomas et al. 2012). However, the presence of gymnodimine A in the Dutch but not the American population would be a major difference of chemotaxonomic significance. In any case, in depth population genetics are needed to evaluate a potential common origin and/or a potential dispersal routes.

Characterization of a novel spirolide

Among the many unidentified or poorly characterized cyclic imine compounds detected, the compound inducing a mass transition at $[M+H]^+$ 696 → 164 m/z attracted attention because this compound, which we identified by a precursor ion scan, had not been detected before (Bernd Krock, pers. com.) and occurred in fairly high concentrations of up to 1.1 pg per cell, albeit just in a very few isolates. For a more detailed structural characterization, an enhanced product ion scan was performed at 696 m/z to determine the fragmentation pattern of this molecule (Figure 44). Here, the residual fragment at m/z 164 was determined (Figure 42), which is regarded as the most characteristic fragment for several other spirolides (Roach et al. 2009) and is also present in the product ion spectra of SPX1 (Figure 39). The structure of this fragment was determined before by several authors and includes the functional imine group of cyclic imine toxins (Hu et al. 2001; Roach et al. 2009). It is obvious that this residual fragment is different from the fragment reported by Ciminiello et al. (2007) for the 27-hydroxy-13,19-didesmethylspirolide C analog which contains a functional hydroxyl group at C27. This hydroxyl at C27 is preserved in a residual fragment at m/z 180 (Figure 43). It is therefore suggested that the novel compound does not contained a hydroxyl at C27, because no respective fragment was found in the product ion spectra. In addition, the unknown compound produced another fragment in the product ion spectra at m/z 446 (Figure 44). A similar fragment with an identical mass-to-charge ratio and corresponding water losses were found in the product ion spectra at m/z 446 for

27-hydroxy-13,19-didesmethylspirolide C (Ciminiello et al. 2007). This indicates that the unknown compound is similar to the reported 27-hydroxy-13,19-didesmethylspirolide C besides a different position of the hydroxyl and differences in the C2-C3 region which is also variable within different types of spirolides. The precursor ion at m/z 696 and corresponding water losses were two masses higher than it was reported by Ciminiello et al. (2007) for the 27-hydroxy-13,19-didesmethylspirolide C analog which was detected at m/z 694. As it is reported by several authors, the mass difference between spirolide C and D is also 2 masses caused by a differing methylation at C2 and C3 (Christian et al. 2008; van Wagoner et al. 2011; Roach et al. 2009). A reasonable possibility is that the unknown compound is a spirolide D analog which is de-methylated at C13 and C19 and contain a hydroxyl not at C27 but somewhere in the m/z 446 fragment. Because of an optimal steric configuration, the unknown compound produced by *A. ostenfeldii* from The Netherlands is thus suggested to be 23-hydroxy-13,19-didesmethyl spirolide D. The MS data of the observed precursor ion were consistent with an elemental composition of $C_{41}H_{61}NO_8$ ($[M+H]^+$ 696.5 m/z).

This suggestion is merely based on LC-MS/MS data and the chemical structure, especially the position of the hydroxyl in the m/z 446 fragment, is thus hypothetical at the moment. Because a larger amount of the new compound is now available, NMR analyses in the near future will be used to elucidate the true structure and to prove or disprove our structural hypothesis.

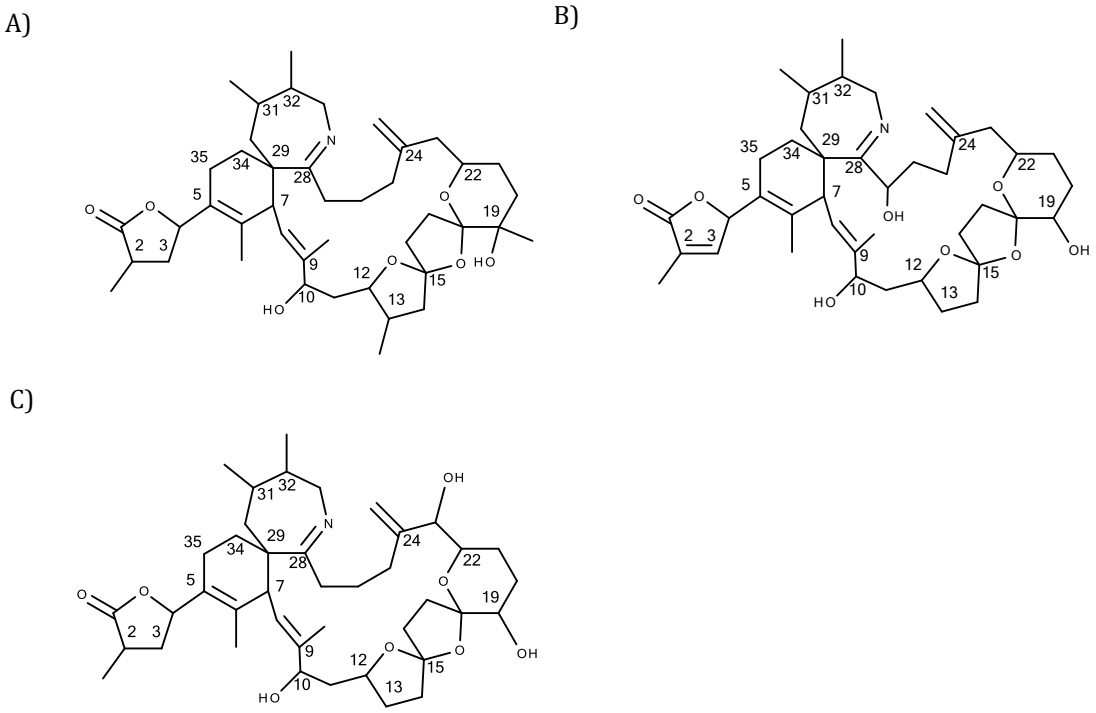

Figure 41: A) Chemical structure of spirolide D (molecular weight: 708.5), **B)** chemical structure of 27-hydroxy-13,19-didesmethyl spirolide C (MW: 694.5; Ciminiello et al. 2007) and **C)** chemical structure of a hypothetical 23-hydroxy-13,19-didesmethyl spirolide D (MW: 696.9). MW are mentioned for $[M+H]^+$ ions.

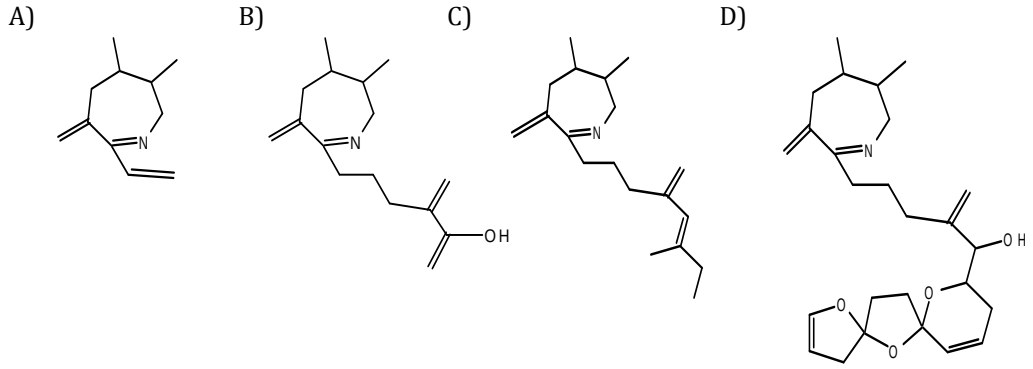

Figure 42: Chemical structures of hypothetical fragment ions of the novel 23-hydroxy-13,19-didesmethyl spirolide D. **A)** MW= 163.2, **B)** MW= 247.4, **C)** MW= 273.5 and **D)** MW= 427.6. MW are mentioned for $[M+H]^+$ ions.

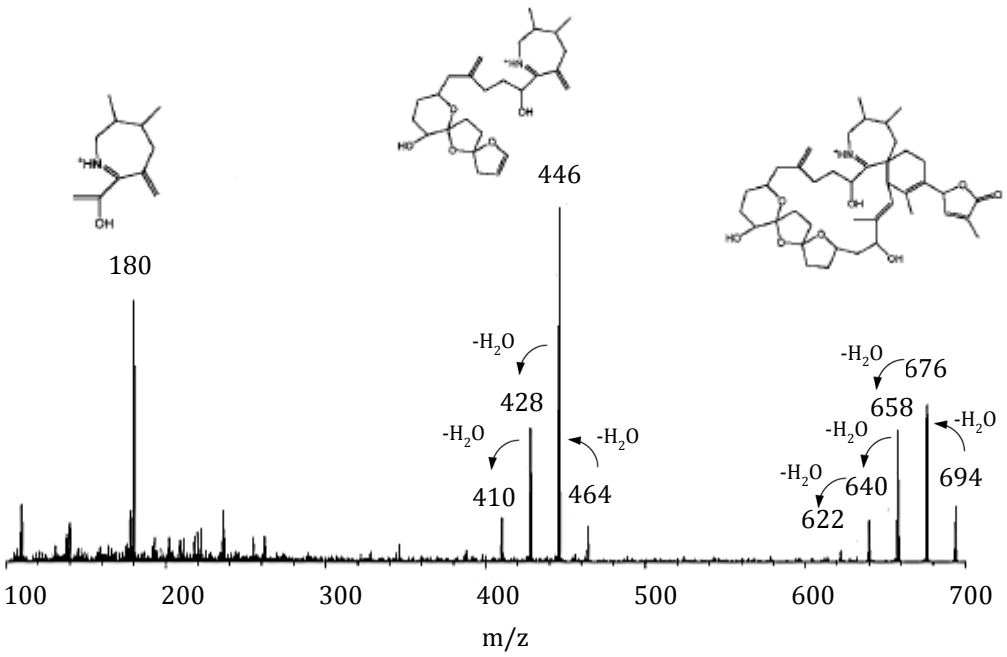

Figure 43: MS2 product ion spectra of the [M+H]+ ion at m/z 694.5 of 27-hydroxy-13,19-didesmethylspirolide C as it is reported by Ciminiello et al. (2007).

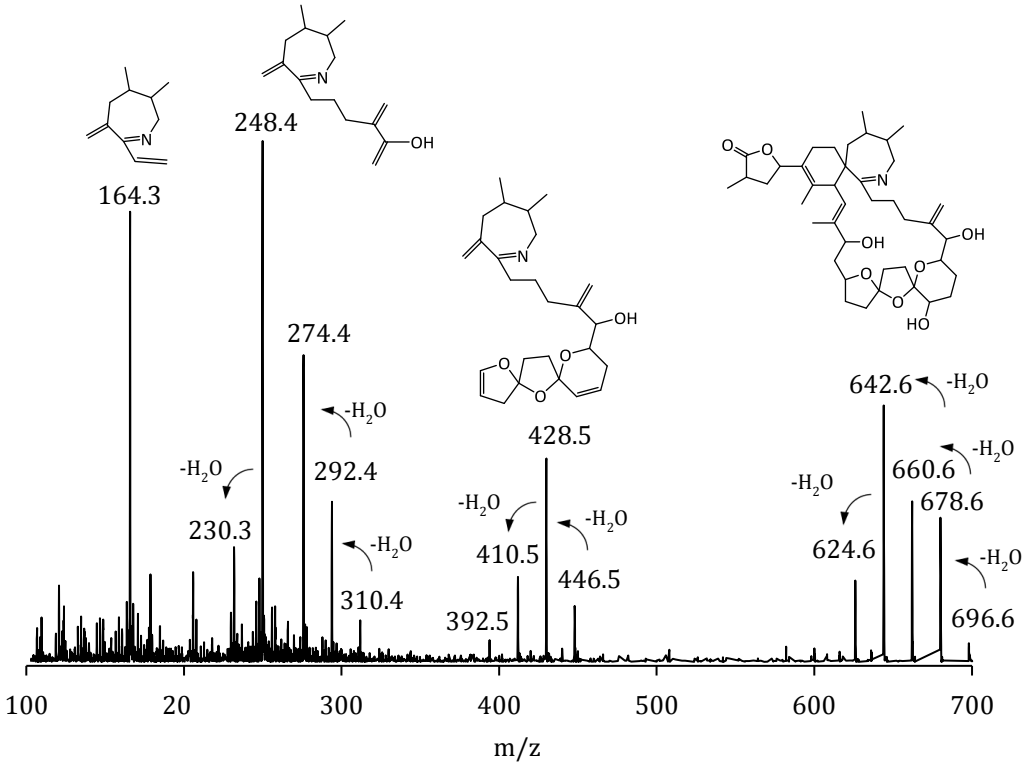

Figure 44: MS² product ion spectra of the [M+H]+ ion at m/z 696.5 of the novel 23-hydroxy-13,19-didesmethyl spirolide D. Hypothetical structures are suggested for the molecule and its fragments based on the LC-MS/MS data.

6.2 Salinity tolerance of a selected *A. ostenfeldii* isolate

A. ostenfeldii populations are found around the world in temperate coastal and estuarine waters with common fluctuations in salinity (Maclean et al. 2003; Balech 1995; Tomas et al. 2012). In this thesis the tolerance of an *A. ostenfeldii* isolate from a brackish water creek with highly variable salinities was tested for salinities from 3 to 34.

Cell size determination

As one of the easiest accessible parameter, cell size in relation to salinity was determined. Generally, cell sizes for all cultures ranged between 25 - 40 µm. This is somewhat smaller as sizes documented for field samples of *A. ostenfeldii* which have been reported to range between 30-50 µm (Paulsen 1904; Balech and Tangen 1985; Moestrup and Hansen 1988). Such a difference in cell sizes of culture samples and field samples is also mentioned by other authors (Kremp et al. 2009; MacKenzie et al. 1996; Jensen and Moestrup 1997). Cells of *A. ostenfeldii* are usually described to be slightly wider than long (Balech and Tangen 1985). In contrast, cell size determinations of strain OKNL21 showed that this isolate, constant over all salinities, was rather longer than wide. This is in agreement with detailed size measurement of 20 isolates of the Ouwerkerkse bloom population, which all had a mean length to width ration > 1 (van de Waal et al., in prep.) as an obviously stable phenotypic trait of the Netherlands *A. ostenfeldii* population. Cell size was significantly affected by salinity with both cell length and width being increased at extreme salinities. In general, increase in cell size will reduce the surface area/volume ratio of the cell. Lim and Ogata (2005) speculated that this might enhance the osmoregulation capability of the cell and therefore allow higher growth rates at low or high salinities. We currently do not have a conclusive explanation as to why stationary phase cells at salinities of 22, 28, and 34 decreased in size, and stationary phase cells at salinities of 6, 10, and 16 did not (Figure 38). We cannot exclude an increased gamete formation (gametes of *Alexandrium* are generally smaller than normal vegetative cells) at higher salinities. Future studies should specifically address the role of different salinities for transitions events in the life cycle of the Dutch *A. ostenfeldii* bloom populations, as formation of sexual resting cysts as seeding stocks for the next season is of outstanding importance for the presence of annually recurrent blooms.

Cell growth determination

Fully acclimated cells were able to grow at or close to their maximal growth rate of about 0.2 d^{-1} over the very wide range of salinities from 6 to 34. Almost optimal growth at such a broad level of salinities with a lower tolerance limit at about 4.5 suggests that the Dutch *A. ostenfeldii* are euryhaline. A lethal barrier for most estuarine planktonic algae at which

the organisms suffers extreme osmotic stresses is at a salinity of nearly 5 (Lim and Ogata 2005). This is consistent with our observation that slow growth at salinity of 4.5 only occurred during pre-acclimation but not in experimental cultures. However, below that level *A. ostenfeldii* cannot survive; cells number in cultures transferred from salinities of 4.5 to 3 rapidly declined in cell numbers. Although growth was similar at all salinities, slightly higher growth was observed for cultures in salinities from 10 to 22 which confirmed salinity-dependant growth response of other *A. ostenfeldii* isolates (Lim and Ogata 2005; Grzebyk et al. 2003; Maclean et al. 2003).

An euryhaline growth response is also reported by another study for Danish isolates of an *A. ostenfeldii* population with good growth between salinities of 15-30 (Jensen and Moestrup 1997). Maclean et al. (2003) also observed an euryhaline response of growth rate over a range of salinities from 25 to 33 for *A. ostenfeldii* cultures from Nova Scotia, Canada. The salinity tolerance of a Baltic population of *A. ostenfeldii* was determined by Kremp et al. (2009) and here growth was optimal for salinities of 6 to 10. Suikkanen et al. (2013) reported about salinities ranging between 6 to 20 for other isolates from the Baltic Sea. For both Baltic populations no growth was determined at salinities below 6. In comparison to Dutch isolates from Ouwerkerkse Kreek the growth performances of *A. ostenfeldii* was distinct lower. A general broad euryhaline growth response as for *A. ostenfeldii* has also been reported for the closely related species *Alexandrium minutum* (Lim and Ogata 2005; Grzebyk et al. 2003), which is also known to form dense blooms in harbours, lagoons and other coastal systems (Hwang and Lu 2000; Chang et al. 1997; Vila et al. 2005).

Generally, growth of isolate OKNL21 was slightly below the range of maximal growth rates (between 0.2 - 0.3 d^{-1}) reported for other *A. ostenfeldii* (Maclean et al. 2003; Jensen and Moestrup 1997). The combination of relatively slow growth (a growth rate of 0.2 d^{-1} correspond to one doubling in 3.5 days) and the obvious formation of dense blooms clearly indicate that *A. ostenfeldii* is very successful in reducing grazing loss and in outcompeting other fast-growing species. It is tempting to speculate that the broad cocktail of bioactive compounds detected here for the Dutch bloom population play an important role in this respect; the role of PSP-toxins in deterring copepod grazers is intensely discussed (Teegarden and Cembella 1996; Bagoien et al. 1996; Selander et al. 2006) and the deleterious role of extracellular lytic compounds towards accompanying protists clearly support the achievement of bloom dominance (Tillmann and John 2002; Tillmann et al. 2007).

Cell yield and growth limiting factors

Salinity did not affect cell yield, i.e the maximum cell density at stationary phase, which for all treatments was about 10,000 cells mL^{-1}. Generally, for our experiments it is difficult to determine the factor(s) responsible for growth cessation and limitation in stationary phase. Growth in un-aerated cultures might lead to carbon limitation and a strong increase in pH in dense cultures has been shown to strongly affect dinoflagellate growth of both photosynthetic and heterotrophic species (Pedersen and Hansen 2003; Hansen 2002). In terms of macronutrient, the K-medium used here has a surplus of nitrate compared to phosphate (465 µM N and 18 µM P in original half-strength K-medium) so – if nutrient limitation is involved in growth limitation - cultures in stationary phase are expected to be phosphorous-limited. A phosphate limitation indeed seem to indicated by high intracellular C/P and N/P ratios of cultures in stationary phase at both low and high salinities. However, almost no increase in elemental ratios from exponential to stationary phase was observed for medium salinities, indicating that salinity had a large effect on which factor became growth limiting at high cell densities. The causation of this salinity effect remains to be elucidated but generally indicate profound differences in cell metabolism and physiology depending on the osmotic status of the cells even when bulk parameters like growth rate and final cell yield obviously are similar.

C, N, P cell quota

A literature search did not reveal specific data on C, N, P cell quota for *Alexandrium ostenfeldii* to be compared to the cell quotas estimated here for isolate OKNL21. Nevertheless, cell quota of C, N, and P of isolate OKNL21 were in the range of values previously published for comparably large *Alexandrium* spp. (John and Flynn 1999; Zhu and Tillmann 2012). For all three elements there was the same tendency for slightly higher cell quotas of exponentially growing cells towards both ends of the salinity scale (Figure 35) with different salinities causing only minor if any changes in the particular C:N:P stoichiometry (as indicated by stable element ratios during exponential growth, Figure 36). Carbon, nitrogen, and phosphorus cell quota at exponential growth now closely mimic the observed changes in cell size (but only P quota was significantly correlated to cell size, $r = 0.58$ for C, $r = 0.72$ for N, $p > 0.05$ for both; $r = 0.87$, $p < 0.05$ for P) implying an interdependence of cell size and cell biomass, both being increased as a response to osmotic stress towards both sides of the salinity scale.

DOC/DON determination

In our study we included analysis of dissolved organic compounds (DOC and DON) in order to test the hypothesis that osmotic stress can cause an increased leakage and/or exudation of organic material from the cells, which then might be measurable as an increase in dissolved organic material. However, the culture medium used in this study obviously contains a large stock of organic carbon, most probably due to the addition of vitamins and, most importantly, of TRIS buffer, which is added to a final concentration of 1 mM. The corresponding large and variable blank values of 2.5 - 4.5 mM DOC in the freshly prepared culture medium thus probably prevented to detect comparably small changes in DOM caused by the *A. ostenfeldii* cells. With just a few exception amounts of DOM (both DOC and DON) were lower in stationary phase compared to exponential phase. Since our culture were not axenic (i.e they contained bacteria) and bacteria are known to increase in abundance in stationary algal cultures (Uribe and Espejo 2003) we assume that bacterial consumption/degradation was responsible for this decrease. However, it was reported that no bacterial degeneration of DOM was observable in *A. tamarense* cultures (Baines and Pace 1991; Chen and Wangersky 1996). Clearly more detailed targeted studies using different culture media and monitoring bacteria density and metabolism are needed when focusing on DOM dynamics in salinity tolerance/stress culture experiments.

Lytic activity

In order to avoid overlap of performing the time and labour intensive lysis bioassays in parallel to the running experiments it was decided to store cell free supernatant and cell extract for later use. Temperature stability experiments with lytic compounds produced by *Alexandrium tamarense* had indicated that lytic compounds did not lose lytic activity upon freezing: after storage at -20 °C for three months, lytic activity was still high (Ma et al. 2009). The lytic activity of *A. ostenfeldii* cultures were thus tested in defrosted culture supernatants and in cell extracts. From the supernatant of a salinity of 16, however, only undiluted samples showed some lytic activity, which is inconsistent with the experiment comparing lytic activity of the three fractions (whole culture, supernatant, cell extract), which was performed with the same sample immediately after sampling and thus should yield comparable results. This comparison, however, now showed at least 50 % loss of lytic activity after freezing. We currently do not know if this loss upon freezing is exceptional for this one sample or can generally be applied to all samples. In any case, a comparison of the EC_{50} of all analysed frozen samples indicate that in both growth phase, supernatants at a salinity of 6 showed an about 2-fold higher lytic capacity than samples at any other salinity. It is supposable that high osmotic stresses at very low salinities caused a higher amount of

extracellular lytic compounds, regardless of being caused by an active excretion or a more passive release as a result of disturbed osmoregulation. Contrary, at very high salinity (S = 34) an accumulation of lytic compounds was observed inside the cells. Therefore it is suggested that there is a distinct difference in release or accumulation of lytic compounds depending on the salinity and osmotic stress.

PSP- and cyclic imine toxin determination

As a main result of our study there was an increase in total PSP and total cyclic imine toxins in *A. ostenfeldii* growing exponentially both at the lower and higher salinities. No similar trend was observed in terms of growth suggesting that there are other mechanisms than growth which control toxin production. The increase of toxin cell quota at lower and higher salinities was most obvious for total PSP content (Figure 29) which was almost 2-fold higher at a salinity of 6 compared to 16 and/or 22. Larger cell size at low salinity might have contributed to these elevated values but are not sufficient to fully explain the large increase in toxin cell quota. In addition, cultures at low salinities tend to produce a higher amount of saxitoxin while cultures at increased salinities tend to produce even more C1/C2 toxins. Saxitoxin is reported as the most toxic PSP-compound with an equivalent toxicity of 2045 MU/µmol. In comparison, the C-toxins are distinctly less toxic (20-300 MU/µmol) (Botana 2014; Genenah and Shimizu 1981). Calculated per cell equivalents of the total toxicity in terms of mouse units (MU; as it is established by Boyer et al. (1986)) showed that at a salinity of 6 cells with a toxicity of 81.4 µMU cell^{-1} were 3-fold more toxic than cells at a salinity of 22 (at which the toxin cell quota is minimal). In comparison to salinity 34, cells at a salinity of 6 were 2-fold more toxic. This salinity-depended shift in production of low-potency C-toxins and highly toxic was not mentioned for other *Alexandrium* isolates.

As for the PSP-toxins, the cellular concentration of cyclic imine toxins was significantly higher at a salinity of 6. At this low salinity under assumed high osmotic stress, total cyclic imine toxins of exponentially growing cells were almost three-fold higher compared to cells grown at a salinity of 22. As has been noted for saxitoxin and C1/C2 toxins there were also clear salinity-dependent shifts in the ratio of single compounds: Depending on the salinity, *A. ostenfeldii* tend to produce a higher amount of gymnodimine A at low salinities or, respectively, a higher amount of 13-desmethyl spirolide C if the salinity is increased (Figure 32).

Even if the underlying physiological mechanisms and metabolic linkages remain unknown, it is clearly shown that the cell quota and relative proportion of single PSTs or spirolides are highly depended on abiotic factors like salinity.

In order to follow the hypothesis of an osmotic stress induced increase of extracellular organic compounds in *A. ostenfeldii*, we intended to detect and quantify both intracellular and extracellular toxins. Whereas initial attempt to quantify extracellular PSP-toxins using Solid Phase Extraction (SPE) or Solid Phase Adsorption Toxin Tracking (SPATT) using HP-20 resins failed because of pretty low recovery (results not shown), recovery of known amount of added dissolved cyclic imine toxins with SPE extraction was close to 100 % and this method was thus applied to the salinity experiments. To the best of our knowledge this is the first study where extracellular cyclic imine toxins have been quantified in cultures of *A. ostenfeldii*. Overall, total cyclic imine concentrations were about 10-fold higher inside the cells than were measured in the extracellular medium. These distinct differences suggest that cyclic imine compounds primarily are intracellular metabolites without an obvious role as extracellular compounds, e.g. involvement in cell communication and/or allelochemical interactions, although we cannot exclude that the molecules, when release into the environment, rapidly become undetectable either because of binding to a target sites or because of bio-transformation and/or degradation. Interestingly, extracellular cyclic imine concentrations were consistently (but more pronounced at lower salinities) higher during exponential phase compared to stationary phase, which might indicate an increased excretion of these compounds by actively growing cells or which might reflect an increased degradation in old cultures as bacterial density usually peak when algae become dense. At low salinities, the extracellular cyclic imine toxin content in exponential phase was up to 2-fold higher than it was observed for higher salinities. It is supposable that high osmotic stresses at low salinities caused a higher amount of extracellular cyclic imine toxin concentrations, regardless of being caused by an active excretion or a passive release as a result of disturbed osmoregulation. The qualitative cyclic imine toxin composition was largely similar for both extracellular and intracellular compounds. Exceptionally, no extracellular 13-desmethyl spirolide D could be detected even though high intracellular concentrations of this spirolide were present. Furthermore, extracellular spirolide D occurred in high relative and absolute amounts but only contributed little to the cyclic imine compounds inside the cells, but without more data it is difficult to speculate on potential explanations for these qualitative and quantitative shifts for certain compounds.

7 Conclusion

In conclusion, our study of multiple isolates of *A. ostenfeldii* from The Netherlands revealed that the bloom population contained the most diverse mixture of various neurotoxins ever reported for that species. Total toxin cell quota compared to other *A. ostenfeldii* isolates were fairly high, especially for the PSP-toxins, underlining the threat of such blooms for the important shellfish farming areas in The Netherlands .

Growth of a selected isolate at fixed laboratory conditions with doubling times of 0.13 to 0.2 d^{-1} was relatively slow suggesting that allelopathy and/or a reduced population loss by grazing, both facilitated by a high lytic capacity and potentially by the copepod deterrent PSP-toxins, played a significant role for bloom formation and persistence. Our data also demonstrate high intra-specific variability with respect to toxin quota, as it was earlier reported for other *A. ostenfeldii* populations. Such a high phenotypic variability may add to the success of genotypically highly diverse *A. ostenfeldii* blooms, and make populations resilient to changes in environmental and climatic conditions.

Local blooms in the brackish water of the Ouwerkerkse Kreek with its special and dynamic hydrographic situation are exposed to varying salinities and thus the ecophysiological flexibility of *A. ostenfeldii* to such variable conditions are of special interest. Growth rates measured over a broad range of salinities now clearly showed that the Dutch population of *A. ostenfeldii* is euryhaline and able to proliferate at a rather wide range of salinities, but that a lower limit for active growth seem to be set at a salinity of 3 to 5. Production of bioactive compounds, including both lytic compounds and phycotoxins, was different for different salinities with a remarkable increase in cellular PSP- and cyclic imine toxin content mainly at low but also at high salinities. Data collected in this thesis will form a scientific base for regional water managers to better understand the development of toxic *A. ostenfeldii* blooms in the creek systems and to mitigate negative effects like seafood contamination in the creek and the adjacent shellfish beds of the Oosterschelde estuary.

8 References

Aasen, J., MacKinnon, S.L., LeBlanc, P., Walter, J.A., Hovgaard, P., Aune, T., Quilliam, M.A. (2005): Detection and identification of spirolides in norwegian shellfish and plankton. *Chemical research in toxicology* **18** (3), pp. 509–515.

AB Sciex (2010): Proven quantitation and reliability. API 4000™ LC/MS/MS System.

Alpermann, T.J., Tillmann, U., Beszteri, B., Cembella, A.D., John, U. (2010): Phenotypic variation and genotypic diversity in a planktonic population of the toxigenic marine dinoflagellate *Alexandrium tamarense* (Dinophyceae). *Journal of Phycology* **46** (1), pp. 18–32.

Anderson, D.M. (1980): Effects of temperature conditioning on development and germination of *Gonyaulax tamarensis* (Dinophyceae) hypozygotes. *Journal of Phycology* **16** (2), pp. 166–172.

Anderson, D.M. (1998): Physiology and bloom dynamics of toxic *Alexandrium* species, with emphasis on life cycle transitions. *NATO ASI series* **G41**.

Anderson, D.M., Alpermann, T.J., Cembella, A.D., Collos, Y., Masseret, E., Montresor, M. (2012): The globally distributed genus *Alexandrium*: multifaceted roles in marine ecosystems and impacts on human health. *Harmful algae* **14**, pp. 10–35.

Anderson, D.M., Kulis, D.M., Binder, B.J. (1984): Sexuality and cyst formation in the dinoflagellate *Gonyaulax tamarensis*: Cyst yield in batch culutres. *Journal of Phycology* **20** (3), pp. 418–425.

Anderson, D.M., Morel, F. (1979): The seeding of two red tide blooms by the germination of benthic *Gonyaulax tamarensis* hypnocysts. *Estuarine and Coastal Marine Science* **8** (3), pp. 279–293.

Asp, T.N., Larsen, S., Aune, T. (2004): Analysis of PSP toxins in Norwegian mussels by a post-column derivatization HPLC method. *Toxicon : official journal of the International Society on Toxinology* **43** (3), pp. 319–327.

Bachvaroff, T.R., Adolf, J.E., Place, A.R. (2009): Strain variation in *Karlodinium veneficum* (Dinophyceae): toxin profiles, pigments, and growth characteristics. *Journal of Phycology* **45** (1), pp. 137–153.

Bagoien, E., Miranda, A., Reguera, B., Franco, J.M. (1996): Effects of two paralytic shellfish toxin producing dinoflagellates on the pelagic harpacticoid copepod *Euterpina acutifrons*. *Marine Biology* **126** (3), pp. 361–369.

Baines, S.B., Pace, M.L. (1991): The production of dissolved organic matter by phytoplankton and its importance to bacteria: Patterns across marine and freshwater systems. *Limnology and Oceanography* **36** (6), pp. 1078–1090.

Balech, E. (1995): The genus *Alexandrium* Halim (Dinoflagellata). Sherkin Island, Co. Cork, Ireland: Sherkin Island Marine Station.

Balech, E., de Mendiola, B.R. (1977): Un nuevo *Gonyaulax* productor de Hemotalasia en Peru. *Neotropica* **23**, pp. 49–54.

Balech, E., Tangen, K. (1985): Morphology and taxonomy of toxic species in the *tamarensis* group (Dinophyceae): *Alexandrium excavatum* (Braarud) comb. nov. and *Alexandrium ostenfeldii* (Paulsen) comb. nov. *Sarsia* **70** (4), pp. 333–343.

Banerjee, S., Mazumdar, S. (2012): Electrospray ionization mass spectrometry: a technique to access the information beyond the molecular weight of the analyte. *International journal of analytical chemistry* **2012**, pp. 1–40.

Biecheler, B. (1957): Recherche sur les peridinens. *Bulletin Biologique de la France et de la Belgique* **36**, pp. 1–149.

Bolch, C.J., Blackburn, S.I., Cannon, J.A., Hallegraeff, G.M. (1991): The resting cyst of the red-tide dinoflagellate *Alexandrium minutum* (Dinophyceae). *Phycologia* **30** (2), pp. 215–219.

Borkman, D.G., Smayda, T.J., Tomas, C.R., York, R., Strangman, W., Wright, J.L. (2012): Toxic *Alexandrium peruvianum* (Balech and de Mendiola) Balech and Tangen in Narragansett Bay, Rhode Island (USA). *Harmful Algae* **19**, pp. 92–100.

Botana, L. M. (2014): Seafood and freshwater toxins. Pharmacology, physiology, and detection. 3rd ed. Boca Raton: CRC Press/Taylor and Francis (Food Science and Technology).

Boyer, G.L., Goddard, G.D. (1999): High performance liquid chromatography coupled with post-column electrochemical oxidation for the detection of PSP toxins. *Natural toxins* **7** (6), pp. 353–359.

Boyer, G.L., Sullivan, J.J., Andersen, R.J., Harrison, P.J., Taylor, F. J. R. (1987): Effects of nutrient limitation on toxin production and composition in the marine dinoflagellate *Protogonyaulax tamarensis*. *Marine Biology* **96** (1), pp. 123–128.

Boyer, G.L., Sullivan, J.J., Andersen, R.J., Taylor, F. J. R., Harrison, P.J., Cembella, A.D. (1986): Use of high-performance liquid chromatography to investigate the production of paralytic shellfish toxins by *Protogonyaulax* spp. in culture. *Marine Biology* **93** (3), pp. 361–369.

Braarud, T. (1945): Morphological observations on marine dinoflagellate cultures (*Porella perforata, Goniaulax tamarensis, Protoceratium reticulatum*). *Avhandlinger ugitt av det Norske Videnskapsakademi i Oslo* **11**, pp. 1–18.

Burkholder, J.M., Glibert, P.M. (2009): The importance of intraspecific variability in harmful algae—Preface to a collection of topical papers. *Harmful Algae* **8** (5), pp. 744–745.

Burson, A., Matthijs, H.C., Bruijne, W. de, Talens, R., Hoogenboom, R., Gerssen, A. et al. (2014): Termination of a toxic *Alexandrium* bloom with hydrogen peroxide. *Harmful Algae* **31**, pp. 125–135.

Campàs, M., Prieto-Simón, B., Marty, J.-L. (2007): Biosensors to detect marine toxins: Assessing seafood safety. *Talanta* **72** (3), pp. 884–895.

Cembella, A., Krock, B. (2008): Cyclic imine toxins: chemistry, biogeography, biosynthesis and pharmacology. In: Luis Botana (Hg.): Seafood and Freshwater Toxins, Bd. 20080673: CRC Press (Food Science and Technology), pp. 561–580.

Cembella, A., Quilliam, M.A., Lewis, N.I., Bauder, A.G., J. L. C. Wright (1998): Identifying the planktonic origin and distribution of spirolides in coastal Nova Scotian waters. *Harmful Algae,* Xunta de Galicia and Intergovernmental Oceanographic Commission (UNESCO), Santiago de Compostela, Spain, Reguera, B., J. Blanco, M.L. Fernandez, T. Wyatt (Eds.).

Cembella, A.D. (2003): Chemical ecology of eukaryotic microalgae in marine ecosystems. *Phycologia* **42** (4), pp. 420–447.

Cembella, A.D., Lewis, N.I., Quilliam, M.A. (2000): The marine dinoflagellate *Alexandrium ostenfeldii* (Dinophyceae) as the causative organism of spirolide shellfish toxins. *Phycologia* **39** (1), pp. 67–74.

Cembella, A.D., Sullivan, J.J., Boyer, G.L., Taylor, F., Andersen, R.J. (1987): Variation in paralytic shellfish toxin composition within the *Protogonyaulax tamaronsis/catenella* species complex; red tide dinoflagellates. *Biochemical Systematics and Ecology* **15** (2), pp. 171–186.

Chang, F., Anderson, D.M., Kulis, D.M., Till, D.G. (1997): Toxin production of *Alexandrium minutum* (Dinophyceae) from the Bay of Plenty, New Zealand. *Toxicon* **35** (3), pp. 393–409.

Chen, W., Wangersky, P.J. (1996): Rates of microbial degradation of dissolved organic carbon from phytoplankton cultures. *Journal of Plankton Research* **18** (9), pp. 1521–1533.

Christian, B., Below, A., Dreßler, N., Scheibner, O., Luckas, B., Gerdts, G. (2008): Are spirolides converted in biological systems?—A study. *Toxicon* **51** (5), pp. 934–940.

Ciminiello, P., Dell'Aversano, C., Fattorusso, E., Magno, S., Tartaglione, L., Cangini, M. et al. (2006): Toxin profile of *Alexandrium ostenfeldii* (Dinophyceae) from the Northern Adriatic Sea revealed by liquid chromatography-mass spectrometry. *Toxicon : official journal of the International Society on Toxinology* **47** (5), pp. 597–604.

Ciminiello, P., Dell'Aversano, C., Fattorusso, E., Forino, M., Grauso, L., Tartaglione, L. et al. (2007): Spirolide Toxin Profile of Adriatic *Alexandrium ostenfeldii* Cultures and Structure Elucidation of 27-Hydroxy-13,19-didesmethyl Spirolide C. *Journal of Natural Products* **70** (12), pp. 1878–1883.

Ciminiello, P., Fattorusso, E. (2006): Bivalve molluscs as vectors of marine biotoxins involved in seafood poisoning. *Progress in molecular and subcellular biology* **43**, pp. 53–82.

Eaton, A. D.; Clesceri, L. S.; Greenberg, A. E.; Franson, Mary Ann H (1998): Standard methods for the examination of water and wastewater. 20th ed. Washington, DC: American Public Health Association.

Ekman, R. (2009): Mass spectrometry. Instrumentation, interpretation, and applications. Hoboken, N.J: John Wiley & Sons (Wiley-Interscience series on mass spectrometry).

Eschbach, E., Scharsack, J.P., John, U., Medlin, L.K. (2001): Improved erythrocyte lysis assay in microtitre plates for sensitive detection and efficient measurement of haemolytic compounds from ichthyotoxic algae. *Journal of applied toxicology : JAT* **21** (6), pp. 513–519.

Fistarol, G. O. (2004): The role of allelopathy in phytoplankton ecology. Kalmar: Dept. of Biology and Environmental Sciences, Univ. (Dissertation series / University of Kalmar, Faculty of Natural Science, 11).

Fux, E., McMillan, D., Bire, R., Hess, P. (2007): Development of an ultra-performance liquid chromatography-mass spectrometry method for the detection of lipophilic marine toxins. *Journal of chromatography. A* **1157** (1-2), pp. 273–280.

Genenah, A.A., Shimizu, Y. (1981): Specific toxicity of paralytic shellfish poisons. *Journal of Agricultural and Food Chemistry* **29** (6), pp. 1289–1291.

Geraci, J.R., Anderson, D.M., Timperi, R.J., St. Aubin, David J., Early, G.A., Prescott, J.H., Mayo, C.A. (1989): Humpback Whales (Megaptera novaeangliae) Fatally Poisoned by Dinoflagellate Toxin. *Canadian Journal of Fisheries and Aquatic Sciences* **46** (11), pp. 1895–1898.

Gerssen, A., Pol-Hofstad, I.E., Poelman, M., Mulder, Patrick P J, van den Top, Hester J, Boer, J. de (2010): Marine toxins: chemistry, toxicity, occurrence and detection, with special reference to the Dutch situation. *Toxins* **2** (4), pp. 878–904.

Gill, S., Murphy, M., Clausen, J., Richard, D., Quilliam, M., MacKinnon, S. et al. (2003): Neural injury biomarkers of novel shellfish toxins, spirolides: a pilot study using immunochemical and transcriptional analysis. *Neurotoxicology* **24** (4-5), pp. 593–604.

Glibert, P., Anderson, D., Gentien, P., Granéli, E., Sellner, K. (2005): The Global, Complex Phenomena of Harmful Algal Blooms. *Oceanography* **18** (2), pp. 136–147.

Gracia, S., Roy, S., Starr, M. (2013): Spatial distribution and viability of *Alexandrium tamarense* resting cysts in surface sediments from the St. Lawrence Estuary, Eastern Canada. *Estuarine, Coastal and Shelf Science* **121-122**, pp. 20–32.

Gribble, K.E., Keafer, B.A., Quilliam, M.A., Cembella, A.D., Kulis, D.M., Manahan, A., Anderson, D.M. (2005): Distribution and toxicity of *Alexandrium ostenfeldii* (Dinophyceae) in the Gulf of Maine, USA. *Deep Sea Research Part II: Topical Studies in Oceanography* **52** (19-21), pp. 2745–2763.

Gross, E., Legrand, C., Rengefors, K., Tillmann, U.: Allelochemical interactions among aquatic primary producers. In: Brönmark C, Hansson LA, (eds) Chemical Ecology in Aquatic Systems. University Press, Oxford, pp. 196–209.

Grzebyk, D., Béchemin, C., Ward, C.J., Vérite, C., Codd, G.A., Maestrini, S.Y. (2003): Effects of salinity and two coastal waters on the growth and toxin content of the dinoflagellate Alexandrium minutum. *Journal of Plankton Research* **25** (10), pp. 1185–1199.

Gu, H. (2011): Morphology, phylogenetic position, and ecophysiology of Alexandrium ostenfeldii (Dinophyceae) from the Bohai Sea, China. *Journal of Systematics and Evolution* **49** (6), pp. 606–616.

Gu, H., Zeng, N., Liu, T., Yang, W., Müller, A., Krock, B. (2013): Morphology, toxicity, and phylogeny of Alexandrium (Dinophyceae) species along the coast of China. *Harmful Algae* **27**, pp. 68–81.

Guéret, S.M., Brimble, M.A. (2010): Spiroimine shellfish poisoning (SSP) and the spirolide family of shellfish toxins: isolation, structure, biological activity and synthesis. *Natural product reports* **27** (9), pp. 1350–1366.

Hakanen, P., Suikkanen, S., Kremp, A. (2014): Allelopathic activity of the toxic dinoflagellate *Alexandrium ostenfeldii*: Intra-population variability and response of co-occurring dinoflagellates. *Harmful Algae* **39**, pp. 287–294.

Hallegraeff, G.M. (1993): A review of harmful algal blooms and their apparent global increase. *Phycologia* **32** (2), pp. 79–99.

Hallegraeff, G.M. (1998): Transport of toxic dinoflagellates via ships' ballast water: bioeconomic risk assessment and efficacy of possible ballast water management strategies. *Marine Ecology Progress Series* **168**, pp. 297–309.

Hansen, P.J. (2002): Effect of high pH on the growth and survival of marine phytoplankton: implications for species succession. *Aquatic Microbial Ecology* **28**, pp. 279–288.

Hansen, P.J., Cembella, A.D., Moestrup, O. (1992): The marine dinoflagellate *Alexandrium ostenfeldii*: Paralytic shellfish toxin concentration, composition, and toxicity to a tintinnid ciliate. *Journal of Phycology* **28** (5), pp. 597–603.

Hesse, M.; Bienz, S.; Meier, H.; Zeeh, B. (2012): Spektroskopische Methoden in der organischen Chemie. 8., überarb. und erw. Aufl. Stuttgart: Thieme.

Hopfgartner, G., Varesio, E., Tschäppät, V., Grivet, C., Bourgogne, E., Leuthold, L.A. (2004): Triple quadrupole linear ion trap mass spectrometer for the analysis of small molecules and macromolecules. *Journal of mass spectrometry : JMS* **39** (8), pp. 845–855.

Hu, T., Burton, I.W., Cembella, A.D., Curtis, J.M., Quilliam, M.A., Walter, J.A., Wright, J.L. (2001): Characterization of spirolides a, c, and 13-desmethyl c, new marine toxins isolated from toxic plankton and contaminated shellfish. *Journal of Natural Products* **64** (3), pp. 308–312.

Hu, T., Curtis, J.M., Oshima, Y., Quilliam, M.A., Walter, J.A., Watson-Wright, W.M., Wright, J.L.C. (1995): Spirolides B and D, two novel macrocycles isolated from the digestive glands of shellfish. *Journal of the Chemical Society, Chemical Communications* (20), pp. 2159.

Hu, T., Curtis, J.M., Walter, J.A., Wright, J.L. (1996): Characterization of biologically inactive spirolides E and F: Identification of the spirolide pharmacophore. *Tetrahedron Letters* **37** (43), pp. 7671–7674.

Hunt, D.F., Shabanowitz, J., Giordani, A.B. (1980): Collision activated decompositions in mixture analysis with a triple quadrupole mass spectrometer. *Analytical Chemistry* **52** (3), pp. 386–390.

Hwang, D.F., Lu, Y.H. (2000): Influence of environmental and nutritional factors on growth, toxicity, and toxin profile of dinoflagellate Alexandrium minutum. *Toxicon* **38** (11), pp. 1491–1503.

Jensen, M.Ø., Moestrup, Ø. (1997): Autecology of the toxic dinoflagellate *Alexandrium ostenfeldii*. Life history and growth at different temperatures and salinities. *European Journal of Phycology* **32** (1), pp. 9–18.

John, E.H., Flynn, K.J. (1999): Amino acid uptake by the toxic dinoflagellate *Alexandrium fundyense*. *Marine Biology* **133** (1), pp. 11–19.

John, U., Cembella, A., Hummert, C., Elbrächter, M., Groben, R., Medlin, L. (2003): Discrimination of the toxigenic dinoflagellates *Alexandrium tamarense* and *A. ostenfeldii* in co-occurring natural populations from Scottish coastal waters. *European Journal of Phycology* **38** (1), pp. 25–40.

Keller, M.D., Selvin, R.C., Claus, W., Guillard, R.R.L. (1987): Media for the culture of oceanic ultraphytoplankton. *Journal of Phycology* **23** (4), pp. 633–638.

Kentala, L.L., Sullivan, J.J., Wekell, M.M. (1985): Application of HPLC for the Determination of PSP Toxins in Shellfish. *Journal of Food Science* **50** (1), pp. 26–29.

Kharrat, R., Servent, D., Girard, E., Ouanounou, G., Amar, M., Marrouchi, R. et al. (2008): The marine phycotoxin gymnodimine targets muscular and neuronal nicotinic acetylcholine receptor subtypes with high affinity. *Journal of Neurochemistry*.

Krauss, M., Singer, H., Hollender, J. (2010): LC-high resolution MS in environmental analysis: from target screening to the identification of unknowns. *Analytical and bioanalytical chemistry* **397** (3), pp. 943–951.

Kremp, A., Lindholm, T., Dreßler, N., Erler, K., Gerdts, G., Eirtovaara, S., Leskinen, E. (2009): Bloom forming *Alexandrium ostenfeldii* (Dinophyceae) in shallow waters of the Åland Archipelago, Northern Baltic Sea. *Harmful Algae* **8** (2), pp. 318–328.

Kremp, A., Tahvanainen, P., Litaker, W., Krock, B., Suikkanen, S., Leaw, C.P. et al. (2014): Phylogenetic relationships, morphological variation, and toxin patterns in the *Alexandrium ostenfeldii* (Dinophyceae) complex: implications for species boundaries and identities. *Journal of Phycology*, pp. 1–20.

Krock, B., Seguel, C.G., Cembella, A.D. (2007): Toxin profile of *Alexandrium catenella* from the Chilean coast as determined by liquid chromatography with fluorescence detection and liquid chromatography coupled with tandem mass spectrometry. *Harmful Algae* **6** (5), pp. 734–744.

Krock, B., Tillmann, U., John, U., Cembella, A. (2008): LC-MS-MS aboard ship: tandem mass spectrometry in the search for phycotoxins and novel toxigenic plankton from the North Sea. *Analytical and bioanalytical chemistry* **392** (5), pp. 797–803.

Legrand, C., Rengefors, K., Fistarol, G.O., Granéli, E. (2003): Allelopathy in phytoplankton - biochemical, ecological and evolutionary aspects. *Phycologia* **42** (4), pp. 406–419.

Li, K.-Y., Tu, H., Ray, A.K. (2005): Charge limits on droplets during evaporation. *Langmuir : the ACS journal of surfaces and colloids* **21** (9), pp. 3786–3794.

Lilly, E.L., Halanych, K.M., Anderson, D.M. (2007): Species boundaries and global biogeography of the Alexandrium tamarense complex (Dinophyceae) 1. *Journal of Phycology* **43** (6), pp. 1329–1338.

Lim, P.-T., Ogata, T. (2005): Salinity effect on growth and toxin production of four tropical *Alexandrium* species (Dinophyceae). *Toxicon* **45** (6), pp. 699–710.

Ma, H., Krock, B., Tillmann, U., Cembella, A. (2009): Preliminary characterization of extracellular allelochemicals of the toxic marine dinoflagellate *Alexandrium tamarense* using a *Rhodomonas salina* bioassay. *Marine drugs* **7** (4), pp. 497–522.

Ma, H., Krock, B., Tillmann, U., Muck, A., Wielsch, N., Svatoš, A., Cembella, A. (2011): Isolation of activity and partial characterization of large non-proteinaceous lytic allelochemicals produced by the marine dinoflagellate *Alexandrium tamarense*. *Harmful Algae* **11**, pp. 65–72.

MacKenzie, L., Salas, M. de, Adamson, J., Beuzenberg, V. (2004): The dinoflagellate genus *Alexandrium* (Halim) in New Zealand coastal waters: comparative morphology, toxicity and molecular genetics. *Harmful Algae* **3** (1), pp. 71–92.

MacKenzie, L., White, D., Oshima, Y., Kapa, J. (1996): The resting cyst and toxicity of Alexandrium ostenfeldii (Dinophyceae) in New Zealand. *Phycologia* **35** (2), pp. 148–155.

MacKinnon, S.L., Cembella, A.D., Burton, I.W., Lewis, N., LeBlanc, P., Walter, J.A. (2006a): Biosynthesis of 13-Desmethyl Spirolide C by the Dinoflagellate *Alexandrium ostenfeldii*. *The Journal of Organic Chemistry* **71** (23), pp. 8724–8731.

MacKinnon, S.L., Walter, J.A., Quilliam, M.A., Cembella, A.D., LeBlanc, P., Burton, I.W. et al. (2006b): Spirolides isolated from Danish strains of the toxigenic dinoflagellate *Alexandrium ostenfeldii*. *Journal of Natural Products* **69** (7), pp. 983–987.

Maclean, C., Cembella, A.D., Quilliam, M.A. (2003): Effects of Light, Salinity and Inorganic Nitrogen on Cell Growth and Spirolide Production in the Marine Dinoflagellate *Alexandrium ostenfeldii* (Paulsen) Balech et Tangen. *Botanica Marina* **46** (5).

Meyer, V. R. (2006): Praxis der Hochleistungs-Flüssigchromatographie. Aktualisierte 9. Aufl. Weinheim: Wiley-VCH.

Miles, C.O., Wilkins, A.L., Stirling, D.J., MacKenzie, A.L. (2000): New Analogue of Gymnodimine from a *Gymnodinium* Species. *Journal of Agricultural and Food Chemistry* **48** (4), pp. 1373–1376.

Miles, C.O., Wilkins, A.L., Stirling, D.J., MacKenzie, A.L. (2003): Gymnodimine C, an isomer of gymnodimine B, from *Karenia selliformis*. *Journal of Agricultural and Food Chemistry* **51** (16), pp. 4838–4840.

Moestrup, Ø., Hansen, P.J. (1988): On the occurrence of the potentially toxic dinoflagellates *Alexandrium tamarense* (= *Gonyaulax excavata*) and *A. ostenfeldii* in Danish and faroese waters. *Ophelia* **28** (3), pp. 195–213.

Molgó, J., Aráoz, R., Benoit, E., Iorga, B. (2014): Cyclic Imine Toxins. Chemistry, Origin, Metabolism, Pharmacology, Toxicology, and Detection. In: Luis Botana (Hg.): Seafood and Freshwater Toxins: CRC Press, pp. 951–990.

Munday, R. (2008): Toxicology of Cyclic Imines. Gymnodimine, Spirolides, Pinnatoxins, Pteriatoxins, Prorocentrolide, Spiro-Prorocentrimine, and Symbioimines. In: Luis Botana (Hg.): Seafood and Freshwater Toxins, Bd. 20080673: CRC Press (Food Science and Technology), pp. 581–594.

Ogata, T., Kodama, M., Ishimaru, T. (1987): Toxin production in the dinoflagellate *Protogonyaulax tamarensis*. *Toxicon* **25** (9), pp. 923–928.

Paulsen, O. (1904): Plankton-Investigations in the waters round Iceland in 1903. *Meddelelser fra Kommissionen for Havundersøgelser. Series: Plankton* **1** (1), pp. 1–40.

Paulsen, O. (1949): Observations on Dinoflagellates. *Biologiske Skrifter / Kongelige Danske Videnskabernes Selskab* **6** (4), pp. 1–67.

Pedersen, F.M., Hansen, P.J. (2003): Effects of high pH on the growth and survival of six marine heterotrophic protists. *Marine Ecology Progress Series* **260**, pp. 33–41.

Quilliam, M.A., Janecek, M., Lawrence, J.F. (1993): Characterization of the oxidation products of paralytic shellfish poisoning toxins by liquid chromatography/mass spectrometry. *Rapid communications in mass spectrometry* **7** (6), pp. 482–487.

Reyero, M., Cacho, E., Martínez, A., Vázquez, J., Marina, A., Fraga, S., Franco, J.M. (1999): Evidence of saxitoxin derivatives as causative agents in the 1997 mass mortality of monk seals in the Cape Blanc Peninsula. *Natural toxins* **7** (6), pp. 311–315.

Rhodes, L., Smith, K., Selwood, A., McNabb, P., Munday, R., Suda, S. et al. (2011): Dinoflagellate *Vulcanodinium rugosum* identified as the causative organism of pinnatoxins in Australia, New Zealand and Japan. *Phycologia* **50** (6), pp. 624–628.

Roach, J.S., LeBlanc, P., Lewis, N.I., Munday, R., Quilliam, M.A., MacKinnon, S.L. (2009): Characterization of a Dispiroketal Spirolide Subclass from *Alexandrium ostenfeldii*. *Journal of Natural Products* **72** (7), pp. 1237–1240.

Röder, K., Fritz, N., Gerdts, G., Luckas, B. (2011): Accumulation and Depuration of Yessotoxin in Two Bivalves. *Journal of Shellfish Research* **30** (1), pp. 167–175.

Sánchez, S., Villanueva, P., Carbajo, L. (2004): Distribution and concentration of *Alexandrium peruvianum* (Balech and de Mendiola) in the Peruvian coast (03°24′–18°20′ LS) between 1982–2004. Cape Town, South Africa, 11/15/2004.

Sato, S., Kodama, M. (2008): Metabolism of Paralytic Shellfish Toxins Incorporated into Bivalves. In: Luis Botana (Hg.): Seafood and Freshwater Toxins, Bd. 20080673: CRC Press (Food Science and Technology), pp. 165–175.

Seki, T., Satake, M., MacKenzie, L., Kaspar, H.F., Yasumoto, T. (1995): Gymnodimine, a new marine toxin of unprecedented structure isolated from New Zealand oysters and the dinoflagellate, *Gymnodinium* sp. *Tetrahedron Letters* **36** (39), pp. 7093–7096.

Selander, E., Thor, P., Toth, G., Pavia, H. (2006): Copepods induce paralytic shellfish toxin production in marine dinoflagellates. *Proceedings. Biological sciences / The Royal Society* **273** (1594), pp. 1673–1680.

Smayda, T.J. (1997): Harmful algal blooms: Their ecophysiology and general relevance to phytoplankton blooms in the sea. *Limnology and Oceanography* **42** (5), pp. 1137–1153.

Sournia, A., Chrdtiennot-Dinet, M.-J., Ricard, M. (1991): Marine phytoplankton: how many species in the world ocean? *Journal of Plankton Research* **13** (5), pp. 1093–1099.

Suikkanen, S., Kremp, A., Hautala, H., Krock, B. (2013): Paralytic shellfish toxins or spirolides? The role of environmental and genetic factors in toxin production of the *Alexandrium ostenfeldii* complex. *Harmful Algae* **26**, pp. 52–59.

Tatters, A.O., van Wagoner, R.M., Wright, J.L., Tomas, C.R. (2012): Regulation of spiroimine neurotoxins and hemolytic activity in laboratory cultures of the dinoflagellate *Alexandrium peruvianum* (Balech & Mendiola) Balech & Tangen. *Harmful Algae* **19**, pp. 160–168.

Teegarden, G.J., Cembella, A.D. (1996): Grazing of toxic dinoflagellates, *Alexandrium* spp., by adult copepods of coastal Maine: Implications for the fate of paralytic shellfish toxins in marine food webs. *Journal of Experimental Marine Biology and Ecology* **196** (1-2), pp. 145–176.

Tillmann, U. (2003): Kill and eat your predator: a winning strategy of the planktonic flagellate *Prymnesium parvum*. *Aquatic Microbial Ecology* **32**, pp. 73–84.

Tillmann, U., Alpermann, T., John, U., Cembella, A. (2008): Allelochemical interactions and short-term effects of the dinoflagellate *Alexandrium* on selected photoautotrophic and heterotrophic protists. *Harmful Algae* **7** (1), pp. 52–64.

Tillmann, U., Alpermann, T.L., da Purificação, R.C., Krock, B., Cembella, A. (2009): Intra-population clonal variability in allelochemical potency of the toxigenic dinoflagellate *Alexandrium tamarense*. *Harmful Algae* **8** (5), pp. 759–769.

Tillmann, U., Hansen, P.J. (2009): Allelopathic effects of *Alexandrium tamarense* on other algae: evidence from mixed growth experiments. *Aquatic Microbial Ecology* **57**, pp. 101–112.

Tillmann, U., John, U. (2002): Toxic effects of *Alexandrium* spp. on heterotrophic dinoflagellates: an allelochemical defence mechanism independent of PSP-toxin content. *Marine Ecology Progress Series* **230**, pp. 47–58.

Tillmann, U., John, U., Cembella, A. (2007): On the allelochemical potency of the marine dinoflagellate *Alexandrium ostenfeldii* against heterotrophic and autotrophic protists. *Journal of Plankton Research* **29** (6), pp. 527–543.

Tillmann, U., Kremp, A., Tahvanainen, P., Krock, B. (2014): Characterization of spirolide producing *Alexandrium ostenfeldii* (Dinophyceae) from the western Arctic. *Harmful Algae* **39**, pp. 259–270.

Tomas, C.R., van Wagoner, R., Tatters, A.O., White, K.D., Hall, S., Wright, J.L. (2012): *Alexandrium peruvianum* (Balech and Mendiola) Balech and Tangen a new toxic species for coastal North Carolina. *Harmful Algae* **17**, pp. 54–63.

Touzet, N., Lacaze, J.P., Maher, M., Turrell, E., Raine, R. (2011): Summer dynamics of *Alexandrium ostenfeldii* (Dinophyceae) and spirolide toxins in Cork Harbour, Ireland. *Marine Ecology Progress Series* **425**, pp. 21–33.

Turrell, E., Stobo, L., Lacaze, J.-P., Piletsky, S., Piletska, E. (2008): Optimization of hydrophilic interaction liquid chromatography/mass spectrometry and development of solid-phase extraction for the determination of paralytic shellfish poisoning toxins. *Journal of AOAC International* **91** (6), pp. 1372–1386.

Uribe, P., Espejo, R.T. (2003): Effect of Associated Bacteria on the Growth and Toxicity of *Alexandrium catenella*. *Applied and Environmental Microbiology* **69** (1), pp. 659–662.

Vale, P. (2008): Fate of benzoate paralytic shellfish poisoning toxins from *Gymnodinium catenatum* in shellfish and fish detected by pre-column oxidation and liquid chromatography with fluorescence detection. *Journal of chromatography. A* **1190** (1-2), pp. 191–197.

van de Waal, D., Tillmann, U., Martens, H., Krock, B., van Scheppingen, Y., John, U. (in prep.): A high intra-specific variability in allelopathy and the production of multiple toxins of isolates from an *Alexandrium ostenfeldii* bloom in The Netherlands.

van Wagoner, R.M., Misner, I., Tomas, C.R., Wright, J.L. (2011): Occurrence of 12-methylgymnodimine in a spirolide-producing dinoflagellate Alexandrium peruvianum and the biogenetic implications. *Tetrahedron Letters* **52** (33), pp. 4243–4246.

Vila, M., Giacobbe, M.G., Masó, M., Gangemi, E., Penna, A., Sampedro, N. et al. (2005): A comparative study on recurrent blooms of *Alexandrium minutum* in two Mediterranean coastal areas. *Harmful Algae* **4** (4), pp. 673–695.

Weissbach, A. (2011): The role of allelopathy in microbial food webs. Växjö, Kalmar: Linnaeus University Press (Linnaeus University Dissertations, 33/2011).

Wong, J.L., Brown, M.S., Matsumoto, K., Oesterlin, R., Rapoport, H. (1971): Degradation of saxitoxin to a pyrimido (2,1-b)purine. *Journal of the American Chemical Society* **93** (18), pp. 4633–4634.

Wyatt, T., Jenkinson, I.R. (1997): Notes on *Alexandrium* population dynamics. *Journal of Plankton Research* **19** (5), pp. 551–575.

Zhu, M., Tillmann, U. (2012): Nutrient starvation effects on the allelochemical potency of *Alexandrium tamarense* (Dinophyceae). *Marine Biology* **159** (7), pp. 1449–1459.

9 List of figures

10 List of tables

Appendix

I Mass transitions and their cyclic imine toxins

Table 12: Mass transitions (m/z; precursor ion → fragment ion) and their cyclic imine toxins.

Mass transition	toxin
508→490	GYM-A
522→504	12-me GYM -A
640→164	undescribed
644→164	undescribed
650→164	H
658→164	undescribed
674→164	undescribed
678→164	13,19-didesme C
678→150	undescribed
692→164	13-desme C, G, undescribed
692→150	A, undescribed
694→164	13-desme D, undescribed, pinnatoxin G
694→150	B
696→164	undescribed
698→164	undescribed
706→164	C, 20-me G
708→164	D
710→164	undescribed
710→150	undescribed
720→164	undescribed
722→164	undescribed
766→164	pinnatoxin F
784→164	pinnatoxin E

II Limits of detection and limits of quantification

PSP-toxin determination with LC-FD

Table 13: Limit of detection and limit of quantification for a tested PSP standard solution. Values are mentioned in ng per sample. For LOQ a signal to noise ratio of 5 and for LOD a signal to noise ratio of 3 were assumed.

Standard	LOQ	LOD
C1/2	0.83	0.50
GTX 4	6.35	3.81
GTX 1	13.75	8.25
dc-GTX2	0.26	0.15
dc-GTX 3	0.23	0.14
GTX 2	0.36	0.21
GTX 5	1.54	0.92
GTX 3	0.41	0.24
NeoSTX	2.94	1.77
dc-STX	0.47	0.28
STX	0.34	0.20

Cyclic imine toxin determination with LC-MS

Table 14: Limit of detection and limit of quantifications for a SPX-1 standard solution. Values are mentioned in pg μL^{-1}. For LOQ a signal to noise ratio of 5 and for LOD a signal to noise ratio of 3 were assumed.

Standard	LOQ	LOD
SPX-1	16.67	10.0

III Experiment 1: Supplemental material

Table 15: Cyclic imine toxin contents of the isolate OKNL 21 (selected for experiment 2) and OKNL 48 (selected for experiment 3) compared to minimum, maximum and mean values of all 68 isolates. All concentrations are in fg cell^{-1}. Transitions of cyclic imine toxins are mentioned in m/z. (ND = not detectable)

Transition	Toxin	Maximum	Mean (%)	SD (%)	Minimum	OKNL21 (%)	OKNL48 (%)
508-490	**GYM-A**	**18046.50**	**4100.16 (47.2)**	**3939.38 (96.1)**	ND	**2524.46 (39.51)**	**9726.12 (80.16)**
522-504	**12-me GYM -A**	**2339.91**	**560.75 (6.5)**	**629.36 (112.2)**	ND	**1015.35 (15.89)**	**21.90 (0.18)**
640-164	undescribed	14.03	1.48 (0.02)	2.29 (155.2)	ND	2.24 (0.04)	2.08 (0.02)
644-164	undescribed	6.37	0.29 (0.00)	0.80 (278.6)	ND	0.56 (0.01)	ND
650-164	H	38.25	3.01 (0.03)	7.19 (238.8)	ND	17.89 (0.28)	ND
658-164	undescribed	54.24	12.89 (0.15)	9.10 (70.6)	1.37	7.81 (0.12)	12.45 (0.10)
674-164	**undescribed**	**1051.50**	**408.34 (4.7)**	**179.05 (43.8)**	**111.21**	**326.62 (5.11)**	**111.21 (0.92)**
678-164	13,19-didesme C	398.89	16.02 (0.18)	61.21 (382.0)	ND	4.43 (0.07)	173.94 (1.43)
678-150	undescribed	16.11	4.62 (0.05)	3.87 (83.8)	ND	4.46 (0.07)	ND
692-164	**13-desme C**	**7359.28**	**2752.23 (31.7)**	**1224.34 (44.5)**	**765.13**	**2073.50 (32.45)**	**765.13 (6.31)**
692-150	A, undescribed	33.75	10.01 (0.12)	6.74 (67.3)	ND	9.45 (0.15)	ND
694-164	**13-desme D**	**1900.74**	**627.80 (7.22)**	**300.69 (47.9)**	**160.63**	**384.42 (6.02)**	**160.63 (1.32)**
694-150	B	10.37	1.94 (0.02)	1.71 (88.2)	ND	1.95 (0.03)	ND
696-164	**undescribed**	**1093.04**	**54.66 (0.63)**	**199.87 (365.6)**	**1.61**	**8.96 (0.14)**	**1093.04 (9.01)**
698-164	undescribed	157.64	30.30 (0.35)	37.73 (124.5)	ND	ND	65.49 (0.54)
706-164	C, 20-me G	2.90	0.05 (0.00)	0.36 (661.2)	ND	ND	ND
708-164	D	14.68	3.85 (0.04)	3.85 (100.0)	ND	0.84 (0.01)	0.87 (0.01)
710-164	undescribed	57.62	21.10 (0.24)	13.87 (65.7)	0.58	5.29 (0.08)	0.58 (0.00)
710-150	undescribed	2.90	0.33 (0.00)	0.48 (148.2)	ND	ND	ND
720-164	undescribed	178.84	50.18 (0.58)	45.44 (90.5)	ND	0.28 (0.00)	ND
722-164	undescribed	60.10	19.61 (0.23)	17.78 (90.6)	ND	0.56 (0.01)	ND
766-164	pinnatoxin F	88.38	9.60 (0.11)	18.35 (191.1)	ND	ND	ND
784-164	pinnatoxin E	5.80	0.34 (0.00)	0.74 (214.4)	ND	0.84 (0.01)	ND

Table 16: The range of variability (minimum and maximum amounts), the mean amount and the standard deviations (SD) are shown for PSP-toxins of all 68 isolates and compared to OKNL 21 (selected for experiment 2) and OKNL48 (selected for experiment 3). All toxin concentrations are mentioned in pg cell^{-1}. (ND = not detectable)

	Maximum	Mean (%)	SD (%)	Minimum	OKNL21 (%)	OKNL48 (%)
C1/C2	74.4	37.9 (82.3)	15.08 (39.8)	7.2	60.81 (85.0)	36.29 (84.0)
dc GTX 2/3	0.1	0.0 (0.1)	0.01 (0.04)	ND	0.03 (0.04)	0.03 (0.07)
GTX5	0.9	0.4 (1.0)	0.20 (0.5)	ND	0.42 (0.58)	0.51 (1.17)
GTX2/3	12.8	5.8 (12.6)	2.68 (7.1)	1.5	8.06 (11.3)	4.92 (11.4)
STX	6.8	1.7 (3.6)	1.05 (2.8)	0.4	2.23 (3.1)	1.44 (3.3)

Table 17: LC-FD data of experiment 1: PSP-toxin content (pg cell^{-1}).

#	Cells mL^{-1}	C1/C2	dc GTX 2/3	GTX5	GTX2/3	STX
11	1740	40.88	ND	0.79	5.63	6.81
12	2550	30.93	0.02	0.19	4.46	0.71
13	2487	31.89	0.02	0.31	5.35	1.14
14	1290	54.90	ND	0.41	7.98	1.06
15	1905	44.19	0.04	0.33	5.79	2.00
16	1395	19.50	ND	0.26	2.41	3.41
17	1567	42.31	ND	0.36	4.02	1.04
18	2725	30.81	0.03	0.21	5.31	0.76
19	2035	69.14	0.04	0.48	9.65	2.50
20	1983	49.66	0.04	0.23	5.15	1.44
21	2497	60.81	0.03	0.42	8.06	2.23
22	1463	66.58	0.06	0.41	12.66	1.91
23	3130	27.59	0.02	0.24	3.79	0.98
24	1540	35.42	0.04	0.33	3.58	1.77
25	240	47.45	ND	ND	7.90	0.91
26	1950	38.41	ND	0.32	6.98	1.36
27	1860	67.42	0.03	0.39	10.67	2.73
28	1440	66.96	0.05	0.56	6.13	2.27
29	2100	29.69	0.02	0.36	7.78	1.91
30	1280	49.23	0.04	0.68	5.62	4.40
31	2570	24.07	0.02	0.40	2.78	2.19
32	1195	40.88	0.04	0.47	6.78	1.34
33	1150	44.76	0.04	0.59	5.25	2.13
34	1245	18.45	ND	0.26	2.79	0.88
35	1740	45.52	0.03	0.67	4.45	2.23
36	2450	32.81	0.03	0.24	4.71	1.31
37	2445	36.84	0.02	0.25	4.00	0.51
38	2705	27.96	0.02	0.28	4.90	1.47
39	1280	33.09	ND	0.22	4.85	0.68
40	1710	45.90	0.03	0.22	6.83	2.07
41	1655	15.19	ND	0.23	1.62	0.82
42	2460	34.36	0.02	0.27	4.44	1.38
43	1090	50.54	0.04	0.68	5.89	3.06
44	2005	35.87	0.03	0.33	5.02	1.89
45	1480	25.69	ND	0.28	3.58	1.02
46	2745	32.84	0.02	0.22	5.90	1.12
47	1430	46.64	0.04	0.68	5.85	3.41

Continuation Table 17

#	Cells mL^{-1}	C1/C2	dc GTX 2/3	GTX5	GTX2/3	STX
48	2410	36.29	0.03	0.51	4.92	1.44
49	1760	39.51	0.03	0.54	5.78	1.70
50	1910	53.19	0.04	0.94	6.14	1.63
51	1790	41.87	0.02	0.88	6.80	2.21
52	1990	32.79	0.02	0.56	4.12	1.27
53	1430	74.36	0.05	0.54	11.72	1.53
54	1020	32.96	0.01	0.60	7.18	1.18
55	2240	32.09	0.02	0.49	3.60	2.53
56	1630	53.76	0.03	0.83	12.35	2.13
57	2730	13.63	0.01	0.54	2.70	0.67
58	1890	43.63	0.03	0.50	7.93	0.91
59	2320	24.79	0.02	0.51	3.61	2.14
60	2900	22.33	0.01	0.41	3.97	1.32
61	2290	29.57	0.01	0.47	4.29	1.21
62	2570	19.53	0.01	0.19	3.18	0.52
63	1490	43.44	0.02	0.69	6.01	0.48
64	2110	57.14	0.04	0.80	12.78	2.31
65	2185	59.24	0.02	0.77	9.03	2.93
66	2735	24.36	0.01	0.45	4.84	1.23
67	2455	44.26	0.02	0.63	7.63	1.01
68	2435	7.20	ND	0.50	6.79	1.65
69	1880	46.47	0.03	0.71	10.85	1.03
70	2240	30.94	0.02	0.39	5.15	1.13
71	1300	59.85	0.02	0.70	11.35	3.12
72	1365	23.02	ND	0.49	3.50	0.52
73	1960	18.45	ND	0.60	3.05	2.56
74	3115	9.00	ND	0.22	1.76	0.37
75	2370	30.15	0.02	0.19	2.67	0.56
76	2165	32.89	0.03	0.33	3.85	0.92
77	3715	12.50	ND	0.12	1.51	0.48
78	3175	29.99	0.02	0.24	4.32	0.72

Table 18: LC-MS data of experiment 1: Cyclic imine toxin concentrations (fg cell^{-1}) of all isolates and their respective transitions (m/z). (ND = not detectable)

#	Cells mL^{-1}	508-490	522-504	640-164	644-164	650-164	658-164	674-164	678-164	678-150	692-164	692-150	694-164	694-150	696-164	698-164	706-164	708-164	710-164	710-150	720-164	722-164	766-164	784-164
11	1740	1122.60	333.79	ND	ND	ND	11.77	558.18	4.00	6.40	3475.45	13.95	702.99	2.80	17.90	ND	ND	2.40	7.60	1.20	85.17	24.35	0.40	0.40
12	2550	2771.26	1034.97	0.58	ND	1.26	9.16	306.32	1.37	3.00	2084.03	12.04	437.47	2.46	7.36	3.00	ND	0.55	2.73	0.27	1.63	0.27	0.27	ND
13	2487	879.78	ND	0.28	ND	0.52	7.06	235.82	2.24	2.52	1538.35	4.20	392.42	1.40	9.30	39.79	ND	0.56	9.13	0.28	0.56	0.56	58.59	0.56
14	1290	2066.05	1534.40	0.54	ND	2.02	17.54	371.12	3.46	3.78	2610.26	2.70	541.58	0.54	12.31	0.54	ND	6.48	20.60	ND	43.15	29.65	ND	1.08
15	1905	18046.50	13.85	4.42	ND	0.37	24.65	634.88	3.66	16.11	4208.52	16.11	984.79	2.19	18.52	14.31	ND	3.29	14.07	ND	ND	0.37	88.38	0.37
16	1395	1835.86	659.67	0.58	0.50	ND	5.57	223.32	3.99	1.50	1449.92	4.50	376.03	0.50	6.73	0.50	ND	2.99	10.38	0.50	31.36	19.54	ND	0.50
17	1567	10029.86	33.69	ND	0.89	0.44	11.57	425.47	4.88	2.22	2661.04	5.34	630.17	3.55	7.37	0.89	ND	5.78	19.74	0.89	ND	ND	ND	0.44
18	2725	2293.82	831.51	3.53	ND	0.26	16.56	534.62	3.32	10.51	3505.30	17.40	791.00	1.53	18.83	9.16	ND	3.32	17.23	0.26	0.26	ND	64.81	0.51
19	2035	3020.38	1360.88	0.73	ND	ND	8.89	272.40	3.80	1.37	1699.69	5.82	354.57	0.68	3.55	ND	ND	0.34	8.55	0.34	ND	ND	48.63	0.34
20	1983	8535.55	53.40	0.35	0.70	0.35	16.52	449.27	5.41	2.46	3002.85	14.09	643.30	3.86	15.25	16.86	ND	1.76	12.94	1.05	ND	ND	ND	0.70
21	2497	2524.46	1015.35	2.24	0.56	17.89	7.81	326.62	4.43	4.46	2073.50	9.45	384.42	1.95	8.96	ND	ND	0.84	5.29	ND	0.28	0.56	ND	0.84
22	1463	12814.55	18.04	0.48	ND	ND	11.41	374.12	0.95	5.23	2379.34	14.28	568.22	0.95	10.36	80.62	ND	0.95	23.64	1.43	78.42	41.33	0.48	ND
23	3130	6601.24	ND	1.90	0.22	0.22	11.12	366.65	4.45	6.67	2480.91	10.68	646.94	0.44	7.61	0.67	ND	0.89	9.37	0.22	56.94	23.13	ND	0.22
24	1540	ND	17.14	0.46	0.45	1.36	2.71	223.11	4.97	0.90	1665.92	4.52	355.49	0.45	4.22	42.54	ND	0.45	12.14	ND	0.45	0.45	0.90	0.45
25	240	2868.50	329.90	2.55	ND	ND	8.70	493.44	ND	5.80	2825.12	11.64	754.00	ND	12.03	2.90	2.90	ND	11.64	2.90	43.52	11.64	46.19	5.80
26	1950	1028.42	650.00	0.87	ND	ND	7.14	287.80	ND	1.79	1762.03	5.36	350.06	1.07	7.04	1.07	ND	1.07	6.79	1.07	53.92	15.39	0.71	0.71
27	1860	938.16	ND	3.17	6.37	ND	19.46	541.87	4.50	4.11	3435.95	13.05	907.63	7.66	18.97	80.42	ND	1.12	17.36	ND	96.55	35.22	0.37	0.37
28	1440	2224.62	ND	ND	ND	ND	21.32	582.20	16.86	ND	4040.43	17.34	854.22	ND	21.63	157.64	ND	ND	31.02	ND	66.17	22.75	ND	ND
29	2100	2100.09	806.14	0.32	0.66	9.64	5.64	215.97	3.64	ND	1407.10	5.64	328.32	ND	5.16	41.12	ND	0.66	21.60	0.33	32.83	12.54	ND	0.66
30	1280	13090.01	ND	ND	ND	0.54	5.98	236.22	3.81	3.26	1644.60	3.81	366.86	1.09	5.64	75.52	ND	ND	8.23	ND	1.09	ND	0.54	1.09
31	2570	1344.44	513.46	ND	0.54	0.54	7.58	219.26	0.81	1.90	1568.68	3.79	319.98	1.90	7.02	0.54	ND	0.27	8.42	0.27	43.32	17.65	0.27	ND
32	1195	2121.33	864.51	0.59	0.58	ND	2.91	291.36	ND	ND	1876.60	ND	348.87	ND	2.42	28.56	ND	ND	44.66	0.58	37.38	5.83	ND	1.17
33	1150	4152.00	2091.10	ND	0.61	0.61	10.90	414.31	4.24	3.03	2629.25	5.44	673.25	1.82	8.78	0.61	ND	7.27	23.70	ND	72.70	33.26	23.50	ND
34	1245	1973.38	1506.18	ND	1.12	20.05	10.06	447.09	2.80	2.80	2667.81	8.39	618.20	1.68	22.08	3.35	ND	2.24	14.30	0.56	64.21	36.43	41.58	0.56
35	1740	1227.38	75.84	14.03	ND	1.20	54.24	776.71	398.89	5.20	5134.18	23.17	1192.71	4.00	970.23	140.86	ND	9.11	32.52	0.40	105.58	36.07	0.40	ND
36	2450	2044.57	776.02	2.94	0.28	ND	9.63	403.90	4.83	3.12	2804.86	10.75	567.52	3.12	7.37	15.89	ND	3.53	12.43	0.85	73.58	36.37	ND	ND
37	2445	4828.95	2339.91	2.97	0.57	ND	11.15	423.46	1.42	5.12	2754.38	15.65	579.92	3.70	13.87	50.68	ND	2.87	17.24	0.28	84.88	42.16	0.57	0.28

Continuation Table 18

#	Cells mL^{-1}	508-490	522-504	640-164	644-164	650-164	658-164	674-164	678-164	678-150	692-164	692-150	694-164	694-150	696-164	698-164	706-164	708-164	710-164	710-150	720-164	722-164	766-164	784-164
38	2705	1726.66	1110.46	1.63	0.26	0.26	10.84	425.10	4.12	3.09	2896.11	12.11	721.49	1.03	12.53	25.24	ND	3.86	19.98	ND	70.29	28.03	0.26	ND
39	1280	5256.35	41.24	ND	ND	3.26	4.35	209.38	ND	2.18	1286.69	1.09	263.07	1.09	3.95	25.59	ND	1.09	18.43	ND	ND	ND	13.37	ND
40	1710	1446.91	ND	1.10	ND	0.41	20.76	541.18	8.14	7.73	3737.35	14.20	896.16	1.22	13.09	31.35	0.81	2.85	25.05	ND	140.65	57.87	0.41	0.41
41	1655	1337.63	655.70	1.56	ND	ND	5.05	262.97	0.42	1.69	1826.97	1.26	487.19	0.84	11.78	0.42	ND	3.78	12.32	0.42	33.63	18.55	ND	ND
42	2460	2329.17	1245.75	1.53	0.28	ND	14.99	593.14	5.04	4.81	3752.55	16.67	889.25	1.98	21.42	84.64	ND	4.25	19.83	ND	92.28	44.97	ND	0.57
43	1090	14177.06	169.65	ND	ND	38.25	16.62	418.20	2.56	0.64	3005.15	10.86	613.64	1.28	9.27	0.64	ND	1.28	16.60	1.28	178.84	60.10	0.64	ND
44	2005	10175.28	26.33	ND	0.35	ND	24.56	660.34	7.64	12.45	4706.94	18.74	1137.89	2.08	16.57	ND	ND	13.60	44.44	ND	121.10	38.50	26.51	ND
45	1480	3795.21	1407.80	3.99	ND	0.94	19.19	676.36	3.30	7.06	4380.07	23.53	1163.89	3.30	22.91	119.48	ND	11.76	55.56	ND	0.94	1.75	0.47	ND
46	2745	6546.67	28.84	1.89	ND	ND	8.24	237.83	1.52	4.06	1468.68	4.56	340.47	1.78	5.00	38.55	ND	0.25	7.35	0.25	0.25	ND	22.11	ND
47	1430	4061.47	1936.63	0.50	0.49	27.23	17.78	430.90	1.95	5.35	2931.37	4.87	539.82	2.43	11.10	0.49	ND	0.97	14.96	ND	0.49	ND	ND	ND
48	2410	9726.12	21.90	2.08	ND	ND	12.45	111.21	173.94	ND	765.13	ND	160.63	ND	1093.04	65.49	ND	0.87	0.58	ND	ND	ND	ND	ND
49	1760	10358.56	ND	2.82	ND	0.79	11.28	372.23	2.37	0.40	2589.98	9.89	590.88	0.40	11.08	94.10	ND	0.40	23.04	0.40	105.55	39.57	1.98	0.40
50	1910	459.07	69.09	3.14	0.73	ND	16.79	574.46	3.65	8.02	3969.64	21.11	979.82	4.38	25.66	ND	ND	7.65	37.18	ND	101.34	52.53	ND	ND
51	1790	6547.47	ND	0.78	ND	0.78	7.32	162.52	ND	0.39	1089.01	0.78	198.35	1.56	1.61	55.67	ND	0.39	11.97	0.78	60.66	10.89	9.43	ND
52	1990	3180.29	1060.10	0.38	ND	1.40	22.45	602.01	8.75	4.20	4143.86	16.12	947.33	2.80	18.53	66.30	ND	10.14	39.14	ND	92.32	27.97	13.24	0.70
53	1430	4686.77	1863.78	ND	ND	0.49	17.46	786.51	2.92	12.17	5173.95	17.94	989.94	4.87	14.64	106.68	ND	9.74	44.37	0.49	164.99	56.55	45.49	ND
54	1020	1063.90	620.47	0.66	ND	18.44	1.37	183.70	2.05	1.37	1367.64	5.46	332.37	1.37	11.32	27.62	ND	6.83	13.52	ND	36.83	5.46	17.05	0.68
55	2240	8293.89	82.55	ND	ND	0.31	9.33	364.05	1.86	5.29	2474.70	7.45	586.98	0.93	12.88	14.32	ND	4.97	16.05	ND	88.56	36.71	ND	ND
56	1630	14486.85	16.19	0.44	ND	0.43	18.41	697.03	6.83	11.96	4721.80	13.24	972.47	2.56	20.38	0.85	ND	12.16	57.62	0.85	82.49	36.68	8.40	ND
57	2730	938.11	569.22	ND	0.26	0.26	8.89	281.92	1.28	3.57	2064.09	8.16	448.06	2.80	11.08	0.26	ND	5.87	15.94	0.26	ND	ND	ND	ND
58	1890	2333.43	1258.58	4.35	0.74	12.12	25.09	705.37	6.63	11.79	4944.86	26.18	1123.50	4.05	19.15	0.74	ND	10.68	45.33	ND	111.99	41.21	9.47	0.37
59	2320	2320.05	752.14	2.47	ND	0.30	6.00	275.47	1.50	4.50	1945.07	9.00	443.32	1.20	12.74	56.08	ND	1.50	9.45	ND	0.90	ND	ND	ND
60	2900	1619.54	526.87	ND	ND	0.24	5.47	251.97	1.92	0.96	1595.55	2.88	379.14	0.48	6.22	ND	ND	2.64	13.66	0.24	0.24	ND	6.51	ND
61	2290	1899.31	689.97	0.31	ND	ND	6.99	264.07	ND	0.91	1870.52	8.21	356.10	1.22	878.24	46.81	ND	1.22	8.25	0.30	ND	ND	14.20	0.30
62	2570	3411.78	10.27	ND	ND	ND	5.17	218.37	1.09	2.71	1452.82	4.61	395.74	0.81	10.70	ND	ND	3.52	18.18	ND	31.73	14.62	ND	0.54
63	1490	2441.30	1241.04	0.45	1.40	0.93	5.13	307.47	0.47	1.40	2306.01	5.13	544.22	1.88	13.08	58.88	ND	0.47	26.44	0.47	0.47	ND	30.75	ND
64	2110	130.84	250.16	1.88	ND	20.08	17.15	517.84	6.60	13.24	3723.64	13.90	803.35	1.65	5.47	22.15	ND	7.91	35.93	ND	123.76	44.51	0.33	ND

Continuation Table 18

#	Cells mL^{-1}	508-490	522-504	640-164	644-164	650-164	658-164	674-164	678-164	678-150	692-164	692-150	694-164	694-150	696-164	698-164	706-164	708-164	710-164	710-150	720-164	722-164	766-164	784-164
65	2185	687.37	12.08	0.32	ND	ND	10.48	444.50	6.37	6.69	3281.32	16.88	730.70	1.91	11.22	37.64	ND	14.68	51.58	0.32	81.25	37.01	1.42	ND
66	2735	3364.66	9.65	0.51	ND	0.25	3.31	201.01	1.02	1.27	1381.92	5.09	370.19	1.02	9.46	0.25	ND	3.31	11.81	ND	28.98	18.59	ND	ND
67	2455	806.26	21.50	1.61	ND	0.28	12.22	467.46	4.12	4.82	3209.69	9.61	712.85	1.42	2.65	ND	ND	4.25	23.05	ND	75.67	27.52	14.93	0.57
68	2435	7344.48	54.19	1.34	ND	0.86	14.58	478.82	7.43	4.57	3094.95	14.30	997.16	3.43	11.01	26.90	ND	7.15	37.72	ND	0.29	ND	0.29	ND
69	1880	5079.58	2050.30	7.36	ND	1.49	40.33	1051.50	11.86	13.65	7359.28	33.75	1900.74	10.37	27.66	61.90	ND	8.15	45.57	ND	6.30	ND	0.74	ND
70	2240	2662.57	1011.55	9.24	0.31	ND	40.90	480.62	285.31	12.78	3159.85	14.93	695.37	2.80	33.85	106.35	ND	2.48	19.33	ND	90.09	35.69	0.62	0.31
71	1300	166.28	81.47	1.50	ND	13.39	16.60	518.04	1.07	2.68	3647.40	8.03	792.91	2.68	19.91	1.07	ND	13.39	55.68	0.54	91.63	23.08	ND	0.54
72	1365	775.93	795.01	0.95	ND	3.57	8.02	273.53	ND	3.05	1778.81	6.13	429.60	1.02	6.34	ND	ND	1.02	18.79	1.02	34.74	17.28	ND	0.51
73	1960	6156.75	ND	ND	0.36	ND	14.26	414.89	12.74	1.43	2921.73	8.52	787.70	1.78	8.84	11.01	ND	4.62	25.94	0.36	68.95	24.54	0.36	ND
74	3115	2870.60	16.94	0.22	0.22	ND	4.20	182.37	0.22	2.46	1103.03	4.25	234.58	0.67	4.63	ND	ND	0.67	9.63	ND	43.39	13.16	ND	ND
75	2370	2238.13	736.28	ND	ND	0.29	8.93	393.37	1.47	6.17	2706.24	8.51	514.18	2.35	7.93	23.78	ND	2.06	20.20	0.29	0.29	0.29	0.29	ND
76	2165	1110.75	ND	1.46	ND	ND	10.90	541.71	4.82	7.08	3904.13	ND	705.71	ND	14.71	ND	ND	1.93	19.68	ND	84.54	33.43	ND	ND
77	3715	2079.81	794.53	ND	0.19	0.19	4.39	167.10	0.19	2.06	1220.85	4.31	210.87	0.75	2.53	9.00	ND	0.94	2.06	ND	31.14	12.39	36.81	0.19
78	3175	6234.25	33.36	0.42	ND	0.22	11.47	385.26	3.73	10.32	2806.48	9.02	632.00	2.63	12.26	32.25	ND	7.86	19.26	0.22	60.96	28.71	0.22	0.22

IV Experiment 2: Supplemental material

Cell counts for growth rate determination

Table 19: Cell counts of the triplicate cultures at S = 4.5. No sample takings were done for toxin and elemental analysis.

Date	Day	Sample [µL]	1st Culture		2nd Culture		3rd Culture	
			Count	Cells mL^{-1}	Count	Cells mL^{-1}	Count	Cells mL^{-1}
10.06.2014	1	1000	184	184	176	176	179	179
12.06.2014	3	1000	134	134	198	198	154	154
14.06.2014	5	1000	162	162	192	192	179	179
16.06.2014	7	1000	148	148	142	142	139	139
18.06.2014	9	1000	156	156	154	154	152	152
20.06.2014	11	1000	174	174	186	186	158	158
22.06.2014	13	1000	121	121	142	142	151	151
24.06.2014	15	1000	154	154	116	116	133	133
26.06.2014	17	1000	141	141	106	106	124	124
28.06.2014	19	1000	127	127	153	153	179	179
30.06.2014	21	1000	151	151	189	189	121	121
02.07.2014	23	1000	154	154	196	196	124	124
04.07.2014	25	1000	122	122	154	154	116	116
06.07.2014	27	1000	156	156	131	131	113	113
08.07.2014	29	1000	124	124	119	119	136	136
10.07.2014	31	1000	123	123	132	132	131	131
12.07.2014	33	1000	132	132	125	125	133	133
14.07.2014	35	1000	127	127	109	109	123	123
16.07.2014	37	1000	120	120	119	119	117	117
18.07.2014	39	1000	112	112	122	122	109	109
20.07.2014	41	1000	106	106	124	124	119	119

Table 20: Cell counts of the triplicate cultures at S = 6. Sample takings are grayed out.

Date	Day	Sample [µL]	1st Culture		2nd Culture		3rd Culture	
			Count	Cells mL^{-1}	Count	Cells mL^{-1}	Count	Cells mL^{-1}
15.05.2014	1	1000	297	297	303	303	297	297
17.05.2014	3	1000	301	301	297	297	296	296
19.05.2014	5	1000	302	302	314	314	364	364
21.05.2014	7	1000	506	506	487	487	469	469
23.05.2014	9	800	494	618	449	561	491	614
25.05.2014	11	500	462	924	429	858	397	794
27.05.2014	13	200	231	1155	239	1195	199	995
29.05.2014	15	200	276	1380	291	1455	269	1345
31.05.2014	17	150	254	1693	258	1720	246	1640
02.06.2014	19	150	356	2373	329	2193	334	2227
04.06.2014	21	100	297	2970	281	2810	287	2870
06.06.2014	23	100	381	3810	386	3860	388	3880
08.06.2014	25	50	229	4580	234	4680	238	4760
10.06.2014	27	50	304	6080	306	6120	318	6360
12.06.2014	29	30	218	7267	224	7467	234	7800
16.06.2014	33	30	292	9733	286	9533	278	9267
18.06.2014	35	30	328	10933	304	10133	301	10033
20.06.2014	37	30	418	13933	358	11933	319	10633
22.06.2014	39	30	384	12800	324	10800	410	13667
24.06.2014	41	30	336	11200	360	12000	361	12033

Table 21: Cell counts of the triplicate cultures at S = 10. Sample takings are grayed out.

Date	Day	Sample [µL]	1st Culture		2nd Culture		3rd Culture	
			Count	Cells mL^{-1}	Count	Cells mL^{-1}	Count	Cells mL^{-1}
11.04.2014	1	1000	337	337	328	328	319	319
13.04.2014	3	1000	436	436	428	428	433	433
15.04.2014	5	1000	526	526	453	453	554	554
17.04.2014	7	800	559	699	491	614	614	768
19.04.2014	9	500	464	928	482	964	543	1086
21.04.2014	11	500	848	1696	829	1658	921	1842
23.04.2014	13	100	298	2980	254	2540	261	2610
25.04.2014	15	100	342	3420	386	3860	364	3640
27.04.2014	17	90	451	5011	467	5189	476	5289
29.04.2014	19	80	547	6838	546	6825	537	6713
01.05.2014	21	40	309	7725	304	7600	321	8025
03.05.2014	23	40	384	9600	388	9700	374	9350
05.05.2014	25	40	494	12350	508	12700	496	12400
07.05.2014	27	30	329	10967	368	12267	324	10800
09.05.2014	29	30	279	9300	382	12733	276	9200

Table 22: Cell counts of the triplicate cultures at S = 16. Sample takings are grayed out.

Date	Day	Sample [µL]	1st Culture		2nd Culture		3rd Culture	
			Count	Cells mL^{-1}	Count	Cells mL^{-1}	Count	Cells mL^{-1}
07.04.2014	1	1000	289	289	286	286	291	291
09.04.2014	3	1000	333	333	332	332	345	345
11.04.2014	5	1000	389	389	401	401	404	404
13.04.2014	7	1000	520	520	528	528	519	519
15.04.2014	9	1000	646	646	681	681	591	591
17.04.2014	11	800	696	870	720	900	614	768
19.04.2014	13	500	716	1432	658	1316	612	1224
21.04.2014	15	500	1012	2024	1098	2196	995	1990
22.04.2014	16	300	771	2570	778	2593	743	2477
23.04.2014	17	150	304	2027	342	2280	343	2287
25.04.2014	19	100	272	2720	296	2960	276	2760
27.04.2014	21	90	334	3711	366	4067	381	4233
29.04.2014	23	80	422	5275	423	5288	431	5388
01.05.2014	25	40	264	6600	266	6650	267	6675
03.05.2014	27	40	339	8475	332	8300	337	8425
05.05.2014	29	40	386	9650	389	9725	386	9650
07.05.2014	31	30	304	10133	314	10467	339	11300
09.05.2014	33	30	346	11533	371	12367	346	11533
11.05.2014	35	30	334	11133	330	11000	336	11200
13.05.2014	37	30	306	10200	294	9800	288	9600

Table 23: Cell counts of the triplicate cultures at S = 22. Sample takings are grayed out.

Date	Day	Sample [µL]	1st Culture		2nd Culture		3rd Culture	
			Count	Cells mL^{-1}	Count	Cells mL^{-1}	Count	Cells mL^{-1}
21.04.2014	1	1000	311	311	297	297	317	317
23.04.2014	3	900	468	520	397	441	412	458
25.04.2014	5	700	446	637	424	606	445	636
27.04.2014	7	600	529	882	538	897	566	943
29.04.2014	9	500	638	1276	665	1330	637	1274
01.05.2014	11	250	614	2456	587	2348	519	2076
03.05.2014	13	100	401	4010	374	3740	341	3410
05.05.2014	15	75	384	5120	362	4827	387	5160
07.05.2014	17	60	342	5700	319	5317	368	6133
09.05.2014	19	50	286	5720	264	5280	316	6320
11.05.2014	21	50	406	8120	416	8320	327	6540
13.05.2014	23	30	284	9467	279	9300	234	7800
15.05.2014	25	30	289	9633	278	9267	298	9933
17.05.2014	27	30	248	8267	279	9300	346	11533

Table 24: Cell counts of the triplicate cultures at S = 28. Sample takings are grayed out.

Date	Day	Sample [µL]	1st Culture		2nd Culture		3rd Culture	
			Count	Cells mL^{-1}	Count	Cells mL^{-1}	Count	Cells mL^{-1}
13.05.2014	1	1000	298	298	289	289	310	310
15.05.2014	3	1000	419	419	413	413	389	389
17.05.2014	5	900	548	609	479	532	482	536
19.05.2014	7	800	606	758	688	860	489	611
21.05.2014	9	400	478	1195	442	1105	319	798
23.05.2014	11	250	372	1488	384	1536	269	1076
25.05.2014	13	150	331	2207	310	2067	271	1807
27.05.2014	15	100	267	2670	289	2890	284	2840
29.05.2014	17	75	329	4387	341	4547	321	4280
31.05.2014	19	50	247	4940	242	4840	247	4940
02.06.2014	21	50	274	5480	276	5520	278	5560
04.06.2014	23	30	184	6133	175	5833	174	5800
06.06.2014	25	30	204	6800	248	8267	252	8400
08.06.2014	27	30	228	7600	301	10033	254	8467
10.06.2014	29	30	279	9300	314	10467	304	10133
12.06.2014	31	30	364	12133	401	13367	336	11200
14.06.2014	33	30	328	10933	401	13367	284	9467
16.06.2014	35	30	301	10033	359	11967	314	10467

Table 25: Cell counts of the triplicate cultures at S = 34. Sample takings are grayed out.

Date	Day	Sample [µL]	1st Culture		2nd Culture		3rd Culture	
			Count	Cells mL^{-1}	Count	Cells mL^{-1}	Count	Cells mL^{-1}
19.05.2014	1	1000	279	279	268	268	291	291
21.05.2014	3	1000	254	254	269	269	241	241
23.05.2014	5	1000	244	244	218	218	207	207
25.05.2014	7	1000	278	278	302	302	322	322
27.05.2014	9	1000	299	299	305	305	453	453
29.05.2014	11	1000	378	378	501	501	720	720
31.05.2014	13	800	386	483	471	589	623	779
02.06.2014	15	500	427	854	473	946	621	1242
04.06.2014	17	250	272	1088	321	1284	409	1636
06.06.2014	19	200	341	1705	330	1650	374	1870
08.06.2014	21	100	308	3080	309	3090	321	3210
10.06.2014	23	75	284	3787	286	3813	309	4120
12.06.2014	25	60	251	4183	266	4433	284	4733
14.06.2014	27	50	249	4980	338	6760	334	6680
16.06.2014	29	30	185	6167	214	7133	212	7067
18.06.2014	31	30	257	8567	238	7933	226	7533
20.06.2014	33	30	256	8533	296	9867	332	11067
22.06.2014	35	30	298	9933	371	12367	334	11133
24.06.2014	37	30	346	11533	331	11033	279	9300
26.06.2014	39	30	274	9133	331	11033	294	9800
28.06.2014	41	30	316	10533	305	10167	301	10033

Quantification of the lytic capacity

Table 26: Comparison of cultures fractions: *R. salina* bioassay of the supernatant fraction of a triplicate culture at S = 16 in exponential growth phase (n = 2, ± 1 SD).

A. ostenfeldii (mL^{-1})	1.) *R. salina* (% of control)	2.) *R. salina* (% of control)	Mean	SD
Culture 1				
2506	13.42	12.92	13.17	0.25
1285	28.02	30.37	29.19	1.17
964	42.95	47.99	45.47	2.52
643	69.63	75.84	72.73	3.10
321	97.82	97.15	97.48	0.34
161	98.32	100.00	99.16	0.84
Culture 2				
2529	13.93	16.28	15.10	1.17
1297	35.91	38.76	37.33	1.43
973	55.54	54.03	54.78	0.76
648	87.92	73.49	80.70	7.21
324	109.56	102.68	106.12	3.44
162	102.01	96.14	99.08	2.94
Culture 3				
2415	12.58	14.60	13.59	1.01
1238	36.58	34.40	35.49	1.09
929	49.16	48.66	48.91	0.25
619	78.19	68.79	73.49	4.70
310	104.03	102.35	103.19	0.84
155	105.70	102.52	104.11	1.59

Table 27: Comparison of cultures fractions: *R. salina* bioassay of the whole cell culture of a triplicate culture at S = 16 in exponential growth phase (n = 2, ± 1 SD)

A. ostenfeldii (mL^{-1})	1.) *R. salina* (% of control)	2.) *R. salina* (% of control)	Mean	SD
Culture 1				
2506	0.17	0.00	0.08	0.08
1285	12.24	19.18	15.71	3.47
964	26.13	29.27	27.70	1.57
643	39.53	52.43	45.98	6.45
321	96.58	101.05	98.81	2.23
161	98.73	101.71	100.22	1.49
Culture 2				
2529	0.00	0.00	0.00	0.00
1297	11.25	16.04	13.64	2.40
973	28.78	26.79	27.78	0.99
648	52.92	58.05	55.49	2.56
324	94.27	106.50	100.39	6.12
162	100.88	107.66	104.27	3.39
Culture 3				
2415	0.17	0.33	0.25	0.08
1238	7.44	10.42	8.93	1.49
929	22.49	22.66	22.57	0.08
619	50.94	37.38	44.16	6.78
310	104.36	86.82	95.59	8.77
155	103.53	100.39	101.96	1.57
93	n/a	100.88	100.88	0.00

Table 28: Comparison of salinity treatments: *R. salina* bioassay of the supernatant fraction of the first culture at a salinity of 6. (n = 2, ± 1 SD)

A. ostenfeldii (mL^{-1})	1.) *R. salina* (% of control)	2.) *R. salina* (% of control)	Mean	SD
Exponential growth phase				
2314	3.6	4.8	4.2	0.6
1187	20.9	29.4	25.1	4.3
890	30.7	41.7	36.2	5.5
593	58.6	63.8	61.2	2.6
297	95.4	81.3	88.3	7.0
148	95.5	99.6	97.6	2.0
Stationary growth phase				
10920	0.0	0.0	0.0	0.0
5600	0.0	0.0	0.0	0.0
2800	0.0	0.2	0.1	0.1
2100	1.1	2.1	1.6	0.5
1400	0.7	1.6	1.1	0.5
840	6.9	7.7	7.3	0.4
560	8.5	11.2	9.8	1.3
280	41.7	47.4	44.5	2.9
140	89.6	83.8	86.7	2.9
70	95.1	92.8	94.0	1.1
28	94.5	97.1	95.8	1.3

Table 29: Comparison of salinity treatments: *R. salina* bioassay of the supernatant fraction of the second culture at a salinity of 6. (n = 2, ± 1 SD)

A. ostenfeldii (mL^{-1})	1.) *R. salina* (% of control)	2.) *R. salina* (% of control)	Mean	SD
Exponential growth phase				
2138	6.95	8.20	7.58	0.62
1097	32.62	34.58	33.60	0.98
822	49.02	52.94	50.98	1.96
548	78.43	67.20	72.82	5.61
274	88.06	94.30	91.18	3.12
137	103.21	95.90	99.55	3.65
Stationary growth phase				
11700	0.00	0.00	0.00	0.00
6000	0.00	0.00	0.00	0.00
3000	0.16	0.16	0.16	0.00
2250	0.16	0.16	0.16	0.00
1500	1.31	0.98	1.15	0.16
900	4.43	5.58	5.00	0.57
600	13.12	14.93	14.02	0.90
300	43.96	44.94	44.45	0.49
150	81.19	86.28	83.73	2.54
75	92.18	92.18	92.18	0.00
30	95.79	96.28	96.04	0.25

Table 30: Comparison of salinity treatments: *R. salina* bioassay of the supernatant fraction of the third culture at a salinity of 6. (n = 2, ± 1 SD)

A. ostenfeldii (mL^{-1})	1.) *R. salina* (% of control)	2.) *R. salina* (% of control)	Mean	SD
Exponential growth phase				
2171	12.83	14.08	13.46	0.62
1114	40.82	39.22	40.02	0.80
835	62.39	66.67	64.53	2.14
557	86.27	86.45	86.36	0.09
278	98.40	91.80	95.10	3.30
139	100.71	100.00	100.36	0.36
Stationary growth phase				
11732	0.00	0.00	0.00	0.00
6017	0.00	0.00	0.00	0.00
3008	0.16	0.00	0.08	0.08
2256	0.16	0.00	0.08	0.08
1504	1.48	2.79	2.13	0.66
902	7.87	11.32	9.60	1.72
602	21.49	18.53	20.01	1.48
301	59.54	52.98	56.26	3.28
150	90.05	97.27	93.66	3.61
75	94.64	97.10	95.87	1.23
30	n/a	100.22	100.22	0.00

Table 31: Comparison of salinity treatments: *R. salina* bioassay of the supernatant fraction of the first culture at a salinity of 16. (n = 2, ± 1 SD)

A. ostenfeldii (mL^{-1})	1.) *R. salina* (% of control)	2.) *R. salina* (% of control)	Mean	SD
Exponential growth phase				
2506	94.81	98.23	96.52	1.71
1285	94.24	100.13	97.18	2.94
964	92.53	88.92	90.72	1.80
Stationary growth phase				
9945	0.00	0.00	0.00	0.00
5100	0.00	0.00	0.00	0.00
2550	0.38	1.34	0.86	0.48
1913	4.41	2.68	3.55	0.86
1275	8.05	8.82	8.43	0.38
765	16.10	21.28	18.69	2.59
510	44.09	55.97	50.03	5.94
255	93.93	97.57	95.75	1.82
128	105.24	101.79	103.51	1.73
64	104.86	104.47	104.66	0.19

Table 32: Comparison of salinity treatments: *R. salina* bioassay of the supernatant fraction of the second culture at a salinity of 16. (n = 2, ± 1 SD)

A. ostenfeldii (mL^{-1})	1.) *R. salina* (% of control)	2.) *R. salina* (% of control)	Mean	SD
Exponential growth phase				
2528	64.22	61.37	62.79	1.42
1297	95.95	93.86	94.90	1.04
972	94.81	100.13	97.47	2.66
Stationary growth phase				
9555	0.00	0.00	0.00	0.00
4900	0.19	0.38	0.29	0.10
2450	2.30	3.83	3.07	0.77
1838	4.41	7.09	5.75	1.34
1225	14.57	18.79	16.68	2.11
735	44.66	33.35	39.01	5.65
490	54.44	55.40	54.92	0.48
245	88.56	88.95	88.75	0.19
123	103.13	101.79	102.46	0.67
61	103.90	97.76	100.83	3.07

Table 33: Comparison of salinity treatments: *R. salina* bioassay of the supernatant fraction of the third culture at a salinity of 16. (n = 2, ± 1 SD)

A. ostenfeldii (mL^{-1})	1.) *R. salina* (% of control)	2.) *R. salina* (% of control)	Mean	SD
Exponential growth phase				
2415	36.48	43.13	39.80	3.32
1239	86.07	99.75	92.91	6.84
929	98.42	91.77	95.09	3.32
Stationary growth phase				
9360	0.00	0.00	0.00	0.00
4800	0.38	0.19	0.29	0.10
2400	1.92	2.11	2.01	0.10
1800	7.48	10.35	8.91	1.44
1200	17.06	14.95	16.01	1.05
720	32.78	30.29	31.53	1.25
480	56.17	57.51	56.84	0.67
240	97.96	93.16	95.56	2.40
120	99.68	97.57	98.63	1.05
60	104.47	110.42	107.44	2.97

Table 34: Comparison of salinity treatments: *R. salina* bioassay of the supernatant fraction of the first culture at a salinity of 22. (n = 2, ± 1 SD)

A. ostenfeldii (mL^{-1})	1.) *R. salina* (% of control)	2.) *R. salina* (% of control)	Mean	SD
Exponential growth phase				
2395	40.76	45.71	43.24	2.48
1228	79.81	78.29	79.05	0.76
921	91.81	89.71	90.76	1.05
614	106.67	104.57	105.62	1.05
307	96.95	97.71	97.33	0.38
Stationary growth phase				
8060	0.00	0.00	0.00	0.00
4134	0.37	0.18	0.28	0.09
2067	1.10	1.84	1.47	0.37
1550	3.49	4.41	3.95	0.46
1033	6.06	11.02	8.54	2.48
620	19.83	23.32	21.57	1.74
413	49.39	30.66	40.02	9.36
207	95.65	93.45	94.55	1.10
103	93.45	93.82	93.64	0.18
52	89.23	102.26	95.75	6.52

Table 35: Comparison of salinity treatments: *R. salina* bioassay of the supernatant fraction of the second culture at a salinity of 22. (n = 2, ± 1 SD)

A. ostenfeldii (mL^{-1})	1.) *R. salina* (% of control)	2.) *R. salina* (% of control)	Mean	SD
Exponential growth phase				
2289	18.86	13.90	16.38	2.48
1174	56.57	59.81	58.19	1.62
881	73.52	83.43	78.48	4.95
587	96.76	100.57	98.67	1.90
294	102.86	107.05	104.95	2.10
Stationary growth phase				
9068	0.00	0.18	0.09	0.09
4650	0.18	0.92	0.55	0.37
2325	5.32	4.04	4.68	0.64
1744	8.08	9.91	9.00	0.92
1163	19.65	22.40	21.02	1.38
698	41.68	37.27	39.47	2.20
465	66.46	67.01	66.74	0.28
233	88.68	96.57	92.63	3.95
116	99.69	99.51	99.60	0.09
58	101.71	99.69	100.70	1.01

Table 36: Comparison of salinity treatments: *R. salina* bioassay of the supernatant fraction of the third culture at a salinity of 22. (n = 2, ± 1 SD)

A. ostenfeldii (mL^{-1})	1.) *R. salina* (% of control)	2.) *R. salina* (% of control)	Mean	SD
Exponential growth phase				
2024	20.76	23.43	22.10	1.33
1038	53.52	48.57	51.05	2.48
779	84.57	77.14	80.86	3.71
519	97.14	97.90	97.52	0.38
260	104.95	104.00	104.48	0.48
Stationary growth phase				
11245	0.00	0.00	0.00	0.00
5767	0.37	0.37	0.37	0.00
2883	1.29	1.65	1.47	0.18
2162	9.18	3.30	6.24	2.94
1442	11.75	13.22	12.48	0.73
865	28.27	27.17	27.72	0.55
577	56.00	68.48	62.24	6.24
288	93.27	93.27	93.27	0.00
144	104.10	103.73	103.92	0.18
72	102.26	94.37	98.32	3.95

Table 37: Comparison of salinity treatments: *R. salina* bioassay of the supernatant fraction of the first culture at a salinity of 34. (n = 2, ± 1 SD)

A. ostenfeldii (mL^{-1})	1.) *R. salina* (% of control)	2.) *R. salina* (% of control)	Mean	SD
Exponential growth phase				
3003	19.54	27.02	23.28	3.74
1540	53.86	52.59	53.23	0.64
1155	64.82	81.98	73.40	8.58
770	92.39	88.92	90.66	1.73
385	87.46	92.94	90.20	2.74
193	98.78	96.23	97.50	1.28
Stationary growth phase				
10270	0.00	0.00	0.00	0.00
5267	0.31	0.16	0.24	0.08
2633	0.16	5.04	2.60	2.44
1975	2.36	4.09	3.23	0.87
1317	18.90	18.43	18.66	0.24
790	29.61	36.85	33.23	3.62
527	54.96	58.11	56.54	1.57
263	83.94	105.04	94.49	10.55
132	94.65	99.37	97.01	2.36
66	99.84	94.96	97.40	2.44

Table 38: Comparison of salinity treatments: *R. salina* bioassay of the supernatant fraction of the second culture at a salinity of 34. (n = 2, ± 1 SD)

A. ostenfeldii (mL^{-1})	1.) *R. salina* (% of control)	2.) *R. salina* (% of control)	Mean	SD
Exponential growth phase				
3013	17.35	18.62	17.99	0.64
1545	25.93	29.03	27.48	1.55
1159	40.54	47.47	44.00	3.47
773	64.82	78.15	71.49	6.66
386	99.51	96.04	97.78	1.73
193	102.43	103.35	102.89	0.46
Stationary growth phase				
9913	0.00	0.16	0.08	0.08
5084	0.16	0.00	0.08	0.08
2542	0.16	3.46	1.81	1.65
1906	6.30	5.20	5.75	0.55
1271	13.70	17.17	15.43	1.73
763	34.49	41.26	37.87	3.39
508	66.30	57.32	61.81	4.49
254	90.24	100.63	95.43	5.20
127	100.16	100.31	100.24	0.08
64	92.60	99.53	96.06	3.46

Table 39: Comparison of salinity treatments: *R. salina* bioassay of the supernatant fraction of the third culture at a salinity of 34. (n = 2, ± 1 SD)

A. ostenfeldii (mL^{-1})	1.) *R. salina* (% of control)	2.) *R. salina* (% of control)	Mean	SD
Exponential growth phase				
3130	10.41	4.56	7.49	2.92
1605	20.09	18.08	19.08	1.00
1204	26.11	24.47	25.29	0.82
803	42.54	36.88	39.71	2.83
401	81.80	83.81	82.81	1.00
201	98.97	100.79	99.88	0.91
Stationary growth phase				
9782	0.00	0.00	0.00	0.00
5017	0.00	0.00	0.00	0.00
2508	2.05	1.57	1.81	0.24
1881	4.72	7.40	6.06	1.34
1254	7.09	3.31	5.20	1.89
752	22.20	22.36	22.28	0.08
502	47.87	50.55	49.21	1.34
251	86.61	78.58	82.60	4.02
125	96.69	91.81	94.25	2.44
63	93.54	92.91	93.23	0.31

Table 40: Comparison of salinity treatments: *R. salina* bioassay of the cell extract fraction of the first culture at a salinity of 6. (n = 2, ± 1 SD)

A. ostenfeldii (mL^{-1})	1.) *R. salina* (% of control)	2.) *R. salina* (% of control)	Mean	SD
Exponential growth phase				
8009	2.47	n/a	2.47	0.00
4983	19.92	4.74	12.33	7.59
3204	54.84	35.48	45.16	9.68
2136	66.22	72.11	69.17	2.94
1157	100.57	99.62	100.09	0.47
712	103.42	96.96	100.19	3.23
445	101.33	94.12	97.72	3.61
Stationary growth phase				
25200	0.00	n/a	0.00	0.00
23520	0.00	0.00	0.00	0.00
15120	0.34	0.00	0.17	0.17
10080	0.34	0.34	0.34	0.00
6720	10.07	0.84	5.45	4.61
4704	18.46	27.52	22.99	4.53
3024	54.70	58.39	56.54	1.85
1680	89.93	94.13	92.03	2.10
840	100.00	101.68	100.84	0.84
420	100.00	96.48	98.24	1.76

Table 41: Comparison of salinity treatments: *R. salina* bioassay of the cell extract fraction of the second culture at a salinity of 6. (n = 2, ± 1 SD)

A. ostenfeldii (mL^{-1})	1.) *R. salina* (% of control)	2.) *R. salina* (% of control)	Mean	SD
Exponential growth phase				
7072	3.04	n/a	3.04	0.00
4605	12.14	3.23	7.69	4.46
2961	42.50	33.02	37.76	4.74
1974	52.94	72.11	62.52	9.58
1069	103.23	111.95	107.59	4.36
658	103.98	108.73	106.36	2.37
411	104.36	99.81	102.09	2.28
Stationary growth phase				
27000	0.00	n/a	0.00	0.00
25200	0.00	0.00	0.00	0.00
16200	0.00	0.17	0.08	0.08
10800	1.01	0.34	0.67	0.34
7200	8.22	9.90	9.06	0.84
5040	28.36	33.22	30.79	2.43
3240	61.91	72.99	67.45	5.54
1800	98.66	94.46	96.56	2.10
900	103.02	97.65	100.34	2.68
450	100.00	103.52	101.76	1.76

Table 42: Comparison of salinity treatments: *R. salina* bioassay of the cell extract fraction of the third culture at a salinity of 6. (n = 2, ± 1 SD)

A. ostenfeldii (mL^{-1})	1.) *R. salina* (% of control)	2.) *R. salina* (% of control)	Mean	SD
Exponential growth phase				
7516	3.23	n/a	3.23	0.00
4677	11.39	11.76	11.57	0.19
3006	27.70	38.71	33.21	5.50
2004	84.06	75.71	79.89	4.17
1086	104.93	94.50	99.72	5.22
668	105.12	102.28	103.70	1.42
418	107.21	103.98	105.60	1.61
Stationary growth phase				
27074	0.00	n/a	0.00	0.00
25269	0.00	0.34	0.17	0.17
16245	0.00	0.17	0.08	0.08
10830	0.67	0.50	0.59	0.08
7220	7.72	8.56	8.14	0.42
5054	22.65	19.97	21.31	1.34
3249	73.32	62.42	67.87	5.45
1805	98.99	99.83	99.41	0.42
902	100.34	103.19	101.76	1.43
451	98.66	104.70	101.68	3.02

Table 43: Comparison of salinity treatments: *R. salina* bioassay of the cell extract fraction of the first culture at a salinity of 16. (n = 2, ± 1 SD)

A. ostenfeldii (mL^{-1})	1.) *R. salina* (% of control)	2.) *R. salina* (% of control)	Mean	SD
Exponential growth phase				
8674	4.26	n/a	4.26	0.00
5397	6.39	10.84	8.61	2.23
3470	21.48	38.32	29.90	8.42
2313	66.97	73.94	70.45	3.48
1253	102.19	98.71	100.45	1.74
771	92.71	107.42	100.06	7.35
482	102.77	99.29	101.03	1.74
Stationary growth phase				
18360	0.00	n/a	0.00	0.00
21420	0.00	0.00	0.00	0.00
13770	0.00	0.82	0.41	0.41
9180	0.33	1.80	1.06	0.73
6120	15.02	5.39	10.20	4.82
4284	50.60	33.95	42.27	8.32
2754	81.45	78.35	79.90	1.55
1530	79.82	95.16	87.49	7.67
765	94.50	97.28	95.89	1.39
383	99.08	101.20	100.14	1.06

Table 44: Comparison of salinity treatments: *R. salina* bioassay of the cell extract fraction of the second culture at a salinity of 16. (n = 2, ± 1 SD)

A. ostenfeldii (mL^{-1})	1.) *R. salina* (% of control)	2.) *R. salina* (% of control)	Mean	SD
Exponential growth phase				
8751	1.55	n/a	1.55	0.00
5445	10.65	10.45	10.55	0.10
3501	42.39	43.55	42.97	0.58
2334	54.77	63.10	58.94	4.16
1264	103.94	102.00	102.97	0.97
778	96.58	97.55	97.06	0.48
486	101.61	97.55	99.58	2.03
Stationary growth phase				
18375	0.00	n/a	0.00	0.00
20580	0.00	0.00	0.00	0.00
13230	0.00	0.00	0.00	0.00
8820	1.31	2.29	1.80	0.49
5880	18.77	16.00	17.38	1.39
4116	47.82	47.66	47.74	0.08
2646	72.63	73.78	73.20	0.57
1470	92.71	103.16	97.93	5.22
735	105.11	101.20	103.16	1.96
368	100.54	105.93	103.24	2.69

Table 45: Comparison of salinity treatments: *R. salina* bioassay of the cell extract fraction of the third culture at a salinity of 16. (n = 2, ± 1 SD)

A. ostenfeldii (mL^{-1})	1.) *R. salina* (% of control)	2.) *R. salina* (% of control)	Mean	SD
Exponential growth phase				
8360	4.06	n/a	4.06	0.00
5202	9.10	7.94	8.52	0.58
3344	47.42	38.52	42.97	4.45
2229	64.45	65.23	64.84	0.39
1208	76.65	96.77	86.71	10.06
743	102.58	95.23	98.90	3.68
464	102.00	100.84	101.42	0.58
Stationary growth phase				
23040	0.00	n/a	0.00	0.00
20160	0.49	0.00	0.24	0.24
12960	1.14	1.31	1.22	0.08
8640	3.26	5.55	4.41	1.14
5760	14.85	19.75	17.30	2.45
4032	54.19	50.11	52.15	2.04
2592	79.65	82.26	80.96	1.31
1440	87.65	95.65	91.65	4.00
720	101.20	101.20	101.20	0.00
360	91.08	99.40	95.24	4.16

Table 46: Comparison of salinity treatments: *R. salina* bioassay of the cell extract fraction of the first culture at a salinity of 22. (n = 2, ± 1 SD)

A. ostenfeldii (mL^{-1})	1.) *R. salina* (% of control)	2.) *R. salina* (% of control)	Mean	SD
Exponential growth phase				
7368	25.84	n/a	25.84	0.00
5158	31.20	37.18	34.19	2.99
3316	71.38	67.59	69.49	1.89
2210	83.04	85.87	84.45	1.42
1197	94.54	104.62	99.58	5.04
737	100.21	103.05	101.63	1.42
Stationary growth phase				
17361	0.16	n/a	0.16	0.00
17361	0.00	0.49	0.24	0.24
11160	2.77	2.29	2.53	0.24
7440	5.06	8.16	6.61	1.55
4960	23.18	26.44	24.81	1.63
3472	44.56	53.05	48.80	4.24
2232	83.24	87.65	85.45	2.20
1240	105.11	98.10	101.61	3.51
620	106.26	106.58	106.42	0.16

Table 47: Comparison of salinity treatments: *R. salina* bioassay of the cell extract fraction of the second culture at a salinity of 22. (n = 2, ± 1 SD)

A. ostenfeldii (mL^{-1})	1.) *R. salina* (% of control)	2.) *R. salina* (% of control)	Mean	SD
Exponential growth phase				
7220	9.45	n/a	9.45	0.00
4931	26.00	25.53	25.76	0.24
3170	59.87	61.61	60.74	0.87
2113	80.51	80.83	80.67	0.16
1145	92.80	99.42	96.11	3.31
704	97.85	95.64	96.74	1.10
Stationary growth phase				
20925	0.65	n/a	0.65	0.00
19530	1.31	0.98	1.14	0.16
12555	3.26	6.69	4.98	1.71
8370	17.79	23.18	20.48	2.69
5580	34.44	44.56	39.50	5.06
3906	75.73	72.80	74.27	1.47
2511	93.85	94.34	94.10	0.24
1395	102.34	93.53	97.93	4.41
698	105.11	107.89	106.50	1.39

Table 48: Comparison of salinity treatments: *R. salina* bioassay of the cell extract fraction of the third culture at a salinity of 22. (n = 2, ± 1 SD)

A. ostenfeldii (mL^{-1})	1.) *R. salina* (% of control)	2.) *R. salina* (% of control)	Mean	SD
Exponential growth phase				
6384	9.61	n/a	9.61	0.00
4360	21.43	20.80	21.11	0.32
2803	44.75	48.84	46.80	2.05
1868	75.79	79.41	77.60	1.81
1012	93.28	91.07	92.17	1.10
623	101.16	98.32	99.74	1.42
Stationary growth phase				
25949	0.00	n/a	0.00	0.00
24219	0.16	0.33	0.24	0.08
15570	0.33	1.14	0.73	0.41
10380	1.96	2.45	2.20	0.24
6920	6.04	5.71	5.88	0.16
4844	21.71	25.95	23.83	2.12
3114	54.68	52.88	53.78	0.90
1730	90.42	87.49	88.96	1.47
865	105.60	105.77	105.69	0.08

Table 49: Comparison of salinity treatments: *R. salina* bioassay of the cell extract fraction of the first culture at a salinity of 34. (n = 2, ± 1 SD)

A. ostenfeldii (mL^{-1})	1.) *R. salina* (% of control)	2.) *R. salina* (% of control)	Mean	SD
Exponential growth phase				
9933	0.00	n/a	0.00	0.00
6468	0.00	0.19	0.09	0.09
4158	1.71	0.95	1.33	0.38
2772	14.80	5.12	9.96	4.84
1502	48.77	33.21	40.99	7.78
924	83.49	88.43	85.96	2.47
578	96.58	97.72	97.15	0.57
277	92.41	103.04	97.72	5.31
139	100.95	109.30	105.12	4.17
Stationary growth phase				
23699	0.00	n/a	0.00	0.00
22119	0.00	0.00	0.00	0.00
14220	0.00	0.00	0.00	0.00
9480	0.33	0.00	0.16	0.16
6320	0.33	0.49	0.41	0.08
4424	3.94	6.56	5.25	1.31
2844	24.78	20.19	22.48	2.30
1580	68.27	58.75	63.51	4.76
790	102.08	90.92	96.50	5.58
395	96.66	101.09	98.88	2.22
197	91.58	98.63	95.10	3.53

Table 50: Comparison of salinity treatments: *R. salina* bioassay of the cell extract fraction of the second culture at a salinity of 34. (n = 2, ± 1 SD)

A. ostenfeldii (mL^{-1})	1.) *R. salina* (% of control)	2.) *R. salina* (% of control)	Mean	SD
Exponential growth phase				
10429	0.00	n/a	0.00	0.00
6489	0.00	0.38	0.19	0.19
4172	0.57	0.95	0.76	0.19
2781	4.17	8.54	6.36	2.18
1506	31.69	16.32	24.00	7.69
927	61.48	68.12	64.80	3.32
579	85.96	80.46	83.21	2.75
278	104.55	92.03	98.29	6.26
139	106.83	99.81	103.32	3.51
Stationary growth phase				
22876	0.00	n/a	0.00	0.00
21351	0.00	0.00	0.00	0.00
13725	0.00	0.00	0.00	0.00
9150	0.00	0.00	0.00	0.00
6100	0.49	0.66	0.57	0.08
4270	1.31	5.91	3.61	2.30
2745	16.41	19.53	17.97	1.56
1525	72.37	80.58	76.48	4.10
763	94.86	92.07	93.46	1.39
381	96.99	94.04	95.51	1.48
191	95.84	96.99	96.42	0.57

Table 51: Comparison of salinity treatments: *R. salina* bioassay of the cell extract fraction of the third culture at a salinity of 34. (n = 2, ± 1 SD)

A. ostenfeldii (mL^{-1})	1.) *R. salina* (% of control)	2.) *R. salina* (% of control)	Mean	SD
Exponential growth phase				
10352	0.00	n/a	0.00	0.00
6741	0.19	0.00	0.09	0.09
4334	0.95	0.57	0.76	0.19
2889	2.47	1.52	1.99	0.47
1565	25.43	14.23	19.83	5.60
963	47.25	48.01	47.63	0.38
602	81.59	86.34	83.97	2.37
289	94.12	95.07	94.59	0.47
144	108.16	96.77	102.47	5.69
Stationary growth phase				
21069	0.00	n/a	0.00	0.00
21069	0.00	0.00	0.00	0.00
13545	0.00	0.00	0.00	0.00
9030	0.00	0.00	0.00	0.00
6020	0.33	0.49	0.41	0.08
4214	0.82	0.66	0.74	0.08
2709	16.74	10.83	13.79	2.95
1505	57.44	49.56	53.50	3.94
752	90.43	87.80	89.11	1.31
376	97.65	94.69	96.17	1.48
188	93.87	102.08	97.98	4.10

Toxin content

Table 52: PSP-toxin content per cell (pg cell^{-1}). Triplicate cultures for exponential phase (Exp.) and for stationary phase (Stat.) were measured in technical duplicates (n = 2, ± 1 SD).

	C1/C2	dc GTX 3	GTX5	STX	GTX2/3
S = 6; Exp.; #1	37.39 ± 0.88	0.03 ± 0.00	0.59 ± 0.05	5.75 ± 0.15	4.41 ± 0.11
S = 6; Exp.; #2	41.41 ± 1.05	0.02 ± 0.01	0.66 ± 0.02	6.30 ± 0.13	4.68 ± 0.11
S = 6; Exp.; #3	40.53 ± 1.31	0.02 ± 0.01	0.58 ± 0.01	6.10 ± 0.17	5.01 ± 0.16
S = 6; Stat.; #1	34.28 ± 0.89	0.04 ± 0.00	1.13 ± 0.01	5.60 ± 0.17	2.00 ± 0.05
S = 6; Stat.; #2	29.57 ± 0.89	0.04 ± 0.00	1.03 ± 0.00	5.04 ± 0.16	1.78 ± 0.06
S = 6; Stat.; #3	28.99 ± 0.16	0.04 ± 0.00	1.05 ± 0.00	5.01 ± 0.02	1.73 ± 0.01
S = 10; Exp.; #1	31.74 ± 0.22	0.01 ± 0.00	0.20 ± 0.01	2.79 ± 0.01	4.62 ± 0.02
S = 10; Exp.; #2	33.73 ± 1.02	0.01 ± 0.00	0.21 ± 0.02	3.03 ± 0.09	5.07 ± 0.15
S = 10; Exp.; #3	41.96 ± 9.88	0.02 ± 0.00	0.28 ± 0.06	3.52 ± 0.83	6.12 ± 1.43
S = 10; Stat.; #1	21.57 ± 2.14	0.02 ± 0.00	0.48 ± 0.04	2.61 ± 0.23	1.58 ± 0.15
S = 10; Stat.; #2	17.71 ± 0.44	0.02 ± 0.00	0.36 ± 0.01	2.06 ± 0.05	1.31 ± 0.03
S = 10; Stat.; #3	23.97 ± 0.22	0.03 ± 0.00	0.51 ± 0.01	2.70 ± 0.05	1.74 ± 0.02
S = 16; Exp.; #1	23.84 ± 2.86	0.01 ± 0.00	0.17 ± 0.00	1.53 ± 0.19	2.32 ± 0.25
S = 16; Exp.; #2	22.31 ± 2.41	0.00 ± 0.00	0.16 ± 0.00	1.44 ± 0.15	2.16 ± 0.24
S = 16; Exp.; #3	21.64 ± 2.80	0.00 ± 0.00	0.19 ± 0.05	1.42 ± 0.18	2.08 ± 0.25
S = 16; Stat.; #1	25.12 ± 0.54	0.03 ± 0.00	0.64 ± 0.01	2.51 ± 0.05	1.17 ± 0.02
S = 16; Stat.; #2	25.12 ± 0.07	0.02 ± 0.00	0.61 ± 0.01	2.44 ± 0.01	1.20 ± 0.00
S = 16; Stat.; #3	26.61 ± 1.88	0.03 ± 0.00	0.65 ± 0.04	2.63 ± 0.18	1.3.0 ± 0.09
S = 22; Exp.; #1	21.40 ± 0.51	0.01 ± 0.00	0.18 ± 0.01	1.22 ± 0.03	1.85 ± 0.06
S = 22; Exp.; #2	21.27 ± 0.43	0.01 ± 0.00	0.28 ± 0.00	1.33 ± 0.01	1.63 ± 0.00
S = 22; Exp.; #3	23.15 ± 0.52	0.02 ± 0.00	0.26 ± 0.01	1.46 ± 0.02	1.88 ± 0.03
S = 22; Stat.; #1	29.09 ± 0.46	0.03 ± 0.00	0.75 ± 0.02	2.45 ± 0.05	1.31 ± 0.02
S = 22; Stat.; #2	25.99 ± 1.96	0.02 ± 0.00	0.73 ± 0.06	2.29 ± 0.16	1.13 ± 0.04
S = 22; Stat.; #3	20.99 ± 1.03	0.02 ± 0.00	0.58 ± 0.03	1.85 ± 0.08	0.94 ± 0.03
S = 28; Exp.; #1	34.95 ± 2.78	0.02 ± 0.01	0.38 ± 0.01	1.90 ± 0.16	2.63 ± 0.21
S = 28; Exp.; #2	34.58 ± 3.02	0.01 ± 0.00	0.35 ± 0.06	1.88 ± 0.19	2.55 ± 0.21
S = 28; Exp.; #3	37.08 ± 1.42	0.03 ± 0.00	0.45 ± 0.05	2.23 ± 0.08	2.68 ± 0.11
S = 28; Stat.; #1	27.63 ± 1.35	0.03 ± 0.00	0.96 ± 0.04	2.24 ± 0.11	1.27 ± 0.04
S = 28; Stat.; #2	25.94 ± 0.74	0.03 ± 0.00	0.81 ± 0.00	2.01 ± 0.04	1.19 ± 0.01
S = 28; Stat.; #3	29.93 ± 0.21	0.03 ± 0.00	0.97 ± 0.00	2.35 ± 0.02	1.42 ± 0.01
S = 34; Exp.; #1	35.48 ± 2.21	0.02 ± 0.00	0.59 ± 0.06	1.91 ± 0.12	2.58 ± 0.17
S = 34; Exp.; #2	42.30 ± 2.21	0.02 ± 0.00	0.73 ± 0.07	2.35 ± 0.12	2.89 ± 0.16
S = 34; Exp.; #3	38.59 ± 2.54	0.02 ± 0.01	0.71 ± 0.04	2.03 ± 0.11	2.58 ± 0.16
S = 34; Stat.; #1	26.16 ± 1.03	0.03 ± 0.00	0.99 ± 0.01	1.86 ± 0.03	1.33 ± 0.04
S = 34; Stat.; #2	27.04 ± 1.38	0.03 ± 0.00	1.00 ± 0.06	1.93 ± 0.14	1.36 ± 0.07
S = 34; Stat.; #3	25.33 ± 1.23	0.03 ± 0.00	1.00 ± 0.06	1.86 ± 0.07	1.23 ± 0.06

Table 53: Intracellular cyclic imine toxin concentrations (fg cell^{-1}) of triplicate cultures in exponential growth phase. (Technical duplicates, n = 2, ± 1 SD; ND = not detectable)

	508-490	522-504	640-164	644-164	650-164	658-164	674-164	678-164	678-150	692-164	692-150	694-164	694-150	696-164	698-164	706-164	708-164	710-164	710-150	720-164	722-164	766-164	784-164
S = 4.5 #1	1551.3	310.7	ND	ND	0.7	0.5	37.0	0.2	4.5	1456.2	7.0	314.4	1.9	10.5	ND	ND	6.1	6.3	ND	0.1	0.1	ND	ND
S = 4.5 #2	1600.7	334.7	ND	ND	0.7	0.8	38.5	0.2	4.9	1520.1	7.3	339.7	1.8	10.8	0.6	ND	3.4	10.1	ND	ND	0.1	ND	ND
S = 4.5 #3	2635.8	541.6	ND	ND	1.0	1.1	59.1	0.1	7.7	2388.5	11.5	532.9	3.0	16.1	0.7	ND	9.1	14.9	ND	ND	0.1	ND	ND
S = 6 #1	6413.1 ± 516.5	1398.8 ± 159.3	0.1 ± 0.0	1.3 ± 0.1	2.8 ± 0.3	1.4 ± 0	122.0 ± 4.9	1.6 ± 0.0	16.3 ± 0.8	5061.5 ± 280.5	22.5 ± 1.3	680.1 ± 38.6	4.8 ± 0.0	15.2 ± 0.4	0.9 ± 0.8	0.1 ± 0.0	8.9 ± 0.2	40.2 ± 2.4	0.1 ± 0.0	0.2 ± 0.0	0.2 ± 0.1	2.4 ± 0.2	ND
S = 6 #2	6427.2 ± 372.6	1385.6 ± 44.2	0.1 ± 0.0	1.5 ± 0.3	3.3 ± 0.1	1.3 ± 0.2	128.5 ± 2.6	0.6 ± 0.6	17.2 ± 0.7	5327.3 ± 92.4	24.2 ± 0.8	717.1 ± 9.7	4.9 ± 0.2	16.6 ± 0.4	1.4 ± 1.3	0.1 ± 0.0	8.1 ± 0.7	42.3 ± 3.3	ND	0.1 ± 0.0	0.4 ± 0.0	4.0 ± 1.2	0.7 ± 0.6
S = 6 #3	7085.8 ± 68.8	1495.1 ± 22.9	0.1 ± 0.1	1.5 ± 0.3	2.9 ± 0.3	1.4 ± 0.2	140.4 ± 1.7	1.4 ± 0.1	19.8 ± 0.3	5757.2 ± 39.0	26.4 ± 0.3	780.2 ± 0.4	5.5 ± 0.9	17.8 ± 0.6	2.8 ± 0.1	0.2 ± 0.1	10.2 ± 1.7	47.4 ± 5.2	ND	0.1 ± 0.0	0.2 ± 0.0	4.0 ± 0.7	1.1 ± 0.4
S = 10 #1	3444.5 ± 17.1	805.4 ± 41.1	0.1 ± 0.0	1.2 ± 0.1	2.4 ± 0.1	1.6 ± 0.3	73.5 ± 1.0	0.3 ± 0.3	8.2 ± 0.0	2984.8 ± 32.4	14.0 ± 0.3	644.2 ± 9.7	3.7 ± 0.2	20.5 ± 1.5	0.1 ± 0.0	0.1 ± 0.0	4.8 ± 0.2	32.3 ± 0.3	0.1 ± 0.0	0.1 ± 0.1	0.1 ± 0.0	2.2 ± 0.4	ND
S = 10 #2	3090.2 ± 90.5	762.0 ± 18.1	0.1 ± 0.0	1.1 ± 0.0	2.5 ± 0.4	1.2 ± 0.1	70.9 ± 3.5	0.6 ± 0.0	8.4 ± 0.0	2898 ± 117.7	12.6 ± 1.0	612.3 ± 13.7	3.4 ± 0.4	17.2 ± 0.5	1.4 ± 1.3	0.2 ± 0.1	5.6 ± 0.3	37.6 ± 0.1	ND	0.1 ± 0.0	0.1 ± 0.0	2.6 ± 1.3	1.0 ± 0.9
S = 10 #3	3424.1 ± 219.1	769.0 ± 45.0	0.1 ± 0.0	1.3 ± 0.1	2.2 ± 0.1	1.2 ± 0.1	68.2 ± 2.0	0.5 ± 0.0	8.0 ± 0.1	2964.4 ± 147.9	13.5 ± 0.3	622.1 ± 24.8	3.5 ± 0.1	19.2 ± 2.2	1.1 ± 1.0	0.1 ± 0.0	6.0 ± 1.0	28.2 ± 3.1	ND	0.1 ± 0.0	0.1 ± 0.0	2.5 ± 0.3	ND
S = 16 #1	1975.2 ± 162.9	478.9 ± 41.7	ND	0.8 ± 0.7	1.3 ± 0.3	1.2 ± 0.3	46.4 ± 5.7	0.3 ± 0.1	5.5 ± 1.0	2012.0 ± 195.2	8.4 ± 0.5	548.4 ± 49.2	2.7 ± 0.9	16.6 ± 0.8	ND	0.1 ± 0.1	2.4 ± 0.5	18.3 ± 2.9	ND	0.1 ± 0.0	0.1 ± 0.0	0.5 ± 0.4	ND
S = 16 #2	1756.8 ± 157.6	500.2 ± 27.6	ND	0.4 ± 0.3	1.6 ± 0.1	1.1 ± 0.2	45.6 ± 2.7	0.7 ± 0.6	5.6 ± 0.7	1923.5 ± 93.0	8.4 ± 0.4	516.0 ± 34.6	3.0 ± 0.1	17.5 ± 1	0.1 ± 0.0	0.1 ± 0.1	2.1 ± 0.1	20.3 ± 1.0	ND	ND	ND	0.8 ± 0.7	ND
S = 16 #3	1814.3 ± 115.5	496.9 ± 26.8	ND	0.6 ± 0.5	1.3 ± 0.2	0.5 ± 0.5	45.6 ± 3.5	0.4 ± 0.0	5.7 ± 1.0	1939.6 ± 163.6	8.7 ± 1.2	522.3 ± 43.2	2.4 ± 0.3	16.2 ± 0.3	0.1 ± 0.0	0.1 ± 0.0	1.6 ± 1.5	19 ± 2.5	ND	ND	0.1 ± 0.0	1.3 ± 0.2	ND
S = 22 #1	1480.5 ± 62.4	419.4 ± 13.1	ND	ND	1.3 ± 0.3	1.0 ± 0.1	38.2 ± 2.4	0.2 ± 0.0	4.8 ± 1.0	1641.9 ± 86.4	7.3 ± 0.4	505.5 ± 27.9	2.6 ± 0.1	17.5 ± 0.4	ND	0.1 ± 0.0	2.1 ± 0.1	13 ± 1.3	ND	ND	0.1 ± 0.0	1.6 ± 0.9	0.1 ± 0.0
S = 22 #2	1294.1 ± 84.8	377.8 ± 6.3	0.1 ± 0.0	ND	0.4 ± 0.3	1.2 ± 0.0	35.3 ± 1.1	0.1 ± 0.0	4.7 ± 0.2	1503.8 ± 74.0	6.1 ± 0.6	456.1 ± 22.2	2.7 ± 0.5	14.4 ± 0.1	ND	0.1 ± 0.0	0.9 ± 0.8	9.1 ± 1.2	ND	ND	0.1 ± 0.1	ND	ND
S = 22 #3	1244.7 ± 339.5	393.1 ± 123.5	0.1 ± 0.0	ND	ND	0.0 ± 0.0	35.3 ± 6.2	0.2 ± 0.2	4.7 ± 0.5	1528.9 ± 292.8	6.8 ± 1.7	456.3 ± 86.4	2.2 ± 0.8	14.8 ± 4.1	0.1 ± 0.0	0.1 ± 0.0	1.5 ± 0.8	13.5 ± 2.4	ND	0.1 ± 0.0	0.1 ± 0.0	ND	ND
S = 28 #1	1844.2 ± 122.6	472.7 ± 17.8	0.1 ± 0.0	0.1 ± 0.0	1.9 ± 0.3	1.8 ± 0.2	57.9 ± 3.8	0.2 ± 0.0	8.0 ± 0.8	2478.5 ± 240.4	10.8 ± 0.7	717.8 ± 57.7	3.6 ± 0.1	21.9 ± 1.8	1.6 ± 1.5	0.3 ± 0.2	2.0 ± 1.8	22.0 ± 2.0	0.1 ± 0.0	0.1 ± 0.0	0.1 ± 0.0	4.8 ± 0.2	1.5 ± 0.5
S = 28 #2	1964.2 ± 155.7	462.0 ± 37.1	0.2 ± 0.0	ND	2.5 ± 0.0	1.7 ± 0.1	67.6 ± 1.5	0.3 ± 0.1	9.7 ± 1.1	2809.7 ± 9.3	12.1 ± 0.5	829.4 ± 10.7	3.9 ± 0.4	22.8 ± 1.4	2.9 ± 0.2	0.1 ± 0.0	3.7 ± 0.0	19.0 ± 0.4	0.1 ± 0.0	0.1 ± 0.1	0.3 ± 0.1	4.6 ± 0.3	1.0 ± 1.0
S = 28 #3	1709.8 ± 178	502.5 ± 35.6	0.1 ± 0.0	ND	2.8 ± 0.3	0.1 ± 0.0	61.9 ± 6.0	0.4 ± 0.2	8.6 ± 0.8	2674.8 ± 197.5	12.0 ± 0.8	776.8 ± 20.8	4.7 ± 0.1	23.9 ± 0.4	2.5 ± 0.0	0.2 ± 0.1	2.8 ± 0.1	19.2 ± 3.0	0.1 ± 0.0	0.1 ± 0.1	0.1 ± 0.0	4.0 ± 0.2	0.1 ± 0.0
S = 34 #1	2014.5 ± 124.4	489.1 ± 24.9	0.3 ± 0.0	ND	ND	0.7 ± 0.6	67.0 ± 1.3	0.3 ± 0.0	8.5 ± 0.7	2750.1 ± 100.2	12.4 ± 0.1	726.7 ± 25.1	4.3 ± 0.3	21 ± 0.6	1.8 ± 0.1	0.1 ± 0.0	4.1 ± 0.4	21.1 ± 2.2	ND	0.1 ± 0.0	0.4 ± 0.4	2.7 ± 0.3	0.7 ± 0.6
S = 34 #2	2003.1 ± 33.1	456.1 ± 6.6	0.1 ± 0.0	ND	ND	0.8 ± 0.8	64.6 ± 7.2	0.2 ± 0.2	8.0 ± 0.9	2663.2 ± 277.9	12.1 ± 1.2	672.5 ± 76.8	3.5 ± 0.2	20.1 ± 2.1	1.8 ± 0.1	0.1 ± 0.0	3.1 ± 0.7	24.9 ± 0.5	ND	0.1 ± 0.0	0.1 ± 0.0	3.2 ± 0.1	0.8 ± 0.7
S = 34 #3	1952.1 ± 33.4	478.9 ± 1.6	0.1 ± 0.0	ND	ND	0.5 ± 0.4	68.2 ± 6.3	0.4 ± 0.2	9.0 ± 1.2	2834.1 ± 225.4	12.6 ± 0.2	679.2 ± 54.1	4.1 ± 0.4	18.7 ± 1.6	2.5 ± 0.3	0.1 ± 0.0	4.5 ± 1.0	21.6 ± 1.6	ND	ND	0.1 ± 0.0	3.9 ± 0.2	0.7 ± 0.6

Table 54: Intracellular cyclic imine toxin concentrations (fg cell^{-1}) of triplicate cultures in stationary growth phase. (Technical duplicates, n = 2, ± 1 SD; ND = not detectable)

	508-490	522-504	640-164	644-164	650-164	658-164	674-164	678-164	678-150	692-164	692-150	694-164	694-150	696-164	698-164	706-164	708-164	710-164	710-150	720-164	722-164	766-164	784-164
S = 6 #1	7117.7 ± 132.2	971.2 ± 4.6	0.1 ± 0.0	1.6 ± 0.1	2.8 ± 0.1	1.4 ± 0.2	118.3 ± 4.4	0.8 ± 0.8	18.4 ± 0.2	4393.0 ± 137.8	23.0 ± 0.8	581.4 ± 16.4	4.7 ± 0.2	14.7 ± 1.2	3.0 ± 0.2	0.2 ± 0.0	4.4 ± 0.7	29.6 ± 6.2	ND	0.1 ± 0.0	0.6 ± 0.2	5.0 ± 0.1	1.6 ± 0.0
S = 6 #2	5949.5 ± 144.7	880.9 ± 21.3	0.1 ± 0.0	1.1 ± 0.0	2.6 ± 0.1	1.0 ± 0.1	95.7 ± 3.0	0.6 ± 0.4	14.6 ± 0.9	3633.8 ± 80.4	18.1 ± 0.7	479.1 ± 17.7	3.7 ± 0.1	10.4 ± 0.3	2.3 ± 0.1	0.2 ± 0.1	3.4 ± 0.0	25.0 ± 0.4	ND	ND	0.2 ± 0.1	4.2 ± 0.6	1.2 ± 0.1
S = 6 #3	6238.7 ± 127.3	899.7 ± 8.5	0.1 ± 0.0	1.1 ± 0.1	2.9 ± 0.3	1.0 ± 0.1	104.3 ± 7.5	0.0 ± 0.0	16 ± 1.0	3848.3 ± 224.5	20.0 ± 1.4	507.5 ± 29.7	4.1 ± 0.0	12.5 ± 0.9	2.2 ± 0.1	0.2 ± 0.0	3.7 ± 0.8	20.4 ± 0.4	ND	0.1 ± 0.0	0.4 ± 0.1	4.3 ± 0.0	0.9 ± 0.3
S = 10 #1	2970.8 ± 137.3	592.5 ± 19.2	ND	0.3 ± 0.3	2.1 ± 0.0	0.8 ± 0.1	70.2 ± 3.0	0.1 ± 0.0	9.4 ± 0.8	2821.6 ± 124.5	13.3 ± 0.7	373.4 ± 18.7	2.6 ± 0.4	9.4 ± 0.8	1.4 ± 0.0	0.1 ± 0.0	2.5 ± 0.2	11.0 ± 0.7	ND	ND	0.1 ± 0.0	2.1 ± 0.1	0.7 ± 0.0
S = 10 #2	2197.9 ± 88.2	462.0 ± 8.8	0.1 ± 0.0	0.4 ± 0.0	1.5 ± 0.0	0.6 ± 0.1	49.7 ± 0.2	0.1 ± 0.0	6.9 ± 0.3	2023.0 ± 7.6	9.4 ± 0.3	277.3 ± 1.5	2.1 ± 0.0	7.4 ± 0.1	1.2 ± 0.1	0.1 ± 0.0	1.6 ± 0.7	9.0 ± 0.7	ND	ND	ND	1.7 ± 0.0	0.6 ± 0.0
S = 10 #3	3319.4 ± 111	631.7 ± 4.4	0.1 ± 0.0	0.6 ± 0.1	2.1 ± 0.0	0.7 ± 0.1	68.1 ± 2.0	1.2 ± 1.1	9.1 ± 0.6	2715.9 ± 115.3	12.8 ± 0.6	383.8 ± 18.9	2.6 ± 0.1	9.7 ± 0.3	1.5 ± 0.2	0.1 ± 0.0	3.0 ± 0.3	15.0 ± 0.8	ND	ND	0.1 ± 0.0	2.5 ± 0.0	0.6 ± 0.1
S = 16 #1	2328.1 ± 15	463.6 ± 3.0	0.2 ± 0.0	2.6 ± 0.3	1.9 ± 0.0	0.9 ± 0.1	64.3 ± 3.2	0.1 ± 0.1	9.3 ± 0.3	2572.6 ± 94.6	12.3 ± 0.4	390.6 ± 18.0	2.7 ± 0.3	10.9 ± 0.4	0.2 ± 0.1	0.1 ± 0.0	2.4 ± 0.0	12.4 ± 0.1	ND	ND	0.6 ± 0.2	2.6 ± 0.1	0.9 ± 0.1
S = 16 #2	2318.9 ± 119.9	448.7 ± 4.7	0.1 ± 0.0	2.3 ± 0.0	2.0 ± 0.1	0.9 ± 0.1	68.5 ± 0.4	0.1 ± 0.0	9.8 ± 0.1	2746.5 ± 9.8	12.9 ± 0.2	425.3 ± 2.0	3.1 ± 0.1	11.0 ± 0.1	1.5 ± 0.1	0.1 ± 0.0	2.1 ± 0.3	10.6 ± 0.3	ND	ND	0.3 ± 0.2	2.4 ± 0.0	0.9 ± 0.0
S = 16 #3	2553.4 ± 63.8	499.0 ± 42.6	0.2 ± 0.0	2.0 ± 0.2	1.7 ± 0.1	0.8 ± 0.1	70.5 ± 4.4	0.2 ± 0.1	10.4 ± 0.6	2803.7 ± 110.5	13.2 ± 0.4	439.2 ± 21.1	3.1 ± 0.1	11.9 ± 0.9	1.8 ± 0.3	0.1 ± 0.0	2.4 ± 0.1	13.6 ± 1.1	ND	ND	0.1 ± 0.1	2.6 ± 0.1	0.9 ± 0.2
S = 22 #1	2248.6 ± 74.1	472.0 ± 19.8	0.3 ± 0.1	1.5 ± 0.2	2.2 ± 0.2	1.0 ± 0.1	74.1 ± 4.3	0.4 ± 0.1	10.5 ± 0.5	2940.8 ± 210.1	13.7 ± 1.3	478.5 ± 37.3	3.5 ± 0.4	12.0 ± 1.1	2.0 ± 0.2	0.1 ± 0.0	2.4 ± 0.3	12.6 ± 0.7	ND	ND	0.1 ± 0.0	3.2 ± 0.1	1.5 ± 0.1
S = 22 #2	1790.1 ± 22	376.7 ± 20.9	0.2 ± 0.0	1.2 ± 0.1	1.8 ± 0.0	0.9 ± 0.0	62.3 ± 0.5	0.5 ± 0.1	9.1 ± 0.2	2510.4 ± 20.7	12.4 ± 0.0	434.6 ± 1.0	2.9 ± 0.0	11.9 ± 0.7	1.8 ± 0.3	0.1 ± 0.0	2.3 ± 0.4	13.0 ± 2.0	ND	ND	0.1 ± 0.0	2.6 ± 0.4	1.2 ± 0.2
S = 22 #3	1545.4 ± 31	311.7 ± 16.8	0.1 ± 0.0	1.0 ± 0.3	1.2 ± 0.0	0.6 ± 0.0	43.1 ± 1.1	0.2 ± 0.0	6.0 ± 0.1	1748.3 ± 8.4	8.3 ± 0.1	289.4 ± 1.7	1.8 ± 0.0	8.1 ± 0.2	1.1 ± 0.1	0.1 ± 0.0	1.8 ± 0.2	8.7 ± 0.6	ND	ND	ND	1.8 ± 0.1	1.0 ± 0.0
S = 28 #1	1593.2 ± 259.6	328.3 ± 28.0	ND	ND	0.6 ± 0.0	0.7 ± 0.1	63.6 ± 7.2	0.2 ± 0.0	9.4 ± 1.7	2528.9 ± 278.9	12.2 ± 1.5	380.8 ± 44.2	2.8 ± 0.2	9.7 ± 1.5	2.1 ± 0.3	0.2 ± 0.0	2.3 ± 1.0	8.3 ± 1.2	ND	ND	0.2 ± 0.2	3.7 ± 0.6	1.1 ± 0.2
S = 28 #2	2052.6 ± 277.4	339.7 ± 32.4	0.1 ± 0.0	ND	1.0 ± 0.2	1.0 ± 0.1	78.6 ± 6.5	0.3 ± 0.1	13.3 ± 0.8	3087.6 ± 217.7	15.4 ± 1.4	492.6 ± 37.9	3.3 ± 0.4	12.0 ± 1.2	3.1 ± 0.2	0.2 ± 0.0	2.6 ± 0.3	11.0 ± 1.0	ND	ND	0.2 ± 0.2	4.3 ± 0.5	1.7 ± 0.5
S = 28 #3	2107.7 ± 68.3	382 ± 0.5	0.1 ± 0.0	ND	0.8 ± 0.1	1.1 ± 0.0	84.2 ± 1.8	0.3 ± 0.0	14.2 ± 0.0	3318.1 ± 36.9	16.2 ± 0.4	544.7 ± 6.5	4.0 ± 0.0	14.2 ± 0.2	3.3 ± 0.2	0.3 ± 0.1	2.6 ± 0.7	13.2 ± 1.5	ND	ND	0.1 ± 0.0	4.7 ± 0.1	1.4 ± 0.0
S = 34 #1	1520.9 ± 573.6	277.8 ± 69.3	0.1 ± 0.0	ND	ND	0.7 ± 0.3	60.5 ± 23.9	0.4 ± 0.2	9.1 ± 4.2	2413.4 ± 902.2	11.6 ± 4.7	348.0 ± 142.9	2.5 ± 1.0	8.3 ± 3.5	1.6 ± 0.8	0.1 ± 0.1	2.1 ± 0.8	8.4 ± 3.1	ND	ND	ND	2.7 ± 1.3	1.0 ± 0.5
S = 34 #2	2250.3 ± 160.7	379.7 ± 9.0	0.1 ± 0.0	ND	0.4 ± 0.4	1.0 ± 0.0	90.0 ± 4.1	0.7 ± 0.1	14.3 ± 0.7	3482.4 ± 161.3	17.4 ± 1.0	522.8 ± 27.5	4.0 ± 0.2	12.3 ± 0.5	2.2 ± 0.0	0.2 ± 0.0	3.0 ± 0.5	14.0 ± 0.4	ND	ND	ND	4.3 ± 0.5	2.1 ± 0.4
S = 34 #3	1908.8 ± 96.7	322.7 ± 8.1	0.3 ± 0.0	ND	0.3 ± 0.3	0.8 ± 0.1	64.2 ± 8.7	0.3 ± 0.1	9.1 ± 1.3	2509.7 ± 317.3	11.8 ± 1.5	376.9 ± 55.8	2.5 ± 0.3	8.5 ± 1.0	1.8 ± 0.1	0.1 ± 0.0	1.8 ± 1.4	11.2 ± 1.1	ND	ND	0.4 ± 0.3	2.3 ± 0.4	1.1 ± 0.2

Table 55: Extracellular cyclic imine toxin concentrations (fg cell^{-1}) of triplicate cultures in exponential growth phase. (Technical duplicates, n = 2, ± 1 SD; ND = not detectable)

	508-490	522-504	640-164	644-164	650-164	658-164	674-164	678-164	678-150	692-164	692-150	694-164	694-150	696-164	698-164	706-164	708-164	710-164	710-150	720-164	722-164	766-164	784-164
S = 6 #1	134.4 ± 17.6	16.2 ± 16.2	0.1 ± 0.0	ND	0.1 ± 0.0	0.1 ± 0.0	7.1 ± 0.5	0.1 ± 0.0	ND	268.0 ± 3.4	0.9 ± 0.0	0.1 ± 0.0	0.1 ± 0.0	0.2 ± 0.0	0.1 ± 0.0	ND	7.1 ± 0.6	36.5 ± 4.1	ND	0.1 ± 0.0	0.1 ± 0.0	0.1 ± 0.1	ND
S = 6 #2	123.6 ± 19.2	25.9 ± 4.1	ND	0.1 ± 0.0	ND	0.1 ± 0.0	6.1 ± 0.2	0.1 ± 0.1	0.1 ± 0.0	242.3 ± 8.6	0.9 ± 0.1	ND	ND	0.2 ± 0.1	0.2 ± 0.0	ND	7.1 ± 0.8	37.8 ± 1.4	0.1 ± 0.1	0.1 ± 0.0	0.1 ± 0.0	0.5 ± 0.5	ND
S = 6 #3	124.9 ± 0.5	13.8 ± 3.6	0.1 ± 0.0	0.1 ± 0.0	0.1 ± 0.0	ND	6.4 ± 0.4	0.2 ± 0.0	0.1 ± 0.0	270.2 ± 16.6	0.9 ± 0.2	0.1 ± 0.0	0.1 ± 0.0	1.3 ± 1.1	0.1 ± 0.1	ND	7.3 ± 0.5	41.3 ± 5.2	ND	0.1 ± 0.0	0.2 ± 0.0	0.1 ± 0.0	ND
S = 10 #1	103.4 ± 17.6	27.8 ± 13.3	ND	2.9 ± 1.7	ND	ND	6.2 ± 0.2	0.2 ± 0.1	0.6 ± 0.1	270.4 ± 42.7	1.1 ± 0.3	ND	ND	4.3 ± 1.5	0.1 ± 0.1	ND	4.6 ± 1.6	25.7 ± 3.6	ND	0.1 ± 0.1	1.3 ± 1.2	1.0 ± 0.0	ND
S = 10 #2	208.6 ± 62.9	51.7 ± 21.4	0.1 ± 0.0	2.0 ± 0.4	ND	ND	10.9 ± 2.1	0.1 ± 0.0	0.6 ± 0.5	436.9 ± 110.8	1.8 ± 0.3	ND	ND	5.1 ± 1.3	0.2 ± 0.1	0.1 ± 0.0	8.0 ± 0.6	34.2 ± 11.6	ND	0.1 ± 0.0	0.1 ± 0.1	1.9 ± 0.4	ND
S = 10 #3	186.8 ± 72.1	41.2 ± 18.6	0.1 ± 0.0	3.4 ± 1.8	ND	0.1 ± 0.0	10.5 ± 3.3	0.3 ± 0.2	0.9 ± 0.0	422.1 ± 145.5	1.9 ± 0.6	ND	ND	8.1 ± 5.2	0.2 ± 0.1	ND	8.2 ± 0.9	32.9 ± 9.3	ND	0.1 ± 0.0	3.3 ± 3.3	1.0 ± 0.4	ND
S = 16 #1	57.3 ± 15	19.9 ± 5.7	ND	ND	ND	ND	2.7 ± 0.2	0.1 ± 0.0	0.1 ± 0.0	118.3 ± 10.9	0.4 ± 0.4	ND	ND	1.1 ± 0.0	0.1 ± 0.0	ND	1.9 ± 0.0	13.1 ± 0.2	ND	ND	0.1 ± 0.0	ND	ND
S = 16 #2	82.3 ± 8.7	31.9 ± 4.8	ND	ND	ND	ND	3.9 ± 0.6	0.1 ± 0.0	0.2 ± 0.2	153.4 ± 7.3	0.5 ± 0.5	ND	ND	1.1 ± 0.1	ND	ND	2.5 ± 0.3	14.5 ± 0.8	ND	ND	0.6 ± 0.6	ND	ND
S = 16 #3	77.4 ± 0.4	16.9 ± 4.1	0.1 ± 0.0	0.1 ± 0.0	ND	ND	4.2 ± 0.4	0.1 ± 0.0	ND	165.7 ± 5.5	0.4 ± 0.3	ND	ND	1.5 ± 0.2	ND	ND	2.4 ± 0.4	14.2 ± 0.4	ND	ND	0.1 ± 0.1	ND	ND
S = 22 #1	50.8 ± 4.5	ND	0.1 ± 0.0	0.1 ± 0.0	ND	ND	2.5 ± 0.5	0.1 ± 0.0	ND	86.0 ± 2.2	0.2 ± 0.1	ND	ND	0.6 ± 0.5	0.1 ± 0.0	ND	3.4 ± 0.3	19.5 ± 1.5	0.1 ± 0.0	0.1 ± 0.0	1.2 ± 0.0	ND	ND
S = 22 #2	55.6 ± 7.2	ND	ND	0.1 ± 0.0	ND	ND	2.4 ± 0.4	0.1 ± 0.0	0.1 ± 0.1	108.7 ± 8.8	0.4 ± 0.1	ND	ND	0.6 ± 0.5	0.1 ± 0.1	ND	4.5 ± 0.6	21.4 ± 1.7	0.1 ± 0.1	0.1 ± 0.0	0.4 ± 0.2	ND	ND
S = 22 #3	59.6 ± 3.8	ND	0.1 ± 0.1	0.1 ± 0.0	ND	ND	2.8 ± 0.1	0.1 ± 0.0	0.1 ± 0.0	108.6 ± 16.5	0.1 ± 0.0	ND	ND	0.1 ± 0.0	0.1 ± 0.0	ND	3.8 ± 0.4	20.1 ± 0.4	ND	0.2 ± 0.0	1.2 ± 0.0	ND	ND
S = 28 #1	31.3 ± 0.5	3.6 ± 3.6	0.1 ± 0.0	0.1 ± 0.1	ND	0.1 ± 0.0	2.5 ± 0.9	0.1 ± 0.0	0.1 ± 0.0	96.4 ± 22.2	0.0 ± 0.0	ND	ND	0.8 ± 0.8	0.1 ± 0.0	ND	2.8 ± 1.5	21.0 ± 2.0	ND	0.2 ± 0.2	1.8 ± 1.4	0.1 ± 0.0	ND
S = 28 #2	27.4 ± 5.5	2.2 ± 2.2	0.1 ± 0.0	0.1 ± 0.0	0.1 ± 0.1	0.1 ± 0.1	1.9 ± 1.8	0.1 ± 0.0	0.1 ± 0.0	93.5 ± 20.9	0.4 ± 0.0	0.1 ± 0.0	0.1 ± 0.0	0.1 ± 0.0	0.1 ± 0.1	ND	3.1 ± 0.4	21.3 ± 2.7	ND	ND	1.3 ± 1.0	0.1 ± 0.0	ND
S = 28 #3	43.9 ± 8.7	ND	0.1 ± 0.0	0.1 ± 0.0	ND	0.1 ± 0.0	3.1 ± 0.0	0.1 ± 0.0	ND	137.8 ± 16.0	0.3 ± 0.3	ND	ND	0.1 ± 0.1	0.1 ± 0.1	0.1 ± 0.0	3.6 ± 0.5	23.2 ± 1.9	0.1 ± 0.0	0.1 ± 0.0	1.1 ± 0.7	0.1 ± 0.0	0.1 ± 0.0
S = 34 #1	131.1 ± 3.7	33.2 ± 3.7	ND	ND	0.1 ± 0.0	ND	6.1 ± 0.3	0.1 ± 0.1	0.3 ± 0.3	212.7 ± 3.5	0.8 ± 0.1	ND	ND	0.1 ± 0.0	0.1 ± 0.0	ND	1.8 ± 0.3	24.9 ± 1.8	ND	ND	0.1 ± 0.0	ND	ND
S = 34 #2	32.6 ± 7.0	3.7 ± 2.9	0.1 ± 0.0	ND	ND	ND	1.0 ± 1.0	0.1 ± 0.0	ND	48.3 ± 17.1	ND	ND	ND	0.4 ± 0.2	0.1 ± 0.0	0.1 ± 0.0	2.5 ± 0.0	10.4 ± 5.6	0.1 ± 0.0	1.1 ± 0.0	14.3 ± 0.7	ND	ND
S = 34 #3	101.8 ± 1.3	25.8 ± 13.0	0.1 ± 0.1	1.6 ± 0.0	ND	ND	3.4 ± 0.2	0.1 ± 0.0	ND	132.7 ± 19.1	0.1 ± 0.1	ND	ND	3.6 ± 0.0	0.1 ± 0.0	ND	4.1 ± 0.1	20.5 ± 1.7	0.1 ± 0.0	1.0 ± 0.3	11.6 ± 0.8	ND	ND

Table 56: Extracellular cyclic imine toxin concentrations (fg cell^{-1}) of triplicate cultures in stationary growth phase. (Technical duplicates, n = 2, ± 1 SD; ND = not detectable)

	508-490	522-504	640-164	644-164	650-164	658-164	674-164	678-164	678-150	692-164	692-150	694-164	694-150	696-164	698-164	706-164	708-164	710-164	710-150	720-164	722-164	766-164	784-164
S = 6 #1	54.7 ± 3.2	10.7 ± 6.3	ND	0.2 ± 0.1	ND	ND	2.7 ± 0.1	ND	0.1 ± 0.1	109.0 ± 0.9	0.4 ± 0.0	ND	ND	1.4 ± 0.1	0.1 ± 0.0	ND	3.2 ± 0.9	10.4 ± 0.1	ND	ND	0.1 ± 0.0	0,5 ± 0,0	ND
S = 6 #2	50.5 ± 7.0	13.0 ± 1.4	ND	0.2 ± 0.0	ND	ND	2.5 ± 0.1	ND	0.3 ± 0.0	107.2 ± 0.3	0.4 ± 0.0	ND	ND	1.4 ± 0.3	0.1 ± 0.0	ND	2.0 ± 0.2	8.3 ± 0.4	ND	ND	ND	0,5 ± 0,1	ND
S = 6 #3	43.5 ± 1.0	12.5 ± 0.9	ND	0.1 ± 0.1	ND	ND	1.9 ± 0	ND	0.3 ± 0.0	84.1 ± 3.3	0.4 ± 0.0	ND	ND	1.4 ± 0.0	ND	ND	2.4 ± 0.4	6.2 ± 0.3	ND	ND	0.1 ± 0.0	0,3 ± 0,1	ND
S = 10 #1	18.7 ± 2.1	5.9 ± 1	ND	ND	ND	ND	1.0 ± 0.1	ND	0.1 ± 0.0	37.3 ± 4.1	0.2 ± 0.0	ND	ND	0.0 ± 0.0	ND	ND	0.8 ± 0.0	4.4 ± 0.2	ND	ND	0.2 ± 0.2	ND	ND
S = 10 #2	21.5 ± 2.8	7.9 ± 0.8	ND	ND	ND	ND	0.8 ± 0	ND	0.1 ± 0.0	35.6 ± 0.8	0.1 ± 0.1	ND	ND	0.0 ± 0.0	ND	ND	0.5 ± 0.0	3.4 ± 0.1	ND	ND	0.0 ± 0.0	ND	ND
S = 10 #3	18.9 ± 3.8	5.7 ± 2.2	ND	0.5 ± 0.5	ND	ND	0.9 ± 0.3	ND	ND	38.1 ± 5.8	0.1 ± 0.1	ND	ND	0.2 ± 0.0	ND	ND	0.8 ± 0.1	4.1 ± 0.4	ND	ND	0.1 ± 0.0	ND	ND
S = 16 #1	30.3 ± 10.3	6.9 ± 2.4	0.1 ± 0.1	ND	ND	ND	1.7 ± 0.1	0.3 ± 0.2	ND	68.5 ± 4.6	0.2 ± 0.2	ND	ND	1.7 ± 0.3	0.1 ± 0.0	ND	2.0 ± 0.6	8.6 ± 0.5	ND	0.1 ± 0.0	1.0 ± 0.6	ND	ND
S = 16 #2	41.4 ± 5.4	9.1 ± 0.8	ND	2.2 ± 0.9	ND	ND	2.3 ± 0.5	ND	0.3 ± 0.0	88.0 ± 8.8	0.4 ± 0.1	ND	ND	1.0 ± 0.0	ND	ND	2.0 ± 0.4	9.2 ± 0.3	ND	ND	0.3 ± 0.0	ND	ND
S = 16 #3	46.2 ± 9.3	10.6 ± 0.9	0.1 ± 0.1	1.8 ± 0.3	ND	ND	2.6 ± 0.1	ND	0.3 ± 0.0	104.8 ± 11.0	0.5 ± 0.0	ND	ND	1.2 ± 0.2	ND	ND	1.7 ± 0.1	11.2 ± 0.9	ND	ND	0.1 ± 0.1	ND	ND
S = 22 #1	39.5 ± 1.1	11.5 ± 1.9	ND	1.8 ± 0.6	ND	ND	2.5 ± 0.3	ND	0.2 ± 0.2	104.8 ± 12.2	0.5 ± 0.1	ND	ND	1.5 ± 0.5	0.1 ± 0.0	ND	2.6 ± 0.7	13.2 ± 0.1	ND	0.1 ± 0.1	1.1 ± 0.3	ND	ND
S = 22 #2	31.7 ± 1.7	7.6 ± 0.2	ND	1.6 ± 0.3	ND	ND	2.4 ± 0.2	ND	0.2 ± 0.0	91.9 ± 0.7	0.4 ± 0.0	ND	ND	1.4 ± 0.0	ND	ND	1.6 ± 0.0	13.6 ± 0.2	ND	0.1 ± 0.0	0.3 ± 0.0	ND	ND
S = 22 #3	25.7 ± 1.9	8.8 ± 0.1	ND	1.1 ± 0.2	ND	ND	1.8 ± 0.2	ND	0.2 ± 0.0	72.7 ± 8.2	0.3 ± 0.1	ND	ND	1.2 ± 0.1	ND	ND	1.3 ± 0.1	9.4 ± 1.4	ND	ND	0.3 ± 0.1	ND	ND
S = 28 #1	39.8 ± 12.7	13.0 ± 3.9	ND	1.5 ± 0.9	ND	ND	3.5 ± 1.2	ND	0.4 ± 0.1	131.1 ± 43.5	0.4 ± 0.2	ND	ND	0.1 ± 0.0	ND	ND	3.5 ± 0.5	14.1 ± 3.8	ND	0.1 ± 0.1	1.6 ± 1.5	ND	ND
S = 28 #2	25.3 ± 5.8	6.5 ± 1.2	ND	0.5 ± 0.2	ND	ND	1.9 ± 0.5	ND	0.3 ± 0.0	78.0 ± 21.3	0.4 ± 0.1	ND	ND	0.8 ± 0.2	ND	ND	2.2 ± 0.2	8.5 ± 2.0	ND	0.2 ± 0.0	3.5 ± 1.2	ND	ND
S = 28 #3	26.4 ± 5.9	7.7 ± 0.6	0.1 ± 0.0	ND	ND	ND	2.0 ± 0.4	ND	0.1 ± 0.1	73.8 ± 21.0	0.3 ± 0.1	ND	ND	1.2 ± 0.3	ND	ND	2.5 ± 0.6	11.4 ± 1.4	ND	0.2 ± 0.1	2.0 ± 1.4	ND	ND
S = 34 #1	24.0 ± 4.6	8.7 ± 1.2	ND	3.7 ± 0.1	ND	ND	1.2 ± 0.2	0.1 ± 0.1	ND	52.3 ± 12.2	0.2 ± 0.0	ND	ND	2.1 ± 0.2	0.1 ± 0.0	ND	5.6 ± 1.3	9.4 ± 1.0	ND	0.3 ± 0.0	3.4 ± 0.1	ND	ND
S = 34 #2	53.7 ± 5.9	17.7 ± 3.0	ND	1.8 ± 0.3	ND	ND	2.9 ± 0.2	0.6 ± 0.0	0.3 ± 0.0	104.1 ± 13.0	0.4 ± 0.1	ND	ND	2.5 ± 0.6	ND	ND	6.0 ± 1.5	15.4 ± 0.3	ND	0.1 ± 0.0	1.3 ± 0.3	ND	ND
S = 34 #3	24.8 ± 2.4	7.6 ± 1.2	0.1 ± 0.1	1.4 ± 0.5	ND	ND	1.0 ± 0.1	0.2 ± 0.1	ND	40.6 ± 0.4	0.2 ± 0.0	ND	ND	1.7 ± 0.0	ND	ND	4.1 ± 0.0	11.1 ± 1.1	ND	0.2 ± 0.0	2.3 ± 0.1	ND	ND

Particulate carbon, nitrogen and phosphorus

Table 57: Cell quotas of particulate carbon in triplicate cultures in exponential growth phase and in stationary growth phase. (ng cell^{-1}, technical duplicates, n = 2, ± 1 SD)

	S = 6	S = 10	S = 16	S = 22	S = 28	S = 34
Exponential growth phase						
Culture 1	2.91 ± 2.98	3.06 ± 0.17	2.77 ± 0.27	3.11 ± 0.39	3.67 ± 0.03	3.96 ± 0.16
Culture 2	4.01 ± 0.14	3.78 ± 0.79	3.10 ± 0.15	2.70 ± 0.01	4.06 ± 0.09	5.18 ± 0.20
Culture 3	4.26 ± 0.64	2.81 ± 0.50	2.18 ± 0.47	3.29 ± 0.17	4.00 ± 0.09	3.45 ± 0.68
Stationary growth phase						
Culture 1	4.29 ± 0.05	2.07 ± 0.00	3.06 ± 0.11	3.47 ± 0.22	3.92 ± 0.07	4.15 ± 0.70
Culture 2	4.59 ± 0.23	1.67 ± 0.03	3.12 ± 0.01	2.89 ± 0.11	3.32 ± 0.08	5.15 ± 1.08
Culture 3	4.61 ± 0.33	2.31 ± 0.06	3.05 ± 0.24	2.52 ± 0.00	3.53 ± 0.01	4.16 ± 0.76

Table 58: Cell quotas of particulate nitrogen in triplicate cultures in exponential growth phase and in stationary growth phase. (ng cell^{-1}, technical duplicates, n = 2, ± 1 SD)

	S = 6	S = 10	S = 16	S = 22	S = 28	S = 34
Exponential growth phase						
Culture 1	0.35 ± 0.35	0.53 ± 0.00	0.49 ± 0.06	0.49 ± 0.03	0.56 ± 0.00	0.60 ± 0.03
Culture 2	0.69 ± 0.02	0.64 ± 0.10	0.53 ± 0.04	0.48 ± 0.01	0.60 ± 0.00	0.79 ± 0.03
Culture 3	0.73 ± 0.04	0.54 ± 0.08	0.38 ± 0.04	0.55 ± 0.02	0.57 ± 0.01	0.55 ± 0.11
Stationary growth phase						
Culture 1	0.45 ± 0.00	0.39 ± 0.00	0.48 ± 0.01	0.58 ± 0.04	0.46 ± 0.00	0.47 ± 0.07
Culture 2	0.51 ± 0.03	0.31 ± 0.00	0.51 ± 0.01	0.49 ± 0.03	0.40 ± 0.01	0.54 ± 0.11
Culture 3	0.53 ± 0.03	0.42 ± 0.00	0.49 ± 0.02	0.43 ± 0.00	0.43 ± 0.01	0.46 ± 0.10

Table 59: Cell quotas of particulate phosphorus in triplicate cultures in exponential growth phase and in stationary growth phase. (pg cell^{-1}, technical duplicates, n = 2, ± 1 SD)

	S = 6	S = 10	S = 16	S = 22	S = 28	S = 34
Expoential growth phase						
Culture 1	108.39 ± 1.77	88.51 ± 0.65	88.63 ± 8.56	78.44 ± 4.41	91.99 ± 2.03	93.57 ± 0.96
Culture 2	108.56 ± 3.76	103.95 ± 0.92	99.99 ± 11.77	73.06 ± 3.17	91.32 ± 1.26	110.46 ± 3.44
Culture 3	113.94 ± 0.43	102.38 ± 10.38	56.08 ± 29.61	81.75 ± 2.49	88.48 ± 2.01	83.24 ± 19.13
Stationary growth phase						
Culture 1	48.82 ± 0.07	65.82 ± 5.66	70.78 ± 0.09	72.63 ± 0.01	57.83 ± 1.43	54.40 ± 5.48
Culture 2	50.82 ± 1.25	49.11 ± 0.10	72.51 ± 0.12	70.72 ± 4.82	47.31 ± 0.71	58.67 ± 13.87
Culture 3	51.68 ± 4.80	67.90 ± 2.93	67.85 ± 0.53	52.94 ± 1.74	55.72 ± 0.30	51.34 ± 9.49

Table 60: Particulate C/N, N/P and C/P ratios of different salinity treatments. Each data point represents a mean of triplicate cultures (n = 3, ± 1 SD)

	S = 6	S = 10	S = 16	S = 22	S = 28	S = 34
Exponential growth phase						
C/N	7.76 ± 1.41	6.53 ± 0.34	6.70 ± 0.13	7.00 ± 0.30	7.92 ± 0.21	7.56 ± 0.16
N/P	11.83 ± 3.33	12.93 ± 0.87	13.00 ± 1.54	14.38 ± 0.40	14.08 ± 0.51	14.89 ± 0.70
C/P	87.13 ± 12.57	84.74 ± 9.94	87.01 ± 9.42	100.62 ± 3.60	111.51 ± 6.09	112.51 ± 6.23
Stationary growth phase						
C/N	10.62 ± 0.45	6.32 ± 0.05	7.32 ± 0.13	6.91 ± 0.08	9.81 ± 0.15	10.60 ± 0.33
N/P	21.73 ± 1.07	13.55 ± 0.40	15.45 ± 0.38	17.00 ± 1.18	17.67 ± 0.65	19.90 ± 0.52
C/P	230.22 ± 2.67	85.68 ± 3.20	113.08 ± 2.29	117.38 ± 8.24	173.43 ± 7.17	211.03 ± 12.03

Dissolved organic carbon and total dissolved nitrogen

Table 61: Dissolved organic carbon in culture media and in triplicate cultures of *A. ostenfeldii* in exponential and stationary growth. All amounts are measured in triplicate cultures (n = 3, ± 1 SD) and presented in µM.

	S = 6	S = 10	S = 16	S = 22	S = 28	S = 34
Exponential growth phase						
Medium	3208.21 ± 295.34	2786.78 ± 94.00	5510.78 ± 1178.00	4004.95 ± 1063.43	4306.37 +77.42	3642.77 ± 139.36
Culture 1	4322.33 ± 289.83	2961.78 ± 637.00	4315.72 ± 591.77	4553.75 ± 31.96	4588.40 ± 257.70	3876.13 ± 94.01
Culture 2	4451.26 ± 233.62	5521.31 ± 519.04	4514.08 ± 926.78	3472.78 ± 72.00	4965.54 ± 37.60	4047.56 ± 134.93
Culture 3	4684.89 ± 683.24	5283.27 ± 170.81	4998.96 ± 292.03	2715.78 ± 21.00	4496.60 ± 86.27	3984.52 ± 12.17
Stationary growth phase						
Medium	2555.82 ± 174.12	4050.14 ± 48.49	4119.56 ± 488.19	4453.47 ± 240.00	4335.12 ± 294.20	2713.78 ± 183.00
Culture 1	2526.07 ± 78.24	2599.78 ± 203.00	3115.64 ± 414.35	3388.39 ± 524.24	3407.19 ± 80.74	2765.78 ± 109.00
Culture 2	2466.56 ± 42.98	4406.08 ± 1.10	3214.82 ± 467.25	4689.04 ± 875.95	3306.54 ± 8.85	2980.78 ± 50.00
Culture 3	2432.40 ± 28.65	4412.78 ± 134.00	3171.84 ± 970.86	4595.03 ± 1633.56	3461.38 ± 101.75	2928.78 ± 54.00

Table 62: Total dissolved nitrogen in culture media and in triplicate cultures of *A. ostenfeldii* in exponential and stationary growth. All amounts are measured in triplicate cultures (n = 3, ± 1 SD) and presented in µM.

	S = 6	S = 10	S = 16	S = 22	S = 28	S = 34
Exponential growth phase						
Medium	1310.97 ± 163.12	991.65 ± 74.19	1994.55 ± 406.12	1164.26 ± 378.17	1659.38 ± 9.18	1420.73 ± 12.33
Culture 1	1552.96 ± 162.97	954.56 ± 203.73	1170.82 ± 284.48	1149.05 ± 11.63	1591.95 ± 35.60	1171.65 ± 50.57
Culture 2	1542.38 ± 118.39	1726.51 ± 287.02	1272.95 ± 338.61	1196.25 ± 15.66	1788.82 ± 23.40	1222.22 ± 6.54
Culture 3	1567.72 ± 314.00	1695.35 ± 38.17	1476.77 ± 123.45	976.37 ± 0.67	1566.28 ± 19.25	1199.2 ± 22.27
Stationary growth phase						
Medium	832.36 ± 53.08	1334.23 ± 6.86	1244.32 ± 237.52	1933.75 ± 114.73	1598.87 ± 108.9	1044.12 ± 56.31
Culture 1	217.17 ± 24.15	684.90 ± 24.22	274.28 ± 140.00	913.13 ± 137.50	693.36 ± 14.09	740.83 ± 65.73
Culture 2	126.52 ± 35.78	862.48 ± 68.88	283.82 ± 151.93	1328.4 ± 240.53	641.78 ± 7.04	1051.91 ± 236.5
Culture 3	193.77 ± 36.53	1136.28 ± 54.87	314.09 ± 194.43	1287.39 ± 493.89	755.13 ± 8.43	1038.36 ± 40.17

Table 63: Dissolved C/N ratios of different salinity treatments. Each data point represents a mean of triplicate cultures (n = 3, ± 1 SD)

	S = 6	S = 10	S = 16	S = 22	S = 28	S = 34
Exponential growth phase						
C/N	3.37 ± 0.10	3.66 ± 0.05	4.13 ± 0.14	3.75 ± 0.62	3.32 ± 0.06	3.87 ± 0.01
Stationary growth phase						
C/N	16.99 ± 4.09	4.97 ± 0.70	12.75 ± 0.68	4.20 ± 0.09	5.70 ± 0.27	3.65 ± 0.50

Cell size determination

Table 64: Cell size measurements of a triplicate culture in exponential growth at S = 6. (µm)

Width	Length	Width	Length	Width	Length
Culture 1		Culture 2		Culture 3	
39.53	44.53	35.49	43.46	36.98	39.17
27.91	30.44	38.49	40.80	35.68	43.03
38.44	40.47	35.26	41.13	37.05	38.89
53.48	56.90	34.44	35.28	34.93	43.89
33.53	36.01	38.13	38.15	35.44	36.88
33.80	37.78	35.80	38.86	33.98	37.93
37.23	42.94	32.52	33.24	33.51	35.41
33.58	33.19	30.54	36.73	36.18	37.73
35.40	42.16	40.74	42.56	44.49	44.53
36.87	44.09	34.44	37.33	35.91	36.70
33.93	36.15	34.51	36.73	38.14	38.49
35.69	36.47	35.08	36.91	35.56	37.23
33.59	34.51	30.13	34.84	40.57	45.89
37.30	40.29	38.81	41.26	38.85	39.01
31.70	31.96	32.06	38.70	42.20	46.31
35.15	41.51	39.11	29.71	41.37	41.33
33.45	37.41	36.18	42.08	40.44	40.19
33.75	38.15	31.00	31.89	41.20	45.15
40.46	48.12	33.21	33.79	38.13	41.98
34.31	28.88	39.66	44.31	37.70	40.14
31.63	37.34	37.97	39.31	36.44	36.45
30.54	36.53	38.44	41.21	33.98	37.94
43.40	40.94	26.44	26.11	37.88	42.94
39.62	39.82	33.55	41.91	38.75	38.72
59.98	61.47	34.72	38.07	29.69	35.84
26.34	33.59	40.43	41.75	33.19	34.00
36.70	36.19	30.92	35.42	34.75	36.18
40.73	45.19	37.81	38.66	30.84	36.45
36.98	39.48	36.48	44.90	33.92	35.75
32.71	37.85	34.56	37.47	36.24	38.77

Table 65: Cell size measurements of a triplicate culture in stationary growth at S = 6. (µm)

Width	Length	Width	Length	Width	Length
Culture 1		Culture 2		Culture 3	
34.58	38.13	35.99	41.37	39.83	44.69
30.40	33.29	37.82	42.37	39.15	41.64
36.57	42.67	38.35	42.76	39.22	46.33
29.37	34.50	37.52	43.99	37.05	39.77
35.25	40.37	31.66	37.21	36.06	40.80
33.94	35.25	38.61	39.13	36.09	41.95
32.66	39.14	36.52	45.92	30.53	35.84
37.96	46.26	39.93	41.10	38.20	45.83
35.70	39.30	35.40	39.47	36.09	45.89
30.65	34.69	27.37	31.72	35.01	40.84
43.35	49.27	31.90	35.28	29.93	36.08
34.84	40.39	40.20	44.51	35.16	35.24
33.45	43.46	37.29	43.58	39.73	46.93
34.30	40.53	42.48	46.08	31.60	37.15
37.97	48.19	38.23	42.34	27.89	33.89
38.16	44.40	29.93	29.80	35.40	39.93
24.99	32.00	32.03	42.01	37.23	43.55
33.25	35.35	35.15	41.03	32.71	39.35
43.66	36.72	29.49	38.13	37.77	48.17
39.27	44.85	32.13	37.99	38.77	40.65
39.13	46.53	32.26	38.44	32.42	38.48
35.45	40.53	31.98	42.66	33.59	38.27
35.91	41.68	35.84	42.46	28.08	34.10
33.40	34.07	35.24	42.00	38.47	41.45
38.38	44.44	37.46	40.83	35.56	43.95
36.25	41.95	27.11	31.36	30.39	35.35
38.06	51.18	35.19	37.77	35.00	43.87
38.37	45.78	39.37	40.94	38.02	44.14
36.14	48.58	37.43	43.73	32.94	34.73
36.81	41.91	33.70	37.80	31.30	37.19

Table 66: Cell size measurements of a triplicate culture in exponential growth at S = 10. (µm)

Width	Length	Width	Length	Width	Length
Culture 1		Culture 2		Culture 3	
32.12	33.57	39.93	43.65	38.35	41.17
29.86	35.74	35.72	41.88	35.94	39.60
34.96	36.62	36.45	37.87	34.91	39.90
26.67	35.83	33.94	47.68	29.49	49.00
35.05	36.89	35.93	38.15	26.31	30.30
38.02	38.32	33.97	38.81	38.96	93.18
34.61	35.36	31.51	39.69	35.99	38.36
37.52	41.64	37.52	42.94	36.83	42.15
28.95	32.65	36.94	42.21	37.97	38.70
33.89	38.70	29.66	32.35	34.10	40.19
30.81	33.38	32.44	41.15	27.76	27.62
33.07	34.50	36.75	41.06	37.57	40.60
30.03	39.34	32.18	35.69	31.25	35.44
40.74	44.49	33.67	41.22	34.73	32.56
26.36	30.76	50.99	57.08	27.66	29.42
24.40	25.78	42.17	40.30	31.51	32.84
31.51	33.51	37.89	43.55	36.57	42.64
25.07	30.13	34.56	35.49	35.40	34.96
30.65	30.84	35.16	38.93	29.32	29.54
30.65	32.43	28.25	27.84	27.92	33.54
35.25	41.47	28.21	32.72	32.22	34.38
38.59	42.42	27.49	29.13	29.02	31.66
32.54	39.54	32.14	33.19	25.58	28.21
31.66	33.84	34.75	36.73	30.40	25.92
31.51	35.35	37.46	49.67	36.38	40.07
39.37	42.59	31.74	34.03	29.69	30.78
38.97	38.14	33.40	36.64	27.86	33.09
34.91	36.75	33.16	38.27	33.10	35.56
32.84	35.59	34.69	36.70	34.19	36.44
34.23	37.83	35.37	37.47	28.21	23.56

Table 67: Cell size measurements of a triplicate culture in stationary growth at S = 10. (µm)

Width	Length	Width	Length	Width	Length
Culture 1		Culture 2		Culture 3	
26.16	32.37	36.97	38.54	30.43	31.26
34.96	37.89	35.41	36.92	47.98	41.22
49.08	55.90	24.94	26.36	37.94	41.05
34.98	41.15	28.88	29.97	33.50	35.42
40.11	45.19	34.29	35.56	36.80	38.72
44.71	51.56	32.31	35.62	31.00	39.32
37.89	46.35	37.21	43.48	26.32	29.36
22.96	27.74	36.48	45.65	29.65	29.16
27.29	32.06	36.45	37.00	34.03	38.05
37.99	48.85	23.81	27.03	28.23	34.98
41.31	42.64	23.81	27.48	33.09	33.79
34.94	31.50	30.23	34.45	31.26	33.98
34.82	42.68	33.63	35.70	31.57	30.13
38.44	40.14	22.24	24.19	26.57	28.44
34.55	38.06	27.63	30.50	35.08	42.00
33.20	34.94	24.56	25.47	27.03	30.64
28.28	32.25	32.88	33.40	39.12	47.79
33.20	38.72	27.76	26.19	26.24	34.59
33.51	41.45	30.65	33.21	33.38	35.41
30.47	31.89	25.77	27.29	45.15	45.48
31.30	35.57	25.43	27.46	27.49	35.55
30.47	32.00	28.44	32.66	27.64	29.96
25.01	25.10	42.59	44.75	42.00	48.27
24.34	24.92	28.48	32.97	37.21	43.73
22.13	21.46	33.45	36.85	37.06	37.56
28.90	33.30	28.13	31.86	33.72	43.14
22.44	26.21	33.20	36.47	33.20	38.72
29.99	37.72	26.71	28.75	31.00	35.92
32.79	38.65	33.69	36.92	36.97	38.54
33.71	41.75	26.85	32.03	28.09	33.57

Table 68: Cell size measurements of a triplicate culture in exponential at S = 16. (µm)

Width	Length	Width	Length	Width	Length
Culture 1		Culture 2		Culture 3	
24.11	25.97	37.53	40.08	26.71	26.53
41.85	47.82	24.90	26.98	33.20	36.45
30.22	32.44	33.31	34.80	26.57	29.16
28.13	32.14	42.99	43.26	37.87	37.87
23.87	26.33	29.20	32.82	31.49	33.67
26.21	29.96	29.49	30.50	33.52	33.92
37.52	38.26	24.88	29.78	42.17	45.49
23.51	23.75	31.19	34.28	20.57	25.93
33.63	32.03	32.20	33.40	32.97	29.45
25.82	27.90	29.91	29.53	29.16	32.23
42.42	43.64	25.91	30.05	35.86	40.97
30.32	34.21	36.50	42.10	26.19	29.97
27.27	28.18	32.90	34.49	33.24	35.99
29.51	31.84	30.98	38.01	25.60	30.69
32.14	38.51	25.40	27.63	27.91	28.09
32.90	33.53	33.55	37.30	26.98	30.49
27.10	27.77	29.48	30.14	29.99	35.56
33.35	34.01	24.91	24.62	24.51	28.21
29.32	30.69	27.10	30.55	36.09	36.65
30.99	30.32	43.89	49.81	22.83	29.90
34.55	37.78	33.51	35.58	28.45	27.64
28.10	32.22	28.63	37.18	39.32	41.04
37.88	41.30	28.60	38.70	37.70	41.33
39.69	45.64	36.37	43.69	27.74	28.41
39.87	40.07	35.51	35.87	27.06	39.94
31.89	33.78	35.54	38.24	24.88	29.78
29.32	32.81	26.97	28.01	26.21	32.75
25.22	26.78	37.14	45.07	30.99	33.53
24.83	32.17	26.43	25.50	25.82	38.70
31.74	38.18	30.01	37.79	30.13	37.10

Table 69: Cell size measurements of a triplicate culture in stationary growth at S = 16. (µm)

Width	Length	Width	Length	Width	Length
Culture 1		Culture 2		Culture 3	
33.57	37.29	37.37	28.68	38.16	44.59
35.89	43.26	38.83	39.37	36.24	45.23
37.04	28.28	27.92	30.69	24.94	30.40
33.10	34.50	23.91	28.76	24.92	29.12
31.93	41.75	25.76	30.13	27.91	33.02
29.58	34.35	28.62	30.88	33.09	37.05
29.57	36.38	32.66	34.92	31.43	40.03
41.98	43.69	33.88	34.03	33.34	35.88
20.90	25.92	41.10	44.44	25.35	26.18
33.19	40.31	32.44	35.23	27.89	35.16
26.66	31.19	34.92	42.49	34.62	39.78
35.42	36.80	42.14	44.37	20.52	23.41
33.80	37.47	32.65	32.68	28.24	31.19
25.52	28.36	37.29	41.43	29.42	31.31
27.31	28.28	32.12	39.56	25.53	37.63
32.49	28.53	28.71	28.63	35.18	38.38
26.93	28.00	31.87	37.94	27.32	25.78
31.89	37.27	36.70	36.52	43.71	44.00
29.37	36.17	33.83	36.01	23.99	26.86
31.02	38.38	33.51	38.86	26.96	30.54
30.43	33.08	30.92	29.13	25.37	27.92
23.26	23.79	30.87	35.31	45.90	43.32
33.46	43.17	28.89	34.60	26.18	28.80
28.14	31.66	31.10	33.71	33.73	39.11
34.16	41.21	24.04	38.83	29.19	31.50
23.69	24.70	27.02	29.27	27.96	27.18
34.52	43.32	24.31	27.73	29.41	21.05
39.36	43.26	23.18	28.60	26.31	30.00
31.55	40.02	33.55	40.03	43.60	49.71
25.58	26.56	24.70	26.78	39.49	43.40

Table 70: Cell size measurements of a triplicate culture in exponential growth at S = 22. (µm)

Width	Length	Width	Length	Width	Length
Culture 1		Culture 2		Culture 3	
34.43	37.79	31.33	32.87	39.22	44.80
27.31	32.36	33.19	33.38	31.13	33.80
27.59	34.78	29.71	36.08	32.47	34.53
32.14	37.29	31.64	35.99	27.75	29.44
33.19	34.54	30.44	35.88	29.16	30.84
27.82	33.82	31.09	32.97	24.53	28.45
33.19	34.54	31.72	34.10	42.16	45.82
36.09	39.88	27.27	28.44	30.19	32.74
33.09	35.74	32.37	36.69	22.71	24.86
41.51	44.57	39.85	42.95	27.54	30.12
27.32	35.00	26.85	30.55	23.74	27.49
34.61	37.56	38.41	40.66	25.45	30.09
47.62	50.27	31.21	35.72	33.03	36.15
40.13	40.68	31.01	32.27	45.14	45.96
29.49	31.55	29.47	29.30	25.58	31.52
39.37	39.71	27.40	32.55	28.77	30.65
29.37	28.68	25.80	30.12	39.37	44.25
37.43	40.89	25.61	25.70	36.81	41.65
35.82	33.70	37.29	40.94	24.05	26.34
44.88	45.10	27.29	30.23	37.80	46.63
27.18	28.73	28.33	32.64	28.37	29.57
36.38	39.53	39.00	41.91	32.14	36.29
35.33	36.14	30.17	34.82	32.59	33.79
33.82	37.25	41.37	44.53	24.56	27.37
38.37	44.44	30.30	38.87	40.14	44.66
29.63	32.18	24.91	27.56	33.12	33.52
31.33	33.19	31.87	39.88	30.65	32.55
32.90	33.97	39.37	44.17	25.84	29.42
34.17	44.75	34.61	34.82	27.99	31.06
31.20	36.25	31.81	38.25	34.56	38.96

Table 71: Cell size measurements of a triplicate culture in stationary growth at S = 22. (µm)

Width	Length	Width	Length	Width	Length
Culture 1		Culture 2		Culture 3	
26.39	26.84	24.83	30.30	30.83	36.47
32.67	36.43	25.78	28.21	24.23	29.20
22.29	28.10	28.63	34.81	28.12	31.42
24.70	30.12	25.04	30.91	24.92	26.01
27.74	27.29	30.22	34.38	35.08	29.65
32.76	28.93	28.10	30.24	22.14	26.91
29.88	32.87	27.74	28.10	30.05	34.44
26.06	27.91	28.67	33.21	29.96	32.78
29.41	31.32	28.24	33.74	22.98	26.16
39.90	41.03	26.78	28.08	30.04	31.27
24.61	29.22	33.98	35.36	31.70	32.26
35.56	38.75	24.66	30.13	26.58	26.79
25.44	26.31	30.29	33.13	28.32	31.90
30.90	34.18	24.80	27.42	24.19	31.71
28.10	32.81	26.35	31.19	26.84	29.86
28.16	31.42	24.58	27.29	30.05	36.16
30.12	32.14	25.40	31.24	23.36	27.15
25.93	26.21	30.13	33.42	23.78	27.65
30.12	32.14	26.79	32.10	34.35	35.71
25.93	26.31	27.19	26.20	25.37	30.75
27.95	32.96	28.28	31.44	32.22	27.56
33.55	38.44	28.01	32.69	30.39	32.12
28.10	29.42	24.71	30.50	24.04	27.57
29.36	31.93	25.67	25.56	28.08	29.13
30.39	36.66	28.01	29.51	21.93	31.26
32.26	28.33	28.89	26.64	21.86	25.11
30.91	31.96	30.86	34.64	40.21	43.95
29.70	31.74	23.46	27.92	24.84	29.50
28.01	33.54	37.10	39.45	41.60	44.62
28.55	31.96	24.45	29.20	23.80	32.07

Table 72: Cell size measurements of a triplicate culture in exponential growth at S = 28. (µm)

Width	Length	Width	Length	Width	Length
Culture 1		Culture 2		Culture 3	
30.66	33.05	37.29	45.61	31.44	37.52
34.71	38.25	30.22	30.87	30.82	33.05
29.41	34.01	26.34	29.96	35.88	36.47
34.98	40.11	35.69	38.38	39.69	43.05
24.53	26.35	28.86	31.30	26.75	28.60
40.89	43.10	42.13	44.41	31.74	33.72
28.58	31.55	30.75	32.76	28.34	30.83
26.78	28.13	40.47	48.79	39.76	40.70
36.80	39.46	44.62	49.72	31.74	32.46
33.48	34.19	30.35	35.41	39.62	47.02
28.88	34.00	32.44	34.47	30.98	39.70
26.81	32.78	27.89	28.38	28.34	30.83
39.23	42.93	23.81	26.91	32.61	36.44
36.18	38.44	22.44	32.50	42.21	47.06
27.84	28.08	25.11	25.92	27.53	29.95
32.74	36.75	24.70	27.86	30.97	33.48
30.15	33.80	28.91	32.48	34.94	40.08
30.24	31.03	36.25	38.73	35.88	40.90
33.70	34.36	40.10	42.78	28.73	30.91
44.59	47.50	26.33	26.72	35.40	35.50
46.60	51.45	27.81	33.21	28.61	32.47
28.63	29.33	32.49	36.24	27.82	28.79
41.13	46.93	24.75	27.18	28.13	30.49
28.73	32.37	29.96	31.31	27.25	28.88
24.22	27.82	33.09	34.49	33.09	35.77
29.77	30.79	34.43	37.14	31.91	33.64
30.69	35.13	26.72	26.33	28.80	34.72
28.14	31.20	27.51	31.22	29.41	35.76
30.11	34.57	25.78	29.44	30.20	35.71
41.25	49.38	29.43	33.10	34.20	43.05

Table 73: Cell size measurements of a triplicate culture in stationary growth at S = 28. (µm)

Width	Length	Width	Length	Width	Length
Culture 1		Culture 2		Culture 3	
23.90	28.08	30.77	36.43	31.21	32.64
34.96	39.83	37.61	42.70	24.65	32.12
28.38	32.72	19.68	22.36	25.80	30.73
23.50	28.13	33.34	35.22	25.06	31.68
26.61	26.75	24.02	25.70	28.64	31.41
25.29	27.19	24.92	29.13	29.96	33.69
32.40	37.29	27.31	38.73	27.98	31.52
29.80	31.24	26.05	29.24	29.42	34.03
28.65	31.25	28.83	28.93	31.97	33.62
28.42	30.13	33.89	38.13	26.72	31.89
31.64	33.62	25.73	28.93	29.04	37.63
34.20	38.13	29.06	32.18	23.06	29.30
31.16	36.56	22.54	22.71	25.05	32.07
21.60	22.94	29.95	33.31	28.68	30.39
23.84	24.87	25.26	31.06	25.51	36.12
28.19	28.60	24.02	27.39	22.45	23.78
30.69	36.70	29.51	31.56	30.15	34.76
24.90	23.06	33.97	34.22	30.76	36.81
30.40	34.89	28.52	32.76	28.87	30.39
23.62	26.98	30.54	30.56	25.78	30.18
28.10	29.51	25.37	29.99	31.28	33.80
29.00	29.69	28.55	29.04	27.49	27.77
25.60	34.19	34.25	37.70	31.14	34.27
28.47	28.58	25.88	26.05	35.59	38.85
30.54	31.59	31.66	38.87	30.43	37.90
26.75	27.26	24.18	31.24	24.02	28.93
26.73	30.76	27.95	24.87	28.07	29.97
32.17	36.56	34.43	37.29	27.78	31.04
31.37	32.76	21.08	31.07	29.10	32.25
24.17	26.78	22.19	26.70	34.96	37.29

Table 74: Cell size measurements of a triplicate culture in exponential growth at S = 34. (µm)

Width	Length	Width	Length	Width	Length
Culture 1		Culture 2		Culture 3	
35.33	38.32	45.74	47.26	34.38	37.21
36.98	38.32	28.89	30.96	31.89	34.69
45.08	52.48	41.71	42.29	27.57	30.91
26.57	28.14	28.61	32.22	45.22	49.34
34.73	35.08	39.45	40.38	37.00	39.60
31.11	34.62	41.73	47.91	33.49	33.46
31.18	32.00	27.75	29.86	33.06	35.58
30.87	32.72	36.18	38.49	36.59	40.59
41.87	45.10	35.43	35.76	32.63	32.25
25.82	26.85	29.47	34.27	26.49	28.61
35.13	40.45	32.27	36.44	27.53	30.01
28.80	31.35	37.78	42.15	40.20	43.70
35.32	37.36	28.55	30.54	33.09	34.71
42.29	49.17	24.95	30.05	31.74	38.46
42.46	47.14	47.08	53.16	27.45	30.08
23.29	28.58	42.76	43.51	41.25	44.71
38.70	41.56	42.01	42.77	26.31	27.90
26.70	28.76	27.29	32.81	26.71	27.54
27.37	28.25	43.48	45.87	32.93	33.16
47.26	49.24	36.98	42.86	36.71	36.83
44.93	47.41	34.59	37.63	32.40	34.73
42.46	46.27	29.77	34.11	33.17	35.36
41.46	48.06	31.87	33.19	39.40	44.44
26.47	28.85	40.79	45.62	27.11	30.70
45.63	48.64	38.47	40.41	32.97	37.94
31.33	34.65	36.62	44.05	37.26	39.04
37.83	42.04	31.30	34.00	39.84	43.35
33.26	35.92	23.64	29.69	33.67	34.36
30.55	32.03	31.36	35.91	39.13	44.74
29.57	32.63	28.75	34.48	25.53	22.94

Table 75: Cell size measurements of a triplicate culture in stationary growth at S = 34. (µm)

Width	Length	Width	Length	Width	Length
Culture 1		Culture 2		Culture 3	
35.15	37.54	25.02	28.25	32.71	37.30
30.44	31.87	25.95	28.86	26.11	29.47
36.60	38.47	31.61	34.65	26.78	31.72
26.27	28.86	31.21	24.40	24.92	28.91
25.84	28.97	24.57	28.25	24.17	26.92
27.71	29.41	27.12	30.88	25.78	32.10
30.79	36.43	28.68	31.42	32.81	38.83
28.89	31.19	33.19	37.59	25.01	28.99
30.29	37.92	31.21	37.30	27.05	29.49
25.41	29.36	31.09	31.74	35.52	37.78
36.85	34.01	28.35	32.66	25.26	28.21
27.18	34.19	30.53	34.56	24.19	28.99
30.18	30.44	31.75	36.26	24.39	25.95
31.92	34.19	29.91	33.38	32.63	40.13
26.58	28.58	27.17	30.01	23.57	33.16
23.78	31.85	24.90	31.70	28.60	34.01
30.55	33.42	26.38	27.15	43.01	38.15
29.51	29.69	27.75	30.73	35.60	36.27
35.51	37.89	26.85	32.03	20.23	21.22
30.98	33.40	24.60	26.71	23.91	25.01
23.51	27.32	24.74	30.77	35.56	42.82
35.84	40.69	26.01	30.09	33.83	40.73
32.10	33.48	28.44	29.54	35.41	42.07
23.51	30.13	23.70	25.36	38.75	39.31
32.60	33.44	27.81	34.35	42.95	48.00
37.47	41.66	29.01	37.40	29.16	33.58
30.57	36.33	36.10	39.16	29.80	38.50
27.03	33.16	26.80	28.23	29.69	33.72
32.97	35.98	27.42	34.35	32.71	38.89
25.64	27.90	29.41	33.35	29.12	29.00